PROTEOMICS TO STUDY RACIAL DISPARITIES IN ALZHEIMER'S DISEASE

By

Kaitlyn Elizabeth Stepler

Dissertation
Submitted to the Faculty of the
Graduate School of Vanderbilt University
in partial fulfillment of the requirements
for the degree of

DOCTOR OF PHILOSOPHY
in
Chemistry
August 31, 2021
Nashville, Tennessee

Approved:

Renã A.S. Robinson, Ph.D.

Lars Plate, Ph.D.

Richard M. Caprioli, Ph.D.

Timothy J. Hohman, Ph.D.

ACKNOWLEDGEMENTS

I would like to thank my advisor, Dr. Renã A. S. Robinson, for her mentoring throughout my time as a graduate student in her lab. She always pushed me to think deeper about my project and the bigger picture to help me grow into the scientist I am today. Thank you, Dr. Robinson, for this journey over the last five years and for making the move from Pittsburgh to Vanderbilt worth it.

I would also like to thank the current and former members of the RASR Lab over the past five years for their advice, feedback, and support. I would especially like to thank Dr. Bushra Amin, Dr. Christina King, and Dr. Mostafa Khan for training me when I first joined the lab knowing nothing about mass spectrometry, and for teaching me the values of a good scientist. I would also like to thank the Dream Team and Bailey Bowser for their friendship and encouragement, without which I would not be here today.

To Dr. Mrs., thank you for lighting the chemistry spark in me and being my first mentor in chemistry.

I would like to thank my family and friends, especially my parents and sisters and Emma's family, for their support and encouragement during the ups and downs of this last five years and for always believing in me.

Lastly, but most importantly, I would like to thank my fiancée, Emma. She has been by my side through every step of this journey, every twist and turn, supporting me and believing in me every step of the way. She has been my rock and has helped me find the joy every day even when I don't feel it. I would not be here without her. We did this together, Em; thanks for being amazing.

TABLE OF CONTENTS

Page

LIST OF TABLES

Table Page

LIST OF FIGURES

CHAPTER 1

Introduction

According to the Alzheimer's Association, approximately 6.2 million Americans have Alzheimer's disease (AD),[1] a devastating neurodegenerative disorder marked by accumulation of extracellular amyloid beta (Aβ) plaques and intracellular hyperphosphorylated tau tangles [also referred to as senile plaques and neurofibrillary tangles, (NFTs)] in the brain. These pathological hallmarks lead to neuronal dysfunction and death and are associated with cognitive decline. However, the number of AD sufferers is not equally spread amongst different subgroups of the population. AD disproportionately affects African American/Black and Hispanic adults,[2-5] which is alarming considering that underrepresented minorities will comprise a larger proportion of both the entire older population and the population of AD sufferers by 2050.[2, 6-7] Though many factors are known to contribute to these disparities, the underlying mechanisms remain unknown. This dissertation will apply proteomics to investigate molecular contributions to AD in African American/Black adults. The following sections of this chapter will summarize the known contributors to racial disparities in AD and introduce the value of proteomics to study these disparities.

1.1 Alzheimer's Disease Disparities

African American/Black adults are two to three and Hispanic adults are one and a half times as likely to develop AD and related-dementias compared to non-Hispanic White adults,[8-9] and African American/Black adults have a 65% higher risk of developing AD than Asian

American adults.[10] African American/Black and Hispanic adults also have a higher prevalence of cognitive impairment at ages 55 and older compared to non-Hispanic White adults.[2] African American/Black and Hispanic adults are more likely to present with more severe symptoms and African American/Black adults are more likely to have an earlier age of onset than non-Hispanic White adults.[6, 9] Several studies demonstrate that African American/Black adults score lower on cognitive tests such as the Mini-Mental State Exam (MMSE) than non-Hispanic White adults,[3, 6, 11] although the rates of cognitive decline are similar between the racial groups.[3] However, MMSE has a much higher rate of false positive diagnosis of cognitive impairment in African American/Black adults than non-Hispanic White adults[9] and is not culturally tailored as a diagnostic test; therefore, MMSE may not be generalizable to racial groups outside of non-Hispanic White adults.

There are no significant differences in the two primary neuropathological hallmarks of AD, Aβ plaques and tau tangles, in the brains of African American/Black and non-Hispanic White adults.[9, 12-14] However, African American/Black adults are more likely to present with mixed AD and other dementia pathologies, particularly Lewy body dementia, infarcts, and cerebrovascular disease,[3, 12, 15-16] though other studies have not replicated this trend.[17-18] Furthermore, differences in total and phosphorylated tau levels in cerebrospinal fluid (CSF), *in vivo* biomarkers for AD,[19-21] have been identified between African American/Black and non-Hispanic White adults.[17, 22-24] This relationship between tau levels and racial background appears to be mediated by apolipoprotein E (*APOE)* genotype, as tau levels were only significantly decreased in individuals with the *APOE* ε4 allele.[17] Tau levels are also associated with other changes in AD that have been uniquely reported in African American/Black adults, including increased CSF interleukin-9 (IL-9) levels[25] and increased connectivity within the default mode

network, an imaging biomarker for AD.[26] Other factors, such as socioeconomic and psychosocial factors, risk genes, and comorbidities, also likely have substantial contributions to higher incidence of AD in African American/Black adults and will be briefly discussed in the following sections, highlighting molecular pathways related to each class of factors.

1.1.1 Socioeconomic & psychosocial factors

Socioeconomic factors include education level, healthcare access, and willingness to seek care and treatment, which are noted as having differences between racial subgroups in AD.[5, 9] African American/Black adults are less likely to seek care for symptoms of mild cognitive impairment (MCI), a preliminary stage of AD, and be prescribed AD pharmacotherapy treatment (e.g., cholinesterase inhibitors or memantine) upon disease diagnosis than non-Hispanic White adults.[6, 27] Psychosocial factors include stresses related to life events, work, family/relationships, finances, living situation, and discrimination. These types of stresses are more prevalent in minority populations,[28] and have been associated with lower executive function and episodic memory in African American/Black adults.[29] Increased perceived stress level was also associated with increased AD biomarker levels in CSF of African American/Black adults with MCI.[30]

Consequently, allostatic load, which is "…a measure of the cumulative physiological burden exacted on the body through attempts to adapt to life's demands,"[31] is also higher in African American/Black adults than non-Hispanic White adults.[32-37] Low socioeconomic status, income level, neighborhood quality, and parental socioeconomic status, high discrimination and adversity, and fewer years of education have all been associated with increased allostatic load.[32] High allostatic load or allostatic overload results in extensive biological disturbances such as suppression of the immune system[32, 38] and disruption of brain architecture and function,[32, 39-42]

which lead to negative health consequences such as physical and cognitive decline and increased incidence of comorbidities such as cardiovascular disease and metabolic syndrome.[31] Systemic racism in the United States is one of the major causes of high allostatic load experienced by African American/Black adults.[28] Increased circulating levels of immune and inflammatory markers such as C-reactive protein (CRP), fibrinogen, interleukin-6 (IL-6), E-selectin, and intracellular adhesion molecule-1 (ICAM-1) are among the biomarkers of allostatic load.[43] Changes in these markers in African American/Black adults are inconsistent, as increased levels of CRP and IL-6 but decreased levels of ICAM-1 have been reported in African American/Black adults compared to non-Hispanic White adults.[44-46]

Inflammatory differences between African American/Black and non-Hispanic White adults have been previously observed in AD. In a cohort of older African American/Black and non-Hispanic White adults, increased IL-9 levels in CSF were associated with AD only in African American/Black adults.[25] Other molecular changes in the brain up- and downstream of IL-9 upregulation also only correlated with AD in African American/Black adults. Another study also observed increased levels of pro-inflammatory cytokines and decreased levels of anti-inflammatory cytokines in postmortem brain tissue from the middle temporal gyrus of African American/Black adults with AD.[47] These findings suggest increased neuroinflammation and apoptosis and decreased protection against Aβ neurotoxicity in brains of African American/Black adults with AD. Therefore, changes in immune and inflammatory pathways in African American/Black adults could potentially contribute to racial disparities in AD, which may be due in part to socioeconomic and psychosocial factors.

1.1.2 Genetic factors

Genetic factors are well-known to play a role in AD risk (**Table 1.1**) and most likely also contribute to racial disparities in AD. Although there is no evidence for a separate genomic region contributing to age-related cognitive decline between non-Hispanic White and African American/Black adults,[48] risk genes such as *APOE*, phospholipid-transporting ATPase ABCA7 (*ABCA7*), and others have been discovered with differing impacts on AD risk across racial groups. Furthermore, in some cases, there are single nucleotide polymorphisms (SNPs) and genes that are only associated with AD for a given racial group. These genes implicate lipid metabolism (**Figures 1.1-1.2**) and immune/inflammatory pathways as potential contributors to racial disparities, which will be highlighted in the discussion of two major risk genes, *APOE* and *ABCA7*, in the remainder of this section. For a full review of genetic contributors to racial disparities in AD related to lipid metabolism, please refer to our published book chapter.[49]

1.1.2.1 APOE ε4

The *APOE* gene codes for apolipoprotein E, a lipoprotein responsible for maintaining lipid and cholesterol homeostasis in the brain, which is important for synapse formation and neuronal functioning.[50] The *APOE* ε4 allele is one of the strongest genetic risk factors for AD,[6, 50-54] conferring two to three times greater risk with one ε4 allele and 12 times greater risk with two ε4 alleles.[55] The ε4 allele has been associated with increased Aβ accumulation and deposition in the brain and cerebral vessels,[53-54, 56] as well as increased tau tangles.[6, 57] The apoE4 protein isoform is less effective at binding and clearing Aβ from the brain[51-52, 58-59] and increases both Aβ production and fibril formation compared to the other two isoforms.[53, 56] The apoE4 isoform also suppresses synaptic protein expression, which impairs synapse transmission and

Table 1.1. Genes known to increase risk of AD.

Gene [a]	Disease-Associated SNP/Allele	References
ABCA1[b]	SNPs rs2230806, rs4149313, rs2230805, rs2230808	Wavrant-De Vrièze et al 2007[60]; Koldamova et al 2010[61]; Fehér et al 2018[62]
ABCA7[b]	SNPs rs11550680, rs142076058, rs3764647, rs3752239, rs3764650, rs3752246, rs78117248, rs4147929, rs3752232	Aikawa et al 2018[63]; Almeida et al 2018[64]; Hollingworth et al 2011[65]; Naj et al 2011[66]; Cuyvers et al 2015[67]; Lambert et al 2013[68]; N'Songo et al 2017[69]
APOC1[b]	Insertion/deletion polymorphism rs11568822, H2 allele	Zhou et al 2014[70]; Petit-Turcotte et al 2001[71]; Ki et al 2002[72]
APOD[b]	Intron 1 polymorphism	Desai et al 2003[73]
APOE[b]	ε4 allele	Barnes & Bennett 2014[6]; El Gaamouch et al 2016[52]; Martins et al 2009[51]; Zhao et al 2017[53]
BIN1[b]	SNPs rs55636820, rs7561528, rs744373	Reitz et al 2013[74]; Reitz & Mayeux 2014[75]; Hollingworth et al 2011[65]; Naj et al 2011[66]; Seshadri et al 2010[76]
CD2AP	SNP rs9349407	Naj et al 2011[66]
CD33	SNPs rs3826656, rs3865444	Bertram et al 2008[77]; Hollingworth et al 2011[65]; Naj et al 2011[66]
CLU[b]	SNPs rs11136000, rs1532278	Lambert et al 2009[78]; Naj et al 2011[66]; Harold et al 2009[79]; Seshadri et al 2010[76]
CR1	SNPs rs3818361, rs6656401, rs6701713	Hollingworth et al 2011[65]; Lambert et al 2009[78]; Naj et al 2011[66]
EPHA1	SNPs rs11771145, rs11767557	Hollingworth et al 2011[65]; Naj et al 2011[66]; Seshadri et al., 2010[76]
MS4A gene cluster	SNP rs610932 in MS4A6A SNP rs670139 in MS4A4E SNP rs4938933 in MS4A4A	Hollingworth et al 2011[65]; Naj et al 2011[66]
PICALM[b]	SNPs rs561655, rs3851179	Reitz & Mayeux 2014[75]; Harold et al 2009[79]; Seshadri et al 2010[76]
SORL1[b]	SNPs rs2298813, rs2070045, rs668387, rs689021, rs641120, rs1784933, rs3824966, rs12285364	Rogaeva et al 2007[80]; Lee et al 2007[81]; Chou et al 2016[82]
SIGMAR1[b]	Long runs of homozygosity in Chr4q313, 15q24.1, 3p21.31 regions	Ghani et al 2015[83]
SREBF2[b]	SNP rs2269657	Picard et al 2018[84]

[a]Abbreviations: ABCA1, phospholipid-transporting ATPase ABCA1; ABCA7, phospholipid-transporting ATPase ABCA7; APOC1, apolipoprotein C-I; APOD, apolipoprotein D; APOE, apolipoprotein E; BIN1, myc box-dependent-interacting protein 1; CD2AP, CD2-associated protein; CD33, myeloid cell surface antigen CD33; CLU, clusterin; CR1, complement receptor type 1; EPHA1, ephrin type-A receptor 1; MS4A, membrane-spanning 4-domains subfamily A; PICALM, phosphatidylinositol-binding clathrin assembly protein; SORL1, sortilin-related receptor; SIGMAR1, sigma non-opioid intracellular receptor 1; SREBF2, sterol regulatory element-binding protein 2. [b]Related to lipid metabolism.

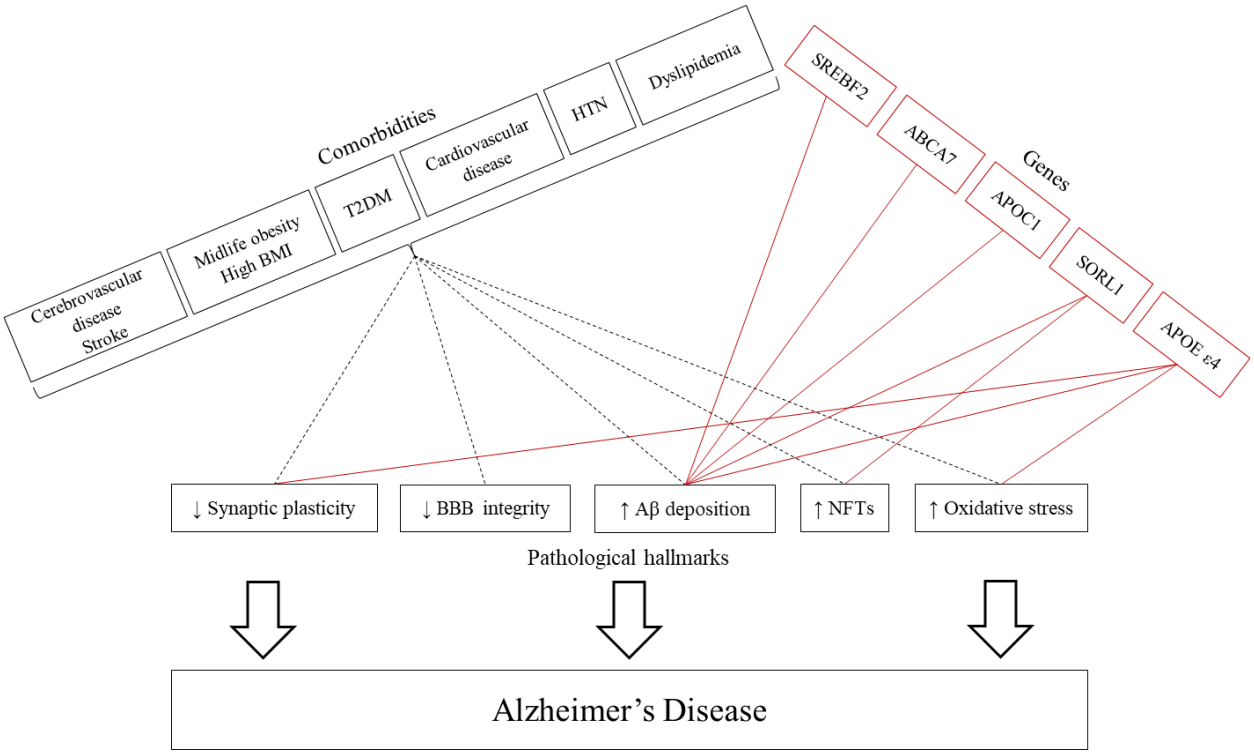

Figure 1.1. The connections amongst AD risk factors with altered lipid metabolism and AD pathological hallmarks. Genes are in red and comorbidities are in black. Abbreviations: BMI, body mass index; T2DM, type 2 diabetes mellitus; HTN, hypertension; SREBF2, sterol regulatory element binding transcription factor 2; ABCA7, phospholipid-transporting ATPase ABCA7; APOC1, apolipoprotein C1; SORL1, sortilin related receptor 1; APOE, apolipoprotein E; BBB, blood-brain barrier; Aβ, amyloid-beta; NFTs, neurofibrillary tangles. Figure reprinted by permission from Springer Nature: The potential of 'omics to link lipid metabolism and genetic and comorbidity risk factors of Alzheimer's disease in African Americans, Stepler, K. E. & Robinson, R. A. S, in Reviews on Biomarker Studies in Psychiatric and Neurodegenerative Disorders, Guest, P. C., ed., Copyright 2019.[49]

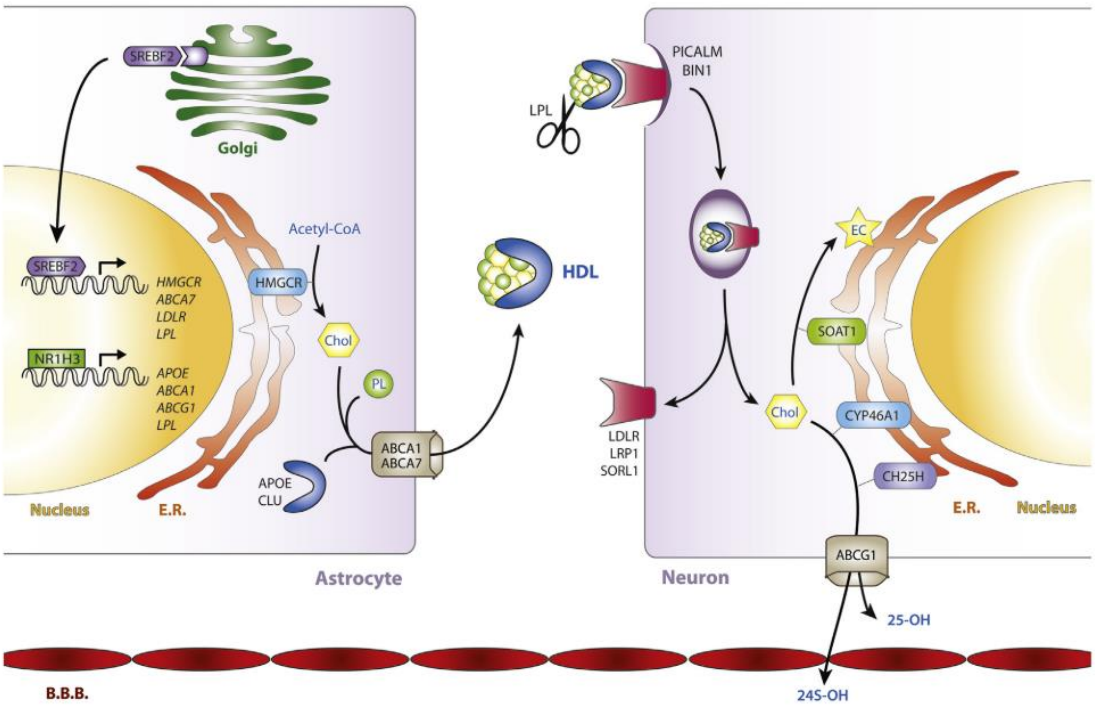

Figure 1.2. Representation of cholesterol metabolism in the brain, including several AD risk genes and their gene products. Abbreviations: SREBF2, sterol regulatory element binding transcription factor 2; NR1H3, oxysterols receptor LXR-alpha; HMGCR, 3-hydroxy-3-methylglutaryl-CoA (HMG-CoA) reductase; ABCA7, phospholipid-transporting ATPase ABCA7; LDLR, LDL receptor; LPL, lipoprotein lipase; APOE, apolipoprotein E; ABCA1, phospholipid-transporting ATPase ABCA1; ABCG1, ATP-binding cassette sub-family G member 1; ER, endoplasmic reticulum; Chol, cholesterol; PL, phospholipid; CLU, clusterin; HDL, high-density lipoprotein; PICALM, phosphatidylinositol-binding clathrin assembly protein; BIN1, Myc box-dependent-interacting protein 1; LRP, LDL receptor-related protein; SORL1, sortilin related receptor 1; EC, esterified cholesterol; SOAT1, sterol O-acyltransferase 1; CYP46A1, cholesterol 24-hydroxylase; CH25H, cholesterol 25-hydroxylase; BBB, blood-brain barrier; 25-OH, 25-hydroxycholesterol; 24S-OH, 24S-hydroxycholesterol. Figure reprinted from Neurobiol. Aging, Vol 66, Picard, C., et al., Alterations in cholesterol metabolism-related genes in sporadic Alzheimer's disease, Pages 180.e1-180.e9, Copyright (2018), with permission from Elsevier.[84]

plasticity and could contribute to synapse dysfunction and loss that occurs early in AD pathology.[53-54]

Disparities in *APOE* allele frequency and association with AD have been noted among racial groups. Multiple studies have determined that there is an increased frequency of the ε4 allele and the ε4/ε4 genotype in African American/Black populations compared to non-Hispanic White adults.[6, 15] *APOE* ε4 has been associated with increased risk of AD in African American/Black adults, although some studies have concluded that it is inconsistently related to AD and cognition in this population.[2, 6] Furthermore, the strength of the association between the *APOE* ε4 allele and AD is weaker in African American/Black adults than non-Hispanic White adults.[2, 4] Overall, the *APOE* ε4 allele represents a major protein in lipid-related pathways critical for AD pathogenesis, and likely has a significant contribution to AD risk in African American/Black adults despite contradictory findings.

1.1.2.2 ABCA7

ABCA7 is a transmembrane protein responsible for moving lipids across the cell membrane using energy from adenosine triphosphate (ATP) and it is involved in three major cellular processes: cholesterol metabolism, phospholipid regulation, and phagocytosis.[85-88] ABCA7 primarily transports phospholipids such as phosphatidylcholines and phosphatidylserines across the cell membranes to apolipoprotein A-I and apoE, though it has a lesser ability to transport cholesterol.[88-89] The endogenous expression of ABCA7 stimulates cholesterol efflux to apoE, in turn suppressing Aβ production.[90] When ABCA7 function is lost (i.e. *ABCA7* knockout), disruption in the microglial Aβ clearance pathway leads to a cholesterol deficiency, triggering accelerated Aβ production[63, 91] and Aβ plaque formation.[92] Altered lipid

homeostasis, caused by decreased levels of ABCA7, can also lead to endoplasmic reticulum (ER) stress and subsequent declines in cognition and synaptic integrity.[93]

ABCA7 is also involved in the phagocytosis of apoptotic cells through the C1q complement pathway in macrophages. Increased ABCA7 expression increases microglial phagocytosis as well as Aβ uptake.[94] On the other hand, *ABCA7* knockout mice showed reduced oligomeric uptake of Aβ proteins in macrophages and microglia.[91, 95] *ABCA7* knockdown in macrophages also results in incomplete phagocytosis of apoptotic debris,[96] which could potentially cause neuroinflammation and thus contribute to AD pathogenesis.[88] When *ABCA7* haplodeficient mice were crossed with amyloid precursor protein ($APP)^{NL\text{-}G\text{-}F}$ mice, these mice had increased Aβ accumulation in the brain and enlarged endosomes in microglia.[97] The observed disruption of cell membrane organization likely alters microglial responses to acute and chronic brain inflammation.

Mutations in *ABCA7* have been associated with increased AD risk in various racial/ethnic groups, including European,[67, 98-99] Latin American,[100] non-Hispanic White,[64, 74] and African American/Black groups[63, 69, 74-75, 101] (**Table 1.2**). Some of these mutations increase AD risk in multiple racial/ethnic groups, such as rs3764650, while others are specific to a given group, such as rs3764647 and rs115550680. Additionally, several of the risk mutations identified across groups have different effect sizes and/or prevalence in different racial/ethnic groups. As a whole, *ABCA7* risk variants have a greater impact on odds of AD diagnosis in African American/Black adults compared to other racial/ethnic groups[102]; *ABCA7* variants have been found to increase AD risk 1.8 times in individuals with African ancestry compared to 1.1-1.2 times in individuals with European ancestry.[74]

Dysregulation of ABCA7's functions in lipid metabolism and phagocytosis has been

Table 1.2. ABCA7 SNPs associated with AD in various racial/ethnic groups.[a]

SNP	Mutation	Populations Associated with AD	Frequency[b]	Effect Size	Sources
rs3752232	Thr319Ala	African American/Black	27.2% AD 23.2% CN	1.24	N'Songo et al 2017[69]; Logue et al 2018[103]
rs3752239	Asn718Thr	African American/Black	1.8% AD 0.4% CN	4.06	N'Songo et al 2017[69]
rs3752246	Gly1527Ala	Multiple racial groups	ND	1.35 1.15	Fehér et al 2019[62]; Hollingworth et al 2011[65]; Naj et al 2011[66]
rs3764647	His395Arg	African American/Black	26.2-29.8% AD 21.6-23.1% CN	1.32 1.29 1.47	Logue et al 2011[101]; Logue et al 2018[103]; N'Songo et al 2017[69]
rs3764650	Intron variant	African American/Black	ND	1.27	Hohman et al 2016[104]; Logue et al 2011[101]
		Asian		8.32 1.09	Li et al 2017[105]; Zhou et al 2017[106]
		Colombian		1.7	Moreno et al 2017[100]
		Non-Hispanic White		1.25 1.25	Almeida et al 2018[64]; Zhou et al 2017[106]
		Multiple racial groups		1.23	Hollingworth et al 2011[65]
rs4147929		Danish	ND	1.07	Kjeldsen et al 2017[99]
		Non-Hispanic White		1.66	Monsell et al 2017[107]
		Multiple racial groups		1.15	Lambert et al 2013[68]
rs59851484		African American/Black	14.8% AD 10.5% CN	1.49	Logue et al 2018[103]
rs78117248	Intron variant	Belgian	3.8% AD 1.8% CN	2.07	Cuyvers et al 2015[67]
		Non-Hispanic White	ND	1.56	Kunkle et al 2017[108]
rs115550680		African American/Black	ND	1.79	Reitz et al 2013[74]
rs142076058	Arg578Alafs	African American/Black	9.2-15.2% AD 7.4-9.7% CN	2.13 1.27	Cukier et al 2016[109] Logue et al 2018[103]

Table 1.2 (continued)

rs200538373	Splice donor variant	Icelandic	ND	1.91	Steinberg et al 2015[98]
		Non-Hispanic White		2.12	Kunkle et al 2017[108]
rs567222111	Leu396fs	African American/Black	1.1% AD 0.3% CN	2.42	Logue et al 2018[103]

[a]Updated from ref **49**. [b]ND indicates that this information was not available for the denoted SNP. Abbreviations: SNP, single nucleotide polymorphism; AD, Alzheimer's disease; CN, cognitively normal.

clearly linked to AD phenotypes and thus implicated in AD racial disparities. However, most studies have probed the impact of ABCA7 deficiency on its protein functions, such that the functional impacts of specific *ABCA7* risk mutations remain unknown. Further mechanistic studies of *ABCA7* mutations prevalent in African American/Black adults are necessary to elucidate their downstream consequences and contributions to AD pathogenesis. One such study of rs3752232 in human embryonic kidney (HEK) 293 cells is described in **Chapter 2** of this dissertation.

1.1.3 Comorbidities

Comorbidities describe health conditions that can increase an individual's risk for diseases, such as AD. Traumatic brain injury, stroke, dyslipidemia/hypercholesterolemia, cardiovascular disease, type 2 diabetes mellitus (T2DM), obesity, and hypertension (HTN) all increase risk of AD (**Figure 1.1**)[4, 6, 58, 110-113] and also disproportionately affect African American/Black adults. Notably, alterations in lipid metabolism are common in AD and these comorbidities, suggesting that lipid metabolism may be an important underlying cause of racial disparities of AD. In the remainder of this section, we will briefly discuss racial disparities in several comorbidities tied to lipid metabolism. For a comprehensive review of comorbidities, lipid metabolism, and AD risk in African American/Black adults, please refer to our published book chapter.[49]

1.1.3.1 Dyslipidemia

Dyslipidemia is a group of lipid disorders that result in abnormal levels of high-density lipoprotein (HDL), low-density lipoprotein (LDL), very-low-density lipoprotein (VLDL), and triglycerides,[58] including high cholesterol levels (hereafter referred to as hypercholesterolemia).

Findings regarding differences in cholesterol levels by racial background have been contradictory. In the Atherosclerosis Risk in Communities study, cholesterol levels in midlife (50-60 years old) were not different between African American/Black and non-Hispanic White adults.[114] However, over the age of 45, there is higher incidence of dyslipidemia in African American/Black adults compared to non-Hispanic White adults,[115-116] which is more noticeable in older age groups (i.e., 65-74 years old).

The connection between AD and cholesterol has been firmly established (**Figure 1.3**),[51, 117-119] and abnormalities in both brain[52] and peripheral[58, 120] cholesterol levels are implicated in AD. Hypercholesterolemia has been associated with AD[50, 112] and in midlife is associated with increased risk of MCI later in life.[116] In a cohort of African American/Black adults without *APOE* ε4 alleles, higher mean serum total cholesterol levels were observed in individuals with AD compared to those that were cognitively normal (CN).[121]

1.1.3.2 Hypertension

Dyslipidemia is also a risk factor for HTN. It is well-known that HTN is more prevalent in African American/Black adults than in non-Hispanic White adults,[3-4, 9, 116, 122-123] affecting 42% and 45% of African American/Black men and women, respectively, including diagnosed and undiagnosed cases.[124] African American/Black adults are less likely to have their blood pressure under control when compared to non-Hispanic White and Hispanic adults, despite the fact that African American/Black adults are more aware of a HTN diagnosis and take medications.[122, 124-125]

HTN is independently associated with increased cognitive decline, MCI and AD,[3, 50, 116] and in midlife is associated with increased AD and dementia risk later in life.[126] High systolic blood pressure is also associated with an increased risk of AD,[127] an increased number of NFTs

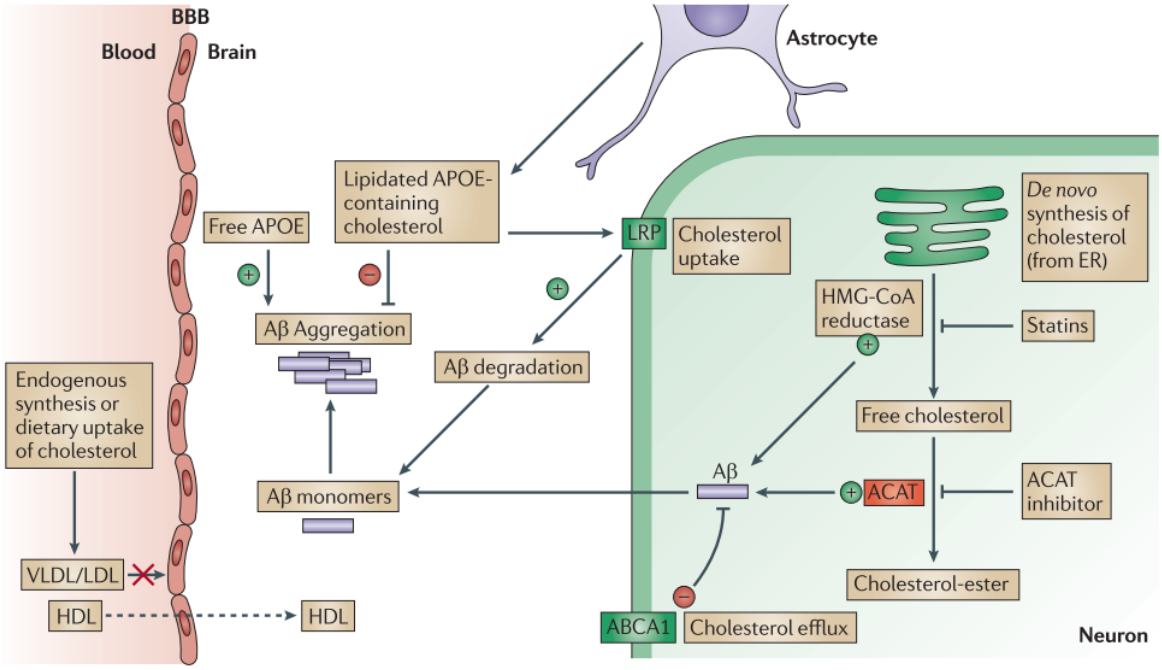

Figure 1.3. Role of cholesterol in Aβ pathology in AD. ApoE is also included in this figure as it is a cholesterol transporter. Proteins highlighted in green reduce decrease Aβ pathology; proteins highlighted in red increase Aβ pathology. Abbreviations: ACAT, acyl-CoA:cholesterol acyltransferase 1 (also known as sterol O-acyltransferase); LRP, LDL receptor-related protein; HMG-CoA, 3-hydroxy-3-methylglutaryl-CoA. Figure reprinted by permission from Springer Nature: Nat. Rev. Neurosci., Linking lipids to Alzheimer's disease: cholesterol and beyond, Di Paolo, G., et al., Copyright 2011.[119]

in postmortem brain tissue, and increased odds of brain infarcts.[128] In individuals with AD, there is a higher prevalence of HTN in African American/Black adults compared to non-Hispanic White adults.[4, 11, 15] HTN among African American/Black adults is also likely to increase risk for certain neurovascular pathologies, such as cerebral amyloid angiopathy, white-matter lesions and vascular endothelial damage.[4]

1.1.3.3 Obesity

A high body mass index (BMI) and obesity are more prevalent in African American/Black adults than non-Hispanic White adults at various ages.[6, 114, 124] BMI has strong effects on risk for other conditions in African American/Black adults, especially diabetes, metabolic syndrome, and HTN.[6] Obesity can lead to neuroinflammation, compromised blood-brain barrier (BBB) integrity, and changes in neuronal structure, synaptic plasticity and memory.[58] Both low and high body mass indices have been associated with cognitive impairment and dementia.[6] A higher BMI ($\geq$30 kg/m^2) in midlife is associated with increased dementia and AD risk, presumably due to increased amyloid deposition.[13] On the other hand, a higher BMI in late life reduces risk of cognitive decline and dementia.[126]

1.1.3.4 Type 2 diabetes mellitus

T2DM is more prevalent in African American/Black[3, 6, 124, 129-130] and Hispanic adults[4, 9] than non-Hispanic White adults. Prevalence estimates are 1.4 to 2.3 times higher in African American/Black adults than in non-Hispanic White adults.[116, 130] Comprehensive discussions of the connections between T2DM, lipid metabolism, and AD can be found in several reviews.[131-134] T2DM has been associated with AD[58, 112, 134] and significantly increases risk for AD.[58, 126] Prediabetes and T2DM are also associated with increased cognitive decline,[135] increased risk of progression from MCI to dementia,[57-58] vascular dementia, and compromised BBB integrity.[131]

T2DM was associated with greater cognitive decline in African American/Black adults,[136] while the Minority Aging Research Study and Memory and Aging Project cohorts found similar effects of diabetes on cognition in African American/Black and non-Hispanic White adults.[137] Glucose levels in African American/Black adults with T2DM were also significantly higher in those who developed dementia than in those who did not develop dementia.[138-139] Although most evidence supports the existence of racial disparities in T2DM, one study did not find an association between T2DM and race.[140]

Overall, this section demonstrates that comorbidities greatly influence risk and incidence of AD among African American/Black adults. Significant evidence has linked dysregulation of lipid metabolism to AD and to these comorbidities.[49, 51, 117-118] Furthermore, the comorbidities discussed here, along with the genetic risk factors discussed in **Section 1.1.2**, clearly highlight the relevance of lipid metabolism pathways in AD and in racial disparities.

1.2 Proteomics Approaches to Study Racial Disparities in AD

The previous section highlights that several molecular pathways, including lipid metabolism, immune system/inflammation, and tau-related pathways, are hypothesized to contribute to racial disparities in AD, and are particularly increased risk in African American/Black adults. However, the mechanisms and roles of these pathways in racial disparities of AD have yet to be fully understood. Fortunately, proteomics is a powerful approach with which to study proteins and pathways in this context and can give systematic insight to changes in these pathways in biological samples. Such insight is important to help with tailored AD prevention, early diagnosis and personalized treatment strategies for racial groups with high

incidences of AD. In this section, we will provide a brief overview of proteomics methods and their value to study racial disparities in AD.

1.2.1 Discovery-based proteomics

Discovery-based proteomics is the global study of all of the proteins (the proteome) of a tissue, cell, or biofluid. Liquid chromatography (LC) coupled with mass spectrometry (MS) is the analytical technique of choice for discovery-based proteomics studies because it allows simultaneous measurement of thousands of proteins with high resolution, mass accuracy, and sensitivity.[141-143] Many applications of discovery-based proteomics rely on shotgun proteomics, analyzing peptides from complex biological samples to provide information about their corresponding proteins.[144-145]

A typical discovery-based proteomics workflow is shown in **Figure 1.4**. Proteins are extracted from biological samples such as cells (via lysis, described in **Chapter 2**) or postmortem tissue (via homogenization, described in **Chapters 3-4**), which are then enzymatically digested into peptides using trypsin or a trypsin/Lys-C mixture. Many workflows include a quantitative labeling strategy that provides relative quantification of peptides and allows multiplexing, or simultaneous analysis of multiple samples in the mass spectrometer. Benefits of label-based quantification include increased throughput as a result of multiplexing and improved quantification accuracy and precision compared to label-free quantification (LFQ), which bases relative quantification on spectral counts or peptide peak area.[146-147] The workflow in **Figure 1.4** shows Tandem Mass Tags (TMT)^{11}-plex as the quantification strategy,[148-149] which was utilized in **Chapters 2-4** of this dissertation. TMT^{11}-plex is a tag that distributes ^{13}C and ^{15}N heavy isotopes in different regions of the tag's chemical structure to create 11 unique tags of the

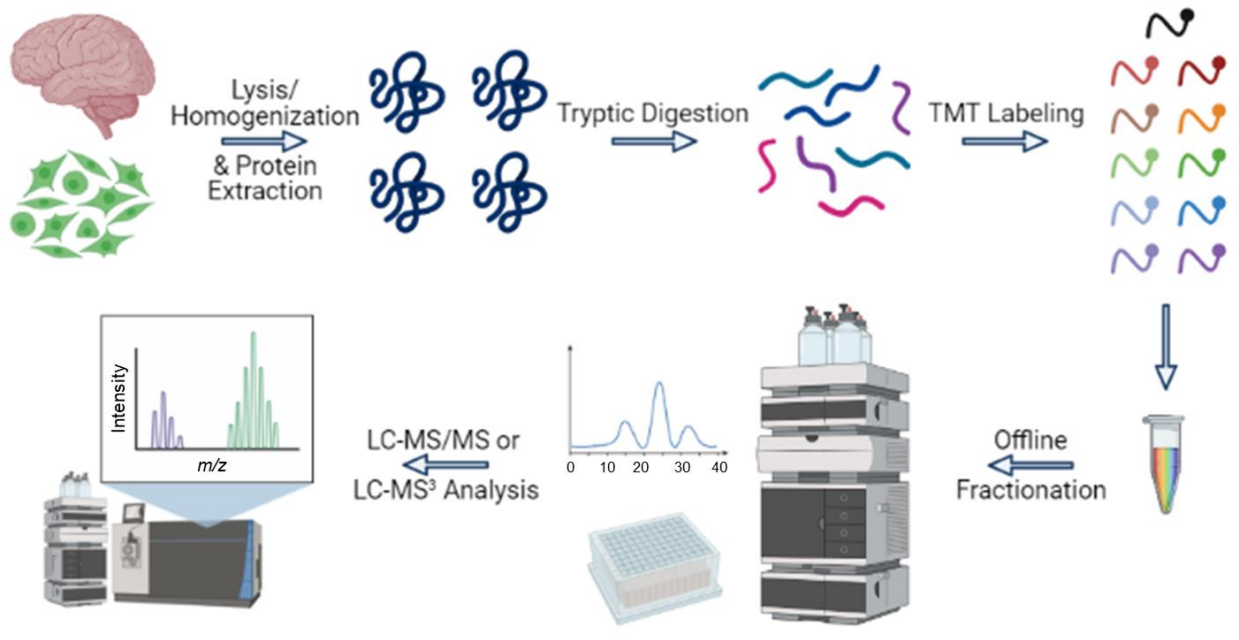

Figure 1.4. TMT-based bottom-up proteomics workflow. Figure created with BioRender.com.

same mass (isobaric), which can be used to label 11 different samples. Labeled samples are then combined for simultaneous LC-tandem mass spectrometry (MS/MS) or LC-MS^3 analysis, where the tags are cleaved into unique reporter ions whose intensities correspond to the intensities of that peptide across the 11 samples (**Figure 1.5**; MS/MS shown). Reporter ion intensities can then be summed across all peptides for a given protein to determine changes in protein intensity across different biological samples or conditions.

Combined labeled peptides may undergo a pre-fractionation step to reduce the complexity of the sample mixture prior to LC-MS/MS or LC-MS^3 analysis. Within the last few years, pre-fractionation has become increasingly common and conducted extensively to improve proteome depth by > 2-3x compared to unfractionated samples (*unpublished data*). High pH reversed-phase fractionation has shown superior performance compared to other separations such as strong cation exchange due to its easier sample processing, better peptide resolution, and improved proteome coverage.[150-153] High pH reversed-phase fractionation has been previously performed by eluting peptides from C_{18} cartridges with discrete organic buffer concentrations[154]; however, an alternative is high-performance liquid chromatography (HPLC)-based fractionation using a buffer gradient, which improves peptide separation and MS identifications from each fraction. Fractions are then analyzed individually using LC-MS/MS or LC-MS^3 for protein identification and quantification.

Detection and quantification of TMT reporter ions can be performed using higher-energy C-trap dissociation (HCD) fragmentation in MS/MS or MS^3 scans, as mentioned above. MS^3-based quantification had previously been considered superior to MS/MS for its improved accuracy and reduced ratio compression, a phenomenon resulting from isolation interferences.[147, 155-156] However, from 2016-2021, there has been a shift in the field back towards MS/MS-based

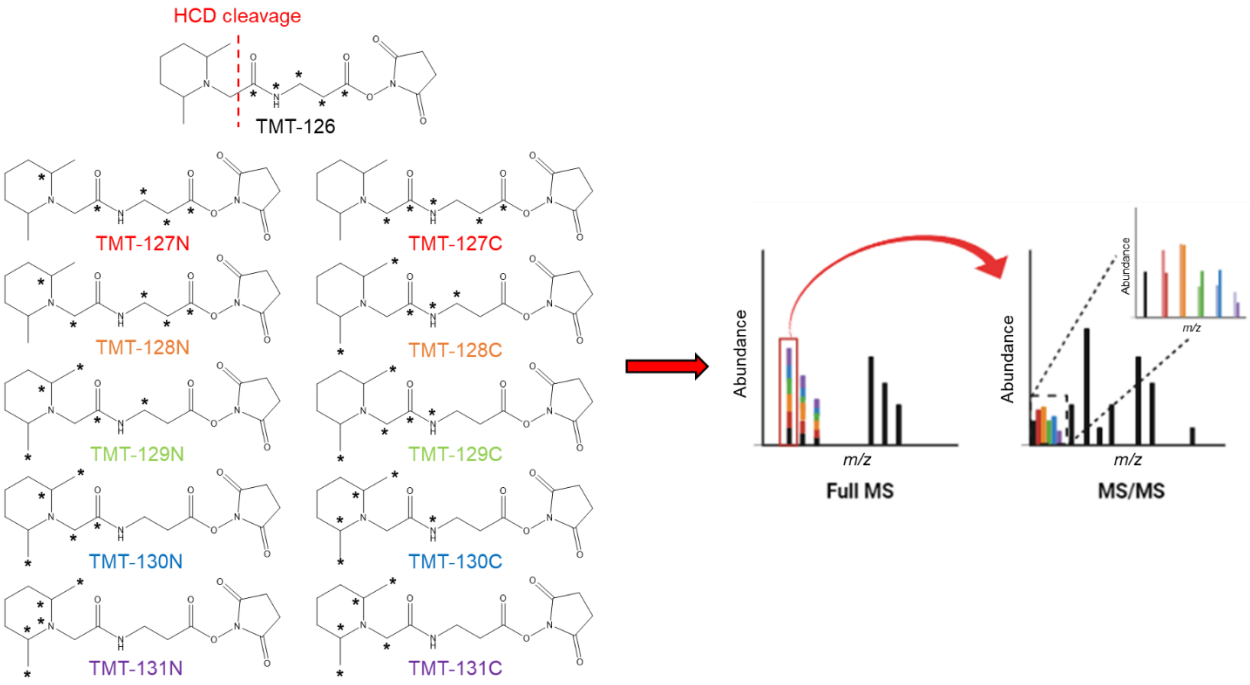

Figure 1.5. TMT^{11}-plex labeling and MS detection. On the left, the chemical structures of the 11 unique TMT^{11}-plex tags are shown.[149] * indicates a heavy isotope at that position. After mixing the 11 TMT-labeled samples together, they will be detected in a single peak in the full MS spectrum and then higher-energy C-trap dissociation (HCD) fragmentation cleaves the tag at the position indicated by the dashed line in the TMT-126 structure. This results in the detection of the 11 unique reporter ions (the part of the structure on the left of the dashed line) corresponding to the 11 different samples, as shown on the right of the figure. Figure partially created using BioRender.com.

TMT quantification. This shift is enabled by measures proven to reduce ratio compression such as pre-fractionation and small isolation windows during LC-MS/MS data acquisition.[157-159] Additionally, these measures also increase proteome coverage compared to MS^3.

LC-MS/MS or LC-MS^3 data are finally searched against a database of known proteins (e.g., UniProt, https://www.uniprot.org/, accessed 6/30/2021) using software such as Thermo Fisher Scientific's Proteome Discoverer to determine which proteins are present in the samples and at what levels, based on the TMT reporter ion abundances. Identified proteins may then undergo further data analysis steps necessary to evaluate data quality and answer the study question, such as normalization[160] and statistical comparisons across groups (i.e., AD compared to CN groups).

1.2.1.1 Machine learning to analyze proteomics data

Another tool that can be applied for proteomics data analysis is machine learning, which is a form of artificial intelligence.[161-162] In machine learning, a system is trained to make the "best" decisions without human subjectiveness. Machine learning applied to quantitative proteomics data can be used to classify, diagnose, or predict disease status or treatment type with clear performance outcomes (e.g., accuracy, sensitivity, specificity).[162] Machine learning can also test the accuracy of various panels of proteins for distinguishing groups to identify biomarker candidates for further investigation. Several applications of machine learning for these purposes have been described previously in different diseases such as cancer[163] and neurodegenerative diseases including amyotrophic lateral sclerosis (ALS)[164] and AD,[165-166] as shown in **Chapter 5**.

1.2.2 Proteomics of postmortem brain tissue in AD

Discovery-based proteomics has been used to examine changes in the overall proteome in aging and MCI or AD[167-176] and to study proteins associated with oxidative stress.[177-181] At the start of this dissertation work, discovery-based proteomics workflows resulted in ~800-3000 proteins from AD postmortem brain tissue,[167-170, 172] or ~5-18% of the human brain proteome reported by the Human Protein Atlas, which is based on transcriptomics expression data and excludes proteoforms[182-185] (see **Chapter 3**). Throughout this dissertation, the advancements in discovery-based proteomics workflows outlined in **Section 1.2.1** have resulted in more extensive proteome coverage in AD postmortem brain tissue, and routinely result in ~6000 to ~14,000 proteins[158, 186-195] or up to ~89% of the human brain proteome[182-185] (see **Chapter 4**). The deep proteome coverage achieved in these studies leads to more comprehensive insights on many biological pathways in AD.

1.3 Overview of Dissertation

Discovery-based proteomics approaches enable comprehensive protein analyses as described in **Sections 1.2.1-1.2.2** and can be broadly used to advance disease understanding and biomarker discovery,[196-197] which are necessary in the study of AD racial disparities. For example, as we have described in **Section 1.1.2**, mutations and alleles in various genes may contribute to racial disparities in AD and increased AD prevalence in African American/Black adults. Though significant research has been performed to identify and study these variants associated with AD at the genetic level, it is necessary to study the functional impacts of these genetic variants, i.e. at the protein level, to elucidate their specific roles in AD. Proteomics can be useful to interrogate the downstream effects of genetic variants in both model systems and

human biospecimens, and provides valuable insight on its own and in combination with other methods. In **Chapter 2** of this dissertation, we applied proteomics along with structural methods to study an *ABCA7* SNP associated with AD in African American/Black adults in HEK 293 cells, allowing us to investigate both structural and functional impacts of this mutation.

There is also a need for discovery-based proteomics in human studies of racial disparities in AD. A majority of discovery-based proteomics studies in AD have been focused on non-Hispanic White adults or other majority populations and grossly exclude African American/Black adults. Specifically within proteomics studies of postmortem brain tissue in AD, few have included individuals from racial backgrounds other than non-Hispanic White, such as African American/Black, Hispanic/Latino, or Asian/Pacific Islander,[170-171, 186-189, 195, 198-199] and, moreover, they only comprise ~2-21% of the total samples included in these studies, besides the rare examples that have solely included Japanese[170] or Mexican individuals.[171] It is important to note that there are also many studies that do not provide information on the race or ethnicity of their participants.[158, 192-194] Studies of postmortem brain tissue from individuals of diverse racial backgrounds are necessary to characterize the proteomic changes induced by AD in these groups, as most of our current knowledge is derived from non-Hispanic White adults. In **Chapters 3 and 4** of this dissertation, we analyzed proteomic differences in postmortem brain tissue in AD in two independent cohorts consisting of African American/Black and non-Hispanic White individuals who were CN or diagnosed with AD.

Combining machine learning with proteomics data is another valuable approach to study racial disparities in AD. Combined proteomics and machine learning approaches demonstrated that a model trained with proteins that were differentially expressed between non-Hispanic White AD and CN groups better differentiated AD and CN individuals within the same racial group.[166]

However, whether that finding is generalizable and relevant in other tissues, such as postmortem brain tissue, has yet to be studied. In **Chapter 5** of this dissertation, we used machine learning to analyze several available AD brain proteomics datasets that include individuals from different racial backgrounds, including the multi-regional set from **Chapter 3**. It is evident that proteomics is valuable to advance understanding of racial disparities in AD, which is necessary to potentially improve AD prevention, diagnosis, and treatment strategies for high-risk populations. Finally, we discuss future directions for this work in **Chapter 6**, including studies designed to link molecular contributors to racial disparities with socioeconomic and comorbidity contributors.

1.4 Acknowledgements

This dissertation chapter was adapted by permission from Springer Nature from a published review titled "The Potential of 'Omics to Link Lipid Metabolism and Genetic and Comorbidity Risk Factors of Alzheimer's Disease in African Americans" by Kaitlyn E. Stepler and Renã A. S. Robinson published in *Reviews on Biomarker Studies in Psychiatric and Neurodegenerative Disorders*, Guest, P. C., Ed. Springer International Publishing: Cham, 2019; Vol. 1118, pp 1-28. The authors acknowledge funding from the Alzheimer's Association (AARGD-17-533405, RASR), Vanderbilt University Start-Up Funds, the University of Pittsburgh Alzheimer Disease Research Center funded by the National Institutes of Health and National Institute on Aging (P50AG005133, RASR), and the Vanderbilt Institute of Chemical Biology (5T32GM065086, fellowship, KES).

1.5 References

1. Alzheimer's Association, 2021 Alzheimer's disease facts and figures. *Alzheimers Dement* **2021,** *17* (3), 327-406.
2. Lines, L.; A Sherif, N.; Wiener, J., *Racial and Ethnic Disparities Among Individuals with Alzheimer's Disease in the United States: A Literature Review*. RTI Press: Research Triangle Park (NC), **2014**; Vol. RR-0024-1412, p 1-30.
3. Gottesman, R. F.; Fornage, M.; Knopman, D. S.; Mosley, T. H., Brain aging in African-Americans: the Atherosclerosis Risk in Communities (ARIC) experience. *Curr Alzheimer Res* **2015,** *12* (7), 607-613.
4. Manly, J. J.; Mayeux, R., Ethnic differences in dementia and Alzheimer's disease. In *Critical Perspectives on Racial and Ethnic Differences in Health in Late Life*, Anderson, N. B.; Bulatao, R. A.; Cohen, B., Eds. National Academies Press: Washington D.C., **2004**.
5. Mehta, K. M.; Yeo, G. W., Systematic review of dementia prevalence and incidence in United States race/ethnic populations. *Alzheimers Dement* **2017,** *13* (1), 72-83.
6. Barnes, L. L.; Bennett, D. A., Alzheimer's disease in African Americans: risk factors and challenges for the future. *Health Aff (Millwood)* **2014,** *33* (4), 580-586.
7. Matthews, K. A.; Xu, W.; Gaglioti, A. H.; Holt, J. B.; Croft, J. B.; Mack, D.; McGuire, L. C., Racial and ethnic estimates of Alzheimer's disease and related dementias in the United States (2015-2060) in adults aged ≥65 years. *Alzheimers Dement* **2018,** *15* (1), 17-24.
8. Alzheimer's Association, Alzheimer's disease facts and figures. *Alzheimers Dement* **2017,** *13*, 325-373.
9. Chin, A. L.; Negash, S.; Hamilton, R., Diversity and disparity in dementia: the impact of ethnoracial differences in Alzheimer disease. *Alzheimer Dis Assoc Disord* **2011,** *25* (3), 187-195.
10. Mayeda, E. R.; Glymour, M. M.; Quesenberry, C. P.; Whitmer, R. A., Inequalities in dementia incidence between six racial and ethnic groups over 14 years. *Alzheimers Dement* **2015,** *12* (3), 216-224.
11. Zamrini, E.; Parrish, J. A.; Parsons, D.; Harrell, L. E., Medical comorbidity in black and white patients with Alzheimer's disease. *South Med J* **2004,** *97* (1), 2-6.
12. Barnes, L. L.; Leurgans, S.; Aggarwal, N. T.; Shah, R. C.; Arvanitakis, Z.; James, B. D.; Buchman, A. S.; Bennett, D. A.; Schneider, J. A., Mixed pathology is more likely in black than white decedents with Alzheimer dementia. *Neurology* **2015,** *85* (6), 528-534.
13. Gottesman, R. F.; Schneider, A. C.; Zhou, Y.; Coresh, J.; Green, E.; Gupta, N.; Knopman, D. S.; Mintz, A.; Rahmim, A.; Sharrett, A. R., et al., Association between midlife vascular risk factors and estimated brain amyloid deposition. *JAMA* **2017,** *317* (14), 1443-1450.
14. Wilkins, C. H.; Grant, E. A.; Schmitt, S. E.; McKeel, D. W.; Morris, J. C., The neuropathology of Alzheimer disease in African American and white individuals. *Arch Neurol* **2006,** *63* (1), 87-90.
15. Graff-Radford, N. R.; Besser, L. M.; Crook, J. E.; Kukull, W. A.; Dickson, D. W., Neuropathological differences by race from the National Alzheimer's Coordinating Center. *Alzheimers Dement* **2016,** *12* (6), 669-677.
16. Brickman, A. M.; Schupf, N.; Manly, J. J.; Luchsinger, J. A.; Andrews, H.; Tang, M. X.; Reitz, C.; Small, S. A.; Mayeux, R.; DeCarli, C., et al., Brain morphology in older African Americans, Caribbean Hispanics, and whites from northern Manhattan. *Arch Neurol* **2008,** *65* (8), 1053-61.

17. Morris, J. C.; Schindler, S. E.; McCue, L. M.; Moulder, K. L.; Benzinger, T. L. S.; Cruchaga, C.; Fagan, A. M.; Grant, E.; Gordon, B. A.; Holtzman, D. M., et al., Assessment of racial disparities in biomarkers for Alzheimer disease. *JAMA Neurol* **2019,** *76* (3), 264-273.
18. Barnes, L. L., Biomarkers for Alzheimer dementia in diverse racial and ethnic minorities—a public health priority. *JAMA Neurol* **2019,** *76* (3), 251-253.
19. Rosenmann, H., CSF biomarkers for amyloid and tau pathology in Alzheimer's disease. *J Mol Neurosci* **2012,** *47* (1), 1-14.
20. Blennow, K.; Vanmechelen, E.; Hampel, H., CSF total tau, Aβ42 and phosphorylated tau protein as biomarkers for Alzheimer's disease. *Mol Neurobiol* **2001,** *24* (1), 87-97.
21. Wallin, Å. K.; Blennow, K.; Andreasen, N.; Minthon, L., CSF biomarkers for Alzheimer's disease: levels of β-amyloid, tau, phosphorylated tau relate to clinical symptoms and survival. *Dement Geriatr Cogn Disord* **2006,** *21* (3), 131-138.
22. Garrett, S. L.; McDaniel, D.; Obideen, M.; Trammell, A. R.; Shaw, L. M.; Goldstein, F. C.; Hajjar, I. Racial disparity in cerebrospinal fluid amyloid and tau biomarkers and associated cutoffs for mild cognitive impairment. *JAMA Netw Open* [Online], **2019**. https://doi.org/10.1001/jamanetworkopen.2019.17363.
23. Howell, J. C.; Watts, K. D.; Parker, M. W.; Wu, J.; Kollhoff, A.; Wingo, T. S.; Dorbin, C. D.; Qiu, D.; Hu, W. T. Race modifies the relationship between cognition and Alzheimer's disease cerebrospinal fluid biomarkers. *Alzheimers Res Ther* [Online], **2017**. https://doi.org/10.1186/s13195-017-0315-1.
24. Chaudhry, A.; Rizig, M. Comparing fluid biomarkers of Alzheimer's disease between African American or Black African and white groups: A systematic review and meta-analysis. *J Neurol Sci* [Online], **2021**. https://www.sciencedirect.com/science/article/pii/S0022510X20306067?via%3Dihub.
25. Wharton, W.; Kollhoff, A. L.; Gangishetti, U.; Verble, D. D.; Upadhya, S.; Zetterberg, H.; Kumar, V.; Watts, K. D.; Kippels, A. J.; Gearing, M., et al., Interleukin 9 alterations linked to Alzheimer disease in African Americans. *Ann Neurol* **2019,** *86*, 407-418.
26. Misiura, M. B.; Howell, J. C.; Wu, J.; Qiu, D.; Parker, M. W.; Turner, J. A.; Hu, W. T. Race modifies default mode connectivity in Alzheimer's disease. *Transl Neurodegen* [Online], **2020**. https://doi.org/10.1186/s40035-020-0186-4.
27. Gilligan, A. M.; Malone, D. C.; Warholak, T. L.; Armstrong, E. P., Racial and ethnic disparities in Alzheimer's disease pharmacotherapy exposure: an analysis across four state Medicaid populations. *Am J Geriatr Pharmacother* **2012,** *10* (5), 303-312.
28. Wilkins, C. H.; Schindler, S. E.; Morris, J. C., Addressing health disparities among minority populations: Why clinical trial recruitment is not enough. *JAMA Neurol* **2020,** *77* (9), 1063-1064.
29. Chen, R.; Weuve, J.; Misra, S.; Cuevas, A.; Kubzansky, L. D.; Williams, D. R., Racial disparities in cognitive function among middle-aged and older adults: the roles of cumulative stress exposures across the life course. *J Gerontol A* **2021**, 10.1093/gerona/glab099.
30. Trammell, A. R.; McDaniel, D. J.; Obideen, M.; Okafor, M.; Thomas, T. L.; Goldstein, F. C.; Shaw, L. M.; Hajjar, I. M., Perceived stress is associated with Alzheimer's disease cerebrospinal fluid biomarkers in African Americans with mild cognitive impairment. *J Alzheimers Dis* **2020,** *77*, 843-853.
31. Seeman, T. E.; McEwen, B. S.; Rowe, J. W.; Singer, B. H., Allostatic load as a marker of cumulative biological risk: MacArthur studies of successful aging. *Proc Natl Acad Sci U S A* **2001,** *98* (8), 4770-4775.

32. Guidi, J.; Lucente, M.; Sonino, N.; Fava, G. A., Allostatic load and its impact on health: A systematic review. *Psychother Psychosom* **2021,** *90* (1), 11-27.
33. Geronimus, A. T.; Hicken, M.; Keene, D.; Bound, J., "Weathering" and age patterns of allostatic load scores among blacks and whites in the United States. *Am J Public Health* **2006,** *96* (5), 826-833.
34. Chyu, L.; Upchurch, D. M., Racial and ethnic patterns of allostatic load among adult women in the United States: findings from the National Health and Nutrition Examination Survey 1999-2004. *J Womens Health (Larchmt)* **2011,** *20* (4), 575-583.
35. Cobb, R. J.; Thomas, C. S.; Laster Pirtle, W. N.; Darity, W. A., Jr., Self-identified race, socially assigned skin tone, and adult physiological dysregulation: Assessing multiple dimensions of "race" in health disparities research. *SSM Popul Health* **2016,** *2*, 595-602.
36. Dormire, S. L., Life stress, race, and abnormal glucose metabolism in postmenopausal women. *J Am Geriatr Soc* **2016,** *64* (9), e46-e48.
37. Thomas Tobin, C. S.; Robinson, M. N.; Stanifer, K., Does marriage matter? Racial differences in allostatic load among women. *Prev Med Rep* **2019,** *15*, 100948.
38. Dhabhar, F. S.; McEwen, B. S., CHAPTER 34 - Bi-directional effects of stress on immune function: Possible explanations for salubrious as well as harmful effects. In *Psychoneuroimmunology (Fourth Edition)*, Ader, R., Ed. Academic Press: Burlington, **2007**, pp 723-760.
39. McEwen, B. S., Physiology and neurobiology of stress and adaptation: central role of the brain. *Physiol Rev* **2007,** *87* (3), 873-904.
40. McEwen, B. S.; Bowles, N. P.; Gray, J. D.; Hill, M. N.; Hunter, R. G.; Karatsoreos, I. N.; Nasca, C., Mechanisms of stress in the brain. *Nat Neurosci* **2015,** *18* (10), 1353-1363.
41. Gray, J. D.; Kogan, J. F.; Marrocco, J.; McEwen, B. S., Genomic and epigenomic mechanisms of glucocorticoids in the brain. *Nat Rev Endocrinol* **2017,** *13* (11), 661-673.
42. Booth, T.; Royle, N. A.; Corley, J.; Gow, A. J.; Valdés Hernández, M. d. C.; Muñoz Maniega, S.; Ritchie, S. J.; Bastin, M. E.; Starr, J. M.; Wardlaw, J. M., et al., Association of allostatic load with brain structure and cognitive ability in later life. *Neurobiol Aging* **2015,** *36* (3), 1390-1399.
43. Fava, G. A.; McEwen, B. S.; Guidi, J.; Gostoli, S.; Offidani, E.; Sonino, N., Clinical characterization of allostatic overload. *Psychoneuroendocrinology* **2019,** *108*, 94-101.
44. Miller, M. A., Association of inflammatory markers with cardiovascular risk and sleepiness. *J Clin Sleep Med* **2011,** *7* (5 Suppl), S31-S33.
45. Paalani, M.; Lee, J. W.; Haddad, E.; Tonstad, S., Determinants of inflammatory markers in a bi-ethnic population. *Ethn Dis* **2011,** *21* (2), 142-9.
46. Miller, M. A.; Cappuccio, F. P., Ethnicity and inflammatory pathways - implications for vascular disease, vascular risk and therapeutic intervention. *Curr Med Chem* **2007,** *14* (13), 1409-25.
47. Ferguson, S. A.; Varma, V.; Sloper, D.; Panos, J. J.; Sarkar, S., Increased inflammation in BA21 brain tissue from African Americans with Alzheimer's disease. *Metab Brain Dis* **2020,** *35* (1), 121-133.
48. Raj, T.; Chibnik, L. B.; McCabe, C.; Wong, A.; Replogle, J. M.; Yu, L.; Gao, S.; Unverzagt, F. W.; Stranger, B.; Murrell, J., et al. Genetic architecture of age-related cognitive decline in African Americans. *Neurol Genet* [Online], **2017**. https://www.ncbi.nlm.nih.gov/pmc/articles/PMC5206965/pdf/NG2016002436.pdf.

49. Stepler, K. E.; Robinson, R. A. S., The potential of 'omics to link lipid metabolism and genetic and comorbidity risk factors of Alzheimer's disease in African Americans. In *Reviews on Biomarker Studies in Psychiatric and Neurodegenerative Disorders*, Guest, P. C., Ed. Springer International Publishing: Cham, **2019**; Vol. 1118, pp 1-28.
50. Burns, M.; Duff, K., Cholesterol in Alzheimer's disease and tauopathy. *Ann N Y Acad Sci* **2002,** *977* (1), 367-375.
51. Martins, I. J.; Berger, T.; Sharman, M. J.; Verdile, G.; Fuller, S. J.; Martins, R. N., Cholesterol metabolism and transport in the pathogenesis of Alzheimer's disease. *J Neurochem* **2009,** *111* (6), 1275-1308.
52. El Gaamouch, F.; Jing, P.; Xia, J.; Cai, D., Alzheimer's disease risk genes and lipid regulators. *J Alzheimers Dis* **2016,** *53*, 15-29.
53. Zhao, N.; Liu, C.-C.; Qiao, W.; Bu, G., Apolipoprotein E, receptors, and modulation of Alzheimer's disease. *Biol Psychiatry* **2017,** *83* (4), 347-357.
54. Bales, K. R., Brain lipid metabolism, apolipoprotein E and the pathophysiology of Alzheimer's disease. *Neuropharmacology* **2010,** *59* (4-5), 295-302.
55. Girard, H.; Potvin, O.; Nugent, S.; Dallaire-Theroux, C.; Cunnane, S.; Duchesne, S., Faster progression from MCI to probable AD for carriers of a single-nucleotide polymorphism associated with type 2 diabetes. *Neurobiol Aging* **2017,** *64*, 157.e11-157.e17.
56. Pirttila, T.; Soininen, H.; Heinonen, O.; Lehtimaki, T.; Bogdanovic, N.; Paljarvi, L.; Kosunen, O.; Winblad, B.; Riekkinen, P., Sr.; Wisniewski, H. M., et al., Apolipoprotein E (apoE) levels in brains from Alzheimer disease patients and controls. *Brain Res* **1996,** *722* (1-2), 71-77.
57. Sato, N.; Morishita, R. The roles of lipid and glucose metabolism in modulation of β-amyloid, tau, and neurodegeneration in the pathogenesis of Alzheimer disease. *Front Aging Neurosci* [Online], **2015**. https://www.frontiersin.org/article/10.3389/fnagi.2015.00199.
58. Nday, C. M.; Eleftheriadou, D.; Jackson, G., Shared pathological pathways of Alzheimer's disease with specific comorbidities: current perspectives and interventions. *J Neurochem* **2017**, 10.1111/jnc.14256.
59. Hall, K.; Murrell, J.; Ogunniyi, A.; Deeg, M.; Baiyewu, O.; Gao, S.; Gureje, O.; Dickens, J.; Evans, R.; Smith-Gamble, V., et al., Cholesterol, APOE genotype, and Alzheimer disease: an epidemiologic study of Nigerian Yoruba. *Neurology* **2006,** *66* (2), 223-227.
60. Vrièze, F. W.-D.; Compton, D.; Womick, M.; Arepalli, S.; Adighibe, O.; Li, L.; Pèrez-Tur, J.; Hardy, J., ABCA1 polymorphisms and Alzheimer's disease. *Neurosci Lett* **2007,** *416* (2), 180-183.
61. Koldamova, R.; Fitz, N. F.; Lefterov, I., The role of ATP-binding cassette transporter A1 in Alzheimer's disease and neurodegeneration. *Biochim Biophys Acta* **2010,** *1801* (8), 824-830.
62. Fehér, Á.; Giricz, Z.; Juhász, A.; Pákáski, M.; Janka, Z.; Kálmán, J., ABCA1 rs2230805 and rs2230806 common gene variants are associated with Alzheimer's disease. *Neurosci Lett* **2018,** *664*, 79-83.
63. Aikawa, T.; Holm, M. L.; Kanekiyo, T. ABCA7 and pathogenic pathways of Alzheimer's disease. *Brain Sci* [Online], **2018**. http://www.mdpi.com/2076-3425/8/2/27/pdf.
64. Almeida, J. F. F.; Dos Santos, L. R.; Trancozo, M.; de Paula, F., Updated meta-analysis of BIN1, CR1, MS4A6A, CLU, and ABCA7 variants in Alzheimer's disease. *J Mol Neurosci* **2018,** *64*, 471-477.
65. Hollingworth, P.; Harold, D.; Sims, R.; Gerrish, A.; Lambert, J. C.; Carrasquillo, M. M.; Abraham, R.; Hamshere, M. L.; Pahwa, J. S.; Moskvina, V., et al., Common variants at ABCA7,

MS4A6A/MS4A4E, EPHA1, CD33 and CD2AP are associated with Alzheimer's disease. *Nat Genet* **2011,** *43* (5), 429-435.
66. Naj, A. C.; Jun, G.; Beecham, G. W.; Wang, L. S.; Vardarajan, B. N.; Buros, J.; Gallins, P. J.; Buxbaum, J. D.; Jarvik, G. P.; Crane, P. K., et al., Common variants at MS4A4/MS4A6E, CD2AP, CD33 and EPHA1 are associated with late-onset Alzheimer's disease. *Nat Genet* **2011,** *43* (5), 436-441.
67. Cuyvers, E.; De Roeck, A.; Van den Bossche, T.; Van Cauwenberghe, C.; Bettens, K.; Vermeulen, S.; Mattheijssens, M.; Peeters, K.; Engelborghs, S.; Vandenbulcke, M., et al., Mutations in ABCA7 in a Belgian cohort of Alzheimer's disease patients: a targeted resequencing study. *Lancet Neurol* **2015,** *14* (8), 814-822.
68. Lambert, J. C.; Ibrahim-Verbaas, C. A.; Harold, D.; Naj, A. C.; Sims, R.; Bellenguez, C.; DeStafano, A. L.; Bis, J. C.; Beecham, G. W.; Grenier-Boley, B., et al., Meta-analysis of 74,046 individuals identifies 11 new susceptibility loci for Alzheimer's disease. *Nat Genet* **2013,** *45* (12), 1452-1458.
69. N'Songo, A.; Carrasquillo, M. M.; Wang, X.; Burgess, J. D.; Nguyen, T.; Asmann, Y. W.; Serie, D. J.; Younkin, S. G.; Allen, M.; Pedraza, O., et al. African American exome sequencing identifies potential risk variants at Alzheimer disease loci. *Neurol Genet* [Online], **2017**. https://ng.neurology.org/content/nng/3/2/e141.full.pdf.
70. Zhou, Q.; Zhao, F.; Lv, Z.-p.; Zheng, C.-g.; Zheng, W.-d.; Sun, L.; Wang, N.-n.; Pang, S.; de Andrade, F. M.; Fu, M., et al. Association between APOC1 polymorphism and Alzheimer's disease: a case-control study and meta-analysis. *PLoS ONE* [Online], **2014**. https://doi.org/10.1371/journal.pone.0087017.
71. Petit-Turcotte, C.; Stohl, S. M.; Beffert, U.; Cohn, J. S.; Aumont, N.; Tremblay, M.; Dea, D.; Yang, L.; Poirier, J.; Shachter, N. S., Apolipoprotein C-I expression in the brain in Alzheimer's disease. *Neurobiol Dis* **2001,** *8* (6), 953-963.
72. Ki, C.-S.; Na, D. L.; Kim, D. K.; Kim, H. J.; Kim, J.-W., Genetic association of an apolipoprotein C-I (APOC1) gene polymorphism with late-onset Alzheimer's disease. *Neurosci Lett* **2002,** *319* (2), 75-78.
73. Desai, P. P.; Hendrie, H. C.; Evans, R. M.; Murrell, J. R.; DeKosky, S. T.; Kamboh, M. I., Genetic variation in apolipoprotein D affects the risk of Alzheimer disease in African-Americans. *Am J Med Genet B Neuropsychiatr Genet* **2003,** *116B* (1), 98-101.
74. Reitz, C.; Jun, G.; Naj, A.; Rajbhandary, R.; Vardarajan, B. N.; Wang, L.-S.; Valladares, O.; Lin, C.-F.; Larson, E. B.; Graff-Radford, N. R., et al., Variants in the ATP-binding cassette transporter (ABCA7), apolipoprotein E ε4, and the risk of late-onset Alzheimer disease in African Americans. *JAMA* **2013,** *309* (14), 1483-1492.
75. Reitz, C.; Mayeux, R., Genetics of Alzheimer's disease in Caribbean Hispanic and African American populations. *Biol Psychiatry* **2014,** *75* (7), 534-541.
76. Seshadri, S.; Fitzpatrick, A. L.; Ikram, M. A.; DeStefano, A. L.; Gudnason, V.; Boada, M.; Bis, J. C.; Smith, A. V.; Carassquillo, M. M.; Lambert, J. C., et al., Genome-wide analysis of genetic loci associated with Alzheimer disease. *JAMA* **2010,** *303* (18), 1832-1840.
77. Bertram, L.; Lange, C.; Mullin, K.; Parkinson, M.; Hsiao, M.; Hogan, M. F.; Schjeide, B. M.; Hooli, B.; Divito, J.; Ionita, I., et al., Genome-wide association analysis reveals putative Alzheimer's disease susceptibility loci in addition to APOE. *Am J Hum Genet* **2008,** *83* (5), 623-632.

78. Lambert, J.-C.; Heath, S.; Even, G.; Campion, D.; Sleegers, K.; Hiltunen, M.; Combarros, O.; Zelenika, D.; Bullido, M. J.; Tavernier, B., et al., Genome-wide association study identifies variants at CLU and CR1 associated with Alzheimer's disease. *Nat Genet* **2009,** *41*, 1094-1099.
79. Harold, D.; Abraham, R.; Hollingworth, P.; Sims, R.; Gerrish, A.; Hamshere, M. L.; Pahwa, J. S.; Moskvina, V.; Dowzell, K.; Williams, A., et al., Genome-wide association study identifies variants at CLU and PICALM associated with Alzheimer's disease. *Nature Genet* **2009,** *41*, 1088-1093.
80. Rogaeva, E.; Meng, Y.; Lee, J. H.; Gu, Y.; Kawarai, T.; Zou, F.; Katayama, T.; Baldwin, C. T.; Cheng, R.; Hasegawa, H., et al., The neuronal sortilin-related receptor SORL1 is genetically associated with Alzheimer's disease. *Nat Genet* **2007,** *39* (2), 168-177.
81. Lee, J. H.; Cheng, R.; Schupf, N.; Manly, J.; Lantigua, R.; Stern, Y.; Tycko, B.; Rogaeva, E.; Wakutani, Y.; Farrer, L., et al., The association between genetic variants in SORL1 and Alzheimer's disease in an urban, multiethnic, community-based cohort. *Arch Neurol* **2007,** *64* (4), 501-506.
82. Chou, C.-T.; Liao, Y.-C.; Lee, W.-J.; Wang, S.-J.; Fuh, J.-L. SORL1 gene, plasma biomarkers, and the risk of Alzheimer's disease for the Han Chinese population in Taiwan. *Alzheimers Res Ther* [Online], **2016**. PMC. http://www.ncbi.nlm.nih.gov/pmc/articles/PMC5200969/.
83. Ghani, M.; Reitz, C.; Cheng, R.; Vardarajan, B. N.; Jun, G.; Sato, C.; Naj, A.; Rajbhandary, R.; Wang, L. S.; Valladares, O., et al., Association of long runs of homozygosity with Alzheimer disease among African American individuals. *JAMA Neurol* **2015,** *72* (11), 1313-1323.
84. Picard, C.; Julien, C.; Frappier, J.; Miron, J.; Théroux, L.; Dea, D.; Breitner, J. C. S.; Poirier, J., Alterations in cholesterol metabolism-related genes in sporadic Alzheimer's disease. *Neurobiol Aging* **2018,** *66*, 180.e1-180.e9.
85. Ikeda, Y.; Abe-Dohmae, S.; Munehira, Y.; Aoki, R.; Kawamoto, S.; Furuya, A.; Shitara, K.; Amachi, T.; Kioka, N.; Matsuo, M., et al., Posttranscriptional regulation of human ABCA7 and its function for the apoA-I-dependent lipid release. *Biochem Biophys Res Commun* **2003,** *311* (2), 313-318.
86. Takahashi, K.; Kimura, Y.; Nagata, K.; Yamamoto, A.; Matsuo, M.; Ueda, K., ABC proteins: key molecules for lipid homeostasis. *Med Mol Morphol* **2005,** *38* (1), 2-12.
87. Abe-Dohmae, S.; Ikeda, Y.; Matsuo, M.; Hayashi, M.; Okuhira, K.; Ueda, K.; Yokoyama, S., Human ABCA7 supports apolipoprotein-mediated release of cellular cholesterol and phospholipid to generate high density lipoprotein. *J Biol Chem* **2004,** *279* (1), 604-11.
88. Zhao, Q. F.; Yu, J. T.; Tan, M. S.; Tan, L., ABCA7 in Alzheimer's disease. *Mol Neurobiol* **2015,** *51* (3), 1008-1016.
89. Quazi, F.; Molday, R. S., Differential phospholipid substrates and directional transport by ATP-binding cassette proteins ABCA1, ABCA7, and ABCA4 and disease-causing mutants. *J Biol Chem* **2013,** *288* (48), 34414-26.
90. Chan, S. L.; Kim, W. S.; Kwok, J. B.; Hill, A. F.; Cappai, R.; Rye, K. A.; Garner, B., ATP-binding cassette transporter A7 regulates processing of amyloid precursor protein in vitro. *J Neurochem* **2008,** *106* (2), 793-804.
91. De Roeck, A.; Van Broeckhoven, C.; Sleegers, K., The role of ABCA7 in Alzheimer's disease: evidence from genomics, transcriptomics and methylomics. *Acta Neuropathol* **2019,** *138* (2), 201-220.

92. Rosenthal, S. L.; Kamboh, M. I., Late-onset Alzheimer's disease genes and the potentially implicated pathways. *Curr Genet Med Rep* **2014,** *2* (2), 85-101.
93. Sakae, N.; Liu, C. C.; Shinohara, M.; Frisch-Daiello, J.; Ma, L.; Yamazaki, Y.; Tachibana, M.; Younkin, L.; Kurti, A.; Carrasquillo, M. M., et al., ABCA7 deficiency accelerates amyloid-beta generation and Alzheimer's neuronal pathology. *J Neurosci* **2016,** *36* (13), 3848-3859.
94. Villegas-Llerena, C.; Phillips, A.; Garcia-Reitboeck, P.; Hardy, J.; Pocock, J. M., Microglial genes regulating neuroinflammation in the progression of Alzheimer's disease. *Curr Opin Neurobiol* **2016,** *36*, 74-81.
95. Kim, W. S.; Li, H.; Ruberu, K.; Chan, S.; Elliott, D. A.; Low, J. K.; Cheng, D.; Karl, T.; Garner, B., Deletion of Abca7 increases cerebral amyloid-beta accumulation in the J20 mouse model of Alzheimer's disease. *J Neurosci* **2013,** *33* (10), 4387-94.
96. Jehle, A. W.; Gardai, S. J.; Li, S.; Linsel-Nitschke, P.; Morimoto, K.; Janssen, W. J.; Vandivier, R. W.; Wang, N.; Greenberg, S.; Dale, B. M., et al., ATP-binding cassette transporter A7 enhances phagocytosis of apoptotic cells and associated ERK signaling in macrophages. *J Cell Biol* **2006,** *174* (4), 547-556.
97. Aikawa, T.; Ren, Y.; Yamazaki, Y.; Tachibana, M.; Johnson, M. R.; Anderson, C. T.; Martens, Y. A.; Holm, M.-L.; Asmann, Y. W.; Saito, T., et al., ABCA7 haplodeficiency disturbs microglial immune responses in the mouse brain. *Proc Natl Acad Sci U S A* **2019,** *116* (47), 23790-23796.
98. Steinberg, S.; Stefansson, H.; Jonsson, T.; Johannsdottir, H.; Ingason, A.; Helgason, H.; Sulem, P.; Magnusson, O. T.; Gudjonsson, S. A.; Unnsteinsdottir, U., et al., Loss-of-function variants in ABCA7 confer risk of Alzheimer's disease. *Nat Genet* **2015,** *47* (5), 445-447.
99. Kjeldsen, E. W.; Tybjaerg-Hansen, A.; Nordestgaard, B. G.; Frikke-Schmidt, R., ABCA7 and risk of dementia and vascular disease in the Danish population. *Ann Clin Transl Neurol* **2018,** *5* (1), 41-51.
100. Moreno, D. J.; Ruiz, S.; Rios, A.; Lopera, F.; Ostos, H.; Via, M.; Bedoya, G., Association of GWAS top genes with late-onset Alzheimer's disease in Colombian population. *Am J Alzheimers Dis Other Demen* **2017,** *32* (1), 27-35.
101. Logue, M. W.; Schu, M.; Vardarajan, B. N.; Buros, J.; Green, R. C.; Go, R. C.; Griffith, P.; Obisesan, T. O.; Shatz, R.; Borenstein, A., et al., A comprehensive genetic association study of Alzheimer disease in African Americans. *Arch Neurol* **2011,** *68* (12), 1569-79.
102. Sinha, N.; Reagh, Z. M.; Tustison, N. J.; Berg, C. N.; Shaw, A.; Myers, C. E.; Hill, D.; Yassa, M. A.; Gluck, M. A., ABCA7 risk variant in healthy older African Americans is associated with a functionally isolated entorhinal cortex mediating deficient generalization of prior discrimination training. *Hippocampus* **2019,** *29* (6), 527-538.
103. Logue, M. W.; Lancour, D.; Farrell, J.; Simkina, I.; Fallin, M. D.; Lunetta, K. L.; Farrer, L. A., Targeted sequencing of Alzheimer disease genes in African Americans implicates novel risk variants. *Front Neurosci* **2018,** *12*, 592.
104. Hohman, T. J.; Cooke-Bailey, J. N.; Reitz, C.; Jun, G.; Naj, A.; Beecham, G. W.; Liu, Z.; Carney, R. M.; Vance, J. M.; Cuccaro, M. L., et al., Global and local ancestry in African-Americans: implications for Alzheimer's disease risk. *Alzheimers Dement* **2016,** *12* (3), 233-243.
105. Li, H.; Zhou, J.; Yue, Z.; Feng, L.; Luo, Z.; Chen, S.; Yang, X.; Xiao, B., A complex association between ABCA7 genotypes and blood lipid levels in Southern Chinese Han patients of sporadic Alzheimer's disease. *J Neurol Sci* **2017,** *382*, 13-17.

106. Zhou, G.; Mao, X. Q.; Chu, J. Q.; Chen, G.; Zhao, Q.; Wang, L. L.; Luo, Y. P., ATP binding cassette subfamily A member 7 rs3764650 polymorphism and the risk of Alzheimer's disease. *Pharmazie* **2017,** *72* (7), 425-427.
107. Monsell, S. E.; Mock, C.; Fardo, D. W.; Bertelsen, S.; Cairns, N. J.; Roe, C. M.; Ellingson, S. R.; Morris, J. C.; Goate, A. M.; Kukull, W. A., Genetic comparison of symptomatic and asymptomatic persons with Alzheimer disease neuropathology. *Alzheimer Dis Assoc Disord* **2017,** *31* (3), 232-238.
108. Kunkle, B. W.; Carney, R. M.; Kohli, M. A.; Naj, A. C.; Hamilton-Nelson, K. L.; Whitehead, P. L.; Wang, L.; Lang, R.; Cuccaro, M. L.; Vance, J. M., et al., Targeted sequencing of ABCA7 identifies splicing, stop-gain and intronic risk variants for Alzheimer disease. *Neurosci Lett* **2017,** *649*, 124-129.
109. Cukier, H. N.; Kunkle, B. W.; Vardarajan, B. N.; Rolati, S.; Hamilton-Nelson, K. L.; Kohli, M. A.; Whitehead, P. L.; Dombroski, B. A.; Van Booven, D.; Lang, R., et al. ABCA7 frameshift deletion associated with Alzheimer disease in African Americans. *Neurol Genet* [Online], **2016**. http://ng.neurology.org/content/2/3/e79.abstract.
110. Ramos-Cejudo, J.; Wisniewski, T.; Marmar, C.; Zetterberg, H.; Blennow, K.; de Leon, M. J.; Fossati, S., Traumatic brain injury and Alzheimer's disease: the cerebrovascular link. *EBioMedicine* **2018,** *28*, 21-30.
111. Honig, L. S.; Tang, M. X.; Albert, S.; Costa, R.; Luchsinger, J.; Manly, J.; Stern, Y.; Mayeux, R., Stroke and the risk of Alzheimer disease. *Arch Neurol* **2003,** *60* (12), 1707-1712.
112. Chakrabarti, S.; Khemka, V. K.; Banerjee, A.; Chatterjee, G.; Ganguly, A.; Biswas, A., Metabolic risk factors of sporadic Alzheimer's disease: implications in the pathology, pathogenesis and treatment. *Aging Dis* **2015,** *6* (4), 282-299.
113. Matsuzaki, T.; Sasaki, K.; Hata, J.; Hirakawa, Y.; Fujimi, K.; Ninomiya, T.; Suzuki, S. O.; Kanba, S.; Kiyohara, Y.; Iwaki, T., Association of Alzheimer disease pathology with abnormal lipid metabolism: the Hisayama Study. *Neurology* **2011,** *77* (11), 1068-1075.
114. Gonzalez, H. M.; Tarraf, W.; Harrison, K.; Windham, B. G.; Tingle, J.; Alonso, A.; Griswold, M.; Heiss, G.; Knopman, D.; Mosley, T. H., Midlife cardiovascular health and 20-year cognitive decline: Atherosclerosis Risk in Communities Study results. *Alzheimers Dement* **2017,** *14* (5), 579-589.
115. Howard, G.; Safford, M. M.; Moy, C. S.; Howard, V. J.; Kleindorfer, D. O.; Unverzagt, F. W.; Soliman, E. Z.; Flaherty, M. L.; McClure, L. A.; Lackland, D. T., et al., Racial differences in the incidence of cardiovascular risk factors in older black and white adults. *J Am Geriatr Soc* **2017,** *65* (1), 83-90.
116. Burke, S. L.; Cadet, T.; Maddux, M., Chronic health illnesses as predictors of mild cognitive impairment among African American older adults. *J Natl Med Assoc* **2017,** *110* (4), 314-325.
117. Liu, Q.; Zhang, J., Lipid metabolism in Alzheimer’s disease. *Neurosci Bull* **2014,** *30* (2), 331-345.
118. Gamba, P.; Testa, G.; Sottero, B.; Gargiulo, S.; Poli, G.; Leonarduzzi, G., The link between altered cholesterol metabolism and Alzheimer's disease. *Ann N Y Acad Sci* **2012,** *1259*, 54-64.
119. Di Paolo, G.; Kim, T. W., Linking lipids to Alzheimer's disease: cholesterol and beyond. *Nat Rev Neurosci* **2011,** *12* (5), 284-296.

120. Martins, I. J. Diabetes and cholesterol dyshomeostasis involve abnormal α-synuclein and amyloid beta transport in neurodegenerative diseases. *Austin Alzheimers J Parkinsons Dis* [Online], **2015**.
121. Evans, R. M.; Emsley, C. L.; Gao, S.; Sahota, A.; Hall, K. S.; Farlow, M. R.; Hendrie, H., Serum cholesterol, APOE genotype, and the risk of Alzheimer's disease: a population-based study of African Americans. *Neurology* **2000,** *54* (1), 240-242.
122. Fuchs, F. D., Why do black Americans have higher prevalence of hypertension? An enigma still unsolved. *Hypertension* **2011,** *57* (3), 379-380.
123. Lackland, D. T., Racial differences in hypertension: implications for high blood pressure management. *Am J Med Sci* **2014,** *348* (2), 135-138.
124. Carnethon, M. R.; Pu, J.; Howard, G.; Albert, M. A.; Anderson, C. A. M.; Bertoni, A. G.; Mujahid, M. S.; Palaniappan, L.; Taylor, H. A., Jr.; Willis, M., et al., Cardiovascular health in African Americans: a scientific statement from the American Heart Association. *Circulation* **2017,** *136* (21), e393-e423.
125. Redmond, N.; Baer, H. J.; Hicks, L. S., Health behaviors and racial disparity in blood pressure control in the National Health and Nutrition Examination Survey. *Hypertension* **2011,** *57* (3), 383-389.
126. Barnes, D. E.; Yaffe, K., The projected effect of risk factor reduction on Alzheimer's disease prevalence. *Lancet Neurol* **2011,** *10* (9), 819-828.
127. Xu, W.; Tan, L.; Wang, H.-F.; Jiang, T.; Tan, M.-S.; Tan, L.; Zhao, Q.-F.; Li, J.-Q.; Wang, J.; Yu, J.-T., Meta-analysis of modifiable risk factors for Alzheimer's disease. *J Neurol Neurosurg Psychiatr* **2015,** *86*, 1299-1306.
128. Arvanitakis, Z.; Capuano, A. W.; Lamar, M.; Shah, R. C.; Barnes, L. L.; Bennett, D. A.; Schneider, J. A., Late-life blood pressure association with cerebrovascular and Alzheimer disease pathology. *Neurology* **2018,** *91* (6), e517-e525.
129. Brancati, F. L.; Kao, W.; Folsom, A. R.; Watson, R. L.; Szklo, M., Incident type 2 diabetes mellitus in African American and white adults: the Atherosclerosis Risk In Communities study. *JAMA* **2000,** *283* (17), 2253-2259.
130. Marshall, M., Diabetes in African Americans. *Postgrad Med J* **2005,** *81* (962), 734-740.
131. Arnold, S. E.; Arvanitakis, Z.; Macauley-Rambach, S. L.; Koenig, A. M.; Wang, H. Y.; Ahima, R. S.; Craft, S.; Gandy, S.; Buettner, C.; Stoeckel, L. E., et al., Brain insulin resistance in type 2 diabetes and Alzheimer disease: concepts and conundrums. *Nat Rev Neurol* **2018,** *14*, 168-181.
132. Boden, G.; Laakso, M., Lipids and glucose in type 2 diabetes: what is the cause and effect? . *Diabetes Care* **2004,** *27* (9), 2253-2259.
133. Savage, D. B.; Petersen, K. F.; Shulman, G. I., Disordered lipid metabolism and the pathogenesis of insulin resistance. *Physiol Rev* **2007,** *87* (2), 507-520.
134. Schilling, M. A., Unraveling Alzheimer's: making sense of the relationship between diabetes and Alzheimer's disease. *J Alzheimers Dis* **2016,** *51* (4), 961-977.
135. Marseglia, A.; Fratiglioni, L.; Kalpouzos, G.; Wang, R.; Bäckman, L.; Xu, W., Prediabetes and diabetes accelerate cognitive decline and predict microvascular lesions: a population-based cohort study. *Alzheimers Dement* **2018,** *15* (1), 25-33.
136. Mayeda, E. R.; Haan, M. N.; Neuhaus, J.; Yaffe, K.; Knopman, D. S.; Sharrett, A. R.; Griswold, M. E.; Mosley, T. H., Type 2 diabetes and cognitive decline over 14 years in middle-aged African Americans and whites: the ARIC Brain MRI Study. *Neuroepidemiology* **2014,** *43* (3-4), 220-227.

137. Arvanitakis, Z.; Bennett, D. A.; Wilson, R. S.; Barnes, L. L., Diabetes and cognitive systems in older black and white persons. *Alzheimer Dis Assoc Disord* **2010,** *24* (1), 37-42.
138. Hendrie, H. C.; Zheng, M.; Lane, K. A.; Ambuehl, R.; Purnell, C.; Li, S.; Unverzagt, F. W.; Murray, M. D.; Balasubramanyam, A.; Callahan, C. M., et al., Changes of glucose levels precede dementia in African-Americans with diabetes but not in Caucasians. *Alzheimers Dement* **2018,** *14* (12), 1572-1579.
139. Hendrie, H. C.; Zheng, M.; Li, W.; Lane, K.; Ambuehl, R.; Purnell, C.; Unverzagt, F. W.; Torke, A.; Balasubramanyam, A.; Callahan, C. M., et al., Glucose level decline precedes dementia in elderly African Americans with diabetes. *Alzheimers Dement* **2017,** *13* (2), 111-118.
140. Pimentel dos Santos Matioli, M. N.; Suemoto, C. K.; Rodriguez, R. D.; Farias, D. S.; da Silva, M. M.; Paraizo Leite, R. E.; Ferretti-Rebustini, R. E. L.; Farfel, J. M.; Pasqualucci, C. A.; Filho, W. J., et al., Diabetes is not associated with Alzheimer's disease neuropathology. *J Alzheimers Dis* **2017,** *60*, 1035-1043.
141. Aebersold, R.; Mann, M., Mass spectrometry-based proteomics. *Nature* **2003,** *422* (6928), 198-207.
142. Angel, T. E.; Aryal, U. K.; Hengel, S. M.; Baker, E. S.; Kelly, R. T.; Robinson, E. W.; Smith, R. D., Mass spectrometry-based proteomics: existing capabilities and future directions. *Chem Soc Rev* **2012,** *41* (10), 3912-3928.
143. Han, X.; Aslanian, A.; Yates, J. R., 3rd, Mass spectrometry for proteomics. *Curr Opin Chem Biol* **2008,** *12* (5), 483-490.
144. McDonald, W. H.; Yates, J. R., Shotgun proteomics and biomarker discovery. *Dis Markers* **2002,** *18*, 99-105.
145. McDonald, W. H.; Yates, J. R., 3rd, Shotgun proteomics: integrating technologies to answer biological questions. *Curr Opin Mol Ther* **2003,** *5* (3), 302-309.
146. Arul, A. B.; Robinson, R. A. S., Sample multiplexing strategies in quantitative proteomics. *Anal Chem* **2019,** *91* (1), 178-189.
147. Pappireddi, N.; Martin, L.; Wühr, M., A review on quantitative multiplexed proteomics. *Chembiochem* **2019,** *20* (10), 1210-1224.
148. Viner, R.; Bomgarden, R.; Blank, M.; Rogers, J. *Increasing the multiplexing of protein quantitation from 6- to 10-plex with reporter ion isotopologues*; Thermo Scientific: **2013**.
149. Thermo Scientific *TMT10plex mass tag labeling kits and reagents: Instructions*; **2017**.
150. Yang, F.; Shen, Y.; Camp, D. G., 2nd; Smith, R. D., High-pH reversed-phase chromatography with fraction concatenation for 2D proteomic analysis. *Expert Rev Proteomics* **2012,** *9* (2), 129-134.
151. Wang, Y.; Yang, F.; Gritsenko, M. A.; Wang, Y.; Clauss, T.; Liu, T.; Shen, Y.; Monroe, M. E.; Lopez-Ferrer, D.; Reno, T., et al., Reversed-phase chromatography with multiple fraction concatenation strategy for proteome profiling of human MCF10A cells. *Proteomics* **2011,** *11* (10), 2019-2026.
152. Cao, Z.; Tang, H. Y.; Wang, H.; Liu, Q.; Speicher, D. W., Systematic comparison of fractionation methods for in-depth analysis of plasma proteomes. *J Proteome Res* **2012,** *11* (6), 3090-100.
153. Gilar, M.; Olivova, P.; Daly, A. E.; Gebler, J. C., Two-dimensional separation of peptides using RP-RP-HPLC system with different pH in first and second separation dimensions. *J Sep Sci* **2005,** *28* (14), 1694-1703.
154. Weston, L. A.; Bauer, K. M.; Hummon, A. B., Comparison of bottom-up proteomic approaches for LC-MS analysis of complex proteomes. *Anal Methods* **2013,** *5* (18), 4615-4621.

155. Ting, L.; Rad, R.; Gygi, S. P.; Haas, W., MS3 eliminates ratio distortion in isobaric multiplexed quantitative proteomics. *Nat Methods* **2011,** *8* (11), 937-940.
156. McAlister, G. C.; Nusinow, D. P.; Jedrychowski, M. P.; Wühr, M.; Huttlin, E. L.; Erickson, B. K.; Rad, R.; Haas, W.; Gygi, S. P., MultiNotch MS3 enables accurate, sensitive, and multiplexed detection of differential expression across cancer cell line proteomes. *Anal Chem* **2014,** *86* (14), 7150-7158.
157. Niu, M.; Cho, J. H.; Kodali, K.; Pagala, V.; High, A. A.; Wang, H.; Wu, Z.; Li, Y.; Bi, W.; Zhang, H., et al., Extensive peptide fractionation and y(1) ion-based interference detection method for enabling accurate quantification by isobaric labeling and mass spectrometry. *Anal Chem* **2017,** *89* (5), 2956-2963.
158. Wang, Z.; Yu, K.; Tan, H.; Wu, Z.; Cho, J.-H.; Han, X.; Sun, H.; Beach, T. G.; Peng, J., 27-plex Tandem Mass Tag mass spectrometry for profiling brain proteome in Alzheimer's disease. *Anal Chem* **2020,** *92* (10), 7162-7170.
159. High, A. A.; Tan, H.; Pagala, V. R.; Niu, M.; Cho, J. H.; Wang, X.; Bai, B.; Peng, J. Deep proteome profiling by isobaric labeling, extensive liquid chromatography, mass spectrometry, and software-assisted quantification. *J Vis Exp* [Online], **2017**. https://www.jove.com/pdf/56474/jove-protocol-56474-deep-proteome-profiling-isobaric-labeling-extensive-liquid.
160. Plubell, D. L.; Wilmarth, P. A.; Zhao, Y.; Fenton, A. M.; Minnier, J.; Reddy, A. P.; Klimek, J.; Yang, X.; David, L. L.; Pamir, N., Extended multiplexing of Tandem Mass Tags (TMT) labeling reveals age and high fat diet specific proteome changes in mouse epididymal adipose tissue. *Mol Cell Proteomics* **2017,** *16* (5), 873-890.
161. Kelchtermans, P.; Bittremieux, W.; De Grave, K.; Degroeve, S.; Ramon, J.; Laukens, K.; Valkenborg, D.; Barsnes, H.; Martens, L., Machine learning applications in proteomics research: How the past can boost the future. *PROTEOMICS* **2014,** *14* (4-5), 353-366.
162. Swan, A. L.; Mobasheri, A.; Allaway, D.; Liddell, S.; Bacardit, J., Application of machine learning to proteomics data: Classification and biomarker identification in postgenomics biology. *Omics* **2013,** *17* (12), 595-610.
163. Zhang, F.; Chen, J. Y. In *A neural network approach to multi-biomarker panel development based on LC/MS/MS proteomics profiles: A case study in breast cancer*, 2009 22nd IEEE International Symposium on Computer-Based Medical Systems, 2-5 Aug. 2009; **2009**; pp 1-6.
164. Ryberg, H.; An, J.; Darko, S.; Lustgarten, J. L.; Jaffa, M.; Gopalakrishnan, V.; Lacomis, D.; Cudkowicz, M.; Bowser, R., Discovery and verification of amyotrophic lateral sclerosis biomarkers by proteomics. *Muscle Nerve* **2010,** *42* (1), 104-111.
165. Hua, D.; Desaire, H., Improved discrimination of disease states using proteomics data with the updated Aristotle Classifier. *J Proteome Res* **2021,** *20* (5), 2823-2829.
166. Khan, M. J.; Desaire, H.; Lopez, O. L.; Kamboh, M. I.; Robinson, R. A. S., Why inclusion matters for Alzheimer's disease biomarker discovery in plasma. *J Alzheimers Dis* **2021,** *79* (3), 1327-1344.
167. Andreev, V. P.; Petyuk, V. A.; Brewer, H. M.; Karpievitch, Y. V.; Xie, F.; Clarke, J.; Camp, D.; Smith, R. D.; Lieberman, A. P.; Albin, R. L., et al., Label-free quantitative LC-MS proteomics of Alzheimer's disease and normally aged human brains. *J Proteome Res* **2012,** *11* (6), 3053-3067.
168. Begcevic, I.; Kosanam, H.; Martinez-Morillo, E.; Dimitromanolakis, A.; Diamandis, P.; Kuzmanov, U.; Hazrati, L. N.; Diamandis, E. P. Semiquantitative proteomic analysis of human

hippocampal tissues from Alzheimer's disease and age-matched control brains. *Clin Proteomics* [Online], **2013**. https://www.ncbi.nlm.nih.gov/pmc/articles/PMC3648498/pdf/1559-0275-10-5.pdf.
169. Hondius, D. C.; van Nierop, P.; Li, K. W.; Hoozemans, J. J. M.; van der Schors, R. C.; van Haastert, E. S.; van der Vies, S. M.; Rozemuller, A. J. M.; Smit, A. B., Profiling the human hippocampal proteome at all pathologic stages of Alzheimer's disease. *Alzheimers Dement* **2016,** *12* (6), 654-668.
170. Manavalan, A.; Mishra, M.; Feng, L.; Sze, S. K.; Akatsu, H.; Heese, K. Brain site-specific proteome changes in aging-related dementia. *Exp Mol Med* [Online], **2013**. http://dx.doi.org/10.1038/emm.2013.76.
171. Minjarez, B.; Calderon-Gonzalez, K. G.; Rustarazo, M. L.; Herrera-Aguirre, M. E.; Labra-Barrios, M. L.; Rincon-Limas, D. E.; Del Pino, M. M.; Mena, R.; Luna-Arias, J. P., Identification of proteins that are differentially expressed in brains with Alzheimer's disease using iTRAQ labeling and tandem mass spectrometry. *J Proteomics* **2016,** *139*, 103-121.
172. Musunuri, S.; Wetterhall, M.; Ingelsson, M.; Lannfelt, L.; Artemenko, K.; Bergquist, J.; Kultima, K.; Shevchenko, G., Quantification of the brain proteome in Alzheimer's disease using multiplexed mass spectrometry. *J Proteome Res* **2014,** *13* (4), 2056-2068.
173. Neuner, S. M.; Wilmott, L. A.; Hoffmann, B. R.; Mozhui, K.; Kaczorowski, C. C., Hippocampal proteomics defines pathways associated with memory decline and resilience in normal aging and Alzheimer's disease mouse models. *Behav Brain Res* **2017,** *322*, 288-298.
174. Sultana, R.; Boyd-Kimball, D.; Cai, J.; Pierce, W. M.; Klein, J. B.; Merchant, M.; Butterfield, D. A., Proteomics analysis of the Alzheimer's disease hippocampal proteome. *J Alzheimers Dis* **2007,** *11* (2), 153-164.
175. Tsuji, T.; Shiozaki, A.; Kohno, R.; Yoshizato, K.; Shimohama, S., Proteomic profiling and neurodegeneration in Alzheimer's disease. *Neurochem Res* **2002,** *27* (10), 1245-1253.
176. Zahid, S.; Oellerich, M.; Asif, A. R.; Ahmed, N., Differential expression of proteins in brain regions of Alzheimer's disease patients. *Neurochem Res* **2014,** *39* (1), 208-215.
177. Aluise, C. D.; Robinson, R. A. S.; Beckett, T. L.; Murphy, M. P.; Cai, J.; Pierce, W. M.; Markesbery, W. R.; Butterfield, D. A., Preclinical Alzheimer disease: brain oxidative stress, Aβ peptide & proteomics. *Neurobiol Dis* **2010,** *39* (2), 221-228.
178. Aluise, C. D.; Robinson, R. A. S.; Cai, J.; Pierce, W. M.; Markesbery, W. R.; Butterfield, D. A., Redox proteomics analyses of brains from subjects with amnestic mild cognitive impairment compared to brains from subjects with preclinical Alzheimer's disease: insights into memory loss in MCI. *J Alzheimers Dis* **2011,** *23*, 257-269.
179. Castegna, A.; Aksenov, M.; Thongboonkerd, V.; Klein, J. B.; Pierce, W. M.; Booze, R.; Markesbery, W. R.; Butterfield, D. A., Proteomic identification of oxidatively modified proteins in Alzheimer's disease brain. Part II: dihydropyrimidinase-related protein 2, alpha-enolase and heat shock cognate 71. *J Neurochem* **2002,** *82* (6), 1524-1532.
180. Reed, T. T.; Pierce, W. M., Jr.; Turner, D. M.; Markesbery, W. R.; Butterfield, D. A., Proteomic identification of nitrated brain proteins in early Alzheimer's disease inferior parietal lobule. *J Cell Mol Med* **2009,** *13* (8b), 2019-2029.
181. Robinson, R. A. S.; Joshi, G.; Huang, Q.; Sultana, R.; Baker, A. S.; Cai, J.; Pierce, W.; St. Clair, D. K.; Markesbery, W. R.; Butterfield, D. A., Proteomics analysis of brain proteins in APP/PS-1 human double mutant knock-in mice with increasing amyloid β-peptide deposition: insights into the effects of in vivo treatment with N-acetylcysteine as a potential therapeutic

intervention in mild cognitive impairment and Alzheimer disease. *Proteomics* **2011,** *11* (21), 4243-4256.
182. Uhlén, M.; Fagerberg, L.; Hallström, B. M.; Lindskog, C.; Oksvold, P.; Mardinoglu, A.; Sivertsson, Å.; Kampf, C.; Sjöstedt, E.; Asplund, A., et al. Tissue-based map of the human proteome. *Science* [Online], **2015**. https://science.sciencemag.org/content/sci/347/6220/1260419.full.pdf.
183. Hawrylycz, M. J.; Lein, E. S.; Guillozet-Bongaarts, A. L.; Shen, E. H.; Ng, L.; Miller, J. A.; van de Lagemaat, L. N.; Smith, K. A.; Ebbert, A.; Riley, Z. L., et al., An anatomically comprehensive atlas of the adult human brain transcriptome. *Nature* **2012,** *489* (7416), 391-399.
184. Sjöstedt, E.; Zhong, W.; Fagerberg, L.; Karlsson, M.; Mitsios, N.; Adori, C.; Oksvold, P.; Edfors, F.; Limiszewska, A.; Hikmet, F., et al. An atlas of the protein-coding genes in the human, pig, and mouse brain. *Science* [Online], **2020**. https://science.sciencemag.org/content/sci/367/6482/eaay5947.full.pdf.
185. The human brain proteome. http://www.proteinatlas.org (accessed 06/23/21).
186. Ping, L.; Duong, D. M.; Yin, L.; Gearing, M.; Lah, J. J.; Levey, A. I.; Seyfried, N. T. Global quantitative analysis of the human brain proteome in Alzheimer's and Parkinson's Disease. *Sci Data* [Online], **2018**. http://dx.doi.org/10.1038/sdata.2018.36.
187. Bai, B.; Wang, X.; Li, Y.; Chen, P.-C.; Yu, K.; Dey, K. K.; Yarbro, J. M.; Han, X.; Lutz, B. M.; Rao, S., et al., Deep multilayer brain proteomics identifies molecular networks in Alzheimer's disease progression. *Neuron* **2020,** *105* (6), 975-991.
188. Ping, L.; Kundinger, S. R.; Duong, D. M.; Yin, L.; Gearing, M.; Lah, J. J.; Levey, A. I.; Seyfried, N. T. Global quantitative analysis of the human brain proteome and phosphoproteome in Alzheimer's disease. *Sci Data* [Online], **2020**. https://www.nature.com/articles/s41597-020-00650-8.pdf.
189. Johnson, E. C. B.; Dammer, E. B.; Duong, D. M.; Ping, L.; Zhou, M.; Yin, L.; Higginbotham, L. A.; Guajardo, A.; White, B.; Troncoso, J. C., et al., Large-scale proteomic analysis of Alzheimer's disease brain and cerebrospinal fluid reveals early changes in energy metabolism associated with microglia and astrocyte activation. *Nat Med* **2020,** *26*, 769-780.
190. Zhang, Q.; Ma, C.; Gearing, M.; Wang, P. G.; Chin, L. S.; Li, L. Integrated proteomics and network analysis identifies protein hubs and network alterations in Alzheimer's disease. *Acta Neuropathol Commun* [Online], **2018**. https://www.ncbi.nlm.nih.gov/pmc/articles/PMC5831854/pdf/40478_2018_Article_524.pdf.
191. Xu, J.; Patassini, S.; Rustogi, N.; Riba-Garcia, I.; Hale, B. D.; Phillips, A. M.; Waldvogel, H.; Haines, R.; Bradbury, P.; Stevens, A., et al. Regional protein expression in human Alzheimer's brain correlates with disease severity. *Commun Biol* [Online], **2019**. https://www.nature.com/articles/s42003-018-0254-9.pdf.
192. McKetney, J.; Runde, R.; Hebert, A. S.; Salamat, S.; Roy, S.; Coon, J. J., Proteomic atlas of the human brain in Alzheimer's disease. *J Proteome Res* **2019,** *18* (3), 1380-1391.
193. Johnson, E. C. B.; Dammer, E. B.; Duong, D. M.; Yin, L.; Thambisetty, M.; Troncoso, J. C.; Lah, J. J.; Levey, A. I.; Seyfried, N. T. Deep proteomic network analysis of Alzheimer's disease brain reveals alterations in RNA binding proteins and RNA splicing associated with disease. *Molec Neurodegen* [Online], **2018**. https://doi.org/10.1186/s13024-018-0282-4.
194. Carlyle, B. C.; Kandigian, S. E.; Kreuzer, J.; Das, S.; Trombetta, B. A.; Kuo, Y.; Bennett, D. A.; Schneider, J. A.; Petyuk, V. A.; Kitchen, R. R., et al., Synaptic proteins associated with cognitive performance and neuropathology in older humans revealed by multiplexed fractionated proteomics. *Neurobiol Aging* **2021,** *105*, 99-114.

195. Higginbotham, L.; Ping, L.; Dammer, E. B.; Duong, D. M.; Zhou, M.; Gearing, M.; Hurst, C.; Glass, J. D.; Factor, S. A.; Johnson, E. C. B., et al., Integrated proteomics reveals brain-based cerebrospinal fluid biomarkers in asymptomatic and symptomatic Alzheimer's disease. *Sci Adv* **2020,** *6* (43).
196. Moya-Alvarado, G.; Gershoni-Emek, N.; Perlson, E.; Bronfman, F. C., Neurodegeneration and Alzheimer's disease. What can proteomics tell us about the Alzheimer's brain? *Mol Cell Proteomics* **2015**, 10.1074/mcp.R115.053330.
197. Robinson, R. A. S.; Amin, B.; Guest, P. C., Multiplexing biomarker methods, proteomics and considerations for Alzheimer's disease. In *Proteomic Methods in Neuropsychiatric Research*, Guest, P. C., Ed. Springer International Publishing: Cham, **2017**, pp 21-48.
198. AD Knowledge Portal. https://www.synapse.org/#!Synapse:syn21347564 (accessed 06/03/2021).
199. Seyfried, N. T.; Dammer, E. B.; Swarup, V.; Nandakumar, D.; Duong, D. M.; Yin, L.; Deng, Q.; Nguyen, T.; Hales, C. M.; Wingo, T., et al., A multi-network approach identifies protein-specific co-expression in asymptomatic and symptomatic Alzheimer's disease. *Cell Syst* **2017,** *4* (1), 60-72.

CHAPTER 2

Investigating the Proteomic and Structural Impact of an Alzheimer's Disease-Associated ABCA7 Mutation

2.1 Introduction

It is well-established that the greatest genetic risk for late-onset Alzheimer's disease (LOAD) in non-Hispanic White adults is conferred by the apolipoprotein E (*APOE*) ε4 allele, which increases LOAD risk by 20-50%.[1] However, in African American/Black adults, mutations in the phospholipid-transporting ATPase ABCA7 *(ABCA7)* gene have stronger associations with LOAD than in non-Hispanic White adults,[2-4] increasing risk by 1.8 times.[2, 5] The *ABCA7* single nucleotide polymorphism (SNP) rs115550680 has an effect size in African American/Black adults comparable to *APOE* ε4.[1-2] In addition, some *ABCA7* variants have also been associated with LOAD more so in African American/Black adults, such as rs3752232, rs3764647, and rs142076058.[6-8]

ABCA7 mutations affecting African American/Black adults can be classified into common mutations with smaller effect sizes and rarer mutations with larger effect sizes (see **Table 1.2** in **Chapter 1**). The more common mutations occur in ~10-25% of individuals with normal cognition and ~15-30% of individuals with AD, and increase AD risk by up to 50%. Most are missense mutations resulting in a single amino acid substitution in the ABCA7 protein. This includes rs3764650, which increases AD risk by 10-20% in African American/Black adults,[9] though it has a larger effect size in non-Hispanic White[2, 10] and Colombian adults.[11] Higher percentages of African ancestry at this locus were also associated with AD.[4] Other

missense mutations include rs3764647 (odds ratio (OR) = 1.32-1.47),[6-7, 9] rs3752246 (OR = 1.15),[12] rs59851484 (OR = 1.49),[13] and rs3752232 (OR = 1.24).[13] The rarer mutations tend to occur in <1% of individuals with normal cognition and <2% of individuals with AD but increase AD risk by >70% (see **Table 1.2** in **Chapter 1**). This group includes rs3752239 (OR = 4.06),[6] the C allele from which has been contrastingly reported to have a protective effect against AD in non-Hispanic White adults.[13] This also includes rs115550680 mentioned above (OR = 1.79),[1-2] and the frameshift mutations rs142076058 and rs567222111, both of which more than double AD risk in African American/Black adults (OR = 2.13 and 2.42, respectively).[7, 13] The potential contributions of these *ABCA7* variants to AD pathogenesis are summarized in **Figure 2.1**.

The ABCA7 protein is a membrane-bound phospholipid transporter composed of 2,146 amino acids with integral functions in lipid metabolism and transport and phagocytosis.[5, 14-15] Its closest homologue is the *ABCA1* gene, the protein from which has also been observed to decrease apoE levels, and thereby increase amyloid deposition.[16] Compared to other members of the ABC transporter superfamily, ABCA1 and ABCA7 are distinctive as both contain two large extracellular domains (ECD1 and ECD2), which are critical for interacting with and transferring lipids to apolipoproteins.[17-18] Multiple studies show that both ABCA1 and ABCA7 mediate export of cholesterol and phospholipids, but with different preferred substrates and efficiencies.[19-20] ABCA7 loss of function can contribute to LOAD-related phenotypes through disruption of lipid rafts, dysregulation of lipid metabolism and amyloid precursor protein (APP) processing, and impaired phagocytic activity that consequently impairs amyloid-beta (Aβ) clearance.[2, 7, 21-22] It is hypothesized that *ABCA7* mutations likely contribute to LOAD risk and pathogenesis via reduced ABCA7 levels or altered/loss of function.[7, 21, 23] For example, the SNP rs3752232 results in a missense mutation causing a threonine to alanine substitution at position

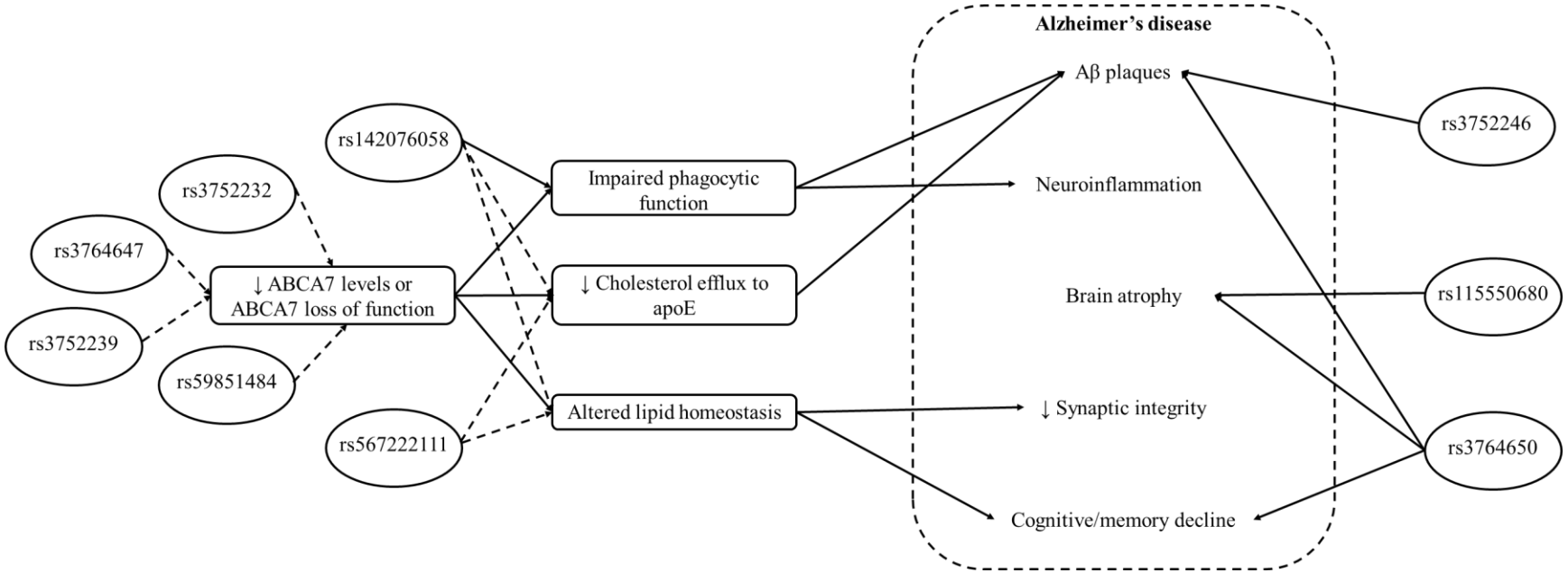

Figure 2.1. Summary of *ABCA7* variant contributions to AD pathogenesis. *ABCA7* SNPs that increase AD risk in African American/Black adults are shown in ovals. Solid arrows indicate proven effects of SNPs; dashed arrows indicate predicted or hypothesized effects of SNPs. Abbreviations: ABCA7, phospholipid-transporting ATPase ABCA7; apoE, apolipoprotein E; Aβ, amyloid-beta.

319 (T319A) in ECD1 of the ABCA7 protein. This mutation is associated with increased LOAD risk in African American/Black adults[6] and also decreased visuospatial and cognitive function in Korean Americans.[24] However, the subcellular effects of this variant remain unclear.

This study examined the impact of the T319A variant on protein structure and binding abilities, in addition to the downstream proteome effects in model human embryonic kidney 293 (HEK 293) cells. Homology models were built and lipid docking simulations were conducted to identify differences in structural conformations of the ECD1 of ABCA7 and to assess the impact of the T319A variant on binding lipid species. Quantitative proteomics was used to compare protein expression across cells transfected with the *ABCA7* T319A mutation, overexpression wild-type (WT) *ABCA7*, or an empty vector (EV). Overall, our findings provide insight into the structural and proteomic impact of the *ABCA7* rs3752232 (T319A) mutation and provide a first step to further understanding of how *ABCA7* variants confer genetic risk in LOAD.

2.2 Methods

2.2.1 Cloning and cell culture

The human *ABCA7* WT and T319A genes were synthesized, cloned into the pcDNA3.1(+) myc/His mammalian expression vector and sequenced (Biomatik, Wilmington, DE, USA). The empty vector pcDNA3.1(+) control was purchased commercially (Thermo Fisher Scientific, Waltham, MA, USA). For cell culture experiments, HEK 293 cells (American Type Culture Collection, Manassas, VA, USA) were maintained in Gibco Dulbecco's Modified Eagle Medium (Thermo Fisher Scientific, Waltham, MA, USA) supplemented with 10% fetal bovine serum (FBS) at 37°C with 5% CO_2. Low-passage cells were seeded in T25 flasks. When cells

were ~80% confluent, they were transfected with each *ABCA7* expression plasmid (WT or T319A) or an EV using polyethylenimine (PEI). After 24 h, the cell media was replaced. Cultures were allowed to grow for 48 h post-transfection then were trypsinized and washed with phosphate-buffered saline (PBS). Each cell type was split into aliquots of 5-6 x 10^6 cells and stored at -80°C.

2.2.2 Immunofluorescence

Adherent HEK 293 cells were cultured in 6-well plates on poly-D-lysine-coated cover slips and were seeded at 0.75 x 10^5 cells per well. The next day, the cells were transfected as described above. After 48 h, the cells were washed twice with PBS and then fixed with 3.7% paraformaldehyde for 15 min. All subsequent steps were conducted at room temperature. Cells were washed 3x with PBS and incubated with blocking/permeabilization buffer (PBS + 10% FBS + 0.1% Triton X-100) for 30 min. Cells were then incubated with ABCA7 antibody (sc-377335, Santa Cruz Biotechnology, Dallas, TX, USA) and the rabbit Na^+/K^+ ATPase antibody (sc-28800, Santa Cruz Biotechnology, Dallas, TX, USA) for 30 min then subjected to 3 x 5 min washes with PBS. Cells were incubated with Alexa Fluor488 goat anti-mouse IgG (Thermo Fisher Scientific, Waltham, MA, USA) or secondary mouse Alexa Fluor 594 (red) antibody for 30 min protected from light. Cells were washed 3 x 5 min with PBS. Cover slips were removed from the 6-well plate and mounted onto a microscope slide dotted with Prolong Gold Antifade mounting medium with DAPI (Thermo Fisher Scientific, Waltham, MA, USA). ABCA7 protein was visualized on a Nikon A1R confocal laser scanning microscope at excitation/emission wavelengths of 488/505-550 nm (green fluorescence).

2.2.3 ABCA7 Western blots

Whole cell lysates were prepared by lysing cells in radioimmunoprecipitation (RIPA) buffer (Research Products International Corporation, Mount Prospect, IL, USA) with the addition of mammalian protease inhibitor cocktail (Millipore Sigma, St. Louis, MO, USA). Equal amounts of protein were separated in 4-12% SDS gel, transferred to a nitrocellulose membrane, and immunoblotted using antibodies against the following proteins: ABCA7 (sc-377335, Santa Cruz Biotechnology, Dallas, TX, USA) and actin (sc-47778, Santa Cruz Biotechnology, Dallas, TX, USA).

2.2.4 Proteomics sample preparation

Two aliquots each of EV, WT, and T319A cells (i.e. workflow replicates) were lysed in RIPA buffer (50 mM Tris pH 7.5, 150 mM NaCl, 0.1% SDS, 1% Triton X-100, 0.5% deoxycholate) with complete mini EDTA-free protease inhibitor cocktail (Roche Diagnostics Gmbh, Mannheim, Germany). Protein concentration was determined using bicinchoninic acid (BCA) assay according to the manufacturer's protocols (Thermo Fisher Scientific, Waltham, MA, USA). A pooled sample containing equal protein amounts from each cell lysate was generated and served as a quality control (QC) sample. Protein integrity of all samples was tested by SDS-PAGE. Protein (50 μg) from each sample and the QC sample was digested using S-Trap™ micro spin columns according to the manufacturer's protocols (ProtiFi, Farmingdale, NY, USA). Briefly, protein was diluted with 10% SDS with 100 mM triethylammonium bicarbonate (TEAB; pH 7.55), reduced for 10 min at 95°C using 20 mM dithiothreitol, and subsequently alkylated with 40 mM iodoacetamide for 30 min at room temperature in the dark. Reduced and alkylated protein was acidified with 12% H_3PO_4 and diluted 6x with 90% aqueous

methanol with 100 mM TEAB, pH 7.1 prior to being loaded onto S-Traps™. Protein was digested with trypsin/Lys-C mix (Promega, Madison, WI, USA) for 1 h at 47 °C (1:25 enzyme:protein ratio). Peptides were then eluted from the S-Trap™ using 50 mM TEAB, 0.2% formic acid (FA), and 0.2% FA in acetonitrile in order. Eluates were pooled and dried prior to tagging. Tandem mass tags $(TMT)^{10}$-plex reagents were used to label 50 µg of each sample, i.e. the complete peptide eluate from S-Trap™ digestion (randomly selected seven channels: 126, 127N, 127C, 128N, 129N, 130C, 131; **Table B2.1**). The TMT-labeled mixture was fractionated using a gradient of acetonitrile at pH 10 to generate 16 fractions (3-8, 10, 12, 14, 16, 18, 20, 25, 30, 40, and 50%). Fractions were dried completely in a SpeedVac (Thermo Fisher Scientific, Waltham, MA, USA) and reconstituted in H_2O with 0.1% FA for liquid chromatography-tandem mass spectrometry (LC-MS/MS) analysis on a Q Exactive HF mass spectrometer (Thermo Fisher Scientific, Waltham, MA, USA). Fractions were randomly injected in triplicates.

2.2.5 LC-MS/MS analysis

An UltiMate 3000 RSLCnano system (Thermo Fisher Scientific, Waltham, MA, USA) was coupled to a Q Exactive HF mass spectrometer operated in positive mode for LC-MS/MS analyses. Peptides (2 µg) were loaded onto a Acclaim™ PepMap™ 100 C18 trap column (75 µm i.d. x 2 cm, 100 Å, 3 µm; Thermo Fisher Scientific, Waltham, MA, USA) prior to separation on an in-house C18 packed column (100 µm i.d. x 25 cm, 100 Å, 2.5 µm; Waters Corporation, Milford, MA, USA). The gradient was 180 min, as follows: 0-7 min, 10% B; 7-120 min, 10-30% B; 120-139 min, 30-60% B; 139-145 min, 60-90% B; 145-159 min, 90% B; 159-160 min, 90-10% B; 160-180 min, 10% B. Mobile phase A was 0.1% FA and mobile phase B was 0.1% FA in acetonitrile. Full MS spectra were collected 300-1,800 *m/z*, 120,000 resolution, automated

gain control (AGC) 1.0E6, and maximum injection time 100 ms. The instrument was operated in data-dependent acquisition (DDA) mode to acquire the top 15 MS/MS spectra using higher-energy collisional dissociation (HCD; normalized collision energy 30%, 45,000 resolution, isolation width 4.0 m/z, AGC 1.0E5, maximum injection time 50 ms) and dynamic exclusion of 10 s. The minimum AGC required for MS/MS scans was 8.0E3. No charge states were excluded for MS/MS selection and peptide match was set to preferred, such that signals with peptide-like isotopic distributions would be preferentially selected for MS/MS scans.

2.2.6 Proteomics data analysis

RAW files were analyzed using Proteome Discoverer software (version 2.4). All technical replicates and fractions were combined into one result file and searched against the UniProt human reviewed protein database (3/16/2020, 25,998 sequences) with the ABCA7 T319A sequence added using SEQUEST-HT. A fixed modification of cysteine carbamidomethylation and variable modifications of methionine oxidation and TMT^{10}-plex (229.163 Da) on lysine residues and peptide N-termini were included in the search. A maximum of two trypsin miscleavages were allowed. Mass tolerances for the search were 10 ppm for precursors and 0.6 Da for fragments. Peptide confidence of high (< 1% false discovery rate (FDR) against decoy database), ≥ 1 unique peptide, and ≥ 2 peptide spectral matches (PSMs) were required for confident protein identification.

The TMT^{10}-plex quantification method in Proteome Discoverer 2.4 was modified to only include TMT^{10}-plex channels utilized in this experiment. Reporter ion quantitation was based on intensity with a reporter signal-to-noise threshold of 10. Protein and peptide groups identified are referred to as proteins and peptides, respectively, throughout.

Processing of data is shown in **Data B2.1**. Post-analysis filtering was performed to only include proteins identified with reporter ion intensities in all seven channels above threshold. These proteins were considered to be quantified proteins, and their TMT reporter ion intensities were normalized to the intensity of the pooled sample.[25-26]

Differentially-expressed proteins were identified between each pair of cell types using two-tailed T-tests ($p < 0.05$) and fold change (FC) cutoffs of < 0.83 and > 1.21, established based on technical and biological variation and level of technical and biological replication.[27] Fold changes between each pair of cell types were calculated using average normalized TMT reporter ion intensities for each cell type. STRING was used to analyze interactions among differentially-expressed proteins.[28]

2.2.7 Computational analyses – 3D structure prediction and validation

An experimental 3D structure of the ABCA7 membrane transport protein is not currently available; however, the structure of the closest homologue, the lipid transporter ABCA1, has been previously determined at 4.1 Å resolution by cryogenic electron microscopy.[29] ABCA7 shares 54% overall sequence identity with ABCA1, and there is ~38% sequence identity shared between the first ECDs of each. For the WT protein, we utilized the Protein Homology/Analogy Recognition Engine V 2.0 (Phyre2) web-based portal for homology modeling using the amino acids (47-629) corresponding to the ECD1 of ABCA7, which used the ABCA1 structure as a template (PDB code: 5xjy).[30] Phyre2 produced a set of potential 3D models. The models were ranked by a raw alignment and assigned a Confidence score that represents the probability that the match is true homology. The best model with the highest Confidence score was chosen. Loop modeling and protein optimization was done using MODELLER.[31] To create the *ABCA7* genetic

T319A variant (rs3752232), we replaced the Thr amino acid with the Ala rotamer and performed energy minimization using University of California San Francisco (UCSF) Chimera.[32] Homology models were validated using various modules in the Structural Analysis and Verification Server (SAVES) server.[33-34] The validated WT and T319A models were used to conduct docking studies of known lipids using the molecular docking software AutoDock Vina[35] and visualization of docking results and identification of putative binding sites was performed using UCSF Chimera.[32]

2.3 Results

HEK 293 cells were transfected with an EV, WT *ABCA7*, or the *ABCA7* T319A mutant and the impact of the T319A mutation on ABCA7 structure, localization, and the proteome were assessed. ABCA7 expression in all three cell types was confirmed via Western blot. Molecular dynamics of the ECD1 of ABCA7 were explored to identify structural effects of the T319A mutation compared to WT ABCA7, including abilities of the ECD1 to bind lipids. Immunofluorescence was used to compare localization of WT ABCA7 and the T319A variant. Two aliquots of EV, WT, and T319A cells with the addition of a pooled sample were analyzed using discovery-based TMT quantitative proteomics to identify downstream proteomic differences among the three cell types.

2.3.1 Structural impact of the T319A mutation

Homology models of the ABCA7 ECD1 suggest regions of the protein result in small conformational changes in the T319A variant compared to WT (**Figure 2.2A**). Based on the model, these differences are in alpha helices distal to the T319A mutation, despite the mutation

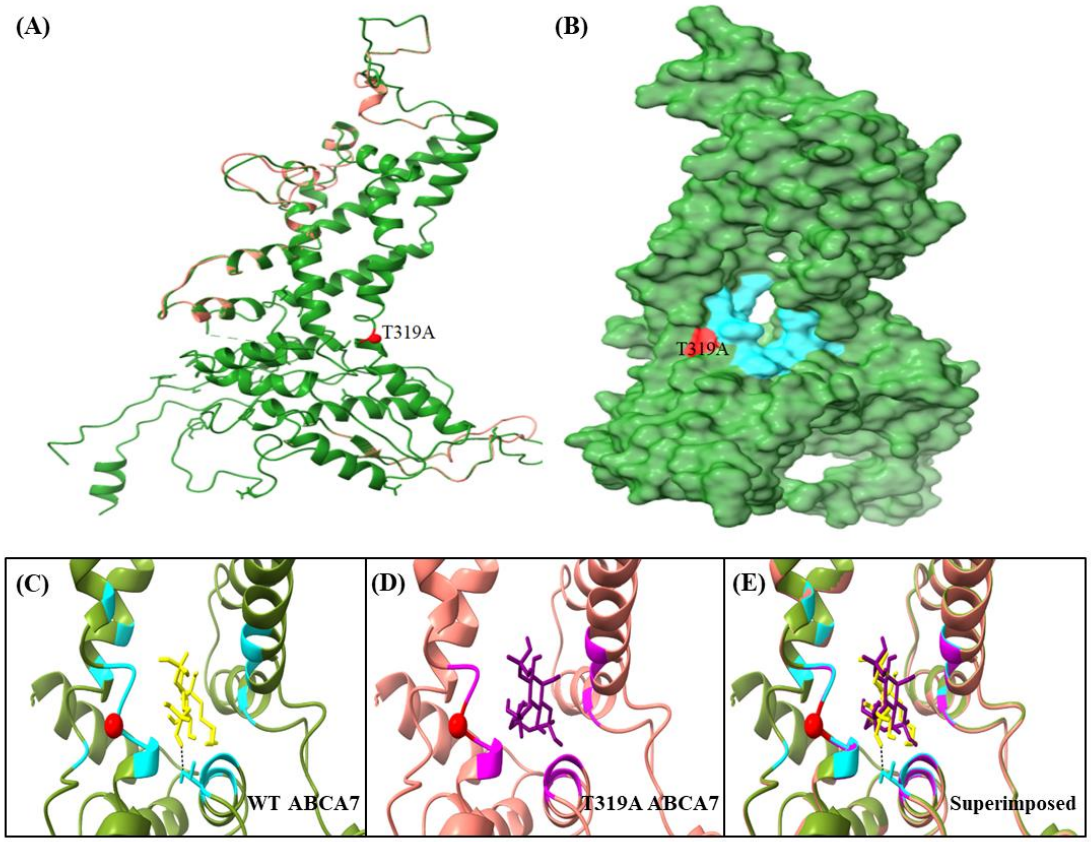

Figure 2.2. Structural comparison of ABCA7 WT and T319A variant and molecular docking. (A) Structural alignment of the ABCA7 ECD homology model. The T319A variant (pink) is superimposed on top of the WT structure (green). The structural impact of the T319A variant (red sphere) are the regions that appear pink. RMSD = 0.963 Å. **(B)** A surface representation of the ABCA7 ECD illustrates that the T319A missense variant (red) resides near a putative binding pocket (cyan) and can potentially impact the binding of various lipid species. **(C)** Cartoon representation of PIP_2 (yellow) docked with WT ABCA7 (green) (ΔG = -4.4 kcal/mol). ABCA7 binding site residues within 4.0 Å of the PIP_2 molecule are shown in cyan. PIP_2 forms a hydrogen bond with Thr66 (shown as a black dashed line). **(D)** Cartoon representation of PIP_2 (purple) docked with T319A ABCA7 (pink) (ΔG = -3.9 kcal/mol). Binding site residues within 4.0 Å of the PIP_2 molecule are shown in magenta. The hydrogen bond observed with Thr66 in the WT model disappears with the T319A mutation. **(E)** Docked cartoon models of WT and T319A ABCA7 were superimposed. Notably, PIP_2 appears to bind to the T319A mutant in a different orientation compared to WT. Abbreviations: RMSD, root-mean-square deviation of atomic positions. Figure contributed by the laboratory of Dr. Jamaine S. Davis.

being situated in close proximity to a putative ligand binding site (**Figure 2.2B**). Subsequently, we used molecular docking software to test the ability of several lipid species (phosphatidylinositol, PI; phosphatidylcholine, PC; phosphatidylglycerol, PG; phosphatidylethanolamine, PE; lysophosphatidylcholine, LPC; and sphingomyelin, SM) to bind in the vicinity of the putative binding pocket. Furthermore, we also specifically assessed the interaction of WT or T319A with a specific PI subspecies member, phosphatidylinositol 4,5-bisphosphate (PIP_2), which is a critical lipid messenger shown to be important in LOAD pathogenesis. The results of our lipid docking studies suggest that the Thr residue interacts with PIP_2, and the T319A variant altered the ability of known lipids to bind the ECD1 of ABCA7 (**Table 2.1**) and has reduced interactions with PIP_2 (**Table 2.2**). In particular, the T319A variant exhibited a decrease in hydrogen bonding between the PIP_2 molecule and binding site residues that was observed in the WT model. It was noted that the PIP_2 molecule interacted with the T319A variant in a different physical orientation than WT. We compared the putative PIP_2 binding site of ABCA7 with the reported binding site of ABCA1 and several residues that interact with PIP_2 are conserved in ABCA7 (**Figure 2.3**). Through this model, we have identified putative lipid binding sites within the ECD1 that may help to regulate the overall function of ABCA7. For example, reduced binding of a class of lipids, like PIP_2, may lead to lower levels in overall lipid signaling, thereby influencing AD pathology.

2.3.2 Effect of ABCA7 expression in HEK 293 cells

To assess the impact of *ABCA7* variants, we used HEK 293 cells to study the overexpression of WT *ABCA7* and expression of the T319A mutant. Western blot results show

Table 2.1. Computed binding free energies of lipid species to WT *ABCA7* and T319A variant.

	Lipid substrate binding free energies (kcal/mol)					
***ABCA7* variant**	**PG**	**PE**	**PI**	**LPC**	**SM**	**PS**
WT	-4.8	-4.6	-4.7	-4.3	-11.1	-4.9
T319A	-5.2	-4.6	-5	-4.2	-10.6	-4.6

Abbreviations: PG, phosphatidylglycerol; PE, phosphatidylethanolamine; PI, phosphatidylinositol; LPC, lysophosphatidylcholine; SM, sphingomyelin; PS, phosphatidylserine. Table contributed by the laboratory of Dr. Jamaine S. Davis.

Table 2.2. Molecular docking results of PIP_2 substrate.

ABCA7 variant	Computed PIP_2 binding free energies (kcal/mol)	Putative Binding Site Residues[a]
WT	-4.4	**Thr66**, Val67, Leu70, Gln71, Ile74, Val102, Leu105, Leu106, Leu224, Glu317, Leu318, **Thr319**, Leu320, Leu321, Val324, Leu400, Val403, Leu407
T319A	-3.9	Thr66, Val67, Leu70, Gln71, Ile74, Leu106, Leu224, Glu317, Leu318, Leu320, Leu321

[a]Residues that were shown to form hydrogen bonds with PIP_2 upon docking are in bold red and the site of the rs3752232 missense variant is in bold. Table contributed by the laboratory of Dr. Jamaine S. Davis.

Figure 2.3. ClustalW sequence alignment of the extracellular domains (ECD1) of ABCA1 (amino acids 45-630) and ABCA7 (amino acids 47-629). The conserved PIP_2 binding residues are shown in green. "*" indicates a conserved residue; ":" indicates conservation between groups of strongly similar amino acid properties; "." indicates conservation between groups of weakly similar amino acid properties. Figure contributed by the laboratory of Dr. Jamaine S. Davis.

that both WT and T319A cells had ABCA7 protein expressed at comparable levels, while ABCA7 was not detected in EV cells (**Figure 2.4**), consistent with previous studies in HEK 293 cells.[36] However, by MS, ABCA7 protein expression was detected in all three cell types and was significantly increased in WT cells compared to EV and T319A cells (**Figure 2.5**). RT-PCR, followed by Sanger sequencing, also confirmed the presence of WT and T319A ABCA7 in transfected cells (**Figure 2.6**). ABCA7 also appeared in the EV samples, suggesting that ABCA7 is indeed expressed. The increased sensitivity of MS and PCR compared to Western blots likely allowed the detection of the relatively low ABCA7 expression in the EV cells.[37] In our proteomics analyses, ABCA7 was identified from 31 peptides and 208 PSMs (**Figure 2.5**, **Table 2.3**). Example MS and MS/MS spectra matching the ABCA7 peptide containing amino acid 319 (TFEEL**T**LLR) – where the T319A mutation is located – are shown in **Figures 2.5A-B**. However, the mutated peptide (TFEEL**A**LLR) was not detected. Additionally, immunofluorescence studies show that the T319A mutation did not impact ABCA7 localization, as both WT ABCA7 and the T319A variant were observed to co-localize with the Na^+/K^+ ATPase in the plasma membrane (**Figure 2.7**). No ABCA7 staining was detected in the EV cells (**Figure 2.7**).

Discovery-based quantitative proteomics analysis of the EV, WT, and T319A cells yielded a total of 3,913 and 30,580 identified proteins and peptides, respectively. Of these proteins, 3,152 were quantified in all cells and replicates. We compared each pair of cell types (EV vs WT, EV vs T319A, WT vs T319A) and identified 202 differentially-expressed proteins across these comparisons (**Figure 2.8, Table B2.2**). There were fewer differentially-expressed proteins between EV and T319A cells (N = 7) compared to EV vs WT cells (N = 168) and WT

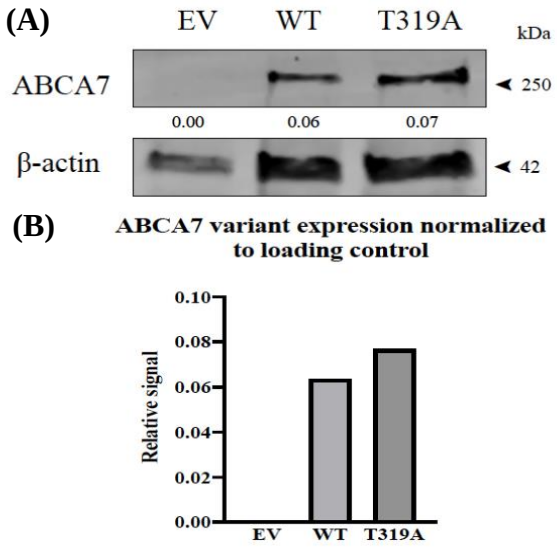

Figure 2.4. Detection of ABCA7 expression in HEK 293 cells. (A) Immunoblot of ABCA7 expression in HEK 293 cells cultured and transfected as described in **Section 2.2.3**. Approximately 50 μg of cell lysate was used in each lane. **(B)** ABCA7 variant expression was normalized to the β-actin loading control. Figure contributed by the laboratory of Dr. Jamaine S. Davis.

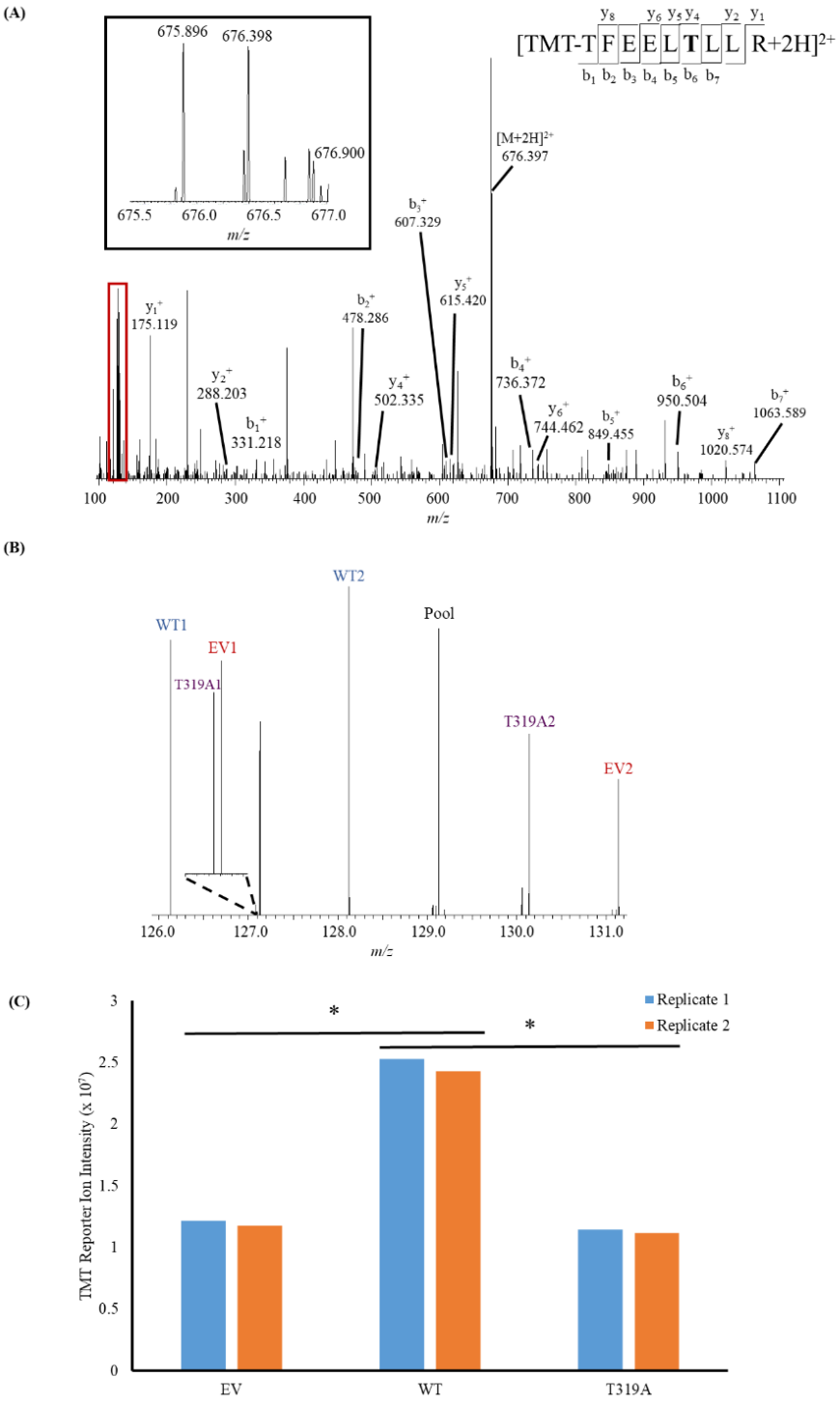

Figure 2.5. ABCA7 identification and expression in EV, WT, and T319A cells from proteomics analyses. (A) MS and MS/MS spectra of peptide [TMT-TFEELTLLR +2H]2+ from ABCA7 with red box indicating **(B)** zoom of TMT reporter ions. **(C)** ABCA7 intensity across cell types. Blue and orange bars indicate replicates 1 and 2 of each cell type, respectively. Two-tailed T-tests were used to compare ABCA7 intensity between each pair of cell types (N = 2 replicates per cell type). * indicates $p < 0.05$.

```
ABCA7 template       GCCCTCTGCAGTGTCAGGGGACCTAGCAGCACAGTGGGCCCCTCCCTCAACTGGTACGAG      120
PCDNA-WT_ABCA7      ---------------------------------------------TNNCANNNGGGNNNN      15
PCDNA-EV            ---------------------------------------------TCAACTGGNTNNGAG      15
PCDNA-319_ABCA7     ---------------------------------------------NCAACTGGTTACGAG      15

ABCA7 template       GCTAGTGACCTGATGGAGCTGGTGGGGCAGGAGCCAGAATCCGCCCTGCCAGACAGCAGC      180
PCDNA-WT_ABCA7      NCTAGTGACCTGATGGAGCTGGTGGGGCAGGAGCCAGAATCCGCCCTGCCAGACAGCAGC      75
PCDNA-EV            GCTAGTGACCTGATGGAGCTGGTGGGGCAGGAGCCAGAATCCGCCCTGCCAGACAGCAGC      75
PCDNA-319_ABCA7     GCTAGTGACCTGATGGAGCTGGTGGGGCAGGAGCCAGAATCCGCCCTGCCAGACAGCAGC      75
                     ************************************************************

ABCA7 template       CTGAGCCCCGCCTGCTCGGAGCTGATTGGAGCCCTGGACAGCCACCCGCTGTCCCGCCTG      240
PCDNA-WT_ABCA7      CTGAGCCCCGCCTGCTCGGAGCTGATTGGAGCCCTGGACAGCCACCCGCTGTCCCGCCTG      135
PCDNA-EV            CTGAGCCCCGCCTGCTCGGAGCTGATTGGAGCCCTGGACAGCCACCCGCTGTCCCGCCTG      135
PCDNA-319_ABCA7     CTGAGCCCCGCCTGCTCGGAGCTGATTGGAGCCCTGGACAGCCACCCGCTGTCCCGCCTG      135
                    ************************************************************

ABCA7 template       CTCTGGAGACGCCTGAAGCCTCTGATCCTCGGGAAGCTACTCTTTGCACCAGATACACCT      300
PCDNA-WT_ABCA7      CTCTGGAGACGCCTGAAGCCTCTGATCCTCGGGAAGCTACTCTTTGCACCAGATACACCT      195
PCDNA-EV            CTCTGGAGACGCCTGAAGCCTCTGATCCTCGGGAAGCTACTCTTTGCACCAGATACACCT      195
PCDNA-319_ABCA7     CTCTGGAGACGCCTGAAGCCTCTGATCCTCGGGAAGCTACTCTTTGCACCAGATACACCT      195
                    ************************************************************

ABCA7 template       TTTACCCGGAAGCTCATGGCCCAGGTGAACCGGACCTTCGAGGAGCTCACCCTGCTGAGG      360
PCDNA-WT_ABCA7      TTTACCCGGAAGCTCATGGCCCAGGTGAACCGGACCTTCGAGGAGCTCACCCTGCTGAGG      255
PCDNA-EV            TTTACCCGGAAGCTCATGGCCCAGGTGAACCGGACCTTCGAGGAGCTCACCCTGCTGAGG      255
PCDNA-319_ABCA7     TTTACCCGGAAGCTCATGGCCCAGGTGAACCGGACCTTCGAGGAGCTCACCCTGCTGAGG      255
                    ************************************************************

ABCA7 template       GATGTCCGGGAGGTGTGGGAGATGCTGGGACCCCGGATCTTCACCTTCATGAACGACAGT      420
PCDNA-WT_ABCA7      GATGTCCGGGAGGTGTGGGAGATGCTGGGACCCCGGATCTTCACCTTCATGAACGACAGT      315
PCDNA-EV            GATGTCCGGGAGGTGTGGGAGATGCTGGGACCCCGGATCTTCACCTTCATGAACGACAGT      315
PCDNA-319_ABCA7     GATGTCCGGGAGGTGTGGGAGATGCTGGGACCCCGGATCTTCACCTTCATGAACGACAGT      315
                    ************************************************************

ABCA7 template       TCCAATGTGGCCATGCTGCAGCGGCTCCTGCAGATGCAGGATGAAGGAAGAAGGCAGCCC      480
PCDNA-WT_ABCA7      TCCAATGTGGCCATGCTGCAGCGGCTCCTGCAGATGCAGGATGAAGGAAGAAGGCAGCCC      375
PCDNA-EV            TCCAATGTGGCCATGCTGCAGCGGCTCCTGCAGATGCAGGATGAAGGAAGAAGGCAGCCC      375
PCDNA-319_ABCA7     TCCAATGTGGCCATGCTGCAGCGGCTCCTGCAGATGCAGGATGAAGGAAGAAGGCAGCCC      375
                    ************************************************************

ABCA7 template       AGACCTGGAGGCCGGGACCACATGGAGGCCCTGCGATCCTTTCTGGACCCTGGGAGCGGT      540
PCDNA-WT_ABCA7      AGACCTGGAGGCCGGGACCACATGGAGGCCCTGCGATCCTTTCTGGACCCTGGGAGCGGT      435
PCDNA-EV            AGACCTGGAGGCCGGGACCACATGGAGGCCCTGCGATCCTTTCTGGACCCTGGGAGCGGT      435
PCDNA-319_ABCA7     AGACCTGGAGGCCGGGACCACATGGAGGCCCTGCGATCCTTTCTGGACCCTGGGAGCGGT      435
                    ************************************************************
```

Figure 2.6. Sequencing of *ABCA7* pcDNA amplicons. Clustal Omega sequence results of pcDNA- empty vector (EV), wild-type *ABCA7* (WT), and T319A *ABCA7* (319) PCR amplicons confirming the presence of the T319A mutation (ACC → GCC). PCR amplification using *ABCA7*-specific primers was performed on cDNA synthesized from RNA isolated from transiently transfected HEK293FT cells. Figure contributed by the laboratory of Dr. Jamaine S. Davis.

Table 2.3. Peptides from ABCA7 identified in proteomics analyses.

Peptide Sequence	Modifications	Sequence Position	PSMs	XCorr Score[a]
QSPLEPPMLDVAELLTSLLR	TMT [N-Term]	146-165	7	5.92
GTSGPLELLSEALCSVR	TMT [N-Term]; Carbamidomethyl [C14]	212-228	2	4.3
LKPLILGK	TMT [N-Term]; TMT [K2]; TMT [K8]	287-294	3	3.1
LLFAPDTPFTR	TMT [N-Term]	295-305	22	3.4
TFEEL**T**LLR[b]	TMT [N-Term]	314-322	11	3.1
EVWEMLGPR	TMT [N-Term]	326-334	10	3.09
LEAAPSEAALVSR	TMT [N-Term]	412-424	12	3.92
ALQLLAEHR	TMT [N-Term]	425-433	18	3.2
MDIDVVTR	TMT [N-Term]	468-475	2	2.6
FWDPGPAADPLTDLR	TMT [N-Term]	483-497	1	2.67
VLVEEAPPGLSPGVSVR	TMT [N-Term]	794-810	7	5.24
GLSAAVVGPEQDR	TMT [N-Term]	910-922	5	3.6
LLQDVGLVSK	TMT [N-Term]; TMT [K10]	923-932	6	3.59
GIWELLLK	TMT [N-Term]; TMT [K8]	977-984	9	2.8
LPLTTNEK	TMT [N-Term]; TMT [K8]	1042-1049	3	2.63
ADTDMEGSVDTR	TMT [N-Term]	1050-1061	2	4.42
VGTPQLLALVQHWVPGAR	TMT [N-Term]	1073-1090	5	6.79
QQLQALLLK	TMT [N-Term]; TMT [K9]	1219-1227	3	3.86
FSAPEVPAEVAK	TMT [N-Term]; TMT [K12]	1318-1329	2	2.36
SVEELWALLSPLPGGALDR	TMT [N-Term]	1435-1453	11	5.52
GWHSMVAFVNR	TMT [N-Term]	1479-1489	2	2.49
NQAMADAFER	TMT [N-Term]	1706-1715	1	3.25
SLPLLGEEDEDVAR	TMT [N-Term]	1765-1778	34	4.84
VVQGATQGDVLVLR	TMT [N-Term]	1783-1796	5	2.32
MVTGDTLASR	TMT [N-Term]	1839-1848	4	2.85
GVPEAQVAQTAGSGLAR	TMT [N-Term]	1896-1912	3	4.12
LGLSWYADRPAGTYSGGNK	TMT [N-Term]; TMT [K19]	1913-1931	1	2.7
LATALALVGDPAVVFLDEPTTGMDPSAR	TMT [N-Term]	1934-1961	1	6.11
FLWNSLLAVVR	TMT [N-Term]	1963-1973	3	3.65
SQPAAAFVAAEFPGAELR	TMT [N-Term]	2031-2048	12	5.35
EAGVGVDPAPGLQHPK	TMT [N-Term]; TMT [K16]	2115-2130	1	3.49

[a]XCorr score is calculated by SEQUEST HT during the Proteome Discoverer search of raw data to score how well a peptide matches to a given spectrum, with a higher score indicating a better match. [b]This is the peptide that contains amino acid 319 where the T319A variant is located. However, only the WT peptide was detected.

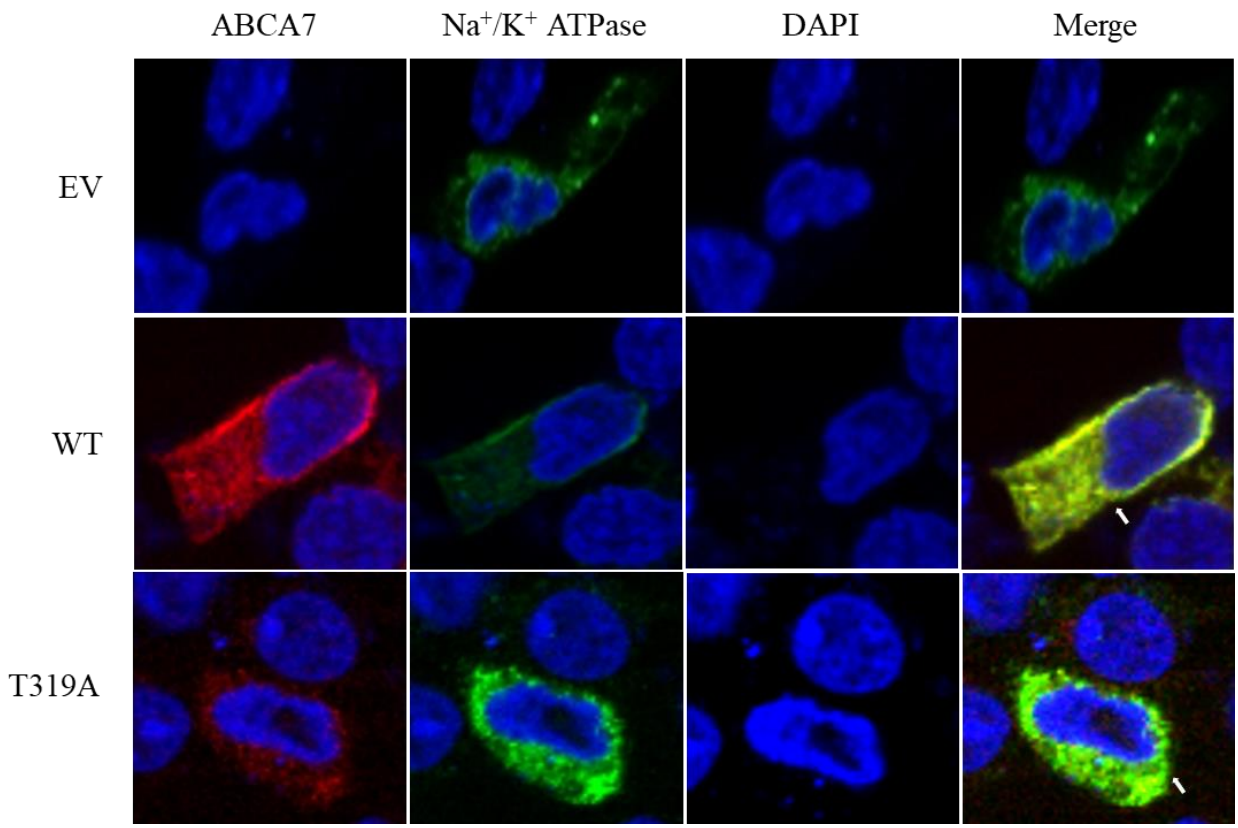

Figure 2.7. Subcellular localization of ABCA7 protein variants. HEK 293 cells were cultured in 35 mm dishes and transfected with the empty vector, *ABCA7* WT or T319A expression plasmids. Immunofluorescence experiments illustrate both WT ABCA7 and the ABCA7 T319A variant localize to the membrane where it is detected by the ABCA7 antibody and visualized using the AlexaFluor 594 (red) antibody using the confocal microscope. The Na^+/K^+ ATPase membrane protein is stained using the AlexaFluor 488 secondary (green) antibody. The nuclei were stained with DAPI (blue). The merged images show areas of co-localization between ABCA7 and Na^+/K^+ ATPase (yellow; white arrows). Figure contributed by the laboratory of Dr. Jamaine S. Davis.

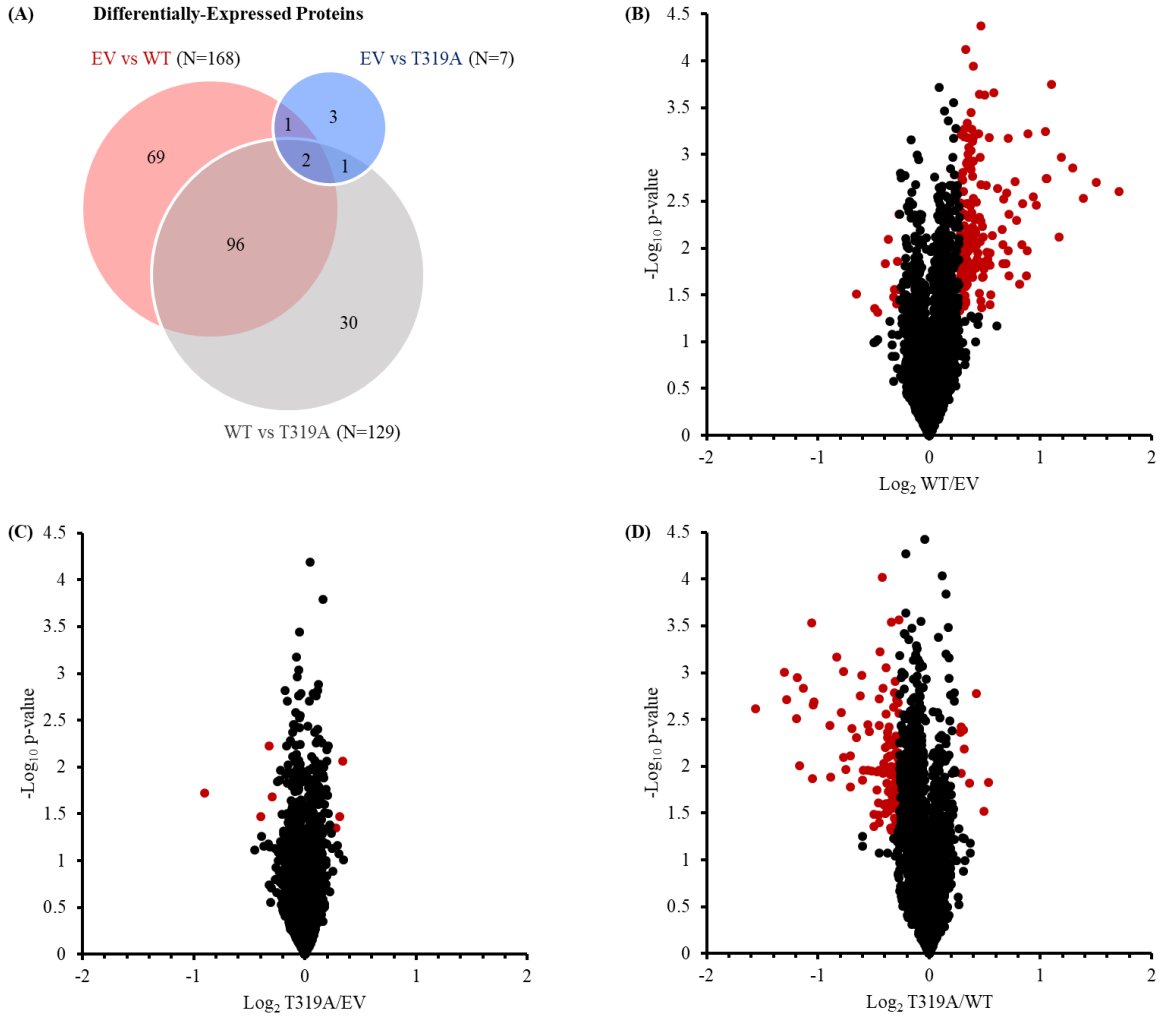

Figure 2.8. Differentially-expressed proteins between EV, WT, and T319A cells from proteomics analyses. (A) Venn diagram showing overlap in differentially-expressed proteins across the three pairwise comparisons with corresponding volcano plots showing comparisons of CV-filtered quantified proteins (N = 2,913) between **(B)** EV and WT, **(C)** EV and T319A, and **(D)** WT and T319A. Red data points indicate proteins with p-value < 0.05 and FC > 1.21 or < 0.83; black data points indicate quantified proteins that did not meet both the p-value and FC cutoffs.

vs T319A cells (N = 129; **Figure 2.8A**). Many differentially-expressed proteins in EV vs WT cells were also differentially expressed in WT vs T319A cells (N = 96). Only two proteins (i.e., cell division cycle protein 123 homolog and ubiquitin-like protein 5) were differentially expressed in all three comparisons. Both proteins were increased in WT and T319A compared to EV cells and decreased in T319A compared to WT cells.

STRING analysis was used to create protein interaction networks of differentially-expressed proteins from EV vs WT and WT vs T319A cell comparisons (**Figure 2.9**). Specific networks were observed for proteins increasing in WT vs EV cells (N = 157) and those decreasing in T319A vs WT cells (N = 120). A total of 96 proteins were significant in both comparisons. Two main clusters of protein interaction networks were found: ribosomal proteins and signal transduction/immune response proteins. Notably, ABCA7 is not in the ribosomal nor signal transduction/immune response clusters, but rather is only connected to one other protein, 5'-3' exonuclease phospholipase D3 (PLD3).

Finally, the proteomics data were mined to examine the expression of proteins in the PIP_2 metabolism pathway across cell types (**Figure 2.10**). Interestingly, 1-phosphatidylinositol 4,5-bisphosphate phosphodiesterase eta-1 (PLCH1), which hydrolyzes PIP_2 into diacylglycerol (DAG) and inositol 1,4,5-trisphosphate (IP_3), was increased in WT compared to EV and T319A cells. However, other enzymes in the PIP_2 metabolism pathway were generally similar across all of the cell types such as 1-phosphatidylinositol 4,5-bisphosphate phosphodiesterase gamma-1 (PLCG1), phosphatidylinositol 4-kinase type 2-alpha (PI4K2A), and phosphatidylinositol 5-phosphate 4-kinase type-2 gamma (PIP4K2C).

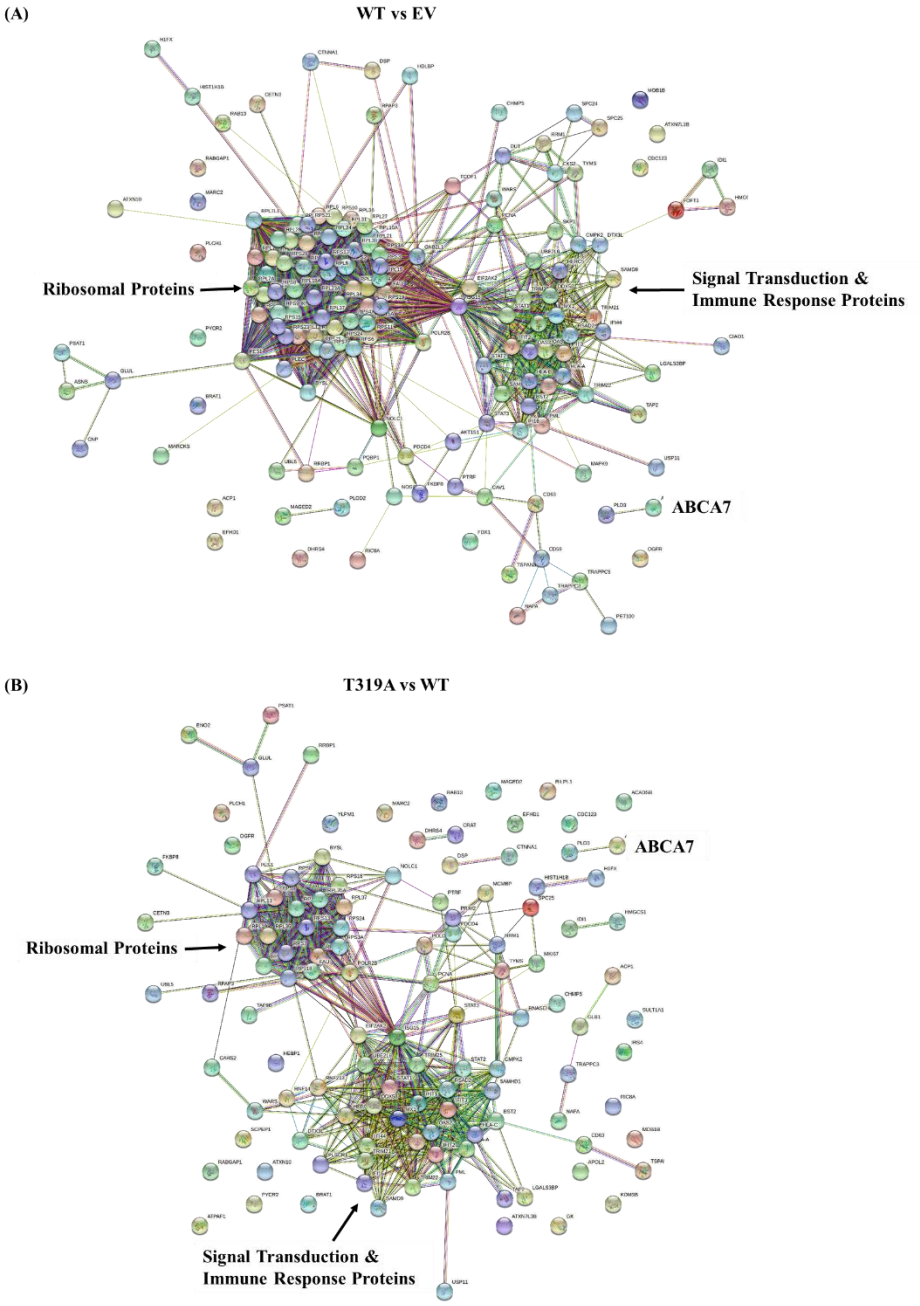

Figure 2.9. STRING protein interaction networks of selected differentially-expressed proteins from proteomics analyses. STRING protein interaction networks of differentially-expressed proteins that were **(A)** increased in WT vs EV cells (N = 157) and **(B)** decreased in T319A vs WT cells (N = 120), many of which (N = 96) were significant in both comparisons. ABCA7 is labeled in each network, and the function associated with each main cluster of proteins is noted.

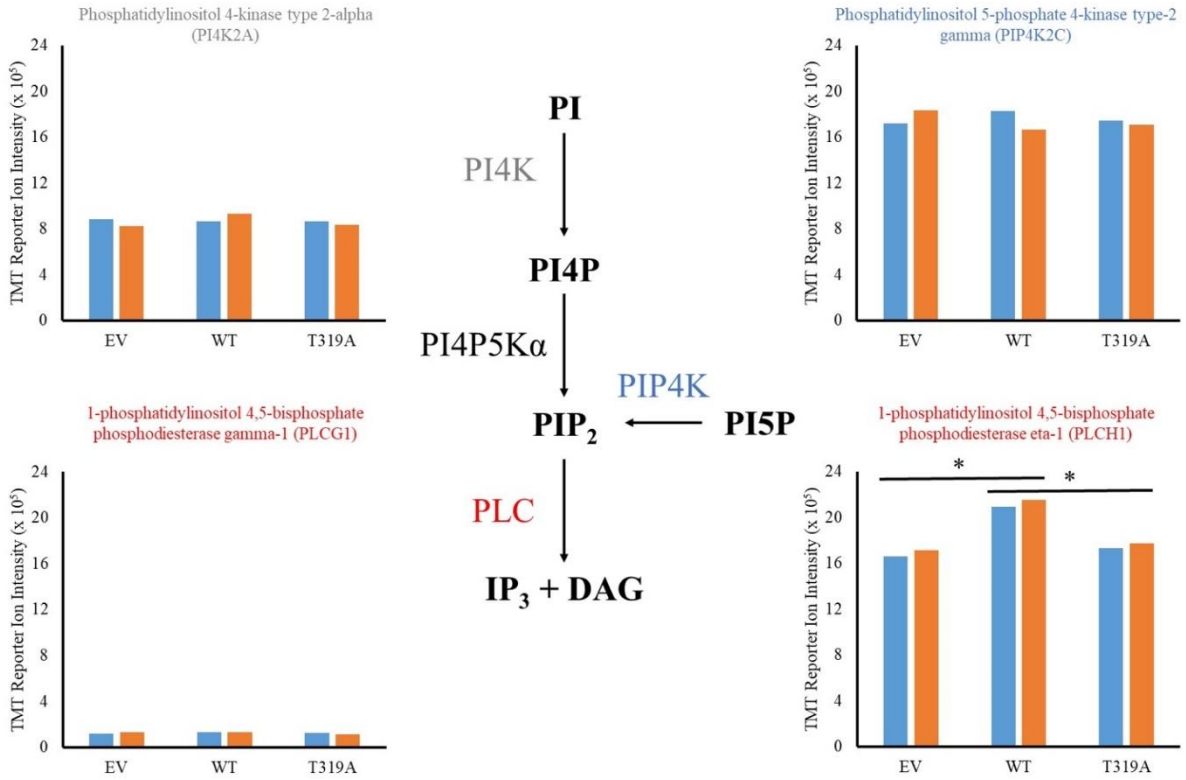

Figure 2.10. Protein expression in the PIP_2 pathway across cell types. PIP_2 metabolism pathway showing corresponding protein expression across cell types for quantified proteins (N = 4). PLCH1 was significantly increased in WT compared to EV and T319A cells, while the other three proteins in this pathway were not differentially expressed. Blue and orange bars represent replicates 1 and 2 of each cell type, respectively. Abbreviations: PI, phosphatidylinositol; PI4K, phosphatidylinositol 4-kinase; PI4P, phosphatidylinositol 4-phosphate; PI4P5Kα, phosphatidylinositol 4-phosphate 5-kinase α; PIP_2, phosphatidylinositol (4,5)-bisphosphate; PI5P, phosphatidylinositol 5-phosphate; PIP4K, phosphatidylinositol 5-phosphate 4-kinase; PLC, phospholipase C; IP_3, inositol 1,4,5-trisphosphate; DAG, diacylglycerol.

2.4 Discussion

LOAD is a complex disease and considerable evidence illustrates that its pathology is linked to disruption of lipid homeostasis.[38-41] Genetic changes in LOAD risk factors, such as *ABCA7,* can impact disease pathogenesis through a variety of mechanisms. Alterations of the brain lipid profile of *ABCA7* knockout mice displayed memory impairment and the accumulation of Aβ peptides.[42] Our study has found subtle structural differences in the protein structure and binding abilities of the ABCA7 ECD1. The flexibility of the ECD1 plays an important role in lipid transport, but the full repertoire of its lipid and protein substrates are unknown. Interestingly, the reduced binding of PIP_2 observed in our study by the T319A variant has implications that may further understanding of the molecular mechanism of ABCA7.

PIP_2 is a major lipid messenger that controls neuronal and synaptic plasticity, and AD brains show reduced levels of PIP_2.[43] ABCA1 has been shown to transport PIP_2 to the cell surface, where it binds to apolipoprotein A-I.[44] The conservation of several residues that line the lipid binding pocket in ABCA7 suggest that PIP_2 may be a critical factor in dissecting the role of ABCA7 in the pathogenesis of AD, as reduced levels of PIP_2 have been reported to influence Aβ toxicity.[45] Increased expression of PLCH1 protein in WT compared to EV and T319A cells suggests that ABCA7 impacts the downstream production of DAG and IP_3 and potentially increases turnover of PIP_2 production. Furthermore, increased DAG levels have been previously reported in plasma and brain of individuals with mild cognitive impairment (MCI) and AD.[46-48] Interestingly, another PLC detected in our data, PLCG1, with a similar function to PLCH1 was not different across cell types (**Figure 2.10**). Therefore, mechanisms that restore levels of lipids like PIP_2 may be an attractive target for novel therapeutics to treat AD in patients with *ABCA7* variants.

Our proteomic analyses revealed significantly increased levels of ABCA7 in WT cells compared to EV and T319A cells, consistent with the overexpression of WT *ABCA7*. On the other hand, EV and T319A cells had similarly lower levels of ABCA7, indicating that levels of ABCA7 in the T319A cells were similar to endogenous levels found in HEK 293 cells. It is interesting to note that expression of the T319A variant did not lead to an increase in ABCA7 above endogenous levels observed in the WT cells. It is possible that this mutation could be causing decreased ABCA7 expression, as is predicted for another LOAD-associated *ABCA7* mutation.[21] This could also be due to increased protein degradation or turnover of the mutant ABCA7 protein. However, further studies are necessary to confirm these hypotheses. These possibilities may further contribute to the reason that the T319A-mutated peptide was not detected in the proteomic experiments. The T319A peptide was likely present in extremely low amounts such that it was below the limit of detection for the LC-MS/MS experiments, while the WT peptide was highly detectable based on its overexpression in the WT cell line. In-gel digestion of gel bands for ABCA7 followed by both untargeted and targeted MS analysis of TFEELTLLR and TFEELALLR peptides did not result in detection of TFEELALLR peptide (*data not shown*). Furthermore, the WT peptide TFEELTLLR was only detected in the WT cell line (and not in EV or T319A).

Across pairwise comparisons of the three cell types, 202 proteins were differentially expressed, most of which occurred in the WT vs EV and WT vs T319A cell comparisons. Significantly fewer proteins were differentially expressed between EV and T319A cells (N = 7; **Table B2.2**), suggesting that the T319A variant does not impart large-scale downstream effects on the proteome. Furthermore, WT *ABCA7* cells had a more significant effect on the proteome

than the T319A mutation, likely due to increased expression of ABCA7 from endogenous and vector-induced levels.

One of the most significant clusters of differentially-expressed proteins in our STRING network analyses was proteins involved in protein translation and regulation. Proteins in these pathways were increased in WT compared to EV cells and decreased in T319A compared to WT cells. Taken together with our data showing localization of ABCA7 in the ER, these results suggest a potential role for ABCA7 in ER function, particularly related to protein synthesis. Interestingly, ABCA7 knockdown in cultured mouse primary neurons has previously been shown to induce ER stress, implicating this as a potential pathway by which ABCA7 contributes to LOAD pathogenesis.[42] Furthermore, increased activation (via phosphorylation) of eukaryotic initiation factor 2α (eIF2α) was associated with this induced ER stress, however, decreased expression of proteins in the eIF2 signaling pathway in T319A compared to WT cells are not consistent with increased eIF2α activation. Nonetheless, our findings provide additional evidence suggesting that further investigation of ABCA7's role in LOAD pathogenesis is necessary.

Additionally, a cluster of proteins related to signal transduction and the immune response was also evident. Proteins in these pathways followed similar expression patterns across cell types as in the translation pathways. Increased expression of proteins in translation and immune response pathways in WT cells may be manifestation of a protective effect of WT ABCA7 overexpression, as has been indicated previously.[7]

On the other hand, ABCA7 was not identified as part of these two main clusters of differentially-expressed proteins. In these STRING network analyses, ABCA7 was only connected to one other protein, PLD3. PLD3 was increased in WT vs EV cells and decreased in T319A vs WT cells. Interestingly, decreased PLD3 mRNA and protein expression has previously

been found in the brains of AD patients compared to controls and was also associated with increased amyloid burden.[49] *PLD3* has also been implicated as a genetic risk factor for LOAD, though its pathological mechanism remains unknown.[39, 50] These findings suggest that the interaction between ABCA7 and PLD3 may be valuable to study in an AD model to further elucidate its role in LOAD pathogenesis.

Though differences in lipid binding affinities between WT ABCA7 and the T319A variant were detected in our structural studies, no lipid transport pathways were significant from the proteomics analyses. To confirm this finding, we manually searched for known lipid transport proteins[51] in the list of differentially-expressed proteins. The only protein identified was apolipoprotein L2, which was decreased in T319A compared to WT cells (**Table B2.2**). Overall, our findings do not suggest downstream effects of the T319A mutation on proteins involved in lipid transport in this cell model.

The primary limitation of this study is that the HEK 293 cell model is not an AD model, and limits the conclusions that can be made about the direct contribution of the T319A variant to AD pathogenesis. However, the HEK 293 cell model provides the basic cellular machinery required to study ABCA7 mechanisms and protein variants without the complex interactions in the neuronal environment, which is an established advantage of these cells for studying neuronal proteins.[52-55] These advantages enabled the primary strength of this study, which is the evaluation of potential mechanisms by which ABCA7 protein may contribute to increased LOAD risk through determining impacted structural binding sites and proteome differences. Future studies with more biological replicates should be performed to verify the discovered impacts of the T319A variant. Additionally, future work could employ cell models which

evaluate ABCA7 effects in the presence of Aβ peptides and also directly monitor lipid expression such as DAG, IP_3, and cholesterol.

2.5 Conclusions

Structural, cellular localization, and proteomic analyses were used to assess the effects of an *ABCA7* variant highly prevalent in African American/Black adults and associated with LOAD, compared to EV and WT *ABCA7* cells. The rs3752232 variant encodes a missense mutation (T319A) in the first extracellular domain of the protein, and the downstream effects of this mutation on ABCA7's function were investigated in HEK 293 cells. Several putative lipid binding sites with subtle differences in binding affinities between WT ABCA7 and the T319A mutant were identified. Furthermore, the T319A variant bound PIP_2 in a different orientation and displayed reduced binding. These results suggest that differences in binding lipids could lead to reductions in signaling molecules that have significant downstream effects. Our proteomics analyses identified many proteins with differences in expression in WT cells that were resolved in the T319A variant. WT ABCA7, in this model, led to higher cellular levels of ABCA7 and increased expression of proteins in pathways involved in protein translation and signal transduction/immune response. Taken together, our findings suggest that the T319A mutation may result in subtle structural and functional differences in ABCA7 and highlight the need for additional studies to further understand the role of this and other *ABCA7* variants in AD.

2.6 Acknowledgements

The authors acknowledge funding from the Vanderbilt Interdisciplinary Training Program in Alzheimer's Disease (T32-AG058524), RCMI Pilot funds from the National Institute

on Minority Health and Health Disparities (U54MD007586, U54MD007586-34), Vanderbilt University Start-Up Funds, and the Vanderbilt University Chancellor's Scholarship. Molecular graphics and analyses performed with UCSF Chimera, developed by the Resource for Biocomputing, Visualization, and Informatics at the University of California, San Francisco, with support from NIH P41-GM103311.

I would like to thank collaborators Dr. Jamaine S. Davis and Dr. Taneisha Gillyard at Meharry Medical College for preparation of the cells and structural and immunofluorescence studies. I would also like to thank Tyra Avery for her contributions to preliminary proteomics experiments for this chapter.

2.7 References

1. Reitz, C.; Mayeux, R., Genetics of Alzheimer's disease in Caribbean Hispanic and African American populations. *Biol Psychiatry* **2014,** *75* (7), 534-541.
2. Reitz, C.; Jun, G.; Naj, A.; Rajbhandary, R.; Vardarajan, B. N.; Wang, L.-S.; Valladares, O.; Lin, C.-F.; Larson, E. B.; Graff-Radford, N. R., et al., Variants in the ATP-binding cassette transporter (ABCA7), apolipoprotein E ε4, and the risk of late-onset Alzheimer disease in African Americans. *JAMA* **2013,** *309* (14), 1483-1492.
3. Barnes, L. L.; Bennett, D. A., Alzheimer's disease in African Americans: risk factors and challenges for the future. *Health Aff (Millwood)* **2014,** *33* (4), 580-586.
4. Hohman, T. J.; Cooke-Bailey, J. N.; Reitz, C.; Jun, G.; Naj, A.; Beecham, G. W.; Liu, Z.; Carney, R. M.; Vance, J. M.; Cuccaro, M. L., et al., Global and local ancestry in African-Americans: implications for Alzheimer's disease risk. *Alzheimers Dement* **2016,** *12* (3), 233-243.
5. Zhao, Q. F.; Yu, J. T.; Tan, M. S.; Tan, L., ABCA7 in Alzheimer's disease. *Mol Neurobiol* **2015,** *51* (3), 1008-1016.
6. N'Songo, A.; Carrasquillo, M. M.; Wang, X.; Burgess, J. D.; Nguyen, T.; Asmann, Y. W.; Serie, D. J.; Younkin, S. G.; Allen, M.; Pedraza, O., et al. African American exome sequencing identifies potential risk variants at Alzheimer disease loci. *Neurol Genet* [Online], **2017**. https://ng.neurology.org/content/nng/3/2/e141.full.pdf.
7. Aikawa, T.; Holm, M. L.; Kanekiyo, T. ABCA7 and pathogenic pathways of Alzheimer's disease. *Brain Sci* [Online], **2018**. http://www.mdpi.com/2076-3425/8/2/27/pdf.
8. Cukier, H. N.; Kunkle, B. W.; Vardarajan, B. N.; Rolati, S.; Hamilton-Nelson, K. L.; Kohli, M. A.; Whitehead, P. L.; Dombroski, B. A.; Van Booven, D.; Lang, R., et al. ABCA7 frameshift deletion associated with Alzheimer disease in African Americans. *Neurol Genet* [Online], **2016**. http://ng.neurology.org/content/2/3/e79.abstract.

9. Logue, M. W.; Schu, M.; Vardarajan, B. N.; Buros, J.; Green, R. C.; Go, R. C.; Griffith, P.; Obisesan, T. O.; Shatz, R.; Borenstein, A., et al., A comprehensive genetic association study of Alzheimer disease in African Americans. *Arch Neurol* **2011,** *68* (12), 1569-79.
10. Almeida, J. F. F.; Dos Santos, L. R.; Trancozo, M.; de Paula, F., Updated meta-analysis of BIN1, CR1, MS4A6A, CLU, and ABCA7 variants in Alzheimer's disease. *J Mol Neurosci* **2018,** *64*, 471-477.
11. Moreno, D. J.; Ruiz, S.; Rios, A.; Lopera, F.; Ostos, H.; Via, M.; Bedoya, G., Association of GWAS top genes with late-onset Alzheimer's disease in Colombian population. *Am J Alzheimers Dis Other Demen* **2017,** *32* (1), 27-35.
12. Naj, A. C.; Jun, G.; Beecham, G. W.; Wang, L. S.; Vardarajan, B. N.; Buros, J.; Gallins, P. J.; Buxbaum, J. D.; Jarvik, G. P.; Crane, P. K., et al., Common variants at MS4A4/MS4A6E, CD2AP, CD33 and EPHA1 are associated with late-onset Alzheimer's disease. *Nat Genet* **2011,** *43* (5), 436-441.
13. Logue, M. W.; Lancour, D.; Farrell, J.; Simkina, I.; Fallin, M. D.; Lunetta, K. L.; Farrer, L. A., Targeted sequencing of Alzheimer disease genes in African Americans implicates novel risk variants. *Front Neurosci* **2018,** *12*, 592.
14. Quazi, F.; Molday, R. S., Differential phospholipid substrates and directional transport by ATP-binding cassette proteins ABCA1, ABCA7, and ABCA4 and disease-causing mutants. *J Biol Chem* **2013,** *288* (48), 34414-26.
15. Takahashi, K.; Kimura, Y.; Nagata, K.; Yamamoto, A.; Matsuo, M.; Ueda, K., ABC proteins: key molecules for lipid homeostasis. *Med Mol Morphol* **2005,** *38* (1), 2-12.
16. Koldamova, R.; Staufenbiel, M.; Lefterov, I., Lack of ABCA1 considerably decreases brain ApoE level and increases amyloid deposition in APP23 mice. *J Biol Chem* **2005,** *280* (52), 43224-43235.
17. Wang, N.; Lan, D.; Gerbod-Giannone, M.; Linsel-Nitschke, P.; Jehle, A. W.; Chen, W.; Martinez, L. O.; Tall, A. R., ATP-binding cassette transporter A7 (ABCA7) binds apolipoprotein A-I and mediates cellular phospholipid but not cholesterol efflux. *J Biol Chem* **2003,** *278* (44), 42906-12.
18. Kawanobe, T.; Shiranaga, N.; Kioka, N.; Kimura, Y.; Ueda, K., Apolipoprotein A-I directly interacts with extracellular domain 1 of human ABCA1. *Biosci Biotechnol Biochem* **2019,** *83* (3), 490-497.
19. Abe-Dohmae, S.; Ikeda, Y.; Matsuo, M.; Hayashi, M.; Okuhira, K.; Ueda, K.; Yokoyama, S., Human ABCA7 supports apolipoprotein-mediated release of cellular cholesterol and phospholipid to generate high density lipoprotein. *J Biol Chem* **2004,** *279* (1), 604-11.
20. Hayashi, M.; Abe-Dohmae, S.; Okazaki, M.; Ueda, K.; Yokoyama, S., Heterogeneity of high density lipoprotein generated by ABCA1 and ABCA7. *J Lipid Res* **2005,** *46* (8), 1703-1711.
21. De Roeck, A.; Van Broeckhoven, C.; Sleegers, K., The role of ABCA7 in Alzheimer's disease: evidence from genomics, transcriptomics and methylomics. *Acta Neuropathol* **2019,** *138* (2), 201-220.
22. Chan, S. L.; Kim, W. S.; Kwok, J. B.; Hill, A. F.; Cappai, R.; Rye, K. A.; Garner, B., ATP-binding cassette transporter A7 regulates processing of amyloid precursor protein in vitro. *J Neurochem* **2008,** *106* (2), 793-804.
23. Kjeldsen, E. W.; Tybjaerg-Hansen, A.; Nordestgaard, B. G.; Frikke-Schmidt, R., ABCA7 and risk of dementia and vascular disease in the Danish population. *Ann Clin Transl Neurol* **2018,** *5* (1), 41-51.

24. Chung, S. J.; Kim, M. J.; Kim, Y. J.; Kim, J.; You, S.; Jang, E. H.; Kim, S. Y.; Lee, J. H., CR1, ABCA7, and APOE genes affect the features of cognitive impairment in Alzheimer's disease. *J Neurol Sci* **2014,** *339* (1-2), 91-96.
25. Plubell, D. L.; Wilmarth, P. A.; Zhao, Y.; Fenton, A. M.; Minnier, J.; Reddy, A. P.; Klimek, J.; Yang, X.; David, L. L.; Pamir, N., Extended multiplexing of Tandem Mass Tags (TMT) labeling reveals age and high fat diet specific proteome changes in mouse epididymal adipose tissue. *Mol Cell Proteomics* **2017,** *16* (5), 873-890.
26. Stepler, K. E.; Mahoney, E. R.; Kofler, J.; Hohman, T. J.; Lopez, O. L.; Robinson, R. A. S. Inclusion of African American/Black adults in a pilot brain proteomics study of Alzheimer's disease. *Neurobiol Dis* [Online], **2020**. http://www.sciencedirect.com/science/article/pii/S0969996120304046.
27. Cao, Z.; Yende, S.; Kellum, J. A.; Angus, D. C.; Robinson, R. A. S., Proteomics reveals age-related differences in the host immune response to sepsis. *J Proteome Res* **2014,** *13* (2), 422-432.
28. Szklarczyk, D.; Gable, A. L.; Lyon, D.; Junge, A.; Wyder, S.; Huerta-Cepas, J.; Simonovic, M.; Doncheva, N. T.; Morris, J. H.; Bork, P., et al., STRING v11: protein–protein association networks with increased coverage, supporting functional discovery in genome-wide experimental datasets. *Nucleic Acids Research* **2018,** *47* (D1), D607-D613.
29. Qian, H.; Zhao, X.; Cao, P.; Lei, J.; Yan, N.; Gong, X., Structure of the Human Lipid Exporter ABCA1. *Cell* **2017,** *169* (7), 1228-1239.e10.
30. Kelley, L. A.; Mezulis, S.; Yates, C. M.; Wass, M. N.; Sternberg, M. J. E., The Phyre2 web portal for protein modeling, prediction and analysis. *Nat Protoc* **2015,** *10* (6), 845-858.
31. Webb, B.; Sali, A., Comparative protein structure modeling using MODELLER. *Curr Protoc Bioinformatics* **2016,** *54*, 5.6.1-5.6.37.
32. Pettersen, E. F.; Goddard, T. D.; Huang, C. C.; Couch, G. S.; Greenblatt, D. M.; Meng, E. C.; Ferrin, T. E., UCSF Chimera--a visualization system for exploratory research and analysis. *J Comput Chem* **2004,** *25* (13), 1605-1612.
33. Benkert, P.; Künzli, M.; Schwede, T., QMEAN server for protein model quality estimation. *Nucleic Acids Res* **2009,** *37* (Web Server issue), W510-4.
34. Benkert, P.; Schwede, T.; Tosatto, S. C. E., QMEANclust: estimation of protein model quality by combining a composite scoring function with structural density information. *BMC Struct Biol* **2009,** *9* (1).
35. Trott, O.; Olson, A. J., AutoDock Vina: improving the speed and accuracy of docking with a new scoring function, efficient optimization, and multithreading. *J Comput Chem* **2010,** *31* (2), 455-461.
36. Satoh, K.; Abe-Dohmae, S.; Yokoyama, S.; St George-Hyslop, P.; Fraser, P. E., ATP-binding cassette transporter A7 (ABCA7) loss of function alters Alzheimer amyloid processing. *J Biol Chem* **2015,** *290* (40), 24152-24165.
37. Aebersold, R.; Burlingame, A. L.; Bradshaw, R. A., Western blots versus selected reaction monitoring assays: time to turn the tables? *Mol Cell Proteomics* **2013,** *12* (9), 2381-2382.
38. El Gaamouch, F.; Jing, P.; Xia, J.; Cai, D., Alzheimer's disease risk genes and lipid regulators. *J Alzheimers Dis* **2016,** *53*, 15-29.
39. Karch, C. M.; Goate, A. M., Alzheimer's disease risk genes and mechanisms of disease pathogenesis. *Biol Psychiatry* **2015,** *77* (1), 43-51.

40. Picard, C.; Julien, C.; Frappier, J.; Miron, J.; Théroux, L.; Dea, D.; Breitner, J. C. S.; Poirier, J., Alterations in cholesterol metabolism-related genes in sporadic Alzheimer's disease. *Neurobiol Aging* **2018,** *66*, 180.e1-180.e9.
41. Chew, H.; Solomon, V. A.; Fonteh, A. N. Involvement of lipids in Alzheimer's disease pathology and potential therapies. *Front Physiol* [Online], **2020**. https://www.frontiersin.org/article/10.3389/fphys.2020.00598.
42. Sakae, N.; Liu, C. C.; Shinohara, M.; Frisch-Daiello, J.; Ma, L.; Yamazaki, Y.; Tachibana, M.; Younkin, L.; Kurti, A.; Carrasquillo, M. M., et al., ABCA7 deficiency accelerates amyloid-beta generation and Alzheimer's neuronal pathology. *J Neurosci* **2016,** *36* (13), 3848-3859.
43. Stokes, C. E.; Hawthorne, J. N., Reduced phosphoinositide concentrations in anterior temporal cortex of Alzheimer-diseased brains. *J Neurochem* **1987,** *48* (4), 1018-21.
44. Gulshan, K.; Brubaker, G.; Conger, H.; Wang, S.; Zhang, R.; Hazen, S. L.; Smith, J. D., PI(4,5)P2 is translocated by ABCA1 to the cell surface where it mediates apolipoprotein A1 binding and nascent HDL assembly. *Circ Res* **2016,** *119* (7), 827-838.
45. Landman, N.; Jeong, S. Y.; Shin, S. Y.; Voronov, S. V.; Serban, G.; Kang, M. S.; Park, M. K.; Di Paolo, G.; Chung, S.; Kim, T. W., Presenilin mutations linked to familial Alzheimer's disease cause an imbalance in phosphatidylinositol 4,5-bisphosphate metabolism. *Proc Natl Acad Sci U S A* **2006,** *103* (51), 19524-19529.
46. Wood, P. L.; Medicherla, S.; Sheikh, N.; Terry, B.; Phillipps, A.; Kaye, J. A.; Quinn, J. F.; Woltjer, R. L., Targeted lipidomics of fontal cortex and plasma diacylglycerols (DAG) in mild cognitive impairment and Alzheimer's disease: validation of DAG accumulation early in the pathophysiology of Alzheimer's disease. *J Alzheimers Dis* **2015,** *48* (2), 537-546.
47. Wood, P. L.; Barnette, B. L.; Kaye, J. A.; Quinn, J. F.; Woltjer, R. L., Non-targeted lipidomics of CSF and frontal cortex grey and white matter in control, mild cognitive impairment, and Alzheimer's disease subjects. *Acta Neuropsychiatr* **2015,** *27* (5), 270-278.
48. Wood, P.; Phillipps, A.; Woltjer, R. L.; Kaye, J.; Quinn, J. Increased lysophosphatidylethanolamine and diacylglycerol levels in Alzheimer's disease plasma. *JSM Alzheimer Dis Rel Dement* [Online], **2014**.
49. Blanco-Luquin, I.; Altuna, M.; Sánchez-Ruiz de Gordoa, J.; Urdánoz-Casado, A.; Roldán, M.; Cámara, M.; Zelaya, V.; Erro, M. E.; Echavarri, C.; Mendioroz, M. PLD3 epigenetic changes in the hippocampus of Alzheimer's disease. *Clin Epigenetics* [Online], **2018**. https://doi.org/10.1186/s13148-018-0547-3.
50. Rosenthal, S. L.; Kamboh, M. I., Late-onset Alzheimer's disease genes and the potentially implicated pathways. *Curr Genet Med Rep* **2014,** *2* (2), 85-101.
51. Wong, L. H.; Gatta, A. T.; Levine, T. P., Lipid transfer proteins: the lipid commute via shuttles, bridges and tubes. *Nat Rev Mol Cell Biol* **2019,** *20* (2), 85-101.
52. Heidarinejad, M.; Nakamura, H.; Inoue, T., Stimulation-induced changes in diffusion and structure of calmodulin and calmodulin-dependent protein kinase II proteins in neurons. *Neurosci Res* **2018,** *136*, 13-32.
53. Ancolio, K.; Alves da Costa, C.; Uéda, K.; Checler, F., Alpha-synuclein and the Parkinson's disease-related mutant Ala53Thr-alpha-synuclein do not undergo proteasomal degradation in HEK293 and neuronal cells. *Neurosci Lett* **2000,** *285* (2), 79-82.
54. Thomas, P.; Smart, T. G., HEK293 cell line: a vehicle for the expression of recombinant proteins. *J Pharmacol Toxicol Methods* **2005,** *51* (3), 187-200.

55. Jiang, S. Z.; Xu, W.; Emery, A. C.; Gerfen, C. R.; Eiden, M. V.; Eiden, L. E. NCS-Rapgef2, the protein product of the neuronal Rapgef2 gene, is a specific activator of D1 dopamine receptor-dependent ERK phosphorylation in mouse brain. *eNeuro* [Online], **2017**. https://www.eneuro.org/content/eneuro/4/5/ENEURO.0248-17.2017.full.pdf.

CHAPTER 3

Inclusion of African American/Black Adults in a Pilot Brain Proteomics Study of Alzheimer's Disease

3.1 Introduction

The Alzheimer's Association estimates that 5.7 million Americans have Alzheimer's disease (AD),[1] although different racial and ethnic subgroups of the population are not affected equally.[2-3] African American/Black adults are 2-3 and Hispanic adults are 1.5-2 times more likely to develop AD and related dementias than non-Hispanic White adults.[4-5] On the other hand, Native American and Asian American adults (i.e., Japanese Americans) have lower prevalence and incidence of AD than non-Hispanic White adults.[1, 4, 6-8] African American/Black and Hispanic minorities will comprise 40% of 65-year and older individuals and AD sufferers by 2050,[7, 9-10] which underscores the urgency of better understanding disparities in this disease.

Significant differences in postmortem disease hallmarks, such as amyloid beta (Aβ) plaques and hyperphosphorylated tau tangles (neurofibrillary tangles; NFTs), between the brains of African American/Black and non-Hispanic White adults have not been observed.[5, 11-13] Cerebral amyloid angiopathy, which often coexists with AD, has similar prevalence and histopathological characteristics between African American/Black and non-Hispanic White adults.[14] Global gray matter change is the best predictor of cognitive decline in both African American/Black and non-Hispanic White adults,[15] however, African American/Black adults are more likely to present with mixed AD pathologies and other dementias, particularly Lewy body dementia, infarcts, and cerebrovascular disease.[11, 16-17]

Socioeconomic factors, genetics, and comorbidities may also have substantial contributions to higher incidence of AD in African American/Black adults, and highlight the importance of carefully designed biological experiments in this context.[18] Socioeconomic factors include education level, healthcare access, and willingness to seek care and treatment (see **Section 1.1.1** for a detailed discussion of these factors).[5, 9, 19-21] African American/Black adults, in one study, were less likely to seek care for symptoms of mild cognitive impairment (MCI)[20] and in other studies, were less likely than non-Hispanic White adults to receive AD pharmacotherapy treatment (e.g., cholinesterase inhibitors or memantine) upon disease diagnosis.[9, 21] Genetic risk factors, particularly the apolipoprotein E (*APOE*) ε4 allele and single nucleotide polymorphisms of the ATP-binding cassette transporter A7 (*ABCA7*) gene, differ in prevalence and effect size amongst different racial and ethnic groups[9, 16, 22-23] (see **Section 1.1.2**). *APOE, ABCA7,* and other risk genes impacting African American/Black adults such as apolipoprotein D (*APOD*),[24] sortilin-related receptor 1 (*SORL1*),[25] and sigma non-opioid intracellular receptor 1 (*SIGMAR1*)[26] are relevant for lipid metabolism and encode proteins involved in lipid transport, homeostasis, regulation, and cholesterol biosynthesis.[23, 27-29] Lipid metabolism plays an important role in AD pathogenesis[27-28, 30-33] and in comorbidities that increase AD risk, such as dyslipidemia, type 2 diabetes mellitus (T2DM), cardiovascular disease, and hypertension[4, 6, 9, 34-36] (see **Section 1.1.3**). These comorbidities are also prevalent in African American/Black adults.[6]

Differences in the immune system and inflammatory pathways are noted in African American/Black compared to non-Hispanic White adults (see **Section 1.1.1**).[37] For example, a recent study reported higher cerebrospinal fluid (CSF) levels of interleukin-9 (IL-9) in African American/Black adults correlate with AD but this is not the case in non-Hispanic White adults.[38]

Cognitively normal (CN) middle-aged African American/Black adults also have lower CSF levels of total and phosphorylated tau, biomarkers for AD,[39-44] and IL-9 compared to non-Hispanic White adults.[38] These findings suggest tau-related pathways may contribute to racial disparities in AD; however, large-scale molecular studies of African American/Black adults using biofluids or postmortem brain are necessary to test this hypothesis.[2]

Discovery-based proteomics can be useful for disease understanding and has been employed broadly to analyze AD postmortem brain.[45-50] Based on an extensive literature search, African American/Black and other underrepresented minorities have been grossly excluded in proteomic studies of AD, especially in brain.[47-48] Significant pathways found in brains of non-Hispanic White adults include innate immune response and the citric acid cycle, while neurotransmitter regulation, monosaccharide/glucose metabolism, and apoptosis/cell cycle regulation primarily differ in regions most severely affected by AD pathology (i.e. hippocampus, entorhinal cortex, and cingulate gyrus).[46] The hippocampus has a well-established role in the early to late stages of AD and undergoes changes in cytoskeletal, metabolic, synaptic, and signaling pathways.[46, 48-49, 51-56] Oxidative posttranslational modifications in the hippocampus and inferior parietal lobule (IPL) increase in amnestic MCI and AD.[57-61] IPL has decreased gray matter volume in AD[62-63] and increased protein phosphorylation.[64] Loss of cholinergic neurons occurs in the globus pallidus (GP) in AD,[65] which may be due to the presence of Aβ oligomers in this region.[66] However, GP has less AD pathology compared to other brain regions.

Understanding the extent of molecular contributions and/or outcomes of racial and ethnic disparities in AD is very necessary to further overall disease understanding and to inform prevention, therapeutic, and personalized medicine strategies. Herein, we present a pilot spatial proteomics study of postmortem brain tissues (i.e. hippocampus, IPL, GP) from African

American/Black and non-Hispanic White adults. This study included participants from the University of Pittsburgh Alzheimer Disease Research Center (ADRC) who were CN or neuropathologically diagnosed with AD at autopsy. Our findings provide new insights regarding the molecular basis of AD and especially highlight the need for more inclusion of racial/ethnic minorities in proteomics studies of AD.

3.2 Methods

3.2.1 Sample selection

Postmortem brain tissues were selected from the University of Pittsburgh ADRC brain bank. The University of Pittsburgh ADRC database was surveyed for African American/Black adults with AD between the time of its inception in 1985 and 12/15/2016 (N = 209; 8.2%). Of these, five were deceased and had brain samples available from hippocampus, IPL, and/or GP. We selected all five of these African American/Black AD brains and the four African American/Black CN brains from these regions, and matched brains from non-Hispanic White adults based on age, sex, and diagnosis. Hippocampal (N = 18), IPL (N = 19), and GP (N = 18) tissues were acquired from African American/Black and non-Hispanic White adults who were CN or neuropathologically diagnosed with AD (**Table 3.1**). Race was self-reported as Black or African American (referred to throughout as African American/Black) or White (referred to throughout as non-Hispanic White). Braak staging[67-68] was completed for all samples. This study was approved by the University of Pittsburgh Institutional Review Board (IRB) and Committee for Oversight of Research and Clinical Training Involving Decedents (CORID).

Table 3.1. Cohort characteristics.[a]

Characteristics	NHW CN	NHW AD	AA CN	AA AD	Diagnosis p-value[b]	Race p-value[b]
Sex	3 F, 2 M	4 F, 2 M	0 F, 4 M	2 F, 3 M	0.301	0.065
Age[c]	65 ± 13	83 ± 8	69 ± 15	80 ± 6	**0.011**	0.986
Years of Education[d]	17	15 ± 4	8	13	0.572	0.050
PMI[e]	14 ± 9	6 ± 2	13 ± 9	11 ± 7	0.142	0.479
***APOE* Genotype**[f]	4 ε3/ε3, 1 ε2/ε2	5 ε3/ε3, 1 ε3/ε4	1 ε3/ε3, 3 N/A	1 ε3/ε3, 2 ε3/ε4, 2 ε4/ε4	--	--
Aβ A4 Positive	4 N 1 Y, rare	6 Y	2 N 1 Y, rare 1 Y	5 Y	--	--
Braak Stage[g]	1 (0-2)	4 (4-5)	1 (0-2)	5 (4-5)	**<0.0001**	0.698

[a]Values for each group are given as average ± standard deviation, unless otherwise noted. [b]p-values were calculated using two-factor ANOVAs with replication; bold indicates $p < 0.05$. [c]Age in years. [d]Years of education was not available for all individuals. Averages and standard deviations were calculated from available samples for each group (NHW CN: N = 2; NHW AD: N = 6; AA CN: N = 1; AA AD: N = 2). [e]Postmortem interval (PMI), in hours. [f]N/A indicates genotype was unavailable. [g]Average Braak stage (range). Abbreviations: NHW, non-Hispanic White; AA, African American/Black.

3.2.2 Sample preparation

Brain tissue (20 mg) was homogenized in 1x phosphate-buffered saline (PBS) with 8 M urea. Briefly, tissues were homogenized with Lysing Matrix A at 4.0 m/s for 20 s using a FastPrep-24™ 5G system (MP Biomedicals). After homogenization, 1x PBS with 8 M urea, 1 mM phenylmethylsulfonyl fluoride (PMSF), and 0.3 μM aprotinin were added. Homogenate was centrifuged at 4 °C, 13,000 rpm for 15 min and supernatant was collected. Protein concentration was determined using bicinchoninic acid (BCA) assay according to the manufacturer's protocols (Thermo Fisher Scientific). A pooled sample containing equimolar amounts of protein from the 18 (hippocampus/GP) or 19 (IPL) samples was generated and served as a quality control (QC). Samples were randomized into two batches of 10 (hippocampus/GP) or 11 (IPL), including at least one QC per batch, and were processed separately (**Table C3.1**). Protein (100 μg) was placed in 50 mM Tris with 8 M urea and was reduced for 30 min using 25 mM dithiothreitol at 37 °C. Protein was subsequently alkylated with 25 mM iodoacetamide for 30 min on ice in the dark and quenched with 25 mM L-cysteine for 30 min with shaking. Samples were diluted to 1 M urea with 20 mM Tris, 10 mM $CaCl_2$ prior to digestion with trypsin/Lys-C mix (Promega) for 6-8 h at 37 °C (1:50 enzyme:protein ratio). Peptides were acidified with formic acid (FA) and desalted with an HLB cartridge (Waters Corporation; 1 cc/10 mg). TMT^{10}-plex (hippocampus/GP) or TMT^{11}-plex (IPL) reagents were used to label 25 μg of each sample. Each batch mixture was desalted and fractionated using a gradient of acetonitrile at pH 10 to generate 12 fractions (2, 4, 6, 8, 10, 12, 14, 16, 20, 25, 35, and 50%). All fractions were analyzed individually via $LC\text{-}MS^3$ on an Orbitrap Fusion Lumos (Thermo Fisher Scientific) with technical duplicates. Fractions were injected in a randomized order.

3.2.3 LC-MS^3 parameters

An UltiMate 3000 RSLCnano system (Thermo) was coupled to an Orbitrap Fusion Lumos mass spectrometer operated in positive mode. Peptides were loaded onto a self-packed C18 trap column (100 μm i.d. x 2.5-2.6 cm, 200 Å, 5 μm; Bruker) prior to separation on an in-house C18 packed column (100 μm i.d. x 20 cm, 100 Å, 2.5 μm; Waters) over the following 100 min gradient: 0-7 min, 10% B; 7-67 min, 10-30% B; 67-75 min, 30-60% B; 75-77 min, 60-90% B; 77-82 min, 90% B; 82-83 min, 90-10% B; 83-100 min, 10% B. Mobile phase A was 0.1% FA and mobile phase B was 0.1% FA in acetonitrile. Full MS spectra were collected in the Orbitrap (375-1,500 *m/z*, 120,000 resolution, automated gain control (AGC) 4.0E5, maximum injection time 50 ms). The instrument was operated in data-dependent acquisition (DDA) mode to acquire the top 7 MS/MS spectra in the ion trap using collision-induced dissociation (CID; normalized collision energy 35%, isolation width 0.7 *m/z*, AGC 1.0E4) and dynamic exclusion of 20 s. Synchronous precursor selection (SPS) mode was used to select the top 8 most intense ions from each MS/MS spectrum for MS^3 in the Orbitrap using higher-energy collisional dissociation (HCD; 100-400 *m/z*, normalized collision energy 55%, resolution 60,000, AGC 5.0E4, maximum injection time 118 ms, isolation width 2 *m/z*).

3.2.4 Data analysis

RAW files were analyzed using Proteome Discoverer software (version 2.2). All technical replicates and fractions for each batch were combined into one result file and searched against the UniProt human reviewed proteins database (hippocampus: 03/22/2018, 20,259 sequences; IPL/GP: 06/25/2018, 20,302 sequences) using SEQUEST-HT. The following modifications were included in this search: fixed modification of cysteine carbamidomethylation

and variable modifications of methionine oxidation and TMT^{10}-plex (229.163 Da) on lysine residues and peptide N-termini for hippocampus and GP and both TMT^{10}-plex and TMT^{11}-plex (229.169 Da) for IPL. A maximum of two trypsin miscleavages were allowed in the search.

TMT^{10}-plex (hippocampus/GP) or TMT^{11}-plex (IPL) was set as the quantification method in Proteome Discoverer, and reporter ion quantitation was based on intensity with a reporter signal-to-noise threshold of 10. Protein groups identified are referred to as proteins throughout. The mass spectrometry proteomics data have been deposited to the ProteomeXchange Consortium (http://proteomecentral.proteomexchange.org/) via the PRIDE[69] partner repository with the dataset identifiers PXD012114 (hippocampus), PXD014372 (IPL), and PXD014371 (GP).

Processed data from hippocampus, IPL, and GP data can be found in **Data C3.1-3.3**, respectively. Peptides were filtered to only include those identified with high confidence (< 1% false discovery rate, FDR) and their corresponding proteins. This list of proteins was further filtered by requiring two peptide spectral matches (PSMs) for a protein identification. Post-analysis filtering was performed to only include proteins identified in both batches with reporter ion intensities in ≥ 80% of samples (≥ 16 of 20 TMT channels for 10-plex or ≥ 17 of 22 for 11-plex), which must include all pooled channels and ≥ 3 samples per group. These proteins were considered to be the quantified proteins from each region. TMT reporter ion intensities of quantified proteins were normalized using a modified two-step process involving within-batch and across-batch normalization (**Figures C3.1-3.2**).[70] The within-batch normalization was based on the intensity of the pooled sample instead of the average across TMT channels, and we adapted the across-batch normalization to having one pool instead of two in most batches.

Differentially-expressed proteins were identified separately for each region. Fold-change cutoffs of < 0.81 and > 1.24 between AD and CN groups were established based on technical and biological variation and level of technical and biological replication.[71] Main effects of diagnosis on protein intensities were assessed using linear regression with models stratified by race. Further, a race x diagnosis interaction term assessed whether race modifies the association between diagnosis and protein intensities. P-values were corrected for the number of proteins tested within each brain region using the FDR procedure. However, use of corrected p-values resulted in no significant proteins (likely due to small sample size); therefore, throughout this manuscript, differentially-expressed proteins refers to those with uncorrected p-values < 0.05. Additionally, unadjusted R^2 values were pulled from the main effects models of race, diagnosis, and race+diagnosis covarying for demographic variables (age, sex, and postmortem interval (PMI)), to assess the additional variance explained by these terms above and beyond demographic variables. Within each region, proteins with coefficients of variation (CVs) greater than two standard deviations from the mean were excluded (CV > 0.49, 0.34, 0.61 in hippocampus, IPL, and GP, respectively; **Figure C3.3**). Ingenuity Pathway Analysis (IPA) was used to identify significant biological pathways ($p < 0.05$; https://www.qiagenbioinformatics.com/products/ingenuitypathway-analysis).[72] TMT reporter ion intensities for differentially-expressed proteins were uploaded into ClustVis to generate heatmaps and cluster data (https://biit.cs.ut.ee/clustvis/).[73]

3.2.5 Western blots

Three samples from each of the four sample groups were randomly selected for verification by Western blot. Protein was fractionated by SDS-PAGE (120 V loading, 160 V for

~80 min). Proteins were transferred to a nitrocellulose membrane using a wet transfer at 100 V for 70 min. After incubation with 5% nonfat milk in Tris-buffered saline with Tween-20 (TBST; 50 mM Tris, 150 mM NaCl, pH 7.4, 0.1% Tween-20) for 30-60 min, the membrane was washed 4 x 4 min with TBST and incubated overnight with antibodies against calcium/calmodulin dependent protein kinase IIα (CAMKIIα; Thermo MA1-048; 1:5,000), peroxiredoxin-2 (PRDX2; abcam ab109367; 1:10,000), or fatty acid-binding protein, heart isoform (H-FABP; Hycult Biotech HM 2016; 1:1,000) at 4°C. Membrane was washed 4 x 4 min with TBST and incubated with a 1:10,000 dilution of fluorescent-labeled anti-mouse (StarBright Blue 700; Bio-Rad Laboratories) or anti-rabbit (IRDye 800CW; Li-Cor Biosciences) secondary antibodies for 30-60 min. For β-actin blots, membrane was incubated with a rhodamine-conjugated anti-β-actin antibody (Bio-Rad 12004164; 1:10,000) overnight (no secondary antibody necessary). Blots were washed 4 x 4 min with TBST prior to imaging using a ChemiDoc MP imaging system (Bio-Rad). ImageLab software (Bio-Rad, version 6.0) was used for band quantification.

3.3 Results

Postmortem hippocampus, IPL, and GP tissues were obtained from the University of Pittsburgh ADRC from African American/Black and non-Hispanic White, CN and AD individuals (**Table 3.1**). The grouping of CN and AD is consistent with disease diagnosis at autopsy, Braak staging, and Aβ staining. Because we were limited by brains from the African American/Black groups, the non-Hispanic White groups were closely matched based on age and sex to the African American/Black groups. We note that CN individuals were younger than those with AD.

3.3.1 Characterization of dataset

Brain samples were analyzed using a discovery-based quantitative proteomics workflow (**Figure 3.1a**). The numbers of proteins (peptides) identified from hippocampus, IPL, and GP based on 1% FDR and ≥ 2 PSMs were 1,883 (8,764), 2,055 (9,071), and 1,656 (9,891), respectively. Overall, 2,613 total unique proteins were identified across the regions with 1,229 common in all three regions (**Figure 3.1b**). These identifications were then filtered to include proteins observed in both TMT batches and with reporter ion signal in ≥ 80% of the TMT channels (including all pools and ≥ 3 per sample group). The numbers of quantified proteins identified from hippocampus, IPL, and GP were 1,414, 1,487, and 1,173 quantified proteins, respectively. This gave a total of 1,801 quantified proteins, 943 of which were common in all three regions (**Figure 3.1c**). The greatest overlap in total and quantified protein identifications was between hippocampus and IPL (**Figure 3.1b-c**). Trends in protein expression for selected proteins (β-actin, PRDX2, CAMKIIα, H-FABP) were verified by Western blots and generally supported MS data (**Figure C3.4**).

3.3.2 Differentially-expressed proteins by region

Quantified proteins were used to assess differences in AD relative to CN individuals within each brain region (implied hereafter). Most differentially-expressed proteins were region-specific, leading to a total of 568 differentially-expressed proteins in AD (**Figure 3.2a**). In these 568 differentially-expressed proteins, covariates (age, sex, PMI, and race) explained 43.42 ± 10.13% of variance in protein intensity, and diagnosis explained an additional 3.24 ± 4.01% of variance in protein intensity above and beyond covariates. In hippocampus, two main clusters of differentially-expressed proteins were observed: a smaller cluster that appears to be mostly

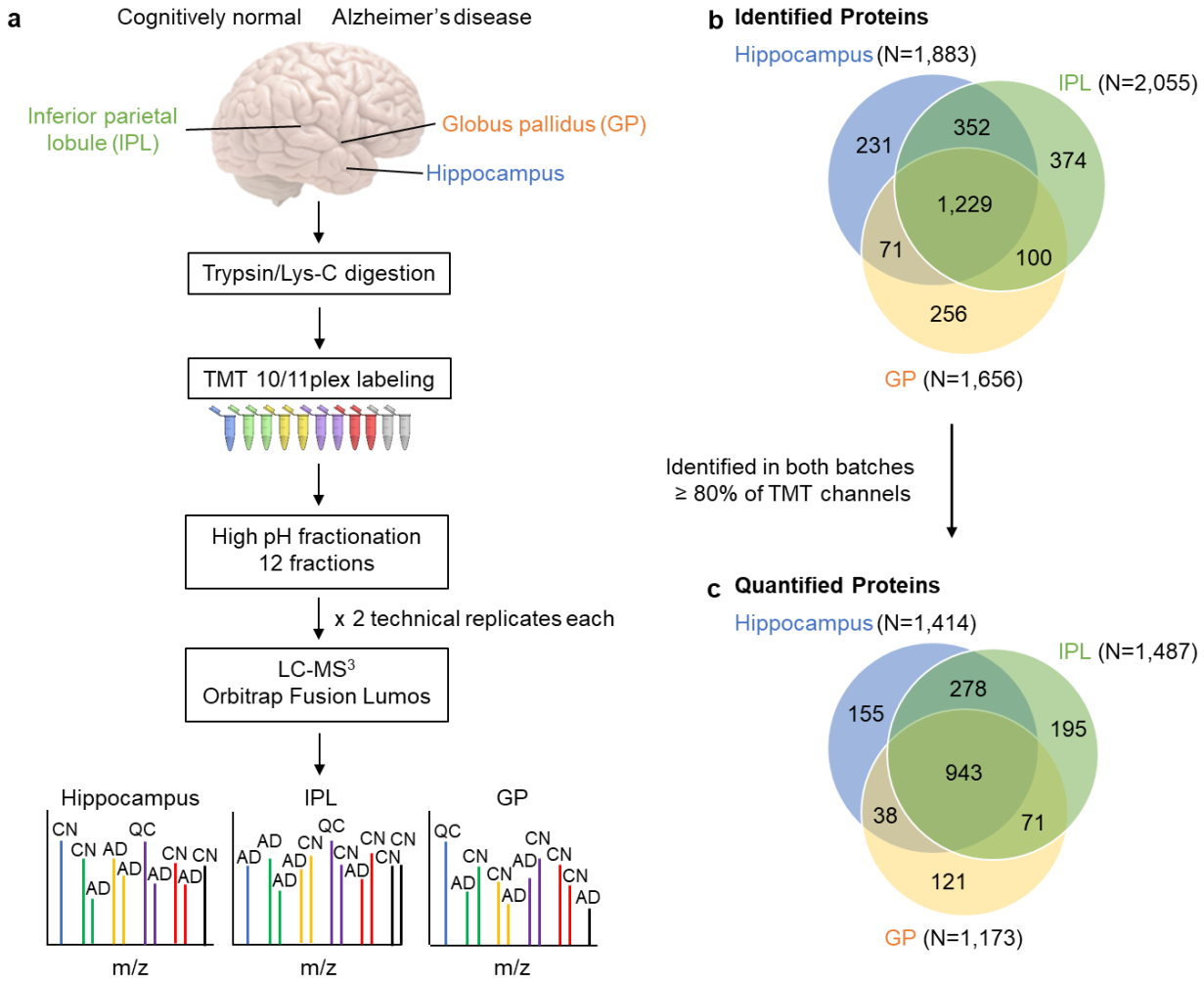

Figure 3.1. Workflow and summary of identified and quantified proteins by region. a, Experimental workflow used in this study. Samples for each region were randomized into two batches such that each batch contained one pool (QC) and at least one individual from each of the four sample groups. The colored tubes indicate the different TMT^{11}-plex reagents. **b**, Overlap of identified proteins across the three brain regions. **c**, Overlap of quantified proteins across the three brain regions. Quantified proteins were identified in both batches with TMT quantification data for ≥ 80% of TMT channels across batches. Brain image modified from "Human brain on white background" by _DJ_ used under CC BY-SA 2.0. Abbreviations: TMT, tandem mass tags; IPL, inferior parietal lobule; GP, globus pallidus; CN, cognitively normal; AD, Alzheimer's disease; QC, quality control. Figure reprinted from Neurobiol. Dis., Vol 146, Stepler, K. E., et al., Inclusion of African American/Black adults in a pilot brain proteomics study of Alzheimer's disease, Article No. 105129, Copyright (2020), with permission from Elsevier.[74]

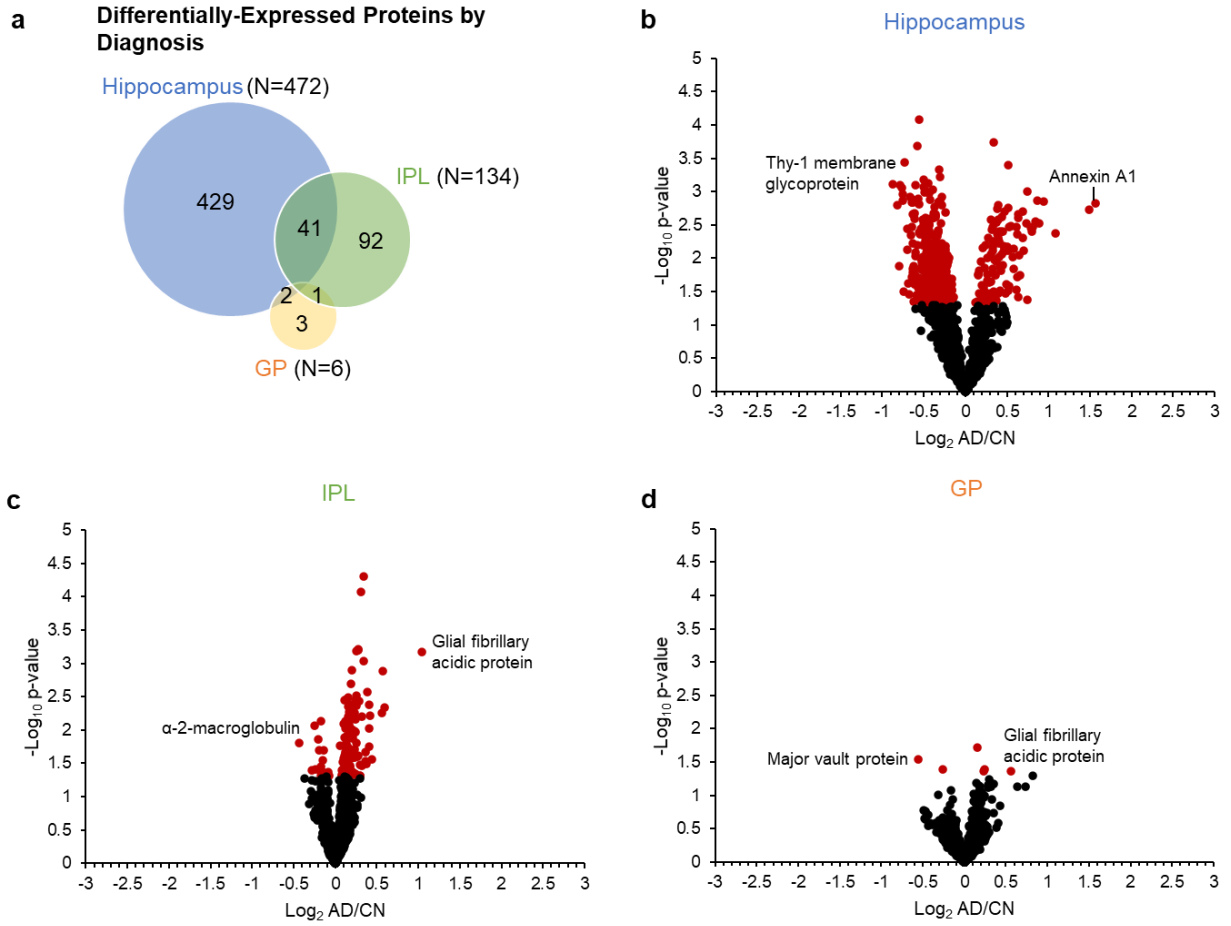

Figure 3.2. Differentially-expressed proteins by diagnosis in each region. a, Venn diagram showing the regional overlap in differentially-expressed proteins by diagnosis and corresponding volcano plots for **b**, hippocampus, **c**, IPL, and **d**, GP. CV-filtered quantified proteins are shown for each region (hippocampus N = 1,338; IPL N = 1,407; GP N = 1,103). Red data points indicate differentially-expressed proteins with uncorrected p-value < 0.05; black data points indicate quantified proteins with nonsignificant p-values. Selected proteins with significant changes in AD are highlighted in each plot. Abbreviations: IPL, inferior parietal lobule; GP, globus pallidus; AD, Alzheimer's disease; CN, cognitively normal. Figure reprinted from Neurobiol. Dis., Vol 146, Stepler, K. E., et al., Inclusion of African American/Black adults in a pilot brain proteomics study of Alzheimer's disease, Article No. 105129, Copyright (2020), with permission from Elsevier.[74]

increased in AD individuals and a larger cluster decreased in AD individuals (**Figure 3.3**). Individuals cluster into either an AD group or an admixed CN group that also includes a few AD cases. Heatmap analysis showed similar clustering of AD and CN groups in IPL and GP (*data not shown*). This suggests that the proteomes for some of the AD individuals are more similar to CN individuals. It is important to note that these neuropathologically diagnosed AD individuals that were clustered with the CN group included non-Hispanic White adults and an African American/Black adult, and two of these AD individuals clustered with the CN group in more than one region. Racial subgroups were not clustered within the AD or CN groups from heatmap analysis, likely due to the small sample size.

Hippocampus had the most differentially-expressed proteins of the three regions in this study (N = 472; **Figure 3.2b, Table C3.2**), consistent with others,[46] with most proteins (N = 359) decreased in AD. Fewer differentially-expressed proteins were observed in IPL (N = 134; **Figure 3.2c, Table C3.3),** most of which (N = 118) were increased in AD, opposite of hippocampus. Only six proteins were differentially expressed in GP, consistent with less noted pathological hallmarks in this region (N = 6; **Figure 3.2d, Table C3.4**). Of the 568 total differentially-expressed proteins, none consistently changed across all regions, though 44 changed in two regions (**Figure 3.2a**). For example, glial fibrillary acidic protein (GFAP) was one of the most robust differentially-expressed proteins across regions and was significantly increased in AD in IPL and GP (**Figure 3.2c-d**) as previously reported.[52, 55] GFAP was the only differentially-expressed protein shared between IPL and GP, and was significantly increased in hippocampus as well but was filtered out due to a high CV within the AD group. The two proteins that were differentially expressed in both hippocampus and GP were methanethiol oxidase (selenium-binding protein 1), which was increased in AD as in previous work,[55] and protein FAM49A,

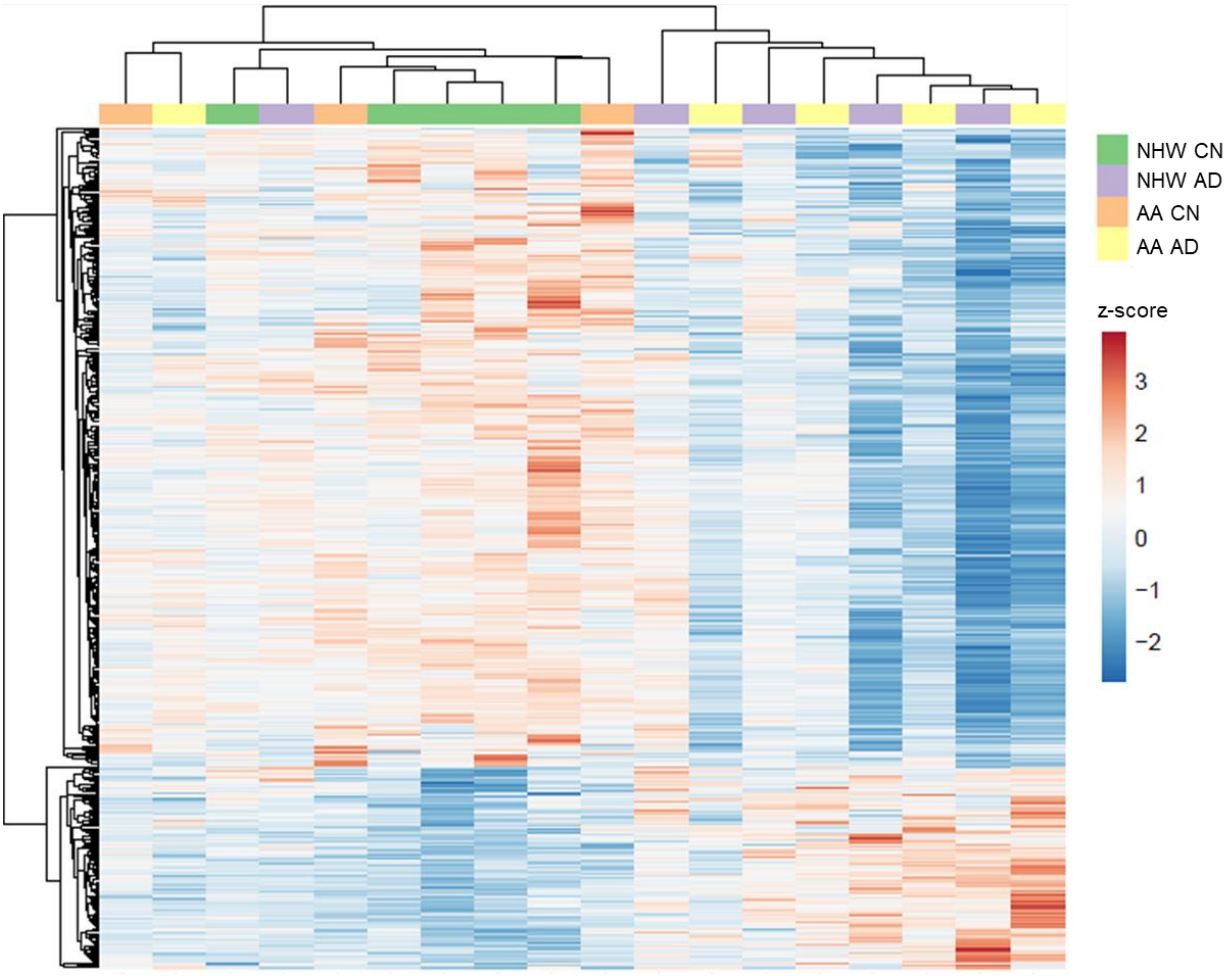

Figure 3.3. Heatmap with clustering of proteins in hippocampus. ClustVis was used to create a heatmap from the TMT reporter ion intensities for the differentially-expressed proteins in hippocampus (N = 472) across individuals (N = 18; see [72]). The columns correspond to the individuals while the rows correspond to the proteins. Rows are centered; unit variance scaling is applied to rows. Both rows and columns are clustered using correlation distance and average linkage. The proteins corresponding to the heatmap can be found in **Data C3.4**. Abbreviations: AA, African American/Black; CN, cognitively normal; NHW, non-Hispanic White; AD, Alzheimer's disease. Figure reprinted from Neurobiol. Dis., Vol 146, Stepler, K. E., et al., Inclusion of African American/Black adults in a pilot brain proteomics study of Alzheimer's disease, Article No. 105129, Copyright (2020), with permission from Elsevier.[74]

which was slightly decreased in AD and has not been reported previously. Forty-one proteins were differentially-expressed in both hippocampus and IPL, including α-2 macroglobulin, glutathione S-transferases Mu 3 and P, peroxiredoxin-1, and annexin A5, which have been reported previously.[49, 52, 55, 75] The majority of these proteins changed similarly across both regions. However, α-2 macroglobulin was decreased in AD in hippocampus while increased in AD in IPL.

On the other hand, the majority of differentially-expressed proteins differed across regions (**Figure 3.2a**). Hippocampus had the most unique differentially-expressed proteins (N = 429) of the three regions. Examples proteins unique to hippocampus include H-FABP, CAMKIIα, PRDX2, annexin A1, thy-1 membrane glycoprotein, α-synuclein, and multiple subunits of hemoglobin, as well as proteins involved in metabolism. IPL also had a significant proportion of unique differentially-expressed proteins (N = 92) including α-enolase, peroxiredoxin-6, acetyl-CoA acetyltransferase, and the brain isoform of fatty acid-binding protein. GP had only three differentially-expressed proteins-elongation factor 2, proteasome subunit α type-3, and major vault protein-none of which have been previously reported in AD.

It is important to note that some of these proteins are blood-derived, including α-2 macroglobulin and the various hemoglobin isoforms. Though it is possible that blood contamination of these brain samples occurred (as is common with human postmortem tissues), several of these proteins have been observed as differentially-expressed in AD brain in prior studies.[49, 55] Furthermore, the presence of these blood-derived proteins in the brain could be due to blood-brain barrier leakage and breakdown known to occur with aging and various forms of dementia including AD.[76-77]

3.3.3 Significant pathways in each brain region

The most significant pathways in AD in were mostly region-specific (**Figure 3.4**). Of the top 10 most significant pathways shared in multiple regions, 14-3-3-mediated signaling, was the only one in both hippocampus and GP regions. In hippocampus, the most significant pathways include mitochondrial dysfunction, oxidative phosphorylation, synaptogenesis and cell junction signaling (**Figure 3.4**; **Table C3.5**). In IPL, most significant pathways were related to oxidative stress or metabolism, including gluconeogenesis, glycolysis, glycogen degradation, and xenobiotic metabolism (**Figure 3.4; Table C3.5**). In GP, the three differentially-expressed proteins represented diphthamide biosynthesis, 14-3-3-mediated signaling, and p70S6K signaling pathways (**Figure 3.4**; **Table C3.5**).

3.3.4 Proteins with significant race x diagnosis interactions

Next, we evaluated if self-reported race had an impact on protein changes in AD. We examined the overlap between the differentially-expressed proteins in each region in all AD compared to CN individuals and the differentially-expressed proteins in a race-stratified analysis between only African American/Black AD compared to CN individuals (**Figure 3.5**). In hippocampus and IPL, about 20% of differentially-expressed proteins were common between the combined and African American/Black race-stratified comparisons, while in GP, no proteins overlapped between the two comparisons. However, in all regions, there were also proteins (N = 24, 78, 46 in hippocampus, IPL, and GP, respectively) that were differentially-expressed between African American/Black AD and CN groups but were not differentially-expressed in the combined analysis, many of which were decreased in AD in hippocampus and IPL and increased

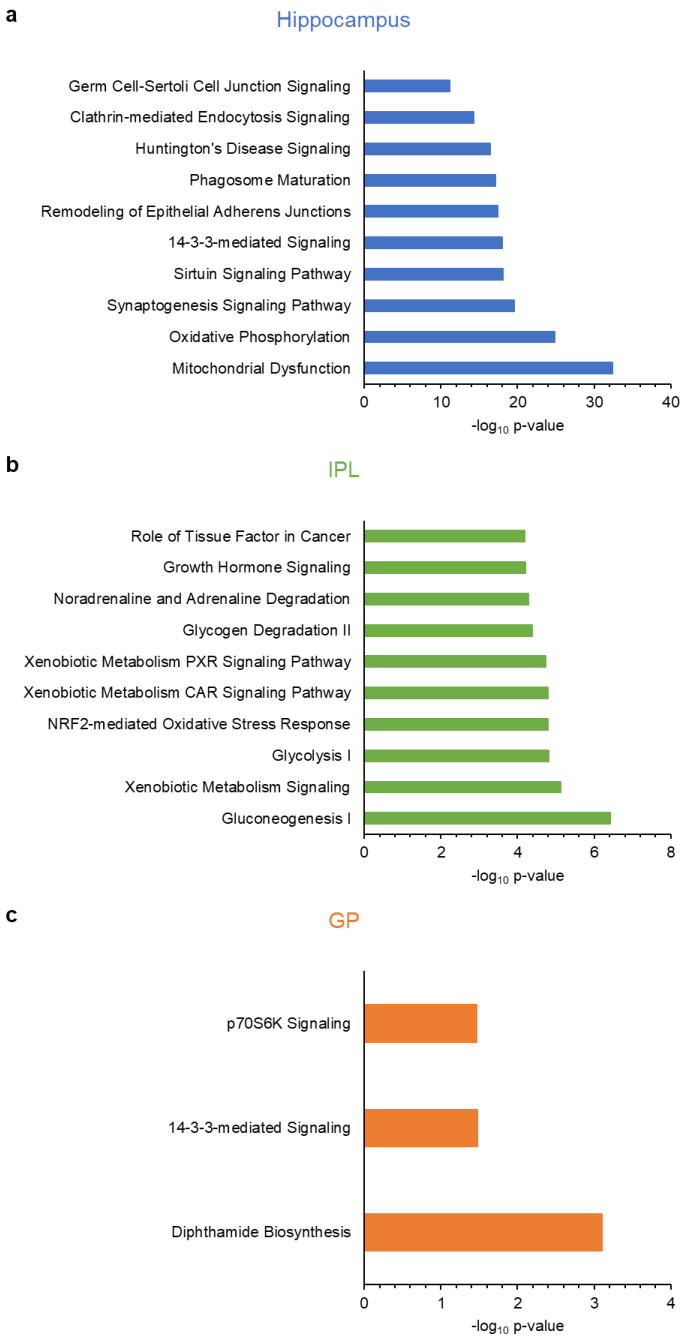

Figure 3.4. Top IPA significant pathways across regions. Bar graphs showing the top 10 significant IPA pathways ($p < 0.05$) in **a**, hippocampus, **b**, IPL, and **c**, GP. Only three pathways were significant in GP. Figure reprinted from Neurobiol. Dis., Vol 146, Stepler, K. E., et al., Inclusion of African American/Black adults in a pilot brain proteomics study of Alzheimer's disease, Article No. 105129, Copyright (2020), with permission from Elsevier.[74]

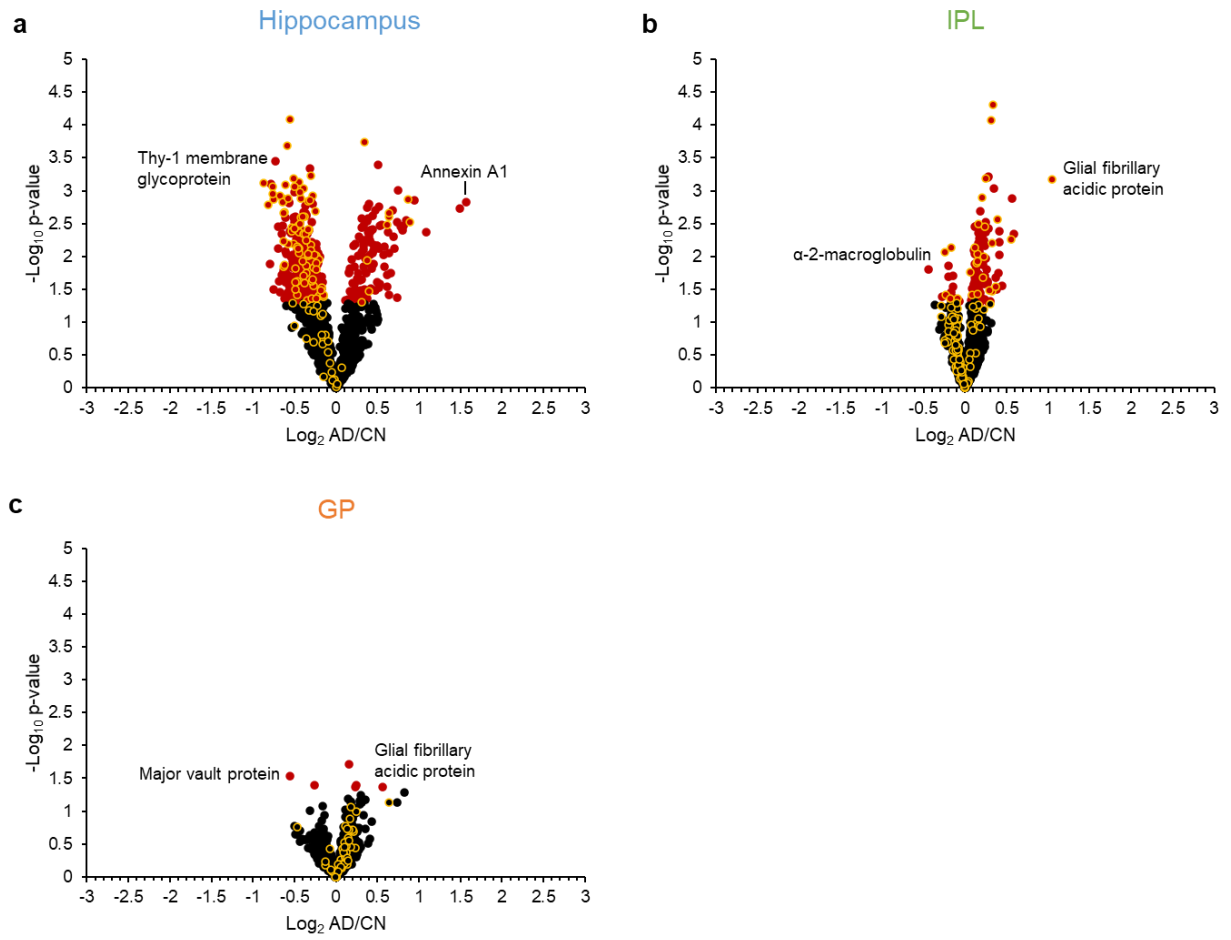

Figure 3.5. Volcano plots highlighting differentially-expressed proteins between African American/Black AD and CN groups. Volcano plots showing differentially-expressed proteins in **a**, hippocampus, **b**, IPL, and **c**, GP, as in **Figure 4.2b-d**, with differentially-expressed proteins between African American/Black AD and CN groups highlighted. CV-filtered quantified proteins are shown for each region (hippocampus N = 1,338; IPL N = 1,407; GP N = 1,103). Red data points indicate differentially-expressed proteins with uncorrected p-value < 0.05; black data points indicate quantified proteins with nonsignificant p-values. Data points with a yellow border indicate proteins that had $p < 0.05$ between African American/Black AD and CN. Selected proteins with significant changes in AD are highlighted in each plot. Abbreviations: IPL, inferior parietal lobule; GP, globus pallidus; AD, Alzheimer's disease; CN, cognitively normal. Figure reprinted from Neurobiol. Dis., Vol 146, Stepler, K. E., et al., Inclusion of African American/Black adults in a pilot brain proteomics study of Alzheimer's disease, Article No. 105129, Copyright (2020), with permission from Elsevier.[74]

in AD in GP (**Figure 3.5**). This suggests that some protein changes in AD would not be detected without examining multiple racial/ethnic groups.

We used linear regression models with a race x diagnosis interaction term to determine whether race modifies the association between diagnosis and protein intensities in each region, which resulted in 185 proteins with significant race x diagnosis interactions (**Figure 3.6**). There were 27, 60, and 105 proteins with significant race x diagnosis interactions in hippocampus, IPL, and GP, respectively (**Tables C3.6-3.8**). Seven proteins with significant interactions overlapped in hippocampus and IPL (**Figure 3.6**). Example proteins are highlighted in **Figure 3.6**. In hippocampus, heterogeneous nuclear ribonucleoprotein D0 increased in non-Hispanic White adults with AD and had no change in African American/Black adults. In IPL, heterogeneous nuclear ribonucleoprotein D0 decreased in African American/Black adults with AD and had no change in non-Hispanic White adults (**Figure 3.6**). Other examples of proteins that differed in the African American/Black and non-Hispanic White AD groups are shown in **Figure 3.6**, for α-2 macroglobulin, α-synuclein, and fructose-bisphosphate aldolase A.

Next, we compared proteins (N=185) with significant race x diagnosis interactions to those significant from the race-stratified linear regression models for the effect of diagnosis (**Table 3.2**). A subset of these proteins were significant in AD in at least one of the race-stratified comparisons: 20 in hippocampus, 39 in IPL, and 40 in GP. Interestingly, most of these proteins changed in AD in one racial/ethnic group and not the other.

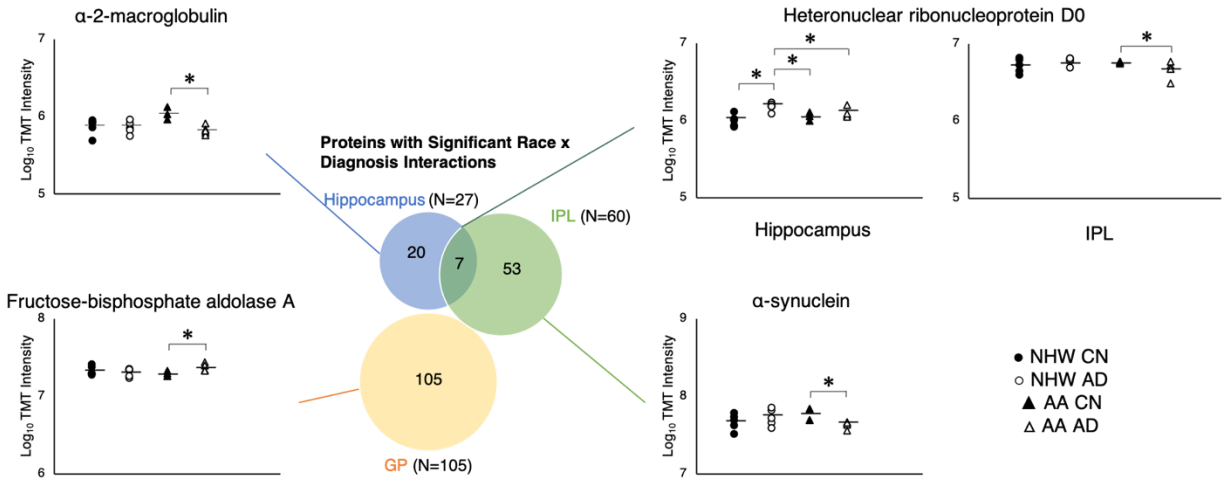

Figure 3.6. Proteins with significant race x diagnosis interactions in each region. Venn diagram showing the regional overlap in proteins with significant race x diagnosis interactions ($p < 0.05$), and plots showing examples of these proteins in different regions: heterogeneous nuclear ribonucleoprotein D0, α-2-macroglobulin, α-synuclein, and fructose-bisphosphate aldolase A. The plots show $\log_{10}$ TMT intensities plotted for each brain sample in the relevant region. Each data point represents one individual; brains of non-Hispanic White CN adults are filled circles, brains of non-Hispanic White AD adults are open circles, brains of African American/Black CN adults are filled triangles, and brains of African American/Black AD adults are open triangles. Horizontal lines indicate group averages (N = 5 per group, except N = 3 for hippocampus from African American/Black CN adults, N = 4 for IPL and GP African American/Black CN and GP African American/Black AD adults). * indicates $p < 0.05$. Abbreviations: AA, African American/Black; CN, cognitively normal; NHW, non-Hispanic White; AD, Alzheimer's disease; IPL, inferior parietal lobule; GP, globus pallidus. Figure reprinted from Neurobiol. Dis., Vol 146, Stepler, K. E., et al., Inclusion of African American/Black adults in a pilot brain proteomics study of Alzheimer's disease, Article No. 105129, Copyright (2020), with permission from Elsevier.[74]

Table 3.2. Overlap of differentially-expressed proteins in AD with ROSMAP TMT dataset.

Brain Region	By Diagnosis in Everyone		By Diagnosis in NHWs		By Diagnosis in AAs		With Race x Diagnosis Interaction	
	Significant in this study	Overlap with ROSMAP	Significant in this study	Overlap with ROSMAP	Significant in this study	Overlap with ROSMAP	Significant in this study	Overlap with ROSMAP
Hippocampus	472	155	199	33	114	2	20	0
IPL	134	59	86	33	105	3	39	1
GP	6	3	23	2	45	3	40	3

Abbreviations: NHW, non-Hispanic White; AA, African American/Black.

3.3.5 Comparison to the Religious Orders Study and Rush Memory and Aging Project (ROSMAP)

Additionally, we compared the differentially-expressed proteins in our study to a TMT dataset of N = 375 dorsolateral prefrontal cortex samples from the Religious Orders Study and Rush Memory and Aging Project (ROSMAP), composed of African American/Black (CN, N = 5 and AD, N = 1) and non-Hispanic White adults (CN, N = 151; MCI N = 90; and AD, N = 120). We performed linear regression analyses and identified 495 significant (corrected $p < 0.05$) proteins in AD. Comparison of these proteins with differentially-expressed proteins in this study (**Figure 3.2**) resulted in 199 overlapping proteins (**Table 3.2**), highlighting the consistency and relevance of our findings. It is apparent that most of our overlap with the ROSMAP dataset occurred in the non-Hispanic White group even despite different brain regions (i.e., hippocampus, IPL, GP vs. prefrontal cortex). Notably, the published ROSMAP dataset included only a single African American/Black AD case, further emphasizing the value of the current dataset despite our limited sample size. Given the number of signals identified in our non-Hispanic White-stratified analysis that were confirmed in the larger non-Hispanic White dataset of ROSMAP, it is likely that many of the novel signals identified in our African American/Black stratified analysis would show similar consistency if a larger African American/Black replication sample were available. Clearly there is a pressing need to increase representation in proteomic analyses of the AD brain.

3.4 Discussion

Our study identified 2,613 total proteins in hippocampus, IPL, and GP which is on par with other proteomics studies of mostly hippocampus and temporal lobe.[46, 48, 50, 52, 55-56, 75, 78-82]

Despite the limited number of brain samples included in this study, 568 total proteins were found to be differentially expressed in AD across hippocampus, IPL, and GP. Hippocampus is the most severely affected brain region in AD and, as such, is previously noted to have substantial protein expression changes.[46] Our data are consistent with this observation. Furthermore, the 568 differentially-expressed proteins in AD from our study, when compared to 709 differentially-expressed proteins compiled from the literature,[48-49, 52, 55, 75, 83-91] reveals an overlap of 217 proteins. Most of the differentially-expressed proteins in our study were region-specific with none observed in all regions and only 44 differentially expressed in two regions, most of which were common between hippocampus and IPL (**Figure 3.2a**). Many of these protein changes have been previously reported in AD brain.[49, 52, 55, 75] Aβ A4 protein was not differentially expressed in any of the regions in our study; it was removed from the analysis in hippocampus and IPL due to high within-group CVs, while it was measured but not differentially expressed in GP. Aβ42 accumulation has been reported in GP neurons,[66] although Aβ accumulation may not be substantial enough for proteomic differences between AD and CN individuals to be detected. Microtubule-associated protein tau was measured in all three regions, but was not differentially expressed in any region or racial group.

It is important to note that existing human AD brain proteomics literature includes studies with a variety of sample sizes (N = 3[50] - ≥ 900[92]) and brain regions such as frontal lobe,[45, 47, 49-50, 84, 88-89, 92-98] temporal lobe (including hippocampus),[46, 48-50, 52, 55, 75, 85-86, 90, 92, 95, 99] and IPL.[50] None included nonpathological regions such as GP. Our study aligns with ~61% of these publications that have had cohorts of N ≤ 20 individuals,[46, 48-50, 55, 75, 84-86, 89-90, 96, 99] resulting in group sizes of N = 1-10. Differentially-expressed proteins in our study (N = 197 and 56, respectively) overlapped with studies of both small (N = 4-20[48-49, 55, 75, 84-86, 89-90]) and large (N = 40-201[52, 88])

sample sizes. Most of these studies also do not include racial/ethnic diversity of participants. For example, one report exclusively studied Mexican[84] and another Japanese[48] adults, while a few included African American/Black, Hispanic, and Native Hawaiian or other Pacific Islander groups representing 11-13% of study participants.[45, 47, 98] Therefore, these consistent findings increase the confidence of this study.

However, a majority of differentially-expressed proteins (i.e., 351 proteins) in our study compared to previous reports[48-49, 52, 55, 75, 83-91] were novel. This is likely due to both the inclusion of a diverse cohort and brain regions: IPL and GP. IPL and GP have been studied in AD,[57-59, 61-65, 100-103] but not in the context of global proteomics analyses. Furthermore, proteomic changes from African American/Black adults or other racial/ethnic AD groups in the U.S. are not well-characterized. There were proteins (N = 24, 78, 46 in hippocampus, IPL, and GP, respectively) that were differentially expressed in AD when evaluating only the African American/Black group that were not differentially-expressed in the combined analysis of both racial groups (**Figure 3.5**). This underscores the need for racial/ethnic diversity in AD cohorts and 'omics studies. We also compared the differentially-expressed proteins in our dataset to an existing ROSMAP TMT dataset from the dorsolateral prefrontal cortex region and identified substantial overlap (**Table 3.2**). It is notable that substantial overlap was observed despite differences in brain regions and geography between the two datasets. Also, this overlap was higher in the non-Hispanic White group than in the African American/Black group. Additionally, fifty-two percent of proteins with significant race x diagnosis interactions also had significant race-stratified changes in AD in one or both racial groups, the majority of which only had significant changes in AD in one racial group but not the other. This could be because the smaller N is more sensitive to heterogeneous changes in AD that could be neutralized in larger groups. However, it

is also possible based on our consistent findings with ROSMAP TMT data that disease pathogenesis is more heterogeneous at the proteome level**,** which highlights the need to conduct larger studies that include diverse participants.

3.4.1 Study strengths and limitations

The most important strength of our study is the inclusion of brain samples from both African American/Black and non-Hispanic White adults. African American/Black adults and adults from other racial/ethnic minorities are highly underrepresented in brain proteomics studies in AD. This is likely due to the need for increased research participation and lower likelihood of some individuals to consent to autopsy to provide brain tissue samples.[104-106] Furthermore, African American/Black and Hispanic adults are at increased risk for AD, making molecular understanding of AD pathogenesis in those groups particularly vital. While we did not study Hispanic or Asian American adults, or adults from other racial/ethnic groups here, we suggest that racial/ethnic diversity be included in future 'omics study designs. However, such studies when including components of race must also consider other social and environmental factors that impact physiological and biological changes.[18] Another strength of our study is that the brain samples from both racial groups and disease states were analyzed within the same experiments. This sample multiplexing minimized error and enabled direct comparison of relative protein abundances across groups. Most brain samples came from the same ADRC, minimizing any potential differences in handling across centers. Although there could be zip code differences, all brains came from the same geographical area.

The inclusion of multiple brain regions in this study is a strength because AD has spatial effects in the brain.[46, 50, 107] The hippocampus is one of the earliest regions affected in AD[53, 108-

[109] making it a valuable region to study disease pathogenesis. Furthermore, IPL and GP are not well-studied in AD using proteomics. Since little is known about proteomic changes in these regions, including them in our study is particularly valuable, especially given the potential role of GP in memory. This study adds to the available proteomics literature with new differentially-expressed proteins for disease insight and confirms others from previous studies. Furthermore, where available, the three brain regions were collected from the same individual, which additionally allows regional comparisons within individuals as well as across individuals and groups.

Proteome depth is greatly influenced by front-end LC separations and MS duty cycles. We used a high pH fractionation approach on a solid-phase extraction cartridge to generate 12 fractions and note that this may have limited our total number of proteins identified compared to column high pH separations and the collection of 24-100 fractions. The inclusion of MS^3 in our proteomics workflow can be viewed as a limitation because MS^3 leads to fewer identified proteins and thus potentially fewer quantified proteins due to longer instrumental duty cycles. However, MS^3 also leads to more robust quantitative measurements from TMT reporter ions, which was vital to this pilot study in order to accurately detect differences between disease states and assess impact of covariates (race, diagnosis, age, sex, PMI).[110-111]

The main challenge of our study was limited sample availability from African American/Black adults, which in turn limited the statistical power of this study. Postmortem brain samples from African American/Black adults are difficult to obtain, particularly from CN individuals, partially because African American/Black adults are less likely to consent to autopsy than non-Hispanic White adults[104-106] and only few centers have been effective in recruitment to brain autopsy programs.[105, 112] Additional brain samples from African American/Black adults

could have been acquired from other ADRCs; however, we thought it detrimental to combine few and unmatched cases and controls from a given center together as it introduces center effects that can impact proteomics results. At the beginning of our study (12/15/2016), African American/Black adults comprised 8.2% of the clinical AD cases in the University of Pittsburgh ADRC (N = 209 African American/Black adults). However, only five African American/Black adults with AD had brain samples available from the selected regions, along with four African American/Black adults that were CN. Thus, we selected all of these brains for our study, and matched brain samples from non-Hispanic White adults based on age, sex, and diagnosis (N = 55).

The limited availability of samples resulted in some differences across the sample groups, specifically in *APOE* genotype, age, and sex (**Table 3.1**). All groups consisted of equal distribution of males and females except the African American/Black CN group, which was all male. There was no significant difference ($p = 0.48$, race; $p = 0.14$, diagnosis) in postmortem interval across groups. The *APOE* genotypes are noted where available and were not used as matching criteria since data was missing in the African American/Black CN group. AD patients were 15 ± 15 years older than CN individuals ($p = 0.010$). Despite this age difference, diagnosis explained additional variance in protein intensity beyond the variance explained by the covariates of age, sex, PMI, and race. There is significant overlap between changes in the brain during normal aging and AD pathogenesis,[92] and due to the age differences across our sample groups, some of the protein expression changes detected in this study could be driven by age-related processes as opposed to disease-related processes. Years of education did not significantly differ between groups ($p = 0.050$, race; $p = 0.572$, diagnosis). However, it is important to note that this data was not available for all individuals, so this study cannot

adequately address the contribution of education, as measured by number of years, to the proteomic findings. Importantly, in future studies, education, the scope by which it is measured, and quality of education[113] must be included. Furthermore, records of vascular comorbidities were not available for all participants, such that incidence of vascular diseases may have differed between the groups and contributed to the observed differences. Nonetheless, significant differences across racial/ethnic backgrounds remain. In future studies, it will be important to collaborate with other ADRCs and brain banks that have greater brain sample availability from African American/Black adults. Such sample sizes will greatly increase statistical power and better normalize racial groups in consideration of socioeconomic and other demographic factors.

3.5 Conclusions

African American/Black adults are disproportionately affected by AD in comparison to non-Hispanic White adults. The molecular basis of this disparity is largely unknown. This pilot study aimed to elucidate molecular pathways that can explain these disparities in postmortem brain tissue from non-Hispanic White and African American/Black adults in a pilot cohort using discovery-based quantitative proteomics. Our study identified many differentially-expressed proteins in AD in hippocampus, IPL, and GP that are consistent with prior AD studies. When race was examined as a covariate, we observed proteins that were differentially-expressed in one racial/ethnic group and not in the other. Overall, our preliminary findings strongly highlight the need for diverse groups, especially African American/Black adults, to be included in proteomics, and likely other ‘omics, studies, to gain a clear picture of disease pathogenesis. The insights gained from this study stress the point that inclusive study designs are necessary in AD research

and at a larger scale, which we took into consideration in the study of brain tissues from a slightly larger cohort from the Rush Alzheimer's Disease Center, described in **Chapter 4**.

3.6 Acknowledgements

This dissertation chapter was adapted from the published paper titled "Inclusion of African American/Black Adults in a Pilot Brain Proteomics Study of Alzheimer's Disease" by Kaitlyn E. Stepler, Emily R. Mahoney, Julia Kofler, Timothy J. Hohman, Oscar L. Lopez, and Renã A. S. Robinson published in *Neurobiology of Disease*, **2020**, *146*, DOI:10.1016/j.nbd.2020.105129.

I would like to thank Dr. Timothy J. Hohman and Emily R. Mahoney for their assistance with statistical analyses. The authors would like to thank the University of Pittsburgh ADRC Neuropathology Core and Data Management and Statistics Core (Heather Eng, Rocco Mercurio, Shelley Ferson) for assistance with sample selection and acquisition. The authors acknowledge pilot funds from the University of Pittsburgh Alzheimer Disease Research Center funded by the National Institutes of Health and National Institute on Aging (P50-AG005133), the Vanderbilt Interdisciplinary Training Program in Alzheimer's Disease (T32-AG058524), the Alzheimer's Association (AARGD-17-533405), the Vanderbilt Institute of Chemical Biology (T32-GM065086), additional grants from the National Institute on Aging (R01-AG064950, K01-AG049164), and Vanderbilt University Start-Up Funds.

3.7 References

1. Association, A. s., 2018 Alzheimer's disease facts and figures. *Alzheimers Dement* **2018,** *14* (3), 367-429.
2. Barnes, L. L., Biomarkers for Alzheimer dementia in diverse racial and ethnic minorities—a public health priority. *JAMA Neurol* **2019,** *76* (3), 251-253.

3. González, H. M.; Tarraf, W.; Fornage, M.; González, K. A.; Chai, A.; Youngblood, M.; Abreu, M. d. l. A.; Zeng, D.; Thomas, S.; Talavera, G. A., et al., A research framework for cognitive aging and Alzheimer's disease among diverse US Latinos: Design and implementation of the Hispanic Community Health Study/Study of Latinos-Investigation of Neurocognitive Aging (SOL-INCA). *Alzheimers Dement* **2019,** *15* (12), 1624-1632.
4. Alzheimer's Association, Alzheimer's disease facts and figures. *Alzheimers Dement* **2017,** *13*, 325-373.
5. Chin, A. L.; Negash, S.; Hamilton, R., Diversity and disparity in dementia: the impact of ethnoracial differences in Alzheimer disease. *Alzheimer Dis Assoc Disord* **2011,** *25* (3), 187-195.
6. Manly, J. J.; Mayeux, R., Ethnic differences in dementia and Alzheimer's disease. In *Critical Perspectives on Racial and Ethnic Differences in Health in Late Life*, Anderson, N. B.; Bulatao, R. A.; Cohen, B., Eds. National Academies Press: Washington D.C., **2004**.
7. Matthews, K. A.; Xu, W.; Gaglioti, A. H.; Holt, J. B.; Croft, J. B.; Mack, D.; McGuire, L. C., Racial and ethnic estimates of Alzheimer's disease and related dementias in the United States (2015-2060) in adults aged ≥65 years. *Alzheimers Dement* **2018,** *15* (1), 17-24.
8. Mayeda, E. R.; Glymour, M. M.; Quesenberry, C. P.; Whitmer, R. A., Inequalities in dementia incidence between six racial and ethnic groups over 14 years. *Alzheimers Dement* **2015,** *12* (3), 216-224.
9. Barnes, L. L.; Bennett, D. A., Alzheimer's disease in African Americans: risk factors and challenges for the future. *Health Aff (Millwood)* **2014,** *33* (4), 580-586.
10. Lines, L.; A Sherif, N.; Wiener, J., *Racial and Ethnic Disparities Among Individuals with Alzheimer's Disease in the United States: A Literature Review*. RTI Press: Research Triangle Park (NC), **2014**; Vol. RR-0024-1412, p 1-30.
11. Barnes, L. L.; Leurgans, S.; Aggarwal, N. T.; Shah, R. C.; Arvanitakis, Z.; James, B. D.; Buchman, A. S.; Bennett, D. A.; Schneider, J. A., Mixed pathology is more likely in black than white decedents with Alzheimer dementia. *Neurology* **2015,** *85* (6), 528-534.
12. Gottesman, R. F.; Schneider, A. C.; Zhou, Y.; Coresh, J.; Green, E.; Gupta, N.; Knopman, D. S.; Mintz, A.; Rahmim, A.; Sharrett, A. R., et al., Association between midlife vascular risk factors and estimated brain amyloid deposition. *JAMA* **2017,** *317* (14), 1443-1450.
13. Wilkins, C. H.; Grant, E. A.; Schmitt, S. E.; McKeel, D. W.; Morris, J. C., The neuropathology of Alzheimer disease in African American and white individuals. *Arch Neurol* **2006,** *63* (1), 87-90.
14. Kamara, D. M.; Gangishetti, U.; Gearing, M.; Willis-Parker, M.; Zhao, L.; Hu, W. T.; Walker, L. C., Cerebral amyloid angiopathy: similarity in African-Americans and Caucasians with Alzheimer's disease. *J Alzheimers Dis* **2018,** *62* (4), 1815-1826.
15. Gavett, B. E.; Fletcher, E.; Harvey, D.; Farias, S. T.; Olichney, J.; Beckett, L.; DeCarli, C.; Mungas, D., Ethnoracial differences in brain structure change and cognitive change. *Neuropsychology* **2018,** *32* (5), 529-540.
16. Graff-Radford, N. R.; Besser, L. M.; Crook, J. E.; Kukull, W. A.; Dickson, D. W., Neuropathological differences by race from the National Alzheimer's Coordinating Center. *Alzheimers Dement* **2016,** *12* (6), 669-677.
17. Filshtein, T. J.; Dugger, B. N.; Jin, L.-W.; Olichney, J. M.; Farias, S. T.; Carvajal-Carmona, L.; Lott, P.; Mungas, D.; Reed, B.; Beckett, L. A., et al., Neuropathological diagnoses of demented Hispanic, black, and non-Hispanic white decedents seen at an Alzheimer's disease center. *J Alzheimers Dis* **2019,** *68*, 145-158.

18. Wilkins, C. H.; Schindler, S. E.; Morris, J. C., Addressing health disparities among minority populations: Why clinical trial recruitment is not enough. *JAMA Neurol* **2020,** *77* (9), 1063-1064.
19. Mehta, K. M.; Yeo, G. W., Systematic review of dementia prevalence and incidence in United States race/ethnic populations. *Alzheimers Dement* **2017,** *13* (1), 72-83.
20. Burke, S. L.; Cadet, T.; Maddux, M., Chronic health illnesses as predictors of mild cognitive impairment among African American older adults. *J Natl Med Assoc* **2017,** *110* (4), 314-325.
21. Gilligan, A. M.; Malone, D. C.; Warholak, T. L.; Armstrong, E. P., Racial and ethnic disparities in Alzheimer's disease pharmacotherapy exposure: an analysis across four state Medicaid populations. *Am J Geriatr Pharmacother* **2012,** *10* (5), 303-312.
22. Hohman, T. J.; Cooke-Bailey, J. N.; Reitz, C.; Jun, G.; Naj, A.; Beecham, G. W.; Liu, Z.; Carney, R. M.; Vance, J. M.; Cuccaro, M. L., et al., Global and local ancestry in African-Americans: implications for Alzheimer's disease risk. *Alzheimers Dement* **2016,** *12* (3), 233-243.
23. Reitz, C.; Jun, G.; Naj, A.; Rajbhandary, R.; Vardarajan, B. N.; Wang, L.-S.; Valladares, O.; Lin, C.-F.; Larson, E. B.; Graff-Radford, N. R., et al., Variants in the ATP-binding cassette transporter (ABCA7), apolipoprotein E ε4, and the risk of late-onset Alzheimer disease in African Americans. *JAMA* **2013,** *309* (14), 1483-1492.
24. Desai, P. P.; Hendrie, H. C.; Evans, R. M.; Murrell, J. R.; DeKosky, S. T.; Kamboh, M. I., Genetic variation in apolipoprotein D affects the risk of Alzheimer disease in African-Americans. *Am J Med Genet B Neuropsychiatr Genet* **2003,** *116B* (1), 98-101.
25. Lee, J. H.; Cheng, R.; Schupf, N.; Manly, J.; Lantigua, R.; Stern, Y.; Tycko, B.; Rogaeva, E.; Wakutani, Y.; Farrer, L., et al., The association between genetic variants in SORL1 and Alzheimer's disease in an urban, multiethnic, community-based cohort. *Arch Neurol* **2007,** *64* (4), 501-506.
26. Ghani, M.; Reitz, C.; Cheng, R.; Vardarajan, B. N.; Jun, G.; Sato, C.; Naj, A.; Rajbhandary, R.; Wang, L. S.; Valladares, O., et al., Association of long runs of homozygosity with Alzheimer disease among African American individuals. *JAMA Neurol* **2015,** *72* (11), 1313-1323.
27. El Gaamouch, F.; Jing, P.; Xia, J.; Cai, D., Alzheimer's disease risk genes and lipid regulators. *J Alzheimers Dis* **2016,** *53*, 15-29.
28. Martins, I. J.; Berger, T.; Sharman, M. J.; Verdile, G.; Fuller, S. J.; Martins, R. N., Cholesterol metabolism and transport in the pathogenesis of Alzheimer's disease. *J Neurochem* **2009,** *111* (6), 1275-1308.
29. Rogaeva, E.; Meng, Y.; Lee, J. H.; Gu, Y.; Kawarai, T.; Zou, F.; Katayama, T.; Baldwin, C. T.; Cheng, R.; Hasegawa, H., et al., The neuronal sortilin-related receptor SORL1 is genetically associated with Alzheimer's disease. *Nat Genet* **2007,** *39* (2), 168-177.
30. Liu, Q.; Zhang, J., Lipid metabolism in Alzheimer's disease. *Neurosci Bull* **2014,** *30* (2), 331-345.
31. Gamba, P.; Testa, G.; Sottero, B.; Gargiulo, S.; Poli, G.; Leonarduzzi, G., The link between altered cholesterol metabolism and Alzheimer's disease. *Ann N Y Acad Sci* **2012,** *1259*, 54-64.
32. Burns, M.; Duff, K., Cholesterol in Alzheimer's disease and tauopathy. *Ann N Y Acad Sci* **2002,** *977* (1), 367-375.

33. Sato, N.; Morishita, R. The roles of lipid and glucose metabolism in modulation of β-amyloid, tau, and neurodegeneration in the pathogenesis of Alzheimer disease. *Front Aging Neurosci* [Online], **2015**. https://www.frontiersin.org/article/10.3389/fnagi.2015.00199.
34. Stepler, K. E.; Robinson, R. A. S., The potential of 'omics to link lipid metabolism and genetic and comorbidity risk factors of Alzheimer's disease in African Americans. In *Reviews on Biomarker Studies in Psychiatric and Neurodegenerative Disorders*, Guest, P. C., Ed. Springer International Publishing: Cham, **2019**; Vol. 1118, pp 1-28.
35. Chakrabarti, S.; Khemka, V. K.; Banerjee, A.; Chatterjee, G.; Ganguly, A.; Biswas, A., Metabolic risk factors of sporadic Alzheimer's disease: implications in the pathology, pathogenesis and treatment. *Aging Dis* **2015,** *6* (4), 282-299.
36. Matsuzaki, T.; Sasaki, K.; Hata, J.; Hirakawa, Y.; Fujimi, K.; Ninomiya, T.; Suzuki, S. O.; Kanba, S.; Kiyohara, Y.; Iwaki, T., Association of Alzheimer disease pathology with abnormal lipid metabolism: the Hisayama Study. *Neurology* **2011,** *77* (11), 1068-1075.
37. Babulal, G. M.; Quiroz, Y. T.; Albensi, B. C.; Arenaza-Urquijo, E.; Astell, A. J.; Babiloni, C.; Bahar-Fuchs, A.; Bell, J.; Bowman, G. L.; Brickman, A. M., et al., Perspectives on ethnic and racial disparities in Alzheimer's disease and related dementias: update and areas of immediate need. *Alzheimers Dement* **2018**, 10.1016/j.jalz.2018.09.009.
38. Wharton, W.; Kollhoff, A. L.; Gangishetti, U.; Verble, D. D.; Upadhya, S.; Zetterberg, H.; Kumar, V.; Watts, K. D.; Kippels, A. J.; Gearing, M., et al., Interleukin 9 alterations linked to Alzheimer disease in African Americans. *Ann Neurol* **2019,** *86*, 407-418.
39. Rosenmann, H., CSF biomarkers for amyloid and tau pathology in Alzheimer's disease. *J Mol Neurosci* **2012,** *47* (1), 1-14.
40. Howell, J. C.; Watts, K. D.; Parker, M. W.; Wu, J.; Kollhoff, A.; Wingo, T. S.; Dorbin, C. D.; Qiu, D.; Hu, W. T. Race modifies the relationship between cognition and Alzheimer's disease cerebrospinal fluid biomarkers. *Alzheimers Res Ther* [Online], **2017**. https://doi.org/10.1186/s13195-017-0315-1.
41. Morris, J. C.; Schindler, S. E.; McCue, L. M.; Moulder, K. L.; Benzinger, T. L. S.; Cruchaga, C.; Fagan, A. M.; Grant, E.; Gordon, B. A.; Holtzman, D. M., et al., Assessment of racial disparities in biomarkers for Alzheimer disease. *JAMA Neurol* **2019,** *76* (3), 264-273.
42. Blennow, K.; Vanmechelen, E.; Hampel, H., CSF total tau, Aβ42 and phosphorylated tau protein as biomarkers for Alzheimer's disease. *Mol Neurobiol* **2001,** *24* (1), 87-97.
43. Wallin, Å. K.; Blennow, K.; Andreasen, N.; Minthon, L., CSF biomarkers for Alzheimer's disease: levels of β-amyloid, tau, phosphorylated tau relate to clinical symptoms and survival. *Dement Geriatr Cogn Disord* **2006,** *21* (3), 131-138.
44. Garrett, S. L.; McDaniel, D.; Obideen, M.; Trammell, A. R.; Shaw, L. M.; Goldstein, F. C.; Hajjar, I. Racial disparity in cerebrospinal fluid amyloid and tau biomarkers and associated cutoffs for mild cognitive impairment. *JAMA Netw Open* [Online], **2019**. https://doi.org/10.1001/jamanetworkopen.2019.17363.
45. Seyfried, N. T.; Dammer, E. B.; Swarup, V.; Nandakumar, D.; Duong, D. M.; Yin, L.; Deng, Q.; Nguyen, T.; Hales, C. M.; Wingo, T., et al., A multi-network approach identifies protein-specific co-expression in asymptomatic and symptomatic Alzheimer's disease. *Cell Syst* **2017,** *4* (1), 60-72.
46. Xu, J.; Patassini, S.; Rustogi, N.; Riba-Garcia, I.; Hale, B. D.; Phillips, A. M.; Waldvogel, H.; Haines, R.; Bradbury, P.; Stevens, A., et al. Regional protein expression in human Alzheimer's brain correlates with disease severity. *Commun Biol* [Online], **2019**. https://www.nature.com/articles/s42003-018-0254-9.pdf.

47. Ping, L.; Duong, D. M.; Yin, L.; Gearing, M.; Lah, J. J.; Levey, A. I.; Seyfried, N. T. Global quantitative analysis of the human brain proteome in Alzheimer's and Parkinson's Disease. *Sci Data* [Online], **2018**. http://dx.doi.org/10.1038/sdata.2018.36.
48. Manavalan, A.; Mishra, M.; Feng, L.; Sze, S. K.; Akatsu, H.; Heese, K. Brain site-specific proteome changes in aging-related dementia. *Exp Mol Med* [Online], **2013**. http://dx.doi.org/10.1038/emm.2013.76.
49. Zahid, S.; Oellerich, M.; Asif, A. R.; Ahmed, N., Differential expression of proteins in brain regions of Alzheimer's disease patients. *Neurochem Res* **2014,** *39* (1), 208-215.
50. McKetney, J.; Runde, R.; Hebert, A. S.; Salamat, S.; Roy, S.; Coon, J. J., Proteomic atlas of the human brain in Alzheimer's disease. *J Proteome Res* **2019,** *18* (3), 1380-1391.
51. Mu, Y.; Gage, F. H. Adult hippocampal neurogenesis and its role in Alzheimer's disease. *Mol Neurodegener* [Online], **2011**. https://www.ncbi.nlm.nih.gov/pmc/articles/PMC3261815/pdf/1750-1326-6-85.pdf.
52. Hondius, D. C.; van Nierop, P.; Li, K. W.; Hoozemans, J. J. M.; van der Schors, R. C.; van Haastert, E. S.; van der Vies, S. M.; Rozemuller, A. J. M.; Smit, A. B., Profiling the human hippocampal proteome at all pathologic stages of Alzheimer's disease. *Alzheimers Dement* **2016,** *12* (6), 654-668.
53. Smith, A. D., Imaging the progression of Alzheimer pathology through the brain. *Proc Natl Acad Sci U S A* **2002,** *99* (7), 4135-4137.
54. Scahill, R. I.; Schott, J. M.; Stevens, J. M.; Rossor, M. N.; Fox, N. C., Mapping the evolution of regional atrophy in Alzheimer's disease: unbiased analysis of fluid-registered serial MRI. *Proc Natl Acad Sci U S A* **2002,** *99* (7), 4703-4707.
55. Begcevic, I.; Kosanam, H.; Martinez-Morillo, E.; Dimitromanolakis, A.; Diamandis, P.; Kuzmanov, U.; Hazrati, L. N.; Diamandis, E. P. Semiquantitative proteomic analysis of human hippocampal tissues from Alzheimer's disease and age-matched control brains. *Clin Proteomics* [Online], **2013**. https://www.ncbi.nlm.nih.gov/pmc/articles/PMC3648498/pdf/1559-0275-10-5.pdf.
56. Schrotter, A.; Oberhaus, A.; Kolbe, K.; Seger, S.; Mastalski, T.; El Magraoui, F.; Hoffmann-Posorske, E.; Bohnert, M.; Deckert, J.; Braun, C., et al., LMD proteomics provides evidence for hippocampus field-specific motor protein abundance changes with relevance to Alzheimer's disease. *Biochim Biophys Acta, Proteins Proteomics* **2017,** *1865* (6), 703-714.
57. Reed, T. T.; Pierce, W. M., Jr.; Turner, D. M.; Markesbery, W. R.; Butterfield, D. A., Proteomic identification of nitrated brain proteins in early Alzheimer's disease inferior parietal lobule. *J Cell Mol Med* **2009,** *13* (8b), 2019-2029.
58. Hensley, K.; Hall, N.; Subramaniam, R.; Cole, P.; Harris, M.; Aksenov, M.; Aksenova, M.; Gabbita, S. P.; Wu, J. F.; Carney, J. M., et al., Brain regional correspondence between Alzheimer's disease histopathology and biomarkers of protein oxidation. *J Neurochem* **1995,** *65* (5), 2146-2156.
59. Dalle-Donne, I.; Giustarini, D.; Colombo, R.; Rossi, R.; Milzani, A., Protein carbonylation in human diseases. *Trends Mol Med* **2003,** *9* (4), 169-176.
60. Sultana, R.; Reed, T.; Perluigi, M.; Coccia, R.; Pierce, W. M.; Butterfield, D. A., Proteomic identification of nitrated brain proteins in amnestic mild cognitive impairment: a regional study. *J Cell Mol Med* **2007,** *11* (4), 839-851.
61. Newman, S. F.; Sultana, R.; Perluigi, M.; Coccia, R.; Cai, J.; Pierce, W. M.; Klein, J. B.; Turner, D. M.; Butterfield, D. A., An increase in S-glutathionylated proteins in the Alzheimer's disease inferior parietal lobule, a proteomics approach. *J Neurosci Res* **2007,** *85* (7), 1506-1514.

62. Wang, Z.; Xia, M.; Dai, Z.; Liang, X.; Song, H.; He, Y.; Li, K., Differentially disrupted functional connectivity of the subregions of the inferior parietal lobule in Alzheimer's disease. *Brain Struct Funct* **2015,** *220* (2), 745-762.
63. Greene, S. J.; Killiany, R. J., Subregions of the inferior parietal lobule are affected in the progression to Alzheimer's disease. *Neurobiol Aging* **2010,** *31* (8), 1304-1311.
64. Triplett, J. C.; Swomley, A. M.; Cai, J.; Klein, J. B.; Butterfield, D. A., Quantitative phosphoproteomic analyses of the inferior parietal lobule from three different pathological stages of Alzheimer's disease. *J Alzheimers Dis* **2016,** *49* (1), 45-62.
65. Lehéricy, S.; Hirsch, E. C.; Hersh, L. B.; Agid, Y., Cholinergic neuronal loss in the globus pallidus of Alzheimer disease patients. *Neurosci Lett* **1991,** *123* (2), 152-155.
66. Baker-Nigh, A.; Vahedi, S.; Davis, E. G.; Weintraub, S.; Bigio, E. H.; Klein, W. L.; Geula, C., Neuronal amyloid-β accumulation within cholinergic basal forebrain in ageing and Alzheimer's disease. *Brain* **2015,** *138* (Pt 6), 1722-1737.
67. Braak, H.; Alafuzoff, I.; Arzberger, T.; Kretzschmar, H.; Del Tredici, K., Staging of Alzheimer disease-associated neurofibrillary pathology using paraffin sections and immunocytochemistry. *Acta Neuropathol* **2006,** *112* (4), 389-404.
68. Braak, H.; Braak, E., Neuropathological stageing of Alzheimer-related changes. *Acta Neuropathol* **1991,** *82* (4), 239-259.
69. Vizcaíno, J. A.; Csordas, A.; del-Toro, N.; Dianes, J. A.; Griss, J.; Lavidas, I.; Mayer, G.; Perez-Riverol, Y.; Reisinger, F.; Ternent, T., et al., 2016 update of the PRIDE database and related tools. *Nucleic Acids Res* **2016,** *44* (D1), D447-D456.
70. Plubell, D. L.; Wilmarth, P. A.; Zhao, Y.; Fenton, A. M.; Minnier, J.; Reddy, A. P.; Klimek, J.; Yang, X.; David, L. L.; Pamir, N., Extended multiplexing of Tandem Mass Tags (TMT) labeling reveals age and high fat diet specific proteome changes in mouse epididymal adipose tissue. *Mol Cell Proteomics* **2017,** *16* (5), 873-890.
71. Cao, Z.; Yende, S.; Kellum, J. A.; Angus, D. C.; Robinson, R. A. S., Proteomics reveals age-related differences in the host immune response to sepsis. *J Proteome Res* **2014,** *13* (2), 422-432.
72. Krämer, A.; Green, J.; Pollard, J., Jr.; Tugendreich, S., Causal analysis approaches in Ingenuity Pathway Analysis. *Bioinformatics* **2014,** *30* (4), 523-530.
73. Metsalu, T.; Vilo, J., ClustVis: a web tool for visualizing clustering of multivariate data using Principal Component Analysis and heatmap. *Nucleic Acids Res* **2015,** *43* (W1), W566-W570.
74. Stepler, K. E.; Mahoney, E. R.; Kofler, J.; Hohman, T. J.; Lopez, O. L.; Robinson, R. A. S. Inclusion of African American/Black adults in a pilot brain proteomics study of Alzheimer's disease. *Neurobiol Dis* [Online], **2020**. http://www.sciencedirect.com/science/article/pii/S0969996120304046.
75. Musunuri, S.; Wetterhall, M.; Ingelsson, M.; Lannfelt, L.; Artemenko, K.; Bergquist, J.; Kultima, K.; Shevchenko, G., Quantification of the brain proteome in Alzheimer's disease using multiplexed mass spectrometry. *J Proteome Res* **2014,** *13* (4), 2056-2068.
76. Halliday, M. R.; Rege, S. V.; Ma, Q.; Zhao, Z.; Miller, C. A.; Winkler, E. A.; Zlokovic, B. V., Accelerated pericyte degeneration and blood-brain barrier breakdown in apolipoprotein E4 carriers with Alzheimer's disease. *J Cereb Blood Flow Metab* **2016,** *36* (1), 216-227.
77. Nelson, A. R.; Sweeney, M. D.; Sagare, A. P.; Zlokovic, B. V., Neurovascular dysfunction and neurodegeneration in dementia and Alzheimer's disease. *Biochim Biophys Acta* **2016,** *1862* (5), 887-900.

78. Martins-de-Souza, D.; Carvalho, P. C.; Schmitt, A.; Junqueira, M.; Nogueira, F. C.; Turck, C. W.; Domont, G. B., Deciphering the human brain proteome: characterization of the anterior temporal lobe and corpus callosum as part of the Chromosome 15-centric Human Proteome Project. *J Proteome Res* **2014,** *13* (1), 147-157.
79. Xu, B.; Gao, Y.; Zhan, S.; Xiong, F.; Qiu, W.; Qian, X.; Wang, T.; Wang, N.; Zhang, D.; Yang, Q., et al., Quantitative protein profiling of hippocampus during human aging. *Neurobiol Aging* **2016,** *39*, 46-56.
80. Xu, B.; Xiong, F.; Tian, R.; Zhan, S.; Gao, Y.; Qiu, W.; Wang, R.; Ge, W.; Ma, C., Temporal lobe in human aging: A quantitative protein profiling study of samples from Chinese Human Brain Bank. *Exp Gerontol* **2016,** *73*, 31-41.
81. Liu, X.; Guo, Z.; Liu, W.; Sun, W.; Ma, C., Differential proteome analysis of hippocampus and temporal cortex using label-free based 2D-LC-MS/MS. *J Proteomics* **2017,** *165*, 26-34.
82. Fernández-Irigoyen, J.; Zelaya, M. V.; Tuñon, T.; Santamaría, E. Anatomo-proteomic characterization of human basal ganglia: focus on striatum and globus pallidus. *Mol Brain* [Online], **2014**. PMC. http://www.ncbi.nlm.nih.gov/pmc/articles/PMC4236423/.
83. Qi, J. P.; Wu, H.; Yang, Y.; Wang, D. D.; Chen, Y. X.; Gu, Y. H.; Liu, T., Cerebral ischemia and Alzheimer's disease: the expression of amyloid-beta and apolipoprotein E in human hippocampus. *J Alzheimers Dis* **2007,** *12* (4), 335-341.
84. Minjarez, B.; Calderon-Gonzalez, K. G.; Rustarazo, M. L.; Herrera-Aguirre, M. E.; Labra-Barrios, M. L.; Rincon-Limas, D. E.; Del Pino, M. M.; Mena, R.; Luna-Arias, J. P., Identification of proteins that are differentially expressed in brains with Alzheimer's disease using iTRAQ labeling and tandem mass spectrometry. *J Proteomics* **2016,** *139*, 103-121.
85. Andreev, V. P.; Petyuk, V. A.; Brewer, H. M.; Karpievitch, Y. V.; Xie, F.; Clarke, J.; Camp, D.; Smith, R. D.; Lieberman, A. P.; Albin, R. L., et al., Label-free quantitative LC-MS proteomics of Alzheimer's disease and normally aged human brains. *J Proteome Res* **2012,** *11* (6), 3053-3067.
86. Sultana, R.; Boyd-Kimball, D.; Cai, J.; Pierce, W. M.; Klein, J. B.; Merchant, M.; Butterfield, D. A., Proteomics analysis of the Alzheimer's disease hippocampal proteome. *J Alzheimers Dis* **2007,** *11* (2), 153-164.
87. Butterfield, D. A.; Lange, M. L., Multifunctional roles of enolase in Alzheimer's disease brain: beyond altered glucose metabolism. *J Neurochem* **2009,** *111* (4), 915-933.
88. Bai, B.; Wang, X.; Li, Y.; Chen, P.-C.; Yu, K.; Dey, K. K.; Yarbro, J. M.; Han, X.; Lutz, B. M.; Rao, S., et al., Deep multilayer brain proteomics identifies molecular networks in Alzheimer’s disease progression. *Neuron* **2020,** *105* (6), 975-991.
89. Wang, Z.; Yu, K.; Tan, H.; Wu, Z.; Cho, J.-H.; Han, X.; Sun, H.; Beach, T. G.; Peng, J., 27-plex Tandem Mass Tag mass spectrometry for profiling brain proteome in Alzheimer's disease. *Anal Chem* **2020,** *92* (10), 7162-7170.
90. Haytural, H.; Mermelekas, G.; Emre, C.; Nigam, S. M.; Carroll, S. L.; Winblad, B.; Bogdanovic, N.; Barthet, G.; Granholm, A.-C.; Orre, L. M., et al., The proteome of the dentate terminal zone of the perforant path indicates presynaptic impairment in Alzheimer disease. *Mol Cell Proteomics* **2020,** *19* (1), 128-141.
91. Vlkolinsky, R.; Cairns, N.; Fountoulakis, M.; Lubec, G., Decreased brain levels of 2',3'-cyclic nucleotide-3'-phosphodiesterase in Down syndrome and Alzheimer's disease. *Neurobiol Aging* **2001,** *22* (4), 547-553.

92. Johnson, E. C. B.; Dammer, E. B.; Duong, D. M.; Ping, L.; Zhou, M.; Yin, L.; Higginbotham, L. A.; Guajardo, A.; White, B.; Troncoso, J. C., et al., Large-scale proteomic analysis of Alzheimer's disease brain and cerebrospinal fluid reveals early changes in energy metabolism associated with microglia and astrocyte activation. *Nat Med* **2020,** *26*, 769-780.
93. Johnson, E. C. B.; Dammer, E. B.; Duong, D. M.; Yin, L.; Thambisetty, M.; Troncoso, J. C.; Lah, J. J.; Levey, A. I.; Seyfried, N. T. Deep proteomic network analysis of Alzheimer's disease brain reveals alterations in RNA binding proteins and RNA splicing associated with disease. *Molec Neurodegen* [Online], **2018**. https://doi.org/10.1186/s13024-018-0282-4.
94. Zhang, Q.; Ma, C.; Gearing, M.; Wang, P. G.; Chin, L. S.; Li, L. Integrated proteomics and network analysis identifies protein hubs and network alterations in Alzheimer's disease. *Acta Neuropathol Commun* [Online], **2018**. https://www.ncbi.nlm.nih.gov/pmc/articles/PMC5831854/pdf/40478_2018_Article_524.pdf.
95. Mendonça, C. F.; Kuras, M.; Nogueira, F. C. S.; Plá, I.; Hortobágyi, T.; Csiba, L.; Palkovits, M.; Renner, É.; Döme, P.; Marko-Varga, G., et al. Proteomic signatures of brain regions affected by tau pathology in early and late stages of Alzheimer's disease. *Neurobiol Dis* [Online], **2019**. http://www.sciencedirect.com/science/article/pii/S096999611930169X.
96. Adav, S. S.; Park, J. E.; Sze, S. K., Quantitative profiling brain proteomes revealed mitochondrial dysfunction in Alzheimer's disease. *Molecular Brain* **2019,** *12* (1), 8.
97. Bereczki, E.; Branca, R. M.; Francis, P. T.; Pereira, J. B.; Baek, J.-H.; Hortobágyi, T.; Winblad, B.; Ballard, C.; Lehtiö, J.; Aarsland, D., Synaptic markers of cognitive decline in neurodegenerative diseases: a proteomic approach. *Brain* **2018,** *141* (2), 582-595.
98. Ping, L.; Kundinger, S. R.; Duong, D. M.; Yin, L.; Gearing, M.; Lah, J. J.; Levey, A. I.; Seyfried, N. T. Global quantitative analysis of the human brain proteome and phosphoproteome in Alzheimer's disease. *Sci Data* [Online], **2020**. https://www.nature.com/articles/s41597-020-00650-8.pdf.
99. Xiong, F.; Ge, W.; Ma, C., Quantitative proteomics reveals distinct composition of amyloid plaques in Alzheimer's disease. *Alzheimers Dement* **2019,** *15* (3), 429-440.
100. Castegna, A.; Aksenov, M.; Thongboonkerd, V.; Klein, J. B.; Pierce, W. M.; Booze, R.; Markesbery, W. R.; Butterfield, D. A., Proteomic identification of oxidatively modified proteins in Alzheimer's disease brain. Part II: dihydropyrimidinase-related protein 2, alpha-enolase and heat shock cognate 71. *J Neurochem* **2002,** *82* (6), 1524-1532.
101. Jacobs, H. I.; Van Boxtel, M. P.; Jolles, J.; Verhey, F. R.; Uylings, H. B., Parietal cortex matters in Alzheimer's disease: an overview of structural, functional and metabolic findings. *Neurosci Biobehav Rev* **2012,** *36* (1), 297-309.
102. Foerde, K.; Shohamy, D., The role of the basal ganglia in learning and memory: insight from Parkinson's disease. *Neurobiol Learn Mem* **2011,** *96* (4), 624-636.
103. Packard, M. G.; Knowlton, B. J., Learning and memory functions of the basal ganglia. *Annu Rev Neurosci* **2002,** *25* (1), 563-593.
104. Bonner, G. J.; Darkwa, O. K.; Gorelick, P. B., Autopsy recruitment program for African Americans. *Alzheimer Dis Assoc Disord* **2000,** *14* (4), 202-208.
105. Barnes, L. L.; Shah, R. C.; Aggarwal, N. T.; Bennett, D. A.; Schneider, J. A., The Minority Aging Research Study: ongoing efforts to obtain brain donation from African Americans without dementia. *Curr Alzheimer Res* **2012,** *9* (6), 734-745.
106. Siminoff, L. A.; Burant, C. J.; Ibrahim, S. A., Racial disparities in preferences and perceptions regarding organ donation. *J Gen Intern Med* **2006,** *21* (9), 995-1000.

107. Ray, M.; Zhang, W. Analysis of Alzheimer's disease severity across brain regions by topological analysis of gene co-expression networks. *BMC Syst Biol* [Online], **2010**. https://doi.org/10.1186/1752-0509-4-136.
108. Halliday, G., Pathology and hippocampal atrophy in Alzheimer's disease. *Lancet Neurol* **2017,** *16* (11), 862-864.
109. West, M. J.; Kawas, C. H.; Martin, L. J.; Troncoso, J. C., The CA1 region of the human hippocampus is a hot spot in Alzheimer's disease. *Ann N Y Acad Sci* **2000,** *908*, 255-259.
110. McAlister, G. C.; Nusinow, D. P.; Jedrychowski, M. P.; Wühr, M.; Huttlin, E. L.; Erickson, B. K.; Rad, R.; Haas, W.; Gygi, S. P., MultiNotch MS3 enables accurate, sensitive, and multiplexed detection of differential expression across cancer cell line proteomes. *Anal Chem* **2014,** *86* (14), 7150-7158.
111. Ting, L.; Rad, R.; Gygi, S. P.; Haas, W., MS3 eliminates ratio distortion in isobaric multiplexed quantitative proteomics. *Nat Methods* **2011,** *8* (11), 937-940.
112. Williams, M. M.; Meisel, M. M.; Williams, J.; Morris, J. C., An interdisciplinary outreach model of African American recruitment for Alzheimer's disease research. *Gerontologist* **2011,** *51* (Suppl 1), S134-S141.
113. Sisco, S.; Gross, A. L.; Shih, R. A.; Sachs, B. C.; Glymour, M. M.; Bangen, K. J.; Benitez, A.; Skinner, J.; Schneider, B. C.; Manly, J. J., The role of early-life educational quality and literacy in explaining racial disparities in cognition in late life. *J Gerontol B Psychol Sci Soc Sci* **2015,** *70* (4), 557-567.

CHAPTER 4

Brain Proteomics Analysis in a Diverse Alzheimer's Disease Cohort

4.1 Introduction

In the United States, Alzheimer's disease (AD) disproportionately burdens different subgroups of the population, including different racial backgrounds. African American/Black adults are about twice as likely while Hispanic adults are about one and a half times as likely to have AD as non-Hispanic White adults.[1-2] No significant differences in the primary neuropathological hallmarks of AD, amyloid-β (Aβ) plaques and neurofibrillary tau tangles, have been discovered in the brains of African American/Black and non-Hispanic White adults,[3-6] though mixed pathology is more likely to be present in African American/Black adults.[4] Consistent with this finding, another study reported higher burden of white matter hyperintensities in brains of non-demented African American/Black and Hispanic adults compared to non-Hispanic White adults.[7] However, these differences may only be relevant for non-community-dwelling cohorts.[8-10] Furthermore, molecular differences within specific brain regions have been previously described. For example, markers of inflammation and neurodegeneration including the 42 amino acid Aβ peptide ($A\beta_{42}$), which is fibrillogenic and the primary component of Aβ plaques in AD,[11] were increased in the middle temporal gyrus region (Brodmann area 21) in African American/Black adults with AD compared to non-Hispanic White adults with AD.[12-13] This study highlights that molecular differences in specific areas of the brain may exist across racial groups and contribute to racial disparities in AD. However,

additional studies across more brain regions in diverse cohorts are necessary to further investigate these potential differences and identify disease changes that are universal.

The inferior parietal lobule (IPL) brain region has functions in sensory and emotional perception and language, but has also been implicated in memory functions.[14-17] Structural changes in subregions of the IPL have been associated with progression from cognitively normal (CN) to mild cognitive impairment (MCI), a preliminary stage of AD.[18] IPL is known to be affected by both Aβ plaques and neurofibrillary tau tangles, in both MCI and AD.[19-20] Lower levels of blood flow to the IPL have also been observed in AD,[21-23] including during performance of memory tasks.[24] The IPL is part of the default mode network (DMN), which is a group of brain regions connected by the fact that they are active when a person is in "active rest" (e.g. background brain activity such as daydreaming or mind wandering)[25] and has also been linked to episodic memory.[26] Functional connectivity (referred to as connectivity) is measured using functional magnetic resonance imaging (fMRI) and indicates the correlation of activity changes between different brain regions.[27] Decreased connectivity is observed between DMN brain regions in AD, reflecting dysfunction of these brain regions related to pathogenic and cognitive changes particularly related to memory impairment.[28-30]

Increased global levels of oxidative stress and oxidative protein modifications (carbonylation, S-glutathionylation, and nitration) were observed in the IPL of individuals with MCI and AD compared to preclinical/asymptomatic AD and individuals who were CN.[31-33] There are two existing global proteomics studies of IPL in AD; one of these is our previous analysis of IPL in a pilot cohort of African American/Black and non-Hispanic White adults from the University of Pittsburgh Alzheimer Disease Research Center (Pitt ADRC), described in

Chapter 3.[34-35] Importantly, both of these studies examined multiple brain regions in AD and highlight the need for additional investigation into IPL-specific changes.

Evidence exists to suggest a role for IPL in racial disparities in AD. Our previous pilot proteomics study of IPL identified a subset of proteins in which race significantly affected protein changes in AD (**Chapter 3**).[34] In preclinical AD, IPL cortical thickness was decreased in African American/Black compared to non-Hispanic White adults.[36] A fMRI study of the DMN found that race affected connectivity between different DMN brain regions at baseline and in AD.[37] Though IPL connectivity with other regions was not affected by race in AD, connectivity between IPL and the parahippocampal gyrus was decreased at baseline in African American/Black compared to non-Hispanic White adults, indicating a weaker correlation between activity of the two regions. Connectivity between these two regions has been previously associated with delayed recall, a measure of episodic memory that tests memory recall 30 minutes after learning.[38] DMN connectivity differences across racial groups were also differentially associated with tau biomarker levels in cerebrospinal fluid (CSF),[37] in which differences between African American/Black and non-Hispanic White adults have been recently identified.[8, 39-41] Importantly, geographic location and selection bias may have an impact on the generalizability of the results from all of these studies. The three mentioned studies recruited participants on a volunteer basis and each from a specific geographic region, which may result in a study population not representative of the entire population.[36, 42] The cortical thickness study attempted to improve the generalizability of their results by including two cohorts of non-Hispanic White adults, one group matched to the African American/Black group and another unmatched to try to account for the differences that one might encounter in the full population.[36] Though these studies have utilized multiple modalities to support the potential involvement of

IPL in AD racial disparities, they also highlight the need for replication of their findings in additional more diverse cohorts and for careful consideration of recruitment strategies.

Herein, we have applied discovery-based quantitative proteomics to characterize the proteomic impact of AD in the IPL region in a diverse cohort of African American/Black and non-Hispanic White adults from the Rush Alzheimer's Disease Center. Our findings highlight the importance of diverse cohorts in proteomic studies of AD brain.

4.2 Methods

4.2.1 Sample selection

Postmortem brain tissues were selected from the Religious Orders Study and Rush Memory and Aging Project (ROSMAP)[43-45] at the Rush Alzheimer's Disease Center. Tissues from IPL (Brodmann area 39/40 [angular gyrus]; N = 40) were acquired from African American/Black and non-Hispanic White adults who were CN or diagnosed with AD (**Table 4.1**). CN and AD classification was based on clinical diagnosis of cognitive status at death of no cognitive impairment and possible or probable AD, respectively. AD cases were neuropathologically confirmed according to NIA-Reagan criteria,[46] which takes into account both Braak staging of tau tangles[47-48] and Consortium to Establish a Registry for Alzheimer's Disease (CERAD) score of amyloid burden.[49] Race was self-reported as Black or African American (referred to throughout as African American/Black) or White (referred to throughout as non-Hispanic White). Group identities were blinded throughout proteomics experiments and data analysis until after validation of the mass spectrometry (MS) results. This study was

approved by the Institutional Review Board (IRB) of Vanderbilt University and the original ROSMAP study was approved by the IRB of Rush University Medical Center.

4.2.2 Sample preparation

IPL tissue (20 mg) was homogenized in 1x phosphate-buffered saline (PBS) with 8 M urea with complete mini EDTA-free protease inhibitor cocktail (Roche Diagnostics Gmbh, Mannheim, Germany). Tissues were homogenized with Lysing Matrix A at 4.0 m/s for 20 s using a FastPrep-24™ 5G system (MP Biomedicals, Santa Ana, CA). Homogenate was centrifuged at 4 °C, 13,000 rpm for 15 min and supernatant was collected. The following BCA assay, protein digestion and desalting, peptide assay, and Tandem Mass Tags (TMT) labeling steps were performed using a Biomek i7 Hybrid Automated Workstation (Beckman Coulter, Brea, CA). Protein concentration was determined using bicinchoninic acid (BCA) assay according to the manufacturer's protocols (Thermo Fisher Scientific, Waltham, MA). A pooled sample containing equimolar amounts of protein from the 40 samples was generated and served as a quality control (QC). Samples were randomized into four batches of 11 with one QC per batch. Prior to sample digestion, protein integrity was assessed via sodium dodecyl sulfate-polyacrylamide gel electrophoresis (SDS-PAGE). Protein (180 μg) was placed in 50 mM Tris with 8 M urea in a 96-well plate and was reduced for 30 min using 25 mM dithiothreitol at 37 °C. Protein was subsequently alkylated with 25 mM iodoacetamide for 30 min in the dark and quenched with 25 mM L-cysteine for 30 min with shaking. Samples were diluted ~8x with 20 mM Tris, 10 mM $CaCl_2$ prior to digestion with trypsin/Lys-C mix (Promega, Madison, WI) for 14-16 h at 37 °C (1:50 enzyme:protein ratio). Peptides were acidified with 5% formic acid (FA) and desalted on a 100 mg Targa C18 FastEQ plate (The Nest Group, Inc., Southborough, MA).

Table 4.1. Cohort demographics.[a]

	African American/Black		Non-Hispanic White		p-value[b]
	CN	AD	CN	AD	
N	6	8	13	13	-
Sex (M/F)	2/4	3/5	4/9	0/13	0.13
Age[c]	80.2 (6.3)	88.7 (7.4)	87.4 (3.9)	92.2 (3.5)	**0.00034**
PMI[d]	13.5 (11.6)	8.5 (5.1)	8.8 (4.6)	6.8 (2.7)	0.15
MMSE score[e]	28.3 (1.5)	17.3 (5.0)	28.3 (1.9)	12.1 (9.1)	**0.000000041**
Braak stage[f]	2.8 (1.2)	4.6 (0.7)	3.4 (0.7)	4.8 (0.4)	**0.0000049**
CERAD score[f]	3.2 (1.3)	1.5 (0.5)	3.2 (1.1)	1.4 (0.9)	**0.00011**
Years of education[g]	13.7 (2.3)	19.3 (3.4)	18.3 (2.9)	16.4 (2.1)	**0.0021**
BMI[h]	34.6 (6.4)	23.9 (5.2)	24.6 (4.8)	26.6 (4.2)	**0.0022**
Hypertension[i]	5	7	9	11	0.72
Diabetes[i]	4	2	1	3	0.051
Stroke[i]	1	3	0	1	0.079
APOE genotype[j]					-
ε2/ε2	0	0	0	0	
ε2/ε3	2	0	4	1	
ε2/ε4	1	3	1	0	
ε3/ε3	1	4	4	6	
ε3/ε4	2	0	4	5	
ε4/ε4	0	1	0	0	

[a]Values for each group are given as average (standard deviation) unless otherwise noted. [b]p-values were calculated using single-factor ANOVAs. [c]Age at death in years. [d]Postmortem interval (PMI) in hours. [e]Mini-Mental State Exam (MMSE) score. [f]Neuropathological data was not available for two participants. Braak stage and Consortium to Establish a Registry for Alzheimer's Disease (CERAD) score average and standard deviation were calculated from N = 12 samples for the non-Hispanic White AD group and N = 5 for the African American/Black CN group. [g]Years of education was available for all but one participant. For the non-Hispanic White AD group, average and standard deviation were calculated from N = 12 samples with this information. [h]Body mass index (BMI). [i]Reported as number of individuals who reported being diagnosed with specified condition at any point. [j]Apolipoprotein E (*APOE*) genotype reported as number of individuals with each genotype. *APOE* genotype was not available from one sample in the non-Hispanic White AD group.

Peptide concentrations were measured using the Pierce™ Quantitative Colorimetric Peptide Assay according to the manufacturer's protocols (Thermo Fisher Scientific, Waltham, MA) prior to labeling 25 µg of each sample using TMT^{11}-plex reagents. Each batch mixture was desalted manually using an HLB cartridge (Waters Corporation, Milford, MA; 1 cc/10 mg), reconstituted in 1 mM ammonium formate in 2% acetonitrile (ACN) at pH 10, and fractionated using the following 96 min gradient on a Zorbax 300Extend-C18 column (4.6 x 250 mm, 5 µm; Agilent Technologies, Santa Clara, CA) on a Waters e2695 separations module with a 2998 PDA detector and a fraction manager: 0-7 min, 0% B; 7-13 min, 0-16% B; 13-73 min, 16-40% B; 73-77 min, 40-44% B; 77-82 min, 44-60% B; 82-96 min, 60% B. Mobile phase A was 4.5 mM ammonium formate in 2% ACN at pH 10 and mobile phase B was 4.5 mM ammonium formate in 90% ACN at pH 10. The flow rate was 0.8 mL/min and the column was kept at 25°C. Fractions were collected every minute and concatenated to 24 fractions (i.e. Fraction 1 was minutes 1, 25, 49, 73; Fraction 2 was minutes 2, 26, 50, 74; etc.). All fractions were analyzed individually via liquid chromatography-tandem mass spectrometry (LC-MS/MS) on an Orbitrap Fusion Lumos (Thermo Fisher Scientific, Waltham, MA) with technical duplicates. Fractions were injected in a randomized order.

4.2.3 LC-MS/MS parameters

An UltiMate 3000 RSLCnano system (Thermo Fisher Scientific, Waltham, MA) was coupled to an Orbitrap Fusion Lumos mass spectrometer operated in positive mode. Peptides were loaded onto an Acclaim™ PepMap™ 100 C18 trap column (75 µm i.d. x 2 cm, 100 Å, 3 µm; Thermo Fisher Scientific, Waltham, MA) prior to separation on an in-house C18 packed column (100 µm i.d. x 30 cm, 100 Å, 2.5 µm; Waters Corporation, Milford, MA) over a 165 min

gradient: 0-3 min, 1-7% B; 3-122 min, 7-30% B; 122-127 min, 30-95% B; 127-142 min, 95% B; 142-145 min, 95-1% B; 145-165 min, 1% B. Mobile phase A was 0.1% FA and mobile phase B was 0.1% FA in 80% ACN. Full MS spectra were collected in the Orbitrap (375-1,500 *m/z*, 120,000 resolution, automated gain control (AGC) 4.0E5, maximum injection time 100 ms). The instrument was operated in data-dependent acquisition (DDA) mode to acquire the top 15 MS/MS spectra using higher-energy collisional dissociation (HCD; normalized collision energy 35%, 50,000 resolution, isolation width 0.7 *m/z*, AGC 5.0E4, maximum injection time 86 ms) and dynamic exclusion of 20 s.

4.2.4 Data analysis

RAW files were analyzed using Proteome Discoverer software (version 2.4). All technical replicates and fractions for each batch were combined into one result file and searched against the UniProt human reviewed proteins database (05/05/2021, 20,309 sequences) using SEQUEST-HT. The following modifications were included in the search: fixed modification of cysteine carbamidomethylation and variable modifications of methionine oxidation and both TMT^{10}-plex (229.163 Da) and TMT^{11}-plex (229.169 Da) on lysine residues and peptide N-termini. A maximum of two trypsin miscleavages were allowed in the search. A false discovery rate (FDR) cutoff of 1% was applied at the peptide level. Mass tolerances for the search were 10 ppm for precursors and 0.05 Da for fragments. At least one unique peptide sequence and two peptide spectral matches (PSMs) were required for protein identification.

TMT^{11}-plex was set as the quantification method in Proteome Discoverer, and reporter ion quantitation was based on intensity with a reporter ion signal-to-noise threshold of 10. Reject

quantitative results with missing values was set to false, and apply quantitative value corrections was set to true. Protein groups identified are hereafter referred to as proteins.

Processed data is shown in **Data D4.1**. Identified proteins were filtered to only include proteins identified in all batches with reporter ion intensities in ≥ 80% of TMT channels across batches (≥ 36 channels), and that includes all pooled channels. Proteins meeting these criteria were considered quantified proteins. TMT reporter ion intensities of quantified proteins were normalized within and across batches to the pooled channels as described previously.[34, 50]

Main effects of diagnosis on protein intensities were assessed using linear regression across the entire cohort and in race-stratified models. A race x diagnosis interaction term was used to determine whether race modifies the association between diagnosis and protein intensities. Age and sex were included as covariates in these models. Similarly, interactions of diagnosis with other variables (age, sex, postmortem interval (PMI), body mass index (BMI), and education) were assessed. Correcting p-values using the FDR procedure resulted in no significant proteins, likely due to small sample size; therefore, differentially-expressed proteins reflects those with uncorrected p-values < 0.05. No imputation was performed for missing values. Proteins with coefficients of variation (CVs) greater than two standard deviations from the mean within race-stratified AD and CN groups were excluded (CV > 0.49; **Figure D4.1**). Fold-change (FC) cutoffs of < 0.81 and > 1.23 were calculated based on biological and technical variation and replication[51] and were used as an additional filter to identify differentially-expressed proteins with the most robust changes. TMT reporter ion intensities for differentially-expressed proteins were uploaded into ClustVis to generate principal component analysis (PCA) plots (https://biit.cs.ut.ee/clustvis/).[52] STRING was used to analyze interactions among differentially-expressed proteins,[53] and Ingenuity Pathway Analysis (IPA) was used to identify

significant biological pathways ($p < 0.05$; https://www.qiagenbioinformatics.com/products/ingenuitypathway-analysis).[54]

4.2.5 Proteomics quality control

QC measures were included during sample preparation, data acquisition, and data analysis. Samples were randomly assigned to TMT channels across batches such that each batch included one QC pool and at least one sample from each group. Prior to protein digestion, all samples and the QC pool were analyzed via SDS-PAGE to confirm protein integrity. During the protein digestion, desalting, and TMT labeling steps, a separate aliquot of the QC pool was digested and labeled with TMT^0 simultaneously with the batches and was checked for digestion efficiency and TMT labeling efficiency. During the TMT labeling step, eleven random samples were digested as a test batch, which was also pooled and used to assess labeling efficiency prior to pooling the patient batches. For the fractionation step, a QC injection of bovine serum albumin (BSA) peptides (100 μg) were analyzed each day prior to any batch fractionations and compared against previous injections for consistency.

The TMT^0-labeled QC pool, sandwiched by blank injections of mobile phase A (0.1% FA), was analyzed approximately every day during LC-MS/MS data acquisition to assess column and instrument performance. Total protein identifications and retention times of twelve peptides of varying abundances were tracked across QC injections. Fractions in each batch were injected in a random order. QC measures applied during data analysis were described in **Section 4.2.4**.

4.3 Results and Discussion

Postmortem brain tissue from the IPL region was acquired from African American/Black and non-Hispanic White adults who were CN or diagnosed with AD in the ROSMAP cohort.[43-45] CN and AD groups are distinguished by clinical diagnosis at death, Mini-Mental State Exam (MMSE) score, Braak stage, and CERAD score. We note that the African American/Black CN group was younger, had fewer years of education, and had a higher average BMI than the rest of the groups. However, there were no differences in prevalence of hypertension, diabetes, or stroke across groups. Age and sex varied the most with race and diagnosis (i.e. AD vs CN) and thus were included as covariates in statistical analyses when determining differentially-expressed proteins.

4.3.1 Overview of proteomics results

IPL tissues were analyzed using a discovery-based proteomics workflow that used TMT^{11}-plex for quantification (see **Figure 1.4** in **Chapter 1**). A total of 9,588 proteins were identified from 121,858 peptides from these samples, 7,276 (75.9%) of which were identified in all batches (**Figure 4.1A)**. After filtering for proteins with reporter ion intensities in ≥ 80% of TMT channels across batches (including all pool channels for normalization), most proteins identified in all batches were considered for further quantification (7,236; **Figure 4.1A**).
The proteins identified in this study represent ~59% of the human brain proteome (human brain proteome based on transcript expression, N = 16,227).[55-58] This is a significant improvement compared to the ~13% of the human brain proteome (N = 2,055) identified in our previous study of IPL tissues from the University of Pittsburgh Alzheimer Disease Research Center (Pitt ADRC; **Chapter 3**).[34] This difference reflects the analytical improvements to our discovery-

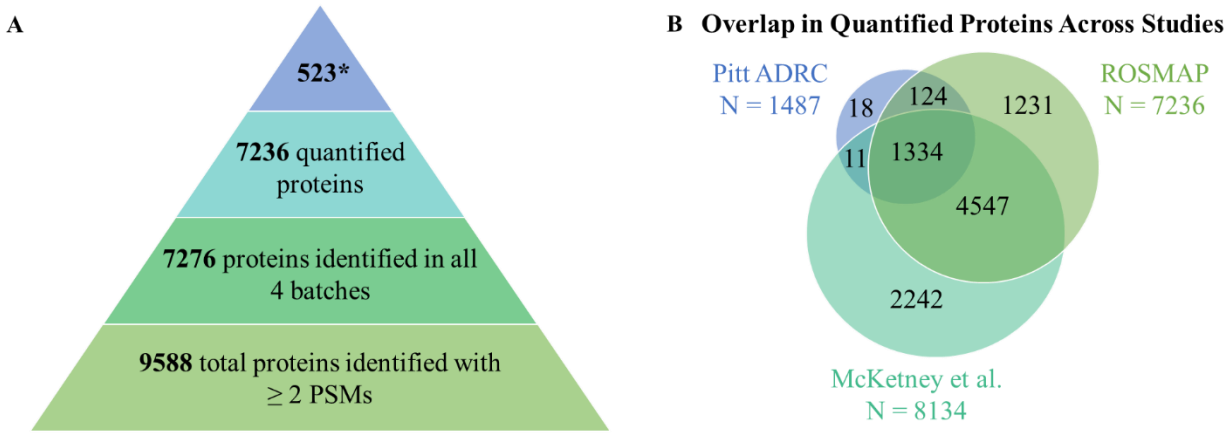

Figure 4.1. Overview of protein identifications and filtering. (A) Filtering of proteins from identified to quantified to differentially expressed proteins. Quantified proteins from this dataset (ROSMAP) had to be identified in both/all batches and have reporter ion intensities in ≥ 80% of TMT channels including the pools (N = 7,236). 523* indicates the number of differentially-expressed proteins with uncorrected $p < 0.05$ between AD and CN groups. **(B)** Overlap of quantified proteins across proteomic studies of IPL in AD. Quantified proteins in the Pitt ADRC dataset met the same criteria as the ROSMAP dataset (N = 1,487), while quantified proteins in the McKetney et al. dataset had label-free quantification intensities in at least 1/3 IPL samples (N = 8,134).[35]

based proteomics workflow, which include high-performance liquid chromatography (HPLC)-based offline fractionation, longer LC gradients, and a longer analytical column for online separation, and LC-MS/MS instead of LC-MS^3 data acquisition. The combination of changes in these parameters yielded improved peptide separation prior and during LC-MS/MS analysis and a shorter MS duty cycle capable of collecting more MS/MS spectra. Overall, this resulted in greater numbers of identified proteins.

Beyond our analysis of IPL in **Chapter 3**,[34] only one other study has used discovery-based proteomics to study IPL in AD.[35] Approximately 83% of proteins identified in this study were identified in one or both of the other IPL studies (**Figure 4.1B**). Ninety percent of proteins identified in the Pitt ADRC dataset were identified in all three studies (N = 1,334), while an additional 4,547 proteins were identified in both this study and the study by McKetney et al.[35]

4.3.2 Differentially-expressed proteins in AD

In our biracial cohort, 523 proteins were differentially expressed between AD and CN groups (**Figure 4.2A, Table D4.2**). These included several proteins with known involvement in AD such as glial fibrillary acidic protein (GFAP; **Figure 4.2B**), neurofilament light polypeptide (NEFL; **Figure 4.2C**), and von Willebrand factor (VWF; **Figure 4.2D**). GFAP, a marker for astrogliosis, and NEFL, a marker for neuronal injury, both increased in AD compared to CN, consistent with previous reports.[59-64] VWF, an endothelial marker involved in hemostasis, was decreased in AD compared to CN in this study. Previous studies have associated increased plasma VWF levels with AD and dementia,[65-66] but no changes in VWF levels in brain have been reported in AD to date. Both amyloid-beta precursor protein (APP) and microtubule-associated protein tau were quantified in this study but their levels were not significantly different between

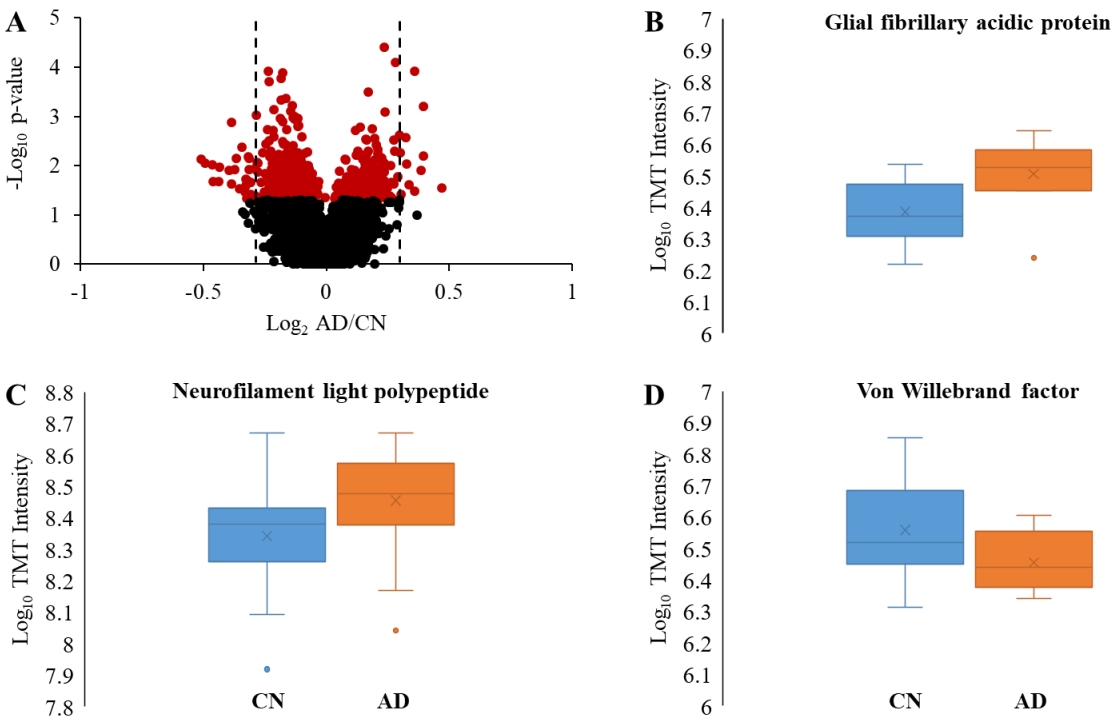

Figure 4.2. Differentially-expressed proteins in AD. (A) Volcano plot showing all quantified proteins (N = 7,236). Red points indicate differentially-expressed proteins in AD (uncorrected $p < 0.05$; N = 523), while black points had non-significant p-values. Dashed lines indicate fold-change cutoffs of < 0.81 and > 1.23. Box plots showing example differentially-expressed proteins: **(B)** glial fibrillary acidic protein (GFAP), **(C)** neurofilament light polypeptide, and **(D)** von Willebrand factor. The center line of each box is the median; the X indicates the mean. The upper and lower limits of the box are the upper and lower quartiles, respectively, and the whiskers reflect the minimum and maximum values. Outlier points are shown where present.

AD and CN groups. These findings are consistent with our previous study of IPL in the Pitt ADRC cohort.[34] APP was not previously reported as a differentially-expressed protein due to high within-group CVs, which was also the case in this study. The McKetney et al. study observed contrasting findings in tau levels, as they reported significantly increased tau levels in AD in this region measured by an α-phosphorylated tau antibody.[35]

Interestingly, when differentially-expressed proteins in AD were compared between this study and the two other studies of IPL in AD, none overlapped in all three studies and the majority were not shared between any of the studies. Twenty proteins, including GFAP, were differentially expressed in AD compared to CN in both this study and the study described in **Chapter 3** (**Table D4.2**).[34] These proteins function in signaling, apoptosis, protein transport/localization, and lipid metabolism/transport pathways, and all but one protein changed in the same direction in both studies. Of the eight differentially-expressed proteins in AD from the McKetney et al. study, only one was also differentially-expressed in this study (DnaJ homolog subfamily C member 12, DNAJC12), while none overlapped with the Pitt ADRC study. DNAJC12 levels were slightly increased in AD in this study, while they were decreased in AD in the McKetney et al. study.[35] DNAJC12 is upregulated in response to endoplasmic reticulum (ER) stress, which has been linked to AD. Additionally, no proteins from this study overlapped with differentially-expressed proteins in MCI or preclinical AD from a two-dimensional gel-based proteomics analysis of IPL,[33] though a few of our differentially-expressed proteins including heat shock protein HSP 90-alpha and alpha-crystallin B chain have been previously reported as oxidatively modified in MCI, preclinical AD, and AD.[32-33]

Demographic differences may contribute to the differences in protein changes in AD across cohorts. Pitt ADRC study participants on average were younger (74 years) than in this

study (87 years) or the McKetney et al. study (80 years), and had fewer years of education (13 years) than the participants in this study (17 years), though this information was not available for all participants. Additional differences in other psychosocial and socioeconomic factors or comorbidities not reported for these cohorts could also play a role. Regarding the proteomics analyses, the overall workflows were similar, though the McKetney et al. study used label-free protein quantification in contrast to TMT-based quantification. Otherwise, the McKetney et al. workflow was similar to the one used in this study, while the Pitt ADRC study had differences in sample preparation and data acquisition that resulted in comparatively fewer proteins identified, as discussed in **Section 4.3.1**. It is also important to note that McKetney et al. used a stricter criterion for differentially-expressed proteins (Bonferroni adjusted $p < 0.05$) than our two studies, such that more overlap may have been present with less stringent criteria for differential expression. In both of our studies, we chose not to use corrected p-values for differential expression because FDR correction resulted in no significant proteins, consistent with previous studies suggesting that multiple hypothesis correction may be overly stringent in some proteomics analyses.[67-69] Overall, this has been the largest study of proteomic changes in IPL in AD to date, at least double the sample sizes in previous global proteomics studies of IPL (N = 10[35] and N = 20[34]). The lack of overlap in differentially-expressed proteins in AD across these studies demonstrates that novel proteomic changes in AD are detected in diverse cohorts and suggests that further characterization of protein changes occurring in this region is necessary.

To identify pathways significantly affected by AD in IPL, we analyzed the differentially-expressed proteins ($p < 0.05$) using IPA (**Figure 4.3A**, **Table D4.3**). Most of the top most significant IPA pathways were metabolic pathways, particularly related to lipid and amino acid metabolism. These include amino acid degradation pathways and lipid degradation and

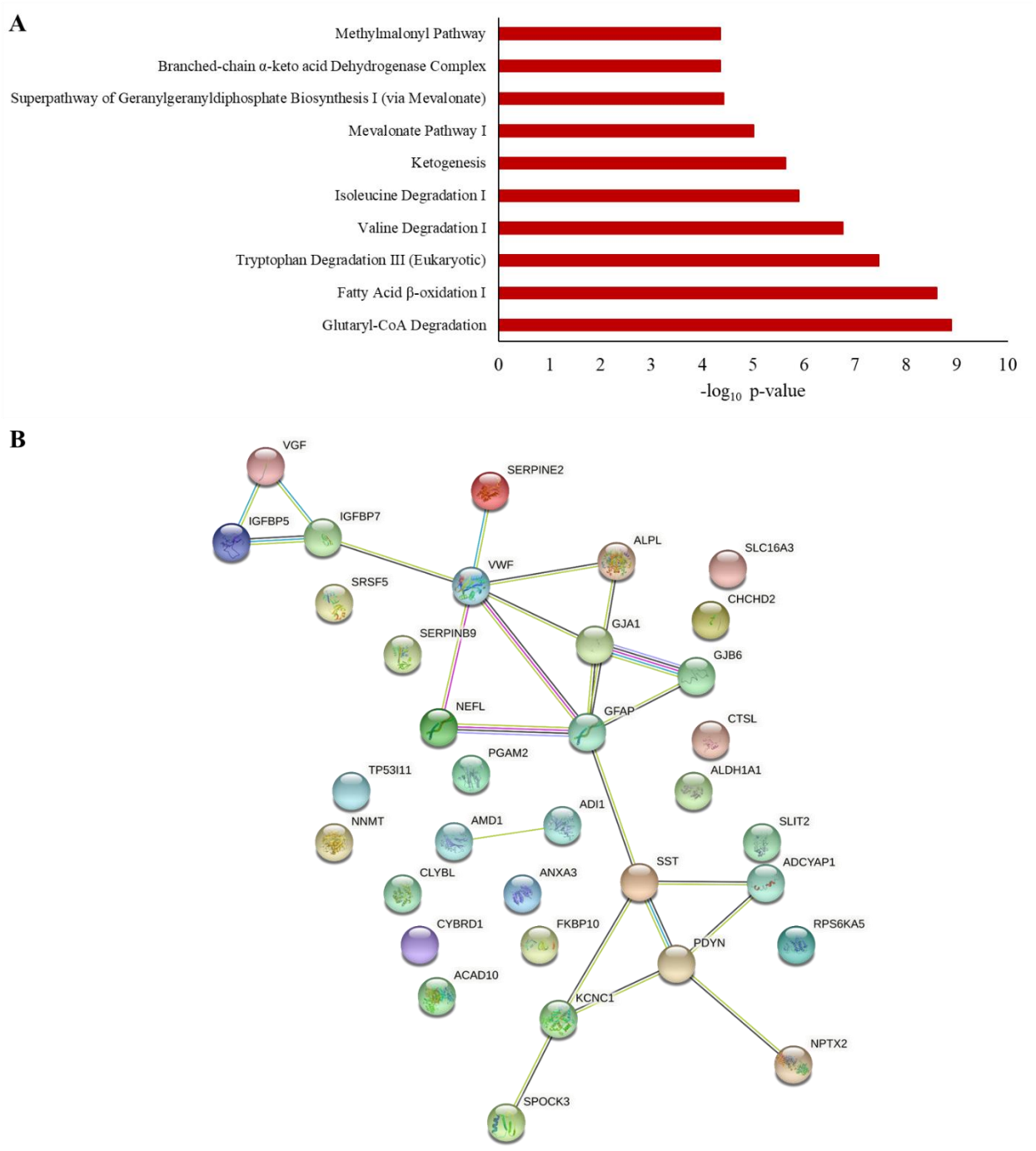

Figure 4.3. Significant pathways in AD. (A) Bar graph showing the top 10 significant IPA pathways ($p < 0.05$) corresponding to differentially-expressed proteins in AD (N = 523). **(B)** STRING network showing the subset of differentially-expressed proteins meeting both p-value and FC cutoffs (N = 34). Abbreviations: VGF, neurosecretory protein VGF; IGFBP5, insulin-like growth factor-binding protein 5; IGFBP7, insulin-like growth factor-binding protein 7; SERPINE2, glia-derived nexin; SRSF5, serine/arginine-rich splicing factor 5; VWF, von Willebrand factor; ALPL, alkaline phosphatase, tissue-nonspecific isozyme; SLC16A3, monocarboxylate transporter 4; SERPINB9, serpin B9; GJA1, gap junction alpha-1 protein;

CHCHD2, coiled-coil-helix-coiled-coil-helix domain-containing protein 2; NEFL, neurofilament light polypeptide; GFAP, glial fibrillary acidic protein; GJB6, gap junction beta-6 protein; TP53I11, tumor protein p53-inducible protein 11; PGAM2, phosphoglycerate mutase 2; CTSL, procathepsin L; NNMT, nicotinamide N-methyltransferase; AMD1, S-adenosylmethionine decarboxylase proenzyme; ADI1, 1,2-dihydroxy-3-keto-5-methylthiopentene dioxygenase; ALDH1A1, retinal dehydrogenase 1; CLYBL, citramalyl-CoA lyase, mitochondrial; ANXA3, annexin A3; SST, somatostatin; SLIT2, slit homolog 2 protein; ADCYAP1, pituitary adenylate cyclase-activating polypeptide; CYBRD1, plasma membrane ascorbate-dependent reductase CYBRD1; FKBP10, peptidyl-prolyl cis-trans isomerase FKBP10; ACAD10, acyl-CoA dehydrogenase family member 10; KCNC1, potassium voltage-gated channel subfamily C member 1; PDYN, proenkephalin-B; RPS6KA5, ribosomal protein S6 kinase alpha-5; SPOCK3, testican-3; NPTX2, neuronal pentraxin-2.

biosynthesis pathways including fatty acid β-oxidation, the mevalonate pathway, and cholesterol biosynthesis, all of which are known to be dysregulated in AD[70-75] and are hypothesized to contribute to racial disparities in AD (see **Chapter 1**). Proteins in all of these pathways were slightly decreased in AD compared to CN groups. The nuclear factor E2-related factor 2 (NRF2)-mediated oxidative stress response pathway was also significant in AD in this study and is consistent with others that have observed oxidative stress in IPL.[31-33] Proteins in this pathway were slightly increased in AD compared to CN groups. NRF2 and other protein levels in this pathway have previously been shown to be decreased in the AD brain,[76-77] though increased levels of proteins in this pathway in AD could indicate an insufficient attempt to combat oxidative stress. Future studies could incorporate measurement of oxidative stress levels to accompany proteomics data to further characterize AD-related changes in diverse cohorts.

To determine the proteins with the most significant changes in AD in this region, we then applied a FC cutoff to the differentially-expressed proteins with $p < 0.05$ ($N = 523$), which reduced the number of significant proteins to 34 (**Figure 4.3B**, **Table D4.2;** see **Section 4.2.4**). This subset of proteins represents the most robust changes resulting from AD in this region and includes several proteins with established changes in AD including GFAP, NEFL, and VWF (**Figure 4.2B-E**). Additionally, compared to proteins with only a p-value < 0.05 (**Figure 4.4A-B**), these 34 proteins showed better discrimination between AD and CN groups (**Figure 4.4C-D**). Using the 523 differentially-expressed proteins resulted in overlap between the AD and CN groups, both with racial groups combined (**Figure 4.4A**) and in race-stratified comparisons (**Figure 4.4B**). The 34 most robust differentially-expressed proteins clearly distinguished the AD and CN groups with less overlap across groups (**Figure 4.4C-D**). This is particularly noticeable in the race-stratified groups, wherein using this subset of proteins led to a clear shift in the

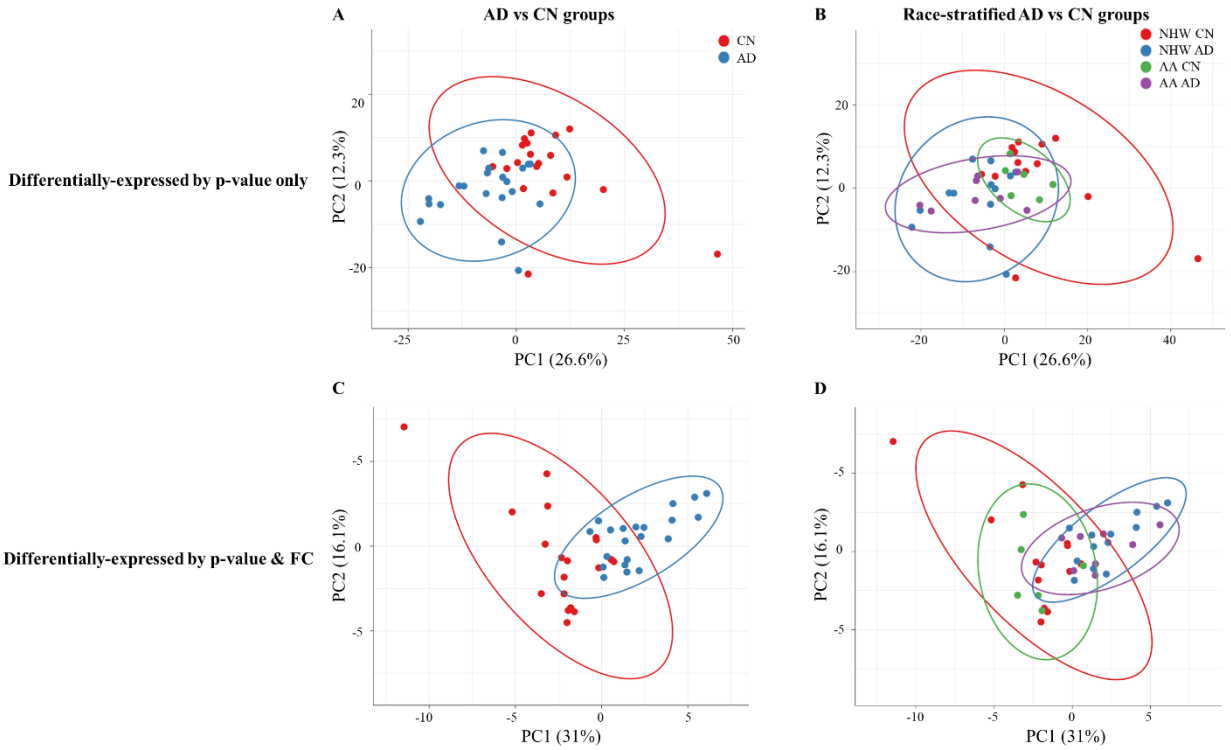

Figure 4.4. PCA plots of differentially-expressed proteins in AD. PCA plots of differentially-expressed proteins significant by p-value only (N = 523 proteins) in **(A)** AD vs CN groups and **(B)** race-stratified AD vs CN groups, and by p-value and fold-change cutoffs (N = 34 proteins) in **(C)** AD vs CN groups and **(D)** race-stratified AD vs CN groups. P-values were uncorrected $p < 0.05$ and significant fold-change values were < 0.81 and > 1.23 per **Section 4.2.4**. Unit variance scaling is applied to rows; singular value decomposition with imputation is used to calculate principal components. X and Y axis show percent of total variance explained by principal component 1 and principal component 2, respectively. Prediction ellipses are such that with probability 0.95, a new observation from the same group will fall inside the ellipse. N = 40 data points. In (A) and (C), the CN group is shown in red and the AD group is shown in blue. In (B) and (D), the non-Hispanic White CN group is shown in red, the non-Hispanic White AD group is shown in blue, the African American/Black CN group is shown in green, and the African American/Black AD group is shown in purple. Abbreviations: AD, Alzheimer's disease; CN, cognitively normal; NHW, non-Hispanic White; AA, African American/Black; FC, fold-change; PC, principal component.

locations of the AD and CN groups on the PCA plot and resulted in more pronounced AD and CN groupings. Racial groups did not separate with either set of differentially-expressed proteins, suggesting that race is not a primary driver of group differences in these specific proteins. We note here that there is more variance within the non-Hispanic White CN group than in the other groups (**Figure 4.4B, D**), which is also evident in the CVs of protein intensities within this group (**Figure D4.1**). However, this variation is not explained by demographic variables or AD neuropathology (**Table 4.1**).

We then used STRING network analysis to examine the interconnectedness of the smaller and more robust subset of differentially-expressed proteins and identified three small protein clusters (**Figure 4.3B**). One of these clusters includes GFAP, NEFL, and VWF, along with two gap junction proteins and glia-derived nexin, which are important for synaptic and neuronal function.[78-82] The other two protein clusters are proteins involved in hormonal and neuropeptide signaling important for many brain functions, some of which have been previously linked to AD.[83-85] Taken together, these findings show that the most robust proteomic changes in AD are amongst proteins and pathways known to be involved in AD pathogenesis, contributing to synaptic and neuronal dysfunction and cognitive decline. Replication of these findings in additional larger cohorts will help further elucidate the most robust proteomic changes in AD in this region.

4.3.3 Impact of race on protein changes in AD

Next, we used a linear regression model with a race x diagnosis interaction term (covaried for age and sex) to evaluate whether race (i.e. self-reported race) had a significant impact on protein changes in AD. From this analysis, 79 proteins had significant race x diagnosis interactions

(uncorrected $p < 0.05$; **Figure 4.5A**, **Table D4.4**). Over half of the proteins with significant race x diagnosis interactions were differentially expressed in race-stratified AD vs CN comparisons. The majority of these proteins were only significant in one racial group and not the other (N = 44; **Figure 4.5B**). This trend is consistent with findings in **Chapter 3**.[34] Thirty proteins were differentially expressed between African American/Black AD and CN groups while 17 were differentially expressed between non-Hispanic White AD and CN groups. Only three proteins were significantly different in both racial groups: C-X-C motif chemokine 14 (CXCL14; **Figure 4.5C**), ankyrin repeat domain-containing protein 36C (ANKRD36C; **Figure 4.5D**), and N^6-adenosine-methyltransferase catalytic subunit (METTL3; **Figure 4.5E**). All three proteins were increased in AD in African American/Black adults. On the other hand, in non-Hispanic White adults, ANKRD36C and METTL3 decreased in AD while there was no change for CXCL14. CXCL14 has not been previously associated with AD, although other chemokines are increased in AD brain to recruit immune cells in response to neuroinflammation.[86] METTL3 functions in N^6-methyladenosine RNA methylation, which is involved in learning and memory. Previous studies have shown conflicting findings on METTL3 levels in AD brain.[87-88] In comparison to **Chapter 3** results, the changes in protein IST1 homolog (IST1) were consistent. IST1 was decreased in African American/Black adults with AD compared to CN adults and did not change between non-Hispanic White AD and CN groups (**Figure 4.5F**). Interestingly, tau protein accumulation has been found to inhibit IST1 expression, corresponding with autophagy deficits and impaired synaptic and cognitive function in mice.[89] Differences in tau CSF biomarkers across racial groups have been reported[8, 39-40]; however, further replication in larger cohorts including African American/Black adults is necessary to determine if IST1 is important for mechanistic follow-up studies.

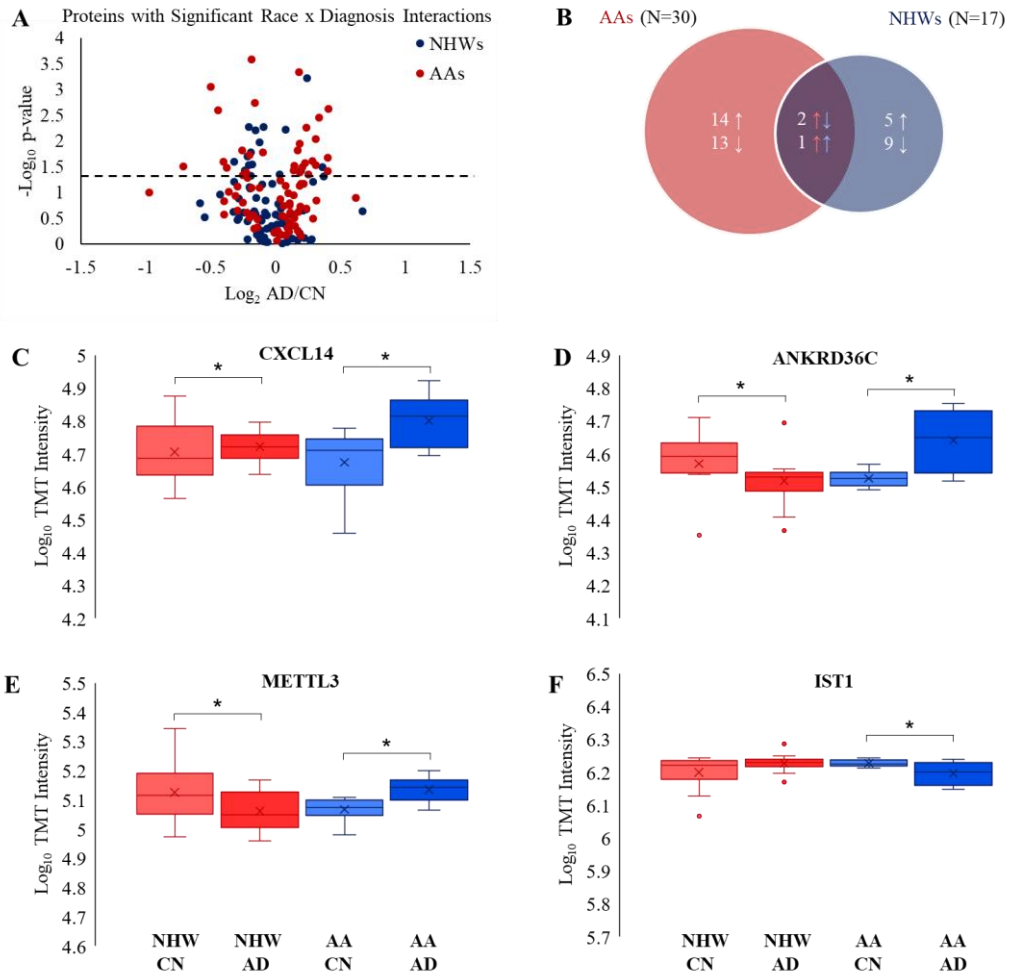

Figure 4.5. Proteins with significant race x diagnosis interactions. (A) Volcano plot showing only proteins with significant race x diagnosis interactions (uncorrected $p < 0.05$; N = 79). Blue and red data points show FC and p-value from non-Hispanic White and African American/Black AD vs CN race-stratified comparisons, respectively. Dashed line indicates $p = 0.05$. **(B)** Venn diagram showing proteins with significant race x diagnosis interactions and significant race-stratified AD vs CN p-value in at least one racial group (N = 44). Arrows indicate direction of change in AD based on FC. For the proteins that had significant race-stratified p-values in both racial groups (N = 3), red and blue arrows indicate direction of change in African American/Black and non-Hispanic White groups, respectively. Box plots showing example proteins with significant race x diagnosis interactions and significant race-stratified AD vs CN differences: **(C)** C-X-C motif chemokine 14 (CXCL14), **(D)** ankyrin repeat domain-containing protein 36C (ANKRD36C), **(E)** N^6-adenosine-methyltransferase catalytic subunit (METTL3), and **(F)** IST1 homolog (IST1). CXCL14, ANKRD36C, and METTL3 all had significant race-stratified changes in both African American/Black and non-Hispanic White groups, while IST1 had significant differences between African American/Black AD and CN groups in both this study and our previous Pitt ADRC study. Abbreviations: NHW, non-Hispanic White; AA, African American/Black; AD, Alzheimer's disease; CN, cognitively normal.

4.3.4 Impact of other covariates on protein changes in AD

After characterizing the impact of race on protein changes in AD, we next sought to evaluate whether additional variables such as age, sex, BMI, PMI, and education also had significant effects on protein changes in AD. This is an important consideration given that samples selected for proteomics studies cannot always be perfectly matched for all variables across groups, especially considering the limited postmortem brain tissue availability from African American/Black adults. To investigate this in our cohort, we independently examined interactions of diagnosis with age, sex, BMI, PMI, and education (**Table 4.2**). Interestingly, more proteins (N = 131-1,041) had significant interactions of other variables with diagnosis than of race (N = 79) with diagnosis. Furthermore, the variables that significantly impacted the most protein changes by diagnosis (education and BMI, N = 1,041 and 316, respectively) also had significant differences across groups (**Table 4.1**). The most proteins (N = 1,041) had significant education x diagnosis interactions, more than three times the number of proteins with significant interactions with diagnosis and any other variable. Educational attainment has been associated with differing levels of both Aβ and tau neuropathology among individuals with the same clinical cognitive status.[90-91] The African American/Black CN group had fewer years of education compared to the other groups in this study. Additionally, the non-Hispanic White AD group had fewer years of education than the African American/Black AD group. A substantial number of proteins also had significant BMI x diagnosis interactions (N = 316). BMI levels have been associated with cognitive decline and dementia[2, 5] and obesity (high BMI) can contribute to neurodegenerative changes in the brain[92] and impact protein expression in microvessels of the blood-brain barrier (**Chapter 1 Section 1.1.3.3**).[93] BMI was highest amongst the African American/Black CN group.

Table 4.2. Variable x diagnosis interactions.

Variable	Number of Proteins with Significant Variable x Diagnosis Interactions[a]
Education	1,041
BMI[b]	316
PMI[c]	283
Age	174
Sex	131
Race	79

[a]Number of proteins with significant variable x diagnosis interactions (uncorrected $p < 0.05$), filtered to remove proteins with high within-group variation (**Section 4.2.4**). [b]Body mass index (BMI). [c]Postmortem interval (PMI).

We observed a subset of proteins with significant race x diagnosis interactions in this study (**Section 4.3.4**); however, there is a clear need for overall diversity of cohorts in AD studies. This includes diversity by racial background, but also extends to other variables noted here such as BMI and education. Given the impact of education on AD-associated proteomic changes in this study, future studies should consider additional educational variables beyond years of education including quality of education,[94-96] early life education,[97] and lifetime cognitive activity.[98-99] These measures have been previously associated with cognition in African American/Black adults and are important to consider in diverse cohorts. The recruitment of diverse cohorts is important to advance AD understanding. The inclusion of both African American/Black and non-Hispanic White adults who were recruited similarly to the ROSMAP study is well-characterized[43-45] and a noteworthy strength of this study. However, one of the known limitations of the ROSMAP cohort is that participants were recruited into the study on a volunteer basis and had to agree to autopsy as a condition of recruitment, such that they may not be representative of the general population.[43-44] Furthermore, though our cohort was biracial, non-Hispanic White adults were still overrepresented and other racial and ethnic groups were excluded. The need for equal representation, oversampling of underrepresented groups, and further studies characterizing changes within exclusively African American/Black adults and other racial and ethnic groups are urgently needed.[100] We have additionally pointed out the demographic differences across groups in our cohort, which is an additional limitation to our study. Though we were able to include age and sex as covariates in our identification of differentially-expressed proteins, we did not include additional covariates with significant differences across groups, such as BMI and education, due to our sample size. It is important to note, on the other hand, that there were no differences across groups in comorbidities that

increase risk for AD and are more prevalent in African American/Black adults, such as hypertension, diabetes, and stroke (**Chapter 1**). This is the largest proteomic study of IPL in AD and furthermore in a diverse cohort; however, larger sample sizes are necessary to account for some of these demographic differences that may exist across groups.

4.4 Conclusions

Herein, we have applied proteomics to globally characterize changes in IPL in AD in a cohort of African American/Black and non-Hispanic White adults. In this cohort, we have identified 523 differentially-expressed proteins in AD, some of which are consistent with known changes in AD and many of which are novel, likely due to the diversity of our cohort and limited existing studies of this region. Thirty-four proteins had robust differences in AD that were able to distinguish AD and CN groups regardless of race that included proteins previously associated with AD including glial fibrillary acidic protein and neurofilament light polypeptide. We also observed a subset of proteins in which changes in AD were significantly impacted by race and that had race-specific patterns of change in AD. In addition to race, we have identified other variables that also significantly affected protein changes in AD, particularly education. Our study revealed novel proteomic changes in the IPL region in AD in a diverse cohort and emphasizes the broad need for diversity in future studies of AD across brain regions.

4.5 Acknowledgements

The authors acknowledge funding from Vanderbilt Interdisciplinary Training Program in Alzheimer's Disease (T32-AG058524) and Vanderbilt University Start-Up Funds. We would like to thank the team at the Rush Alzheimer's Disease Center funded by the National Institutes

of Health and National Institute on Aging (P30-AG010161, center director Dr. David A. Bennett) for their assistance in sample selection and acquisition (Ryan Johnson and Gregory Klein). We would also like to thank Dr. Timothy J. Hohman, Julia O'Malley, and Emily R. Mahoney for their assistance with statistical analyses.

4.6 References

1. Alzheimer's Association, 2021 Alzheimer's disease facts and figures. *Alzheimers Dement* **2021,** *17* (3), 327-406.
2. Barnes, L. L.; Bennett, D. A., Alzheimer's disease in African Americans: risk factors and challenges for the future. *Health Aff (Millwood)* **2014,** *33* (4), 580-586.
3. Chin, A. L.; Negash, S.; Hamilton, R., Diversity and disparity in dementia: the impact of ethnoracial differences in Alzheimer disease. *Alzheimer Dis Assoc Disord* **2011,** *25* (3), 187-195.
4. Barnes, L. L.; Leurgans, S.; Aggarwal, N. T.; Shah, R. C.; Arvanitakis, Z.; James, B. D.; Buchman, A. S.; Bennett, D. A.; Schneider, J. A., Mixed pathology is more likely in black than white decedents with Alzheimer dementia. *Neurology* **2015,** *85* (6), 528-534.
5. Gottesman, R. F.; Schneider, A. C.; Zhou, Y.; Coresh, J.; Green, E.; Gupta, N.; Knopman, D. S.; Mintz, A.; Rahmim, A.; Sharrett, A. R., et al., Association between midlife vascular risk factors and estimated brain amyloid deposition. *JAMA* **2017,** *317* (14), 1443-1450.
6. Wilkins, C. H.; Grant, E. A.; Schmitt, S. E.; McKeel, D. W.; Morris, J. C., The neuropathology of Alzheimer disease in African American and white individuals. *Arch Neurol* **2006,** *63* (1), 87-90.
7. Brickman, A. M.; Schupf, N.; Manly, J. J.; Luchsinger, J. A.; Andrews, H.; Tang, M. X.; Reitz, C.; Small, S. A.; Mayeux, R.; DeCarli, C., et al., Brain morphology in older African Americans, Caribbean Hispanics, and whites from northern Manhattan. *Arch Neurol* **2008,** *65* (8), 1053-61.
8. Morris, J. C.; Schindler, S. E.; McCue, L. M.; Moulder, K. L.; Benzinger, T. L. S.; Cruchaga, C.; Fagan, A. M.; Grant, E.; Gordon, B. A.; Holtzman, D. M., et al., Assessment of racial disparities in biomarkers for Alzheimer disease. *JAMA Neurol* **2019,** *76* (3), 264-273.
9. Barnes, L. L., Biomarkers for Alzheimer dementia in diverse racial and ethnic minorities—a public health priority. *JAMA Neurol* **2019,** *76* (3), 251-253.
10. Nag, S.; Barnes, L. L.; Yu, L.; Buchman, A. S.; Bennett, D. A.; Schneider, J. A.; Wilson, R. S. Association of Lewy bodies with age-related clinical characteristics in Black and White decedents. *Neurology* [Online], **2021**. https://n.neurology.org/content/neurology/early/2021/06/04/WNL.0000000000012324.full.pdf.
11. Iwatsubo, T.; Odaka, A.; Suzuki, N.; Mizusawa, H.; Nukina, N.; Ihara, Y., Visualization of Aβ42(43) and Aβ40 in senile plaques with end-specific Aβ monoclonals: Evidence that an initially deposited species is Aβ42(43). *Neuron* **1994,** *13* (1), 45-53.
12. Ferguson, S. A.; Panos, J. J.; Sloper, D.; Varma, V., Neurodegenerative markers are increased in postmortem BA21 tissue from African Americans with Alzheimer's disease. *J Alzheimers Dis* **2017,** *59*, 57-66.

13. Ferguson, S. A.; Varma, V.; Sloper, D.; Panos, J. J.; Sarkar, S., Increased inflammation in BA21 brain tissue from African Americans with Alzheimer's disease. *Metab Brain Dis* **2020,** *35* (1), 121-133.
14. O'Connor, A. R.; Han, S.; Dobbins, I. G., The inferior parietal lobule and recognition memory: Expectancy violation or successful retrieval? *J Neurosci* **2010,** *30* (8), 2924-2934.
15. Alain, C.; He, Y.; Grady, C., The contribution of the inferior parietal lobe to auditory spatial working memory. *J Cogn Neurosci* **2008,** *20* (2), 285-295.
16. Igelström, K. M.; Graziano, M. S. A., The inferior parietal lobule and temporoparietal junction: A network perspective. *Neuropsychologia* **2017,** *105*, 70-83.
17. Friedman, H.; Goldman-Rakic, P., Coactivation of prefrontal cortex and inferior parietal cortex in working memory tasks revealed by 2DG functional mapping in the rhesus monkey. *J Neurosci* **1994,** *14* (5), 2775-2788.
18. Greene, S. J.; Killiany, R. J., Subregions of the inferior parietal lobule are affected in the progression to Alzheimer's disease. *Neurobiol Aging* **2010,** *31* (8), 1304-1311.
19. Markesbery, W. R.; Schmitt, F. A.; Kryscio, R. J.; Davis, D. G.; Smith, C. D.; Wekstein, D. R., Neuropathologic substrate of mild cognitive impairment. *Arch Neurol* **2006,** *63* (1), 38-46.
20. Nelson, P. T.; Abner, E. L.; Scheff, S. W.; Schmitt, F. A.; Kryscio, R. J.; Jicha, G. A.; Smith, C. D.; Patel, E.; Markesbery, W. R., Alzheimer's-type neuropathology in the precuneus is not increased relative to other areas of neocortex across a range of cognitive impairment. *Neurosci Lett* **2009,** *450* (3), 336-339.
21. Scarmeas, N.; Habeck, C. G.; Zarahn, E.; Anderson, K. E.; Park, A.; Hilton, J.; Pelton, G. H.; Tabert, M. H.; Honig, L. S.; Moeller, J. R., et al., Covariance PET patterns in early Alzheimer's disease and subjects with cognitive impairment but no dementia: utility in group discrimination and correlations with functional performance. *NeuroImage* **2004,** *23* (1), 35-45.
22. Devanand, D. P.; Habeck, C. G.; Tabert, M. H.; Scarmeas, N.; Pelton, G. H.; Moeller, J. R.; Mensh, B. D.; Tarabula, T.; Van Heertum, R. L.; Stern, Y., PET network abnormalities and cognitive decline in patients with mild cognitive impairment. *Neuropsychopharmacol* **2006,** *31* (6), 1327-1334.
23. Tranfaglia, C.; Palumbo, B.; Siepi, D.; Sinzinger, H.; Parnetti, L., Semi-quantitative analysis of perfusion of Brodmann areas in the differential diagnosis of cognitive impairment in Alzheimer's disease, fronto-temporal dementia and mild cognitive impairment. *Hell J Nuc Med* **2009,** *12* (2), 110-114.
24. Rémy, F.; Mirrashed, F.; Campbell, B.; Richter, W., Verbal episodic memory impairment in Alzheimer's disease: a combined structural and functional MRI study. *NeuroImage* **2005,** *25* (1), 253-266.
25. Buckner, R. L.; Andrews-Hanna, J. R.; Schacter, D. L., The brain's default network: anatomy, function, and relevance to disease. *Ann N Y Acad Sci* **2008,** *1124*, 1-38.
26. Dickerson, B. C.; Sperling, R. A., Large-scale functional brain network abnormalities in Alzheimer's disease: Insights from functional neuroimaging. *Behav Neurol* **2009,** *21* (1-2), 63-75.
27. Eickhoff, S. B.; Müller, V. I., Functional Connectivity. In *Brain Mapping*, Toga, A. W., Ed. Academic Press: Waltham, **2015**; Vol. 2, pp 187-201.
28. Badhwar, A.; Tam, A.; Dansereau, C.; Orban, P.; Hoffstaedter, F.; Bellec, P., Resting-state network dysfunction in Alzheimer's disease: A systematic review and meta-analysis. *Alzheimers Dement (Amst)* **2017,** *8*, 73-85.

29. Zhu, D. C.; Majumdar, S.; Korolev, I. O.; Berger, K. L.; Bozoki, A. C., Alzheimer's disease and amnestic mild cognitive impairment weaken connections within the default-mode network: A multi-modal imaging study. *J Alzheimers Dis* **2013,** *34* (4), 969-984.
30. Nuttall, R.; Pasquini, L.; Scherr, M.; Sorg, C., Degradation in intrinsic connectivity networks across the Alzheimer's disease spectrum. *Alzheimers Dement (Amst)* **2016,** *5*, 35-42.
31. Reed, T. T.; Pierce, W. M., Jr.; Turner, D. M.; Markesbery, W. R.; Butterfield, D. A., Proteomic identification of nitrated brain proteins in early Alzheimer's disease inferior parietal lobule. *J Cell Mol Med* **2009,** *13* (8b), 2019-2029.
32. Newman, S. F.; Sultana, R.; Perluigi, M.; Coccia, R.; Cai, J.; Pierce, W. M.; Klein, J. B.; Turner, D. M.; Butterfield, D. A., An increase in S-glutathionylated proteins in the Alzheimer's disease inferior parietal lobule, a proteomics approach. *J Neurosci Res* **2007,** *85* (7), 1506-1514.
33. Aluise, C. D.; Robinson, R. A. S.; Cai, J.; Pierce, W. M.; Markesbery, W. R.; Butterfield, D. A., Redox proteomics analyses of brains from subjects with amnestic mild cognitive impairment compared to brains from subjects with preclinical Alzheimer's disease: insights into memory loss in MCI. *J Alzheimers Dis* **2011,** *23*, 257-269.
34. Stepler, K. E.; Mahoney, E. R.; Kofler, J.; Hohman, T. J.; Lopez, O. L.; Robinson, R. A. S. Inclusion of African American/Black adults in a pilot brain proteomics study of Alzheimer's disease. *Neurobiol Dis* [Online], **2020**. http://www.sciencedirect.com/science/article/pii/S0969996120304046.
35. McKetney, J.; Runde, R.; Hebert, A. S.; Salamat, S.; Roy, S.; Coon, J. J., Proteomic atlas of the human brain in Alzheimer's disease. *J Proteome Res* **2019,** *18* (3), 1380-1391.
36. McDonough, I. M., Beta-amyloid and cortical thickness reveal racial disparities in preclinical Alzheimer's disease. *NeuroImage Clin* **2017,** *16*, 659-667.
37. Misiura, M. B.; Howell, J. C.; Wu, J.; Qiu, D.; Parker, M. W.; Turner, J. A.; Hu, W. T. Race modifies default mode connectivity in Alzheimer's disease. *Transl Neurodegen* [Online], **2020**. https://doi.org/10.1186/s40035-020-0186-4.
38. Huo, L.; Li, R.; Wang, P.; Zheng, Z.; Li, J. The default mode network supports episodic memory in cognitively unimpaired elderly individuals: Different contributions to immediate recall and delayed recall. *Front Aging Neurosci* [Online], **2018**. https://www.frontiersin.org/article/10.3389/fnagi.2018.00006.
39. Howell, J. C.; Watts, K. D.; Parker, M. W.; Wu, J.; Kollhoff, A.; Wingo, T. S.; Dorbin, C. D.; Qiu, D.; Hu, W. T. Race modifies the relationship between cognition and Alzheimer's disease cerebrospinal fluid biomarkers. *Alzheimers Res Ther* [Online], **2017**. https://doi.org/10.1186/s13195-017-0315-1.
40. Garrett, S. L.; McDaniel, D.; Obideen, M.; Trammell, A. R.; Shaw, L. M.; Goldstein, F. C.; Hajjar, I. Racial disparity in cerebrospinal fluid amyloid and tau biomarkers and associated cutoffs for mild cognitive impairment. *JAMA Netw Open* [Online], **2019**. https://doi.org/10.1001/jamanetworkopen.2019.17363.
41. Chaudhry, A.; Rizig, M. Comparing fluid biomarkers of Alzheimer's disease between African American or Black African and white groups: A systematic review and meta-analysis. *J Neurol Sci* [Online], **2021**. https://www.sciencedirect.com/science/article/pii/S0022510X20306067?via%3Dihub.
42. Guo, X.; Vittinghoff, E.; Olgin, J. E.; Marcus, G. M.; Pletcher, M. J. Volunteer participation in the Health eHeart study: A comparison with the US population. *Sci Rep* [Online], **2017**. https://doi.org/10.1038/s41598-017-02232-y (accessed 2017/05/16).

43. Bennett, D. A.; Schneider, J. A.; Arvanitakis, Z.; Wilson, R. S., Overview and findings from the Religious Orders Study. *Curr Alzheimer Res* **2012,** *9* (6), 628-645.
44. Bennett, D. A.; Schneider, J. A.; Buchman, A. S.; Barnes, L. L.; Boyle, P. A.; Wilson, R. S., Overview and findings from the Rush Memory and Aging Project. *Curr Alzheimer Res* **2012,** *9* (6), 646-663.
45. Bennett, D. A.; Buchman, A. S.; Boyle, P. A.; Barnes, L. L.; Wilson, R. S.; Schneider, J. A., Religious Orders Study and Rush Memory and Aging Project. *J Alzheimers Dis* **2018,** *64* (s1), S161-S189.
46. The National Institute on Aging and Reagan Institute Working Group on Diagnostic Criteria for the Neuropathological Assessment of Alzheimer's Disease, Consensus recommendations for the postmortem diagnosis of Alzheimer's disease. *Neurobiol Aging* **1997,** *18* (4 Suppl), S1-S2.
47. Braak, H.; Braak, E., Neuropathological stageing of Alzheimer-related changes. *Acta Neuropathol* **1991,** *82* (4), 239-259.
48. Braak, H.; Alafuzoff, I.; Arzberger, T.; Kretzschmar, H.; Del Tredici, K., Staging of Alzheimer disease-associated neurofibrillary pathology using paraffin sections and immunocytochemistry. *Acta Neuropathol* **2006,** *112* (4), 389-404.
49. Mirra, S. S.; Heyman, A.; McKeel, D.; Sumi, S. M.; Crain, B. J.; Brownlee, L. M.; Vogel, F. S.; Hughes, J. P.; Belle, G. v.; Berg, L., The Consortium to Establish a Registry for Alzheimer's Disease (CERAD). Part II. Standardization of the neuropathologic assessment of Alzheimer's disease. *Neurology* **1991,** *41* (4), 479-486.
50. Plubell, D. L.; Wilmarth, P. A.; Zhao, Y.; Fenton, A. M.; Minnier, J.; Reddy, A. P.; Klimek, J.; Yang, X.; David, L. L.; Pamir, N., Extended multiplexing of Tandem Mass Tags (TMT) labeling reveals age and high fat diet specific proteome changes in mouse epididymal adipose tissue. *Mol Cell Proteomics* **2017,** *16* (5), 873-890.
51. Cao, Z.; Yende, S.; Kellum, J. A.; Angus, D. C.; Robinson, R. A. S., Proteomics reveals age-related differences in the host immune response to sepsis. *J Proteome Res* **2014,** *13* (2), 422-432.
52. Metsalu, T.; Vilo, J., ClustVis: a web tool for visualizing clustering of multivariate data using Principal Component Analysis and heatmap. *Nucleic Acids Res* **2015,** *43* (W1), W566-W570.
53. Szklarczyk, D.; Gable, A. L.; Lyon, D.; Junge, A.; Wyder, S.; Huerta-Cepas, J.; Simonovic, M.; Doncheva, N. T.; Morris, J. H.; Bork, P., et al., STRING v11: protein–protein association networks with increased coverage, supporting functional discovery in genome-wide experimental datasets. *Nucleic Acids Research* **2018,** *47* (D1), D607-D613.
54. Krämer, A.; Green, J.; Pollard, J., Jr.; Tugendreich, S., Causal analysis approaches in Ingenuity Pathway Analysis. *Bioinformatics* **2014,** *30* (4), 523-530.
55. Uhlén, M.; Fagerberg, L.; Hallström, B. M.; Lindskog, C.; Oksvold, P.; Mardinoglu, A.; Sivertsson, Å.; Kampf, C.; Sjöstedt, E.; Asplund, A., et al. Tissue-based map of the human proteome. *Science* [Online], **2015**.
https://science.sciencemag.org/content/sci/347/6220/1260419.full.pdf.
56. Hawrylycz, M. J.; Lein, E. S.; Guillozet-Bongaarts, A. L.; Shen, E. H.; Ng, L.; Miller, J. A.; van de Lagemaat, L. N.; Smith, K. A.; Ebbert, A.; Riley, Z. L., et al., An anatomically comprehensive atlas of the adult human brain transcriptome. *Nature* **2012,** *489* (7416), 391-399.
57. Sjöstedt, E.; Zhong, W.; Fagerberg, L.; Karlsson, M.; Mitsios, N.; Adori, C.; Oksvold, P.; Edfors, F.; Limiszewska, A.; Hikmet, F., et al. An atlas of the protein-coding genes in the

human, pig, and mouse brain. *Science* [Online], **2020**. https://science.sciencemag.org/content/sci/367/6482/eaay5947.full.pdf.
58. The human brain proteome. http://www.proteinatlas.org (accessed 06/23/21).
59. Andreev, V. P.; Petyuk, V. A.; Brewer, H. M.; Karpievitch, Y. V.; Xie, F.; Clarke, J.; Camp, D.; Smith, R. D.; Lieberman, A. P.; Albin, R. L., et al., Label-free quantitative LC-MS proteomics of Alzheimer's disease and normally aged human brains. *J Proteome Res* **2012,** *11* (6), 3053-3067.
60. Begcevic, I.; Kosanam, H.; Martinez-Morillo, E.; Dimitromanolakis, A.; Diamandis, P.; Kuzmanov, U.; Hazrati, L. N.; Diamandis, E. P. Semiquantitative proteomic analysis of human hippocampal tissues from Alzheimer's disease and age-matched control brains. *Clin Proteomics* [Online], **2013**. https://www.ncbi.nlm.nih.gov/pmc/articles/PMC3648498/pdf/1559-0275-10-5.pdf.
61. Hondius, D. C.; van Nierop, P.; Li, K. W.; Hoozemans, J. J. M.; van der Schors, R. C.; van Haastert, E. S.; van der Vies, S. M.; Rozemuller, A. J. M.; Smit, A. B., Profiling the human hippocampal proteome at all pathologic stages of Alzheimer's disease. *Alzheimers Dement* **2016,** *12* (6), 654-668.
62. Wang, Z.; Yu, K.; Tan, H.; Wu, Z.; Cho, J.-H.; Han, X.; Sun, H.; Beach, T. G.; Peng, J., 27-plex Tandem Mass Tag mass spectrometry for profiling brain proteome in Alzheimer's disease. *Anal Chem* **2020,** *92* (10), 7162-7170.
63. Haytural, H.; Mermelekas, G.; Emre, C.; Nigam, S. M.; Carroll, S. L.; Winblad, B.; Bogdanovic, N.; Barthet, G.; Granholm, A.-C.; Orre, L. M., et al., The proteome of the dentate terminal zone of the perforant path indicates presynaptic impairment in Alzheimer disease. *Mol Cell Proteomics* **2020,** *19* (1), 128-141.
64. Musunuri, S.; Wetterhall, M.; Ingelsson, M.; Lannfelt, L.; Artemenko, K.; Bergquist, J.; Kultima, K.; Shevchenko, G., Quantification of the brain proteome in Alzheimer's disease using multiplexed mass spectrometry. *J Proteome Res* **2014,** *13* (4), 2056-2068.
65. Wolters, F.; Boender, J.; Hofman, A.; De Maat, M.; Koudstaal, P.; Leebeek, F.; Ikram, M., Von Willebrand factor and the risk of dementia: A population-based study (P1.092). *Neurology* **2016,** *86* (16 Supplement), P1.092.
66. Hagnelius, N.-O.; Boman, K.; Nilsson, T. K., Fibrinolysis and von Willebrand factor in Alzheimer's disease and vascular dementia – a case-referent study. *Thromb Res* **2010,** *126* (1), 35-38.
67. Amin, B.; Ford, K. I.; Robinson, R. A. S. Quantitative proteomics to study aging in rabbit liver. *Mech Ageing Dev* [Online], **2020**. https://www.ncbi.nlm.nih.gov/pmc/articles/PMC7138690/pdf/nihms-1575385.pdf.
68. Pascovici, D.; Handler, D. C. L.; Wu, J. X.; Haynes, P. A., Multiple testing corrections in quantitative proteomics: A useful but blunt tool. *Proteomics* **2016,** *16* (18), 2448-2453.
69. Wang, W.; Sue, A. C.; Goh, W. W. B., Feature selection in clinical proteomics: with great power comes great reproducibility. *Drug Discov Today* **2017,** *22* (6), 912-918.
70. Polis, B.; Samson, A. O., Role of the metabolism of branched-chain amino acids in the development of Alzheimer's disease and other metabolic disorders. *Neural Regen Res* **2020,** *15* (8), 1460-1470.
71. Griffin, J. W.; Bradshaw, P. C. Amino acid catabolism in Alzheimer's disease brain: Friend or foe? *Oxid Med Cell Longev* [Online], **2017**. https://www.ncbi.nlm.nih.gov/pmc/articles/PMC5316456/pdf/OMCL2017-5472792.pdf.

72. Stepler, K. E.; Robinson, R. A. S., The potential of ‘omics to link lipid metabolism and genetic and comorbidity risk factors of Alzheimer’s disease in African Americans. In *Reviews on Biomarker Studies in Psychiatric and Neurodegenerative Disorders*, Guest, P. C., Ed. Springer International Publishing: Cham, **2019**; Vol. 1118, pp 1-28.
73. Varma, V. R.; Büşra Lüleci, H.; Oommen, A. M.; Varma, S.; Blackshear, C. T.; Griswold, M. E.; An, Y.; Roberts, J. A.; O’Brien, R.; Pletnikova, O., et al. Abnormal brain cholesterol homeostasis in Alzheimer’s disease—a targeted metabolomic and transcriptomic study. *npj Aging Mech Dis* [Online], **2021**. https://doi.org/10.1038/s41514-021-00064-9.
74. Mohamed, A.; Smith, K.; Posse de Chaves, E., The mevalonate pathway in Alzheimer's disease - cholesterol and non-sterol isoprenoids. In *Alzheimer's Disease: Challenges for the Future*, Zerr, I., Ed. InTech: Rijeka, Croatia, **2015**, 10.5772/59904pp 167-222.
75. Moutinho, M.; Nunes, M. J.; Rodrigues, E., The mevalonate pathway in neurons: It's not just about cholesterol. *Exp Cell Res* **2017,** *360* (1), 55-60.
76. Ramsey, C. P.; Glass, C. A.; Montgomery, M. B.; Lindl, K. A.; Ritson, G. P.; Chia, L. A.; Hamilton, R. L.; Chu, C. T.; Jordan-Sciutto, K. L., Expression of Nrf2 in neurodegenerative diseases. *J Neuropathol Exp Neurol* **2007,** *66* (1), 75-85.
77. Gan, L.; Johnson, J. A., Oxidative damage and the Nrf2-ARE pathway in neurodegenerative diseases. *Biochim Biophys Acta Mol Basis Dis* **2014,** *1842* (8), 1208-1218.
78. Pittman, R. N.; Buettner, H. M., Degradation of extracellular matrix by neuronal proteases. *Dev Neurosci* **1989,** *11* (4-5), 361-375.
79. Hoffmann, M. C.; Nitsch, C.; Scotti, A. L.; Reinhard, E.; Monard, D., The prolonged presence of glia-derived nexin, an endogenous protease inhibitor, in the hippocampus after ischemia-induced delayed neuronal death. *Neuroscience* **1992,** *49* (2), 397-408.
80. Kajiwara, Y.; Wang, E.; Wang, M.; Sin, W. C.; Brennand, K. J.; Schadt, E.; Naus, C. C.; Buxbaum, J.; Zhang, B. GJA1 (connexin43) is a key regulator of Alzheimer's disease pathogenesis. *Acta Neuropathol Commun* [Online], **2018**. PubMed. https://pubmed.ncbi.nlm.nih.gov/30577786.
81. Mayorquin, L. C.; Rodriguez, A. V.; Sutachan, J.-J.; Albarracín, S. L. Connexin-mediated functional and metabolic coupling between astrocytes and neurons. *Front Molec Neurosci* [Online], **2018**. https://www.frontiersin.org/article/10.3389/fnmol.2018.00118.
82. Pannasch, U.; Freche, D.; Dallérac, G.; Ghézali, G.; Escartin, C.; Ezan, P.; Cohen-Salmon, M.; Benchenane, K.; Abudara, V.; Dufour, A., et al., Connexin 30 sets synaptic strength by controlling astroglial synapse invasion. *Nat Neurosci* **2014,** *17* (4), 549-558.
83. Beckmann, N. D.; Lin, W.-J.; Wang, M.; Cohain, A. T.; Charney, A. W.; Wang, P.; Ma, W.; Wang, Y.-C.; Jiang, C.; Audrain, M., et al. Multiscale causal networks identify VGF as a key regulator of Alzheimer’s disease. *Nat Comm* [Online], **2020**. https://doi.org/10.1038/s41467-020-17405-z.
84. Yakovleva, T.; Marinova, Z.; Kuzmin, A.; Seidah, N. G.; Haroutunian, V.; Terenius, L.; Bakalkin, G., Dysregulation of dynorphins in Alzheimer disease. *Neurobiol Aging* **2007,** *28* (11), 1700-1708.
85. Ménard, C.; Herzog, H.; Schwarzer, C.; Quirion, R., Possible role of dynorphins in Alzheimer's disease and age-related cognitive deficits. *Neurodegener Dis* **2014,** *13* (2-3), 82-85.
86. Cartier, L.; Hartley, O.; Dubois-Dauphin, M.; Krause, K.-H., Chemokine receptors in the central nervous system: role in brain inflammation and neurodegenerative diseases. *Brain Res Rev* **2005,** *48* (1), 16-42.

87. Han, M.; Liu, Z.; Xu, Y.; Liu, X.; Wang, D.; Li, F.; Wang, Y.; Bi, J. Abnormality of m6A mRNA methylation Is involved in Alzheimer's disease. *Front Neurosci* [Online], **2020**. https://www.frontiersin.org/article/10.3389/fnins.2020.00098.
88. Huang, H.; Camats-Perna, J.; Medeiros, R.; Anggono, V.; Widagdo, J. Altered expression of the m6A methyltransferase METTL3 in Alzheimer's disease. *eNeuro* [Online], **2020**. https://www.ncbi.nlm.nih.gov/pmc/articles/PMC7540926/pdf/ENEURO.0125-20.2020.pdf.
89. Feng, Q.; Luo, Y.; Zhang, X. N.; Yang, X. F.; Hong, X. Y.; Sun, D. S.; Li, X. C.; Hu, Y.; Li, X. G.; Zhang, J. F., et al., MAPT/Tau accumulation represses autophagy flux by disrupting IST1-regulated ESCRT-III complex formation: a vicious cycle in Alzheimer neurodegeneration. *Autophagy* **2020,** *16* (4), 641-658.
90. Hoenig, M. C.; Bischof, G. N.; Hammes, J.; Faber, J.; Fliessbach, K.; van Eimeren, T.; Drzezga, A., Tau pathology and cognitive reserve in Alzheimer's disease. *Neurobiol Aging* **2017,** *57*, 1-7.
91. Kemppainen, N. M.; Aalto, S.; Karrasch, M.; Någren, K.; Savisto, N.; Oikonen, V.; Viitanen, M.; Parkkola, R.; Rinne, J. O., Cognitive reserve hypothesis: Pittsburgh Compound B and fluorodeoxyglucose positron emission tomography in relation to education in mild Alzheimer's disease. *Ann Neurol* **2008,** *63* (1), 112-118.
92. Nday, C. M.; Eleftheriadou, D.; Jackson, G., Shared pathological pathways of Alzheimer's disease with specific comorbidities: current perspectives and interventions. *J Neurochem* **2017**, 10.1111/jnc.14256.
93. Ouyang, S.; Hsuchou, H.; Kastin, A. J.; Wang, Y.; Yu, C.; Pan, W., Diet-induced obesity suppresses expression of many proteins at the blood–brain barrier. *J Cereb Blood Flow Metab* **2013,** *34* (1), 43-51.
94. Chin, A. L.; Negash, S.; Xie, S.; Arnold, S. E.; Hamilton, R., Quality, and not just quantity, of education accounts for differences in psychometric performance between African Americans and White Non-Hispanics with Alzheimer's disease. *J Int Neuropsychol Soc* **2012,** *18* (2), 277-285.
95. Manly, J. J.; Jacobs, D. M.; Sano, M.; Bell, K.; Merchant, C. A.; Small, S. A.; Stern, Y., Cognitive test performance among nondemented elderly African Americans and whites. *Neurology* **1998,** *50* (5), 1238-1245.
96. Fyffe, D. C.; Mukherjee, S.; Barnes, L. L.; Manly, J. J.; Bennett, D. A.; Crane, P. K., Explaining differences in episodic memory performance among older African Americans and Whites: The roles of factors related to cognitive reserve and test bias. *J Int Neuropsychol Soc* **2011,** *17* (4), 625-638.
97. Sisco, S.; Gross, A. L.; Shih, R. A.; Sachs, B. C.; Glymour, M. M.; Bangen, K. J.; Benitez, A.; Skinner, J.; Schneider, B. C.; Manly, J. J., The role of early-life educational quality and literacy in explaining racial disparities in cognition in late life. *J Gerontol B Psychol Sci Soc Sci* **2015,** *70* (4), 557-567.
98. Barnes, L. L.; Wilson, R. S.; Mendes de Leon, C. F.; Bennett, D. A., The relation of lifetime cognitive activity and lifetime access to resources to late-life cognitive function in older African Americans. *Neuropsychol Dev Cogn B Aging Neuropsychol Cogn* **2006,** *13* (3-4), 516-528.
99. Barnes, L. L.; Wilson, R. S.; Everson-Rose, S. A.; Hayward, M. D.; Evans, D. A.; Mendes de Leon, C. F., Effects of early-life adversity on cognitive decline in older African Americans and whites. *Neurology* **2012,** *79* (24), 2321-2327.

100. Whitfield, K. E.; Allaire, J. C.; Belue, R.; Edwards, C. L., Are comparisons the answer to understanding behavioral aspects of aging in racial and ethnic groups? *J Gerontol B Psychol Sci Soc Sci* **2008,** *63* (5), P301-P308.

CHAPTER 5

Machine Learning to Classify Individuals with Alzheimer's Disease in a Diverse Cohort

5.1 Introduction

African American/Black and Hispanic adults are more likely to develop Alzheimer's disease (AD) than other racial groups.[1-2] Neuropathological differences in AD hallmarks (amyloid-beta plaques and tau tangles) have not been reported between the brains of African American/Black and non-Hispanic White adults.[2-5] Some studies have observed that African American/Black adults are more likely to present with both AD and other dementia pathologies,[3, 6-8] though these findings have not been consistent across studies.[9-10] However, differences at the molecular level between African American/Black and non-Hispanic White adults have recently been discovered, particularly in levels of tau biomarkers for AD in cerebrospinal fluid (CSF).[9, 11-13] CSF levels of total tau and tau phosphorylated at position 181 (p-tau$_{181}$) were lower overall in African American/Black adults than non-Hispanic White adults regardless of cognitive status,[9, 11-13] and furthermore smaller changes in tau levels occurred in African American/Black adults with cognitive decline.[11]

Proteomics has been widely used to study molecular changes in the AD brain and many proteins have different levels between AD and cognitively normal (CN) groups across various brain regions.[14-26] However, many existing brain proteomics datasets have included primarily non-Hispanic White adults,[14-19] such that characterization of proteomic changes in AD brain in other racial and ethnic groups has been very limited. Availability of postmortem brain tissue from African American/Black adults is significantly limited due to difficulties around

recruitment into AD studies,[27] particularly related to organ donation.[28] Some studies have worked to develop effective strategies for recruiting African American/Black adults into AD research, such as culturally informed storytelling materials, community engagement and AD education, and making CSF and/or organ donation optional instead of required.[29-31] These strategies have been applied in the Minority Aging Research Study (MARS) at the Rush Alzheimer's Disease Center[30] and the Washington University Alzheimer's Disease Research Center[31] among others, though the majority of studies of postmortem brain tissue to date still only include small proportions of African American/Black adults and other racial/ethnic groups.

Few brain proteomics studies in AD have included diverse racial groups. In **Chapters 3-4**, we used proteomics to analyze postmortem brain tissue from two distinct cohorts, both of which included African American/Black and non-Hispanic White adults, and identified subsets of proteins in each with race-specific changes in AD.[20] Furthermore, markers of inflammation and neurodegeneration were increased in the middle temporal gyrus region (Brodmann area 21) in African American/Black adults with AD compared to non-Hispanic White adults with AD.[32-33] These studies suggest that there is heterogeneity in protein changes in the brain in AD across racial groups, though these studies have had relatively small sample sizes ranging from N = 20-40 total and require further studies to better characterize these changes in diverse cohorts.

Machine learning, an artificial intelligence tool that uses a system or model to make decisions without human involvement,[34-35] can use proteomics data to classify or predict disease status or treatment type and test the accuracy of various protein panels for distinguishing sample groups.[35] Machine learning has been previously used for these purposes in AD research.[36-37] For example, various machine learning algorithms including XGBoost,[38] Support Vector Machine (SVM),[39] and the Aristotle Classifier[40] were able to successfully classify brain proteomics data

from AD and CN groups[15] across two brain regions.[36] Both SVM and XGBoost, a decision tree-based algorithm,[38] are well-established supervised classification tools in machine learning and have been used previously for predictive purposes in AD.[37, 41-43] In these studies, XGBoost was able to distinguish AD and CN groups using demographic and clinical cognitive data,[43] neuroimaging data,[42] AD CSF biomarkers, and metabolites measured in blood plasma.[41] Notably, two of these studies reported improved classification of groups using XGBoost compared to other strategies.[41-42]

Moreover, machine learning has specifically been applied with proteomics data to study racial disparities in AD. Our laboratory demonstrated that a machine learning model trained with plasma proteins that were differentially expressed between non-Hispanic White AD and CN groups from proteomics analyses better differentiated AD and CN groups within the same racial group.[37] In African American/Black groups, this model was much less accurate in distinguishing AD and CN groups (47% accuracy), suggesting that proteomic biomarkers should be established using diverse cohorts. However, whether this finding is generalizable and relevant in other tissues, such as postmortem brain tissue, has yet to be studied.

Few studies have investigated AD-related proteomic changes in the brain in diverse cohorts, yet the brain's direct involvement in AD makes it a valuable tissue in which to initially characterize these changes. Analyses in postmortem brain tissue could identify important target proteins that could later be measured in more accessible biological samples such as plasma or CSF. Machine learning offers a strategy to leverage existing brain proteomics datasets and identify proteins that most effectively differentiate AD and CN individuals in these studies. Herein, we applied machine learning to available AD brain proteomics datasets,[14-15, 19, 44] composed primarily of non-Hispanic White adults, to evaluate whether proteins distinguishing

AD and CN groups can successfully classify AD and CN individuals in a diverse cohort, described in **Chapter 3**[20] (**Figure 5.1**). Our findings show that brain proteins can differentiate AD and CN groups across various AD brain proteomics datasets, and highlight the need for diversity in such brain proteomics studies.

5.2 Methods

5.2.1 Proteomics dataset selection & preparation for machine learning

Available proteomics datasets of postmortem brain tissue from CN and AD individuals were included in this study. Datasets were limited to those analyzed using Tandem Mass Tags (TMT), an isobaric tagging strategy that allows multiplexing of up to 18 samples in a single experiment, for protein quantification.[45-46] This criterion was necessary to ensure that the proteomics sample preparation and analysis process was largely similar for all datasets. This resulted in inclusion of five datasets from different cohorts: (1) dorsolateral prefrontal cortex (DLPFC; Brodmann area 9) from the Emory Alzheimer's Disease Research Center (ADRC) (N = 40)[15]; (2) DLPFC from Religious Orders Study and Rush Memory and Aging Project (ROSMAP; N = 318)[14]; (3-4) parahippocampal gyrus (PHG; Brodmann area 36) from the Mount Sinai/JJ Peters VA Medical Center Brain Bank (MSBB-Bai, N = 62[19] and MSBB-Full, N = 190[44]); (5) hippocampus, inferior parietal lobule (IPL), and globus pallidus (GP) from the University of Pittsburgh ADRC (Pitt ADRC; N = 20), described in **Chapter 3**.[20] We note that the samples in the MSBB-Bai dataset are also part of the larger MSBB-Full dataset. All cohorts included participants from multiple self-reported racial groups (**Table 5.1**).

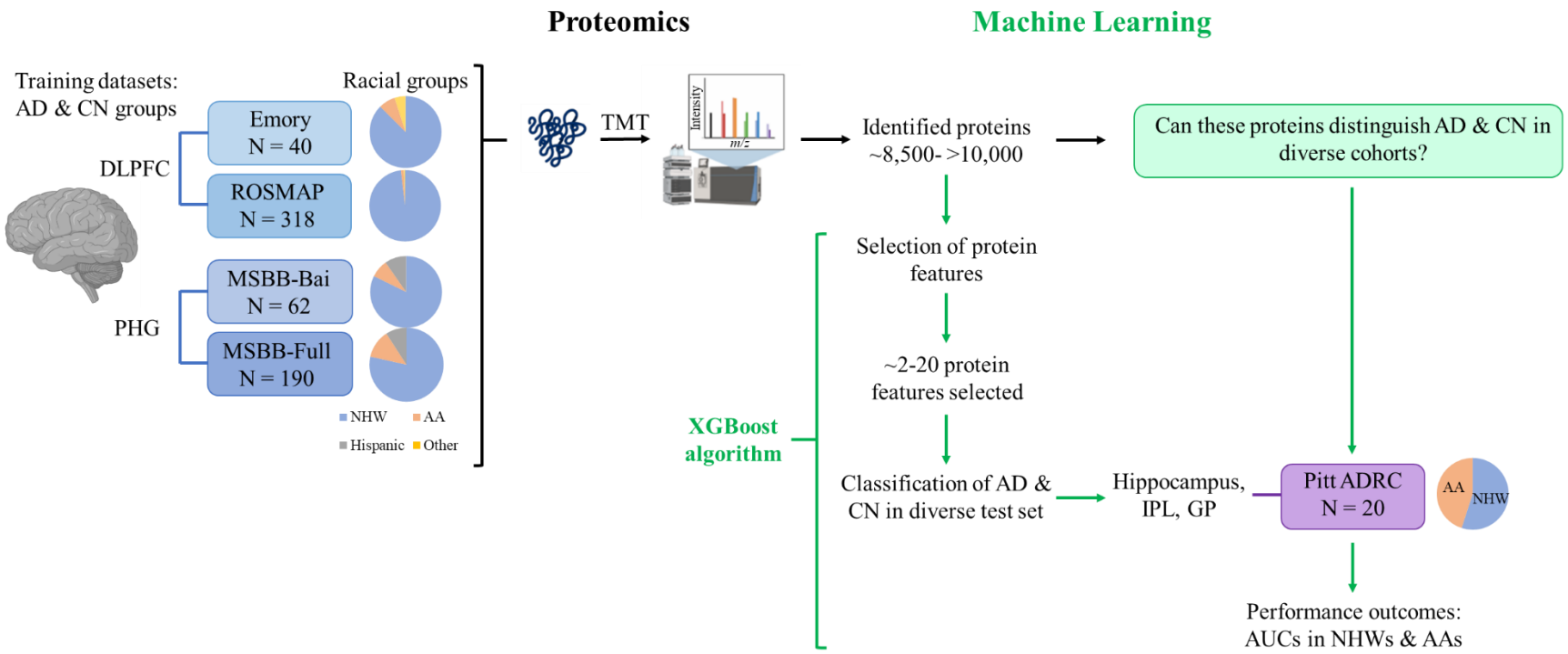

Figure 5.1. Overview of proteomics and machine learning to differentiate AD and CN groups. Proteomics was first used to analyze postmortem brain tissue samples from AD and CN groups in four cohorts (training datasets, shown in blue). These groups were composed of mostly non-Hispanic White adults, as shown by the accompanying pie charts for each dataset. Proteins were extracted from these brain tissues and prepared and analyzed using discovery-based quantitative proteomics workflows using TMT for relative quantification of proteins (black arrows), resulting in the identification of ~8,500 to > 10,000 proteins. From these proteomics results, we then wanted to answer the question of whether any of these proteins distinguish AD and CN groups in more diverse cohorts, for which we utilized machine learning (green arrows). XGBoost was used to select protein features that distinguished AD and CN groups in the four brain proteomics datasets, resulting in ~2-20 selected features per dataset, and use these selected features to classify AD and CN groups in a separate test dataset (shown in purple) that was more diverse (45% African American/Black) than the training datasets. Performance of each machine learning model was evaluated based on the AUCs in African American/Black and non-Hispanic White groups. Abbreviations: AD, Alzheimer's disease; CN, cognitively normal; DLPFC, dorsolateral prefrontal cortex;

ROSMAP, Religious Orders Study and Rush Memory and Aging Project; PHG, parahippocampal gyrus; MSBB, Mount Sinai Brain Bank; NHW, non-Hispanic White; AA, African American/Black; TMT, Tandem Mass Tags; Pitt ADRC, University of Pittsburgh Alzheimer Disease Research Center; IPL, inferior parietal lobule; GP, globus pallidus; AUC, area under the receiver-operator curve. Figure partially created using BioRender.com.

Table 5.1. Demographics of patients in proteomics datasets.

	Emory[a]		ROSMAP[b]		MSBB-Bai		MSBB-Full[c]		Pitt ADRC	
	CN	**AD**	**CN**	**AD**	**CN**	**AD**	**CN**	**AD**	**CN**	**AD**
N	20	20	96	222	23	39	63	127	9	11
Age at death[d]	67 ± 8	68 ± 8	85 ± 5	88 ± 4	81 ± 10	84 ± 10	81 ± 8	80 ± 7	67 ± 13	82 ± 8
Sex (M/F)	14/6	11/9	36/60	67/155	12/11	12/27	29/34 2 ND	41/84 2 ND	6/3	5/6
Race[e]	17 W 1 B 2 PI	18 W 2 B	93 W 2 B 1 U	219 W 2 B 1 AI	17 W 2 B 4 H	34 W 3 B 2 H	44 W 7 B 10 H 2 ND	102 W 16 B 7 H 2 ND	5 W 4 B	6 W 5 B
% African American/Black	7.5%		1.3%		8.1%		12.1%		45.0%	

[a]CN and individuals with Parkinson's disease were grouped together as the CN group; individuals with AD and individuals with both AD and Parkinson's disease were grouped together as the AD group. [b]Individuals with AD and individuals with other dementia were grouped together as the AD group. [c]ND indicates no data was available for N individuals in the designated variable. [d]Reported as mean ± standard deviation. [e]Race was self-reported. W = non-Hispanic White; B = African American/Black; H = Hispanic; PI = Native Hawaiian or other Pacific Islander; AI = American Indian or Alaska native; U = race unknown. Abbreviations: CN, cognitively normal; AD, Alzheimer's disease; ROSMAP, Religious Orders Study and Rush Memory and Aging Project; MSBB, Mount Sinai Brain Bank; Pitt ADRC, University of Pittsburgh Alzheimer Disease Research Center.

Only CN and AD individuals from each dataset were included for machine learning analyses. Individuals with asymptomatic AD or mild cognitive impairment were excluded. In the Emory dataset, CN and individuals with Parkinson's disease were grouped together as the CN group; individuals with AD and individuals with both AD and Parkinson's disease were grouped together as the AD group. These groups were combined in such a way after preliminary comparisons showed no differences between the samples with and without Parkinson's disease (*data not shown*).

TMT protein intensity data for all quantified proteins from each dataset were used for machine learning analysis (**Figure 5.2**). TMT quantification information for all identified proteins were used from the Emory dataset.[15] Quantified proteins from the ROSMAP dataset had <50% missing TMT intensities. Data for these proteins were normalized to pools (samples containing equal amounts of protein from all samples included in each batch), batch-corrected, regressed for age, sex, and postmortem interval, median-centered, and $\log_2$ transformed.[14] Both MSBB datasets included TMT quantification at the peptide spectral match (PSM) level, which involved removing PSMs with low intensities prior to normalizing to the median intensity across all PSMs and mean-centering the data. PSMs were averaged per protein to provide protein-level quantification, which was batch-corrected based on the pools.[19, 44] Quantified proteins in the Pitt ADRC dataset were identified across both TMT batches of samples with intensities present for ≥ 80% of channels including all pools and data for these proteins were normalized to the pools; quantified proteins were determined and normalized per region (see **Chapter 3 Section 3.2.4**).[20]

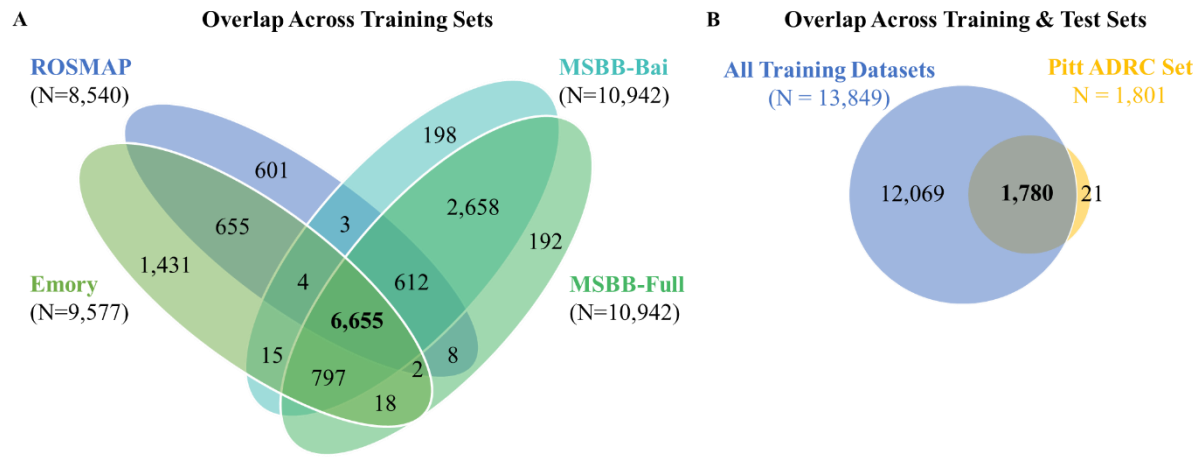

Figure 5.2. Overlap in quantified proteins across proteomics datasets. Venn diagrams showing overlap in quantified proteins across **(A)** the four training datasets and **(B)** the combined quantified proteins from the training datasets (N = 13,849) and the Pitt ADRC test set (N = 1,801). Quantified proteins included in the Pitt ADRC dataset include those from all three regions (hippocampus, IPL, and GP); see **Chapter 3 Figure 3.1c** for overlap across these regions. Criteria for quantified proteins in each study are described in **Section 5.2.1**. Abbreviations: ROSMAP, Religious Orders Study and Rush Memory and Aging Project; MSBB, Mount Sinai Brain Bank; Pitt ADRC, University of Pittsburgh Alzheimer Disease Research Center; IPL, inferior parietal lobule; GP, globus pallidus.

5.2.2 Machine learning

Supervised classification was performed using RStudio, R version 4.0.3. XGBoost was used for feature selection and AD and CN group classification using the xgboost R package version 1.4.1.1.[38] Each brain region of the Pitt ADRC dataset was initially classified independently without any feature selection, using all protein features in that dataset per region. Models were then trained using the Emory, ROSMAP, MSBB-Bai, and MSBB-Full datasets, and each was tested in the Pitt ADRC dataset, as shown in **Figure 5.1**. For each training set, the proteins that were common with the Pitt ADRC test dataset were first identified. XGBoost was then used to select protein features that differentiated AD and CN groups based on feature importance score. These selected features were then used to build a separate XGBoost model for each brain region to classify AD vs CN from the Pitt ADRC dataset using the same parameters as were used initially in the feature selection step. In this second round of XGBoost, each sample was classified using a leave-one-out cross validation to minimize overfitting. From each training dataset, different numbers of protein features, from 2-20 (or the maximum number of features selected if < 20), were used to classify the Pitt ADRC dataset. Area under the receiver-operator curve (AUC) values were calculated for each number of features using the R package pROC[47] for classification of AD and CN groups in the full dataset. Additionally, AUC values were calculated specifically only within African American/Black and only within non-Hispanic White groups. The optimal number of protein features for each dataset, determined by the highest summed AUCs for African American/Black and non-Hispanic White groups, was evaluated across datasets and regions (**Table 5.2**).

Table 5.2. Optimal number of protein features selected from each training dataset.

	Number of protein features		
Training dataset	**Hippocampus**	**IPL**	**GP**
Emory	7	7	8
ROSMAP	6	2	14
MSBB-Bai	5	2	10
MSBB-Full	5	4	2

[a]Optimal number of protein features selected for each dataset and Pitt ADRC test set region, which had the highest summed AUC from African American/Black and non-Hispanic White groups (see **Section 5.2.2**). Abbreviations: IPL, inferior parietal lobule; GP, globus pallidus; ROSMAP, Religious Orders Study and Rush Memory and Aging Project; MSBB, Mount Sinai Brain Bank; AUC, area under the receiver-operator curve; Pitt ADRC, University of Pittsburgh Alzheimer Disease Research Center.

5.3 Results

Machine learning was used to classify AD and CN groups from available proteomics datasets of postmortem brain tissue in AD. Five datasets were selected for machine learning analyses, all of which used TMT for relative quantification of proteins and included individuals of African American/Black racial backgrounds (**Figure 5.1**). These datasets varied in size from N = 20-318 total samples and the proportion of African American/Black adults ranged from ~1-45% (**Table 5.1**). Fewer samples were included from other racial groups including Hispanic, Native American/other Pacific Islander, and American Indian/Alaska Native. The number of proteins quantified across datasets also encompassed a wide range, from ~1,800 to > 10,000 proteins, depending on the proteomics methodologies used for sample preparation and data acquisition. Across the training datasets, a total of 13,849 proteins were quantified, with approximately half of these in common across all four datasets (N = 6,655; **Figure 5.2A**). Similar overlap was observed across the three brain regions within the Pitt ADRC test set (see **Chapter 3 Figure 3.1c**). Importantly, 98.8% of the proteins in the test dataset were also identified across the training sets (N = 1,780; **Figure 5.2B**), showing that most of these protein features were able to be used for feature selection (see **Section 5.2.2**).

5.3.1 Results from optimization of feature selection

We first evaluated whether AD and CN groups in the Pitt ADRC set could be classified using all of the protein features in this dataset, without selecting any features within this or other datasets. Without feature selection, classification of AD and CN groups resulted in higher AUCs in non-Hispanic White adults than African American/Black adults, averaging 0.80 and 0.67 across regions, respectively. Classification for the Pitt ADRC IPL set is shown in **Figure 5.3**.

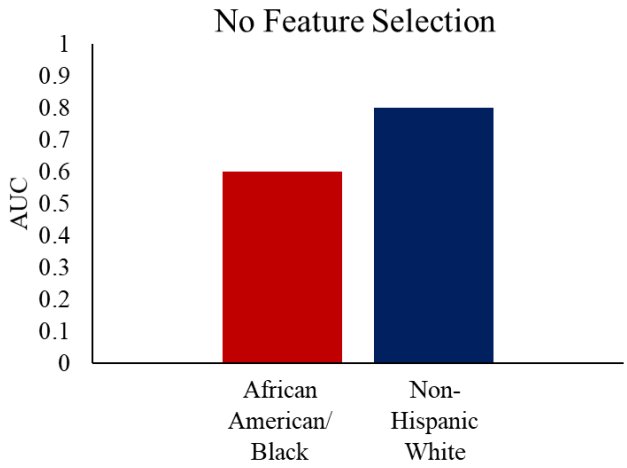

Figure 5.3. Classification of Pitt ADRC test dataset without feature selection. Bar graph of AUCs for classification of AD and CN groups in the Pitt ADRC IPL dataset using all protein features in the Pitt ADRC set (no feature selection). Abbreviations: AUC, area under the receiver-operator curve; AD, Alzheimer's disease; CN, cognitively normal; Pitt ADRC, University of Pittsburgh Alzheimer Disease Research Center; IPL, inferior parietal lobule.

We then tested whether selecting the top N features (i.e. 2-20) that best classified AD and CN groups in the training datasets could improve discrimination of AD and CN groups in the Pitt ADRC dataset. We evaluated the AUCs resulting from each classification (*data not shown*) to determine the optimal number of features (**Table 5.2**) from each dataset to classify each region of the Pitt ADRC dataset. Feature selection resulted in an overall improvement in classification of AD and CN groups in the Pitt ADRC test dataset compared to the model without feature selection (*data not shown*). These improvements were evident across racial groups, whereas without feature selection, the model clearly performed better in non-Hispanic White than African American/Black groups. Choosing the optimal number of protein features with the best performance in each dataset and region resulted in improved classification of AD and CN groups in the Pitt ADRC dataset.

5.3.2 Comparison of classification results across brain regions

Protein features selected from all of the training datasets in this study were able to distinguish AD and CN groups regardless of racial background in the three brain regions from the Pitt ADRC test dataset (**Figure 5.4**). Overall AUCs from all three regions fell within the 0.80-1 range. By region, classification was the best in IPL from all datasets, with overall AUCs of 0.94-0.96. Notably, classification in the GP was the least consistent across racial groups and training datasets. Given that the training datasets were not all from the same brain region and were not from the same regions as those in the test dataset, we evaluated trends in the performance of the training datasets by brain region. We did not observe any effects of the training dataset brain region on performance, as AUCs were similar across the four training datasets for each test dataset brain region (**Figure 5.4**). This supports that machine learning

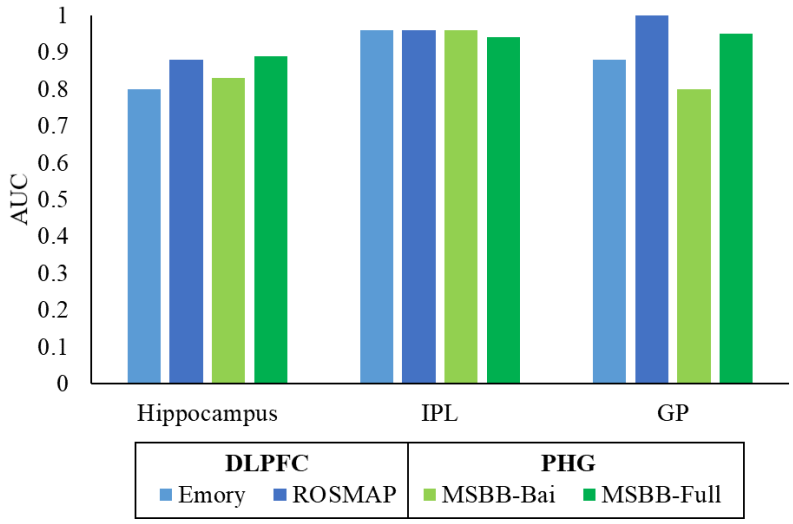

Figure 5.4. Overall AUCs for classification of Pitt ADRC test dataset across brain regions. Bar graph showing AUCs for overall classification of AD and CN groups (no stratification by racial groups) in each region of the Pitt ADRC test dataset using the optimal number of features from each training dataset. Bar colors indicate the brain region of each training dataset: DLPFC datasets are shown in shades of blue (Emory and ROSMAP) and PHG datasets are shown in shades of green (MSBB-Bai and MSBB-Full). Abbreviations: AUC, area under the receiver-operator curve; IPL, inferior parietal lobule; GP, globus pallidus; DLPFC, dorsolateral prefrontal cortex; PHG, parahippocampal gyrus; ROSMAP, Religious Orders Study and Rush Memory and Aging Project; MSBB, Mount Sinai Brain Bank; Pitt ADRC, University of Pittsburgh Alzheimer Disease Research Center; AD, Alzheimer's disease; CN, cognitively normal.

models can successfully use brain proteomics datasets from different brain regions to distinguish AD and CN groups in datasets of similar or differing brain regions.

5.3.3 Comparison of classification results across racial groups

In addition to distinguishing AD and CN groups in general, the optimal protein features selected from the four training datasets were also able to make this distinction between race-stratified AD and CN groups (**Figure 5.5**). This is important to note given that the Pitt ADRC test dataset was composed of a larger proportion of African American/Black adults (45%) than the training datasets (~1-12%). We did not observe an impact of proportion of African American/Black adults in the training datasets on classification performance, i.e. the ROSMAP dataset did not classify African American/Black AD and CN groups worse than the other datasets even though it had the smallest proportion of African American/Black adults. However, classification of race-stratified groups did not show consistent trends across regions, though most race-stratified AUCs ranged between 0.80-1. For example, all datasets classified non-Hispanic White groups with higher AUCs in IPL (**Figure 5.5B**), while most datasets classified African American/Black groups with higher AUCs in hippocampus (**Figure 5.5A**). Our work emphasizes the importance of including individuals from different racial backgrounds in proteomics and machine learning analyses and highlights the need for additional studies to further evaluate classification performance across racial groups.

5.4 Discussion

Many existing proteomics datasets of postmortem brain tissue in AD have included primarily individuals of non-Hispanic White racial background.[14-19] In this study, we applied

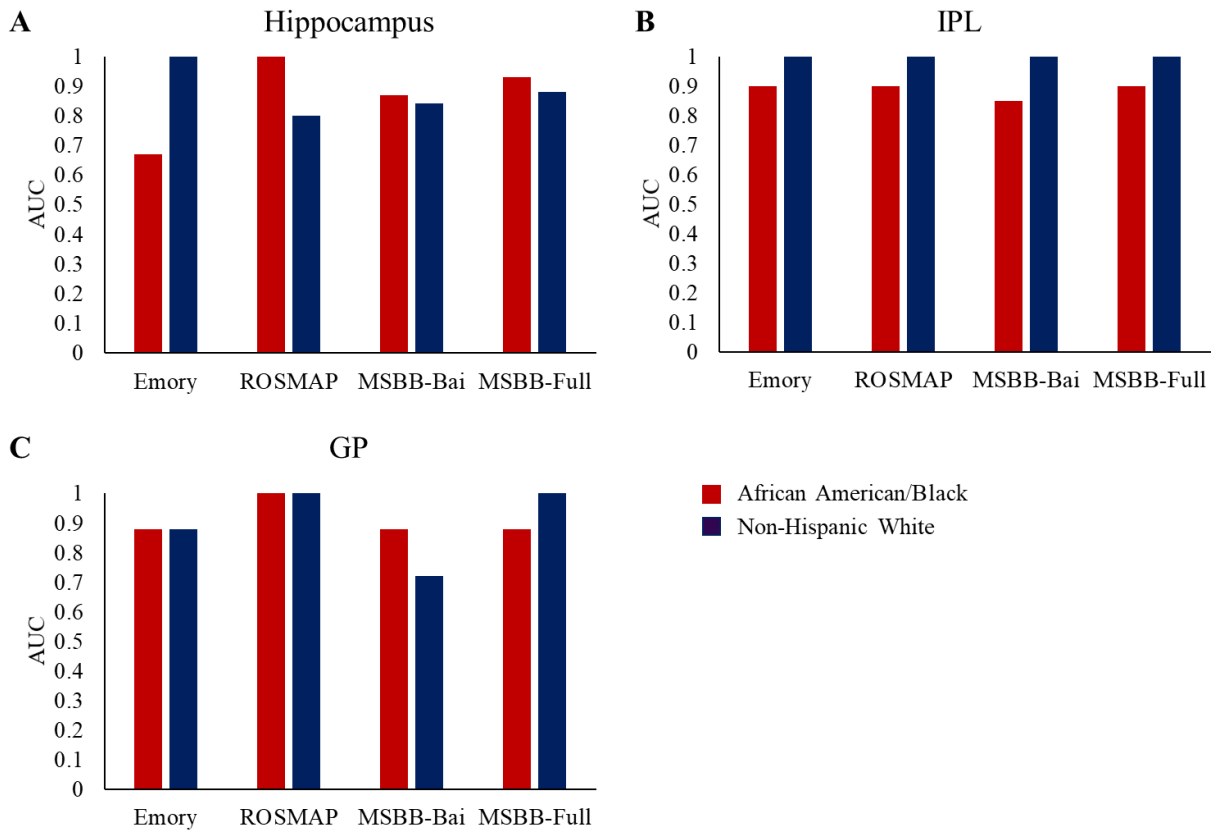

Figure 5.5. Classification of Pitt ADRC test dataset across racial groups. Bar graphs showing AUCs from classification of AD and CN groups within African American/Black and non-Hispanic White adults in the Pitt ADRC test dataset regions of **(A)** hippocampus, **(B)** IPL, and **(C)** GP using each training dataset. The optimal number of selected protein features from each training dataset was used for classification of the Pitt ADRC test dataset. AUCs for classification of African American/Black and non-Hispanic White AD and CN groups are shown in red and blue bars, respectively. Abbreviations: AUC, area under the receiver-operator curve; ROSMAP, Religious Orders Study and Rush Memory and Aging Project; MSBB, Mount Sinai Brain Bank; IPL, inferior parietal lobule; GP, globus pallidus; Pitt ADRC, University of Pittsburgh Alzheimer Disease Research Center; AD, Alzheimer's disease; CN, cognitively normal.

machine learning to identify protein features from existing, primarily non-Hispanic White brain proteomics datasets and tested whether they could accurately classify AD and CN groups in a more diverse cohort including African American/Black adults. We first optimized protein feature selection and then evaluated performance of optimal features from each training dataset in classifying AD and CN groups across brain regions and racial groups of our test dataset.

Selecting top protein features that discriminated AD and CN groups from four different training datasets[14-15, 19, 44] improved overall classification of AD and CN individuals in the Pitt ADRC multi-regional (hippocampus, IPL, and GP) test dataset.[20] Optimizing the number of features selected from each dataset enabled the best possible classification from the models, which would not have been the case if the same number of features had been selected across datasets and brain regions. This analysis highlights the importance of the feature selection step in AD machine learning analyses to provide the best model for classifying AD and CN groups.

When evaluating the classifications using the optimal protein features selected across training datasets and brain regions, this study showed differences in classification of AD and CN groups across the three regions of the Pitt ADRC test set. Notably, the highest overall AUCs and therefore best AD and CN classification were achieved in IPL, which was consistent across datasets (**Figure 5.4**). We expected consistent high performance of the classification to also occur in hippocampus, due to its extensive involvement in AD pathology.[21-22, 48-54] However, the AUCs in hippocampus ranged from 0.80-0.89 and was less consistent than IPL. IPL is also involved in memory function[55-58] and is affected by both amyloid and tau pathology during mild cognitive impairment (MCI) and AD.[59-60] On the other hand, classification of AD and CN groups in GP was more inconsistent compared to hippocampus and IPL. This is likely due to the lack of

AD pathology in this region, suggesting that the proteomic changes observed in this region are not as useful to distinguish AD and CN groups.

Previous proteomics studies, including the Pitt ADRC study described in **Chapter 3**, have shown that differentially-expressed proteins in AD are largely region-specific, with only a small proportion of shared changes across multiple regions.[20, 23, 49] These findings would suggest that training and testing models across different brain regions may not be an effective strategy to classify AD and CN groups. However, in this study we selected protein features that distinguish AD and CN groups in two different brain regions (DLPFC and PHG) and found that they were also able to successfully classify AD and CN groups in a test dataset derived from three different brain regions (hippocampus, IPL, GP). Though the brain regions differed, over 98% of the proteins in the Pitt ADRC test dataset were also identified in the training datasets (**Figure 5.2B**). We observed that all four training datasets, regardless of region, resulted in similar overall classifications of the Pitt ADRC set (**Figure 5.4**). Furthermore, the two PHG training datasets (MSBB-Bai and MSBB-Full) did not classify hippocampus with higher AUCs than IPL and GP, despite the physical proximity of PHG and hippocampus and their shared involvement in memory.[61-62] Therefore, we do not believe that training and testing datasets derived from different brain regions negatively affected model performance in this study. Additionally, others have shown that modules of differentially-expressed proteins in AD brain are largely conserved across multiple cohorts and brain regions.[14, 63] In fact, the identification of protein features that distinguish AD and CN groups across multiple brain regions could result better potential targets to follow up in more accessible biofluids (e.g. plasma or urine). Future studies could train and test machine learning models in datasets from the same brain regions; however, the ability to

accomplish this is currently limited by the lack of diversity in racial background and brain regions studied in existing AD brain proteomics studies.

We have demonstrated in this study that protein features selected from datasets containing mostly non-Hispanic White adults (~79-99%) are able to distinguish AD and CN groups in a more diverse cohort (45% African American/Black; **Figure 5.5**). These models led to race-stratified AUCs that mainly ranged between 0.80-1, though classification of AD and CN groups was not consistent across racial groups and regions. In IPL, non-Hispanic White AD and CN groups were consistently classified with higher AUCs than African American/Black groups, while in hippocampus, three out of four training datasets classified African American/Black AD and CN groups with higher AUCs. No clear trend emerged across racial groups in GP, consistent with lack of pathology and low discrimination performance in this region. Interestingly, there was also no apparent association between proportion of African American/Black adults in the training dataset and the model performance in African American/Black AD and CN groups in the test dataset.

Overall, the optimal protein features from the training datasets had positive performance in both African American/Black and non-Hispanic White groups, resulting in AUCs ranging from 0.67-1 and 0.72-1, respectively. The primary limitations of this study are the small sample size and dataset size of the test cohort, which led to inconsistencies in classification by racial group. The quantified proteins from the Pitt ADRC set in this study were only ~16-21% of the quantified proteins from the training datasets, likely due to differences in sample preparation and data acquisition, which have been discussed in both **Chapters 3-4**. The smaller size of the test dataset significantly limited the protein features that could be matched between the training and test datasets and thus considered for feature selection. Therefore, it is possible that larger test

datasets would yield additional or different top features to differentiate AD and CN groups. Determining how these training datasets (Emory, ROSMAP, and MSBB) perform across additional larger test datasets will be an important next step for this work. Larger, and more diverse datasets could also enable feature selection that achieves high performance in all individuals, regardless of racial background. This study provides initial evidence that proteins distinguishing AD and CN groups in primarily non-Hispanic White adults can also classify AD and CN groups in a more diverse cohort. However, whether this classification is equally accurate across racial groups requires further investigation.

5.5 Conclusions

Machine learning approaches offer unique advantages to analyze proteomics datasets and further pull out the most important proteins that allow discrimination of sample groups by disease state. Proteomics has been extensively used to characterize the AD brain; however, many of these studies have primarily included non-Hispanic White adults and thus knowledge of proteomic changes due to AD in other racial and ethnic groups is quite limited. In this study, we used machine learning to analyze existing brain proteomics datasets in AD that included mainly non-Hispanic White adults to identify proteins that discriminated between AD and CN groups. We demonstrated proteins that successfully classified AD and CN groups in an additional, more diverse dataset across different brain regions, and that these selected proteins resulted in improved classification of AD compared to use of all the protein features in a dataset. Furthermore, selected protein features were able to distinguish AD and CN groups amongst both African American/Black and non-Hispanic White adults overall. However, further investigation into the impact of racial group on classification of AD and CN groups is necessary. Use of

proteomics and machine learning methods in larger, more diverse cohorts in the future will further elucidate the best protein features to classify AD for everyone.

5.6 Acknowledgements

The authors acknowledge funding from Vanderbilt Interdisciplinary Training Program in Alzheimer's Disease (T32-AG058524). We would like to thank Dr. Heather Desaire at the University of Kansas for designing and performing the machine learning analyses for this work. We would also like to thank Drs. Junmin Peng and Xusheng Wang at St. Jude's Children's Research Hospital and Dr. Vahram Haroutunian at Icahn School of Medicine at Mount Sinai and the James J. Peters VA Medical Center for sharing a training dataset for this work.

5.7 References

1. Alzheimer's Association, 2021 Alzheimer's disease facts and figures. *Alzheimers Dement* **2021,** *17* (3), 327-406.
2. Chin, A. L.; Negash, S.; Hamilton, R., Diversity and disparity in dementia: the impact of ethnoracial differences in Alzheimer disease. *Alzheimer Dis Assoc Disord* **2011,** *25* (3), 187-195.
3. Barnes, L. L.; Leurgans, S.; Aggarwal, N. T.; Shah, R. C.; Arvanitakis, Z.; James, B. D.; Buchman, A. S.; Bennett, D. A.; Schneider, J. A., Mixed pathology is more likely in black than white decedents with Alzheimer dementia. *Neurology* **2015,** *85* (6), 528-534.
4. Gottesman, R. F.; Schneider, A. C.; Zhou, Y.; Coresh, J.; Green, E.; Gupta, N.; Knopman, D. S.; Mintz, A.; Rahmim, A.; Sharrett, A. R., et al., Association between midlife vascular risk factors and estimated brain amyloid deposition. *JAMA* **2017,** *317* (14), 1443-1450.
5. Wilkins, C. H.; Grant, E. A.; Schmitt, S. E.; McKeel, D. W.; Morris, J. C., The neuropathology of Alzheimer disease in African American and white individuals. *Arch Neurol* **2006,** *63* (1), 87-90.
6. Graff-Radford, N. R.; Besser, L. M.; Crook, J. E.; Kukull, W. A.; Dickson, D. W., Neuropathological differences by race from the National Alzheimer's Coordinating Center. *Alzheimers Dement* **2016,** *12* (6), 669-677.
7. Gottesman, R. F.; Fornage, M.; Knopman, D. S.; Mosley, T. H., Brain aging in African-Americans: the Atherosclerosis Risk in Communities (ARIC) experience. *Curr Alzheimer Res* **2015,** *12* (7), 607-613.
8. Brickman, A. M.; Schupf, N.; Manly, J. J.; Luchsinger, J. A.; Andrews, H.; Tang, M. X.; Reitz, C.; Small, S. A.; Mayeux, R.; DeCarli, C., et al., Brain morphology in older African

Americans, Caribbean Hispanics, and whites from northern Manhattan. *Arch Neurol* **2008,** *65* (8), 1053-61.
9. Morris, J. C.; Schindler, S. E.; McCue, L. M.; Moulder, K. L.; Benzinger, T. L. S.; Cruchaga, C.; Fagan, A. M.; Grant, E.; Gordon, B. A.; Holtzman, D. M., et al., Assessment of racial disparities in biomarkers for Alzheimer disease. *JAMA Neurol* **2019,** *76* (3), 264-273.
10. Barnes, L. L., Biomarkers for Alzheimer dementia in diverse racial and ethnic minorities—a public health priority. *JAMA Neurol* **2019,** *76* (3), 251-253.
11. Howell, J. C.; Watts, K. D.; Parker, M. W.; Wu, J.; Kollhoff, A.; Wingo, T. S.; Dorbin, C. D.; Qiu, D.; Hu, W. T. Race modifies the relationship between cognition and Alzheimer's disease cerebrospinal fluid biomarkers. *Alzheimers Res Ther* [Online], **2017**. https://doi.org/10.1186/s13195-017-0315-1.
12. Garrett, S. L.; McDaniel, D.; Obideen, M.; Trammell, A. R.; Shaw, L. M.; Goldstein, F. C.; Hajjar, I. Racial disparity in cerebrospinal fluid amyloid and tau biomarkers and associated cutoffs for mild cognitive impairment. *JAMA Netw Open* [Online], **2019**. https://doi.org/10.1001/jamanetworkopen.2019.17363.
13. Chaudhry, A.; Rizig, M. Comparing fluid biomarkers of Alzheimer's disease between African American or Black African and white groups: A systematic review and meta-analysis. *J Neurol Sci* [Online], **2021**. https://www.sciencedirect.com/science/article/pii/S0022510X20306067?via%3Dihub.
14. Johnson, E. C. B.; Dammer, E. B.; Duong, D. M.; Ping, L.; Zhou, M.; Yin, L.; Higginbotham, L. A.; Guajardo, A.; White, B.; Troncoso, J. C., et al., Large-scale proteomic analysis of Alzheimer's disease brain and cerebrospinal fluid reveals early changes in energy metabolism associated with microglia and astrocyte activation. *Nat Med* **2020,** *26*, 769-780.
15. Ping, L.; Duong, D. M.; Yin, L.; Gearing, M.; Lah, J. J.; Levey, A. I.; Seyfried, N. T. Global quantitative analysis of the human brain proteome in Alzheimer's and Parkinson's Disease. *Sci Data* [Online], **2018**. http://dx.doi.org/10.1038/sdata.2018.36.
16. Ping, L.; Kundinger, S. R.; Duong, D. M.; Yin, L.; Gearing, M.; Lah, J. J.; Levey, A. I.; Seyfried, N. T. Global quantitative analysis of the human brain proteome and phosphoproteome in Alzheimer's disease. *Sci Data* [Online], **2020**. https://www.nature.com/articles/s41597-020-00650-8.pdf.
17. Andreev, V. P.; Petyuk, V. A.; Brewer, H. M.; Karpievitch, Y. V.; Xie, F.; Clarke, J.; Camp, D.; Smith, R. D.; Lieberman, A. P.; Albin, R. L., et al., Label-free quantitative LC-MS proteomics of Alzheimer's disease and normally aged human brains. *J Proteome Res* **2012,** *11* (6), 3053-3067.
18. Seyfried, N. T.; Dammer, E. B.; Swarup, V.; Nandakumar, D.; Duong, D. M.; Yin, L.; Deng, Q.; Nguyen, T.; Hales, C. M.; Wingo, T., et al., A multi-network approach identifies protein-specific co-expression in asymptomatic and symptomatic Alzheimer's disease. *Cell Syst* **2017,** *4* (1), 60-72.
19. Bai, B.; Wang, X.; Li, Y.; Chen, P.-C.; Yu, K.; Dey, K. K.; Yarbro, J. M.; Han, X.; Lutz, B. M.; Rao, S., et al., Deep multilayer brain proteomics identifies molecular networks in Alzheimer's disease progression. *Neuron* **2020,** *105* (6), 975-991.
20. Stepler, K. E.; Mahoney, E. R.; Kofler, J.; Hohman, T. J.; Lopez, O. L.; Robinson, R. A. S. Inclusion of African American/Black adults in a pilot brain proteomics study of Alzheimer's disease. *Neurobiol Dis* [Online], **2020**. http://www.sciencedirect.com/science/article/pii/S0969996120304046.

21. Manavalan, A.; Mishra, M.; Feng, L.; Sze, S. K.; Akatsu, H.; Heese, K. Brain site-specific proteome changes in aging-related dementia. *Exp Mol Med* [Online], **2013**. http://dx.doi.org/10.1038/emm.2013.76.
22. Begcevic, I.; Kosanam, H.; Martinez-Morillo, E.; Dimitromanolakis, A.; Diamandis, P.; Kuzmanov, U.; Hazrati, L. N.; Diamandis, E. P. Semiquantitative proteomic analysis of human hippocampal tissues from Alzheimer's disease and age-matched control brains. *Clin Proteomics* [Online], **2013**. https://www.ncbi.nlm.nih.gov/pmc/articles/PMC3648498/pdf/1559-0275-10-5.pdf.
23. McKetney, J.; Runde, R.; Hebert, A. S.; Salamat, S.; Roy, S.; Coon, J. J., Proteomic atlas of the human brain in Alzheimer's disease. *J Proteome Res* **2019,** *18* (3), 1380-1391.
24. Wang, Z.; Yu, K.; Tan, H.; Wu, Z.; Cho, J.-H.; Han, X.; Sun, H.; Beach, T. G.; Peng, J., 27-plex Tandem Mass Tag mass spectrometry for profiling brain proteome in Alzheimer's disease. *Anal Chem* **2020,** *92* (10), 7162-7170.
25. Minjarez, B.; Calderon-Gonzalez, K. G.; Rustarazo, M. L.; Herrera-Aguirre, M. E.; Labra-Barrios, M. L.; Rincon-Limas, D. E.; Del Pino, M. M.; Mena, R.; Luna-Arias, J. P., Identification of proteins that are differentially expressed in brains with Alzheimer's disease using iTRAQ labeling and tandem mass spectrometry. *J Proteomics* **2016,** *139*, 103-121.
26. Johnson, E. C. B.; Dammer, E. B.; Duong, D. M.; Yin, L.; Thambisetty, M.; Troncoso, J. C.; Lah, J. J.; Levey, A. I.; Seyfried, N. T. Deep proteomic network analysis of Alzheimer’s disease brain reveals alterations in RNA binding proteins and RNA splicing associated with disease. *Molec Neurodegen* [Online], **2018**. https://doi.org/10.1186/s13024-018-0282-4.
27. Stahl, S. M.; Vasquez, L., Approaches to improving recruitment and retention of minority elders participating in research: examples from selected research groups including the National Institute on Aging's Resource Centers for Minority Aging Research. *J Aging Health* **2004,** *16* (5 Suppl), 9s-17s.
28. Boulware, L. E.; Ratner, L. E.; Cooper, L. A.; Sosa, J. A.; LaVeist, T. A.; Powe, N. R., Understanding disparities in donor behavior: race and gender differences in willingness to donate blood and cadaveric organs. *Med Care* **2002,** *40* (2), 85-95.
29. Robinson, R. A. S.; Williams, I. C.; Cameron, J. L.; Ward, K.; Knox, M.; Terry, M.; Tamres, L.; Mbawuike, U.; Garrett, M.; Lingler, J. H. Framework for creating storytelling materials to promote African American/Black adult enrollment in research on Alzheimer's disease and related disorders. *Alzheimers Dement (N Y)* [Online], **2020**. PubMed. https://pubmed.ncbi.nlm.nih.gov/32995472.
30. Barnes, L. L.; Shah, R. C.; Aggarwal, N. T.; Bennett, D. A.; Schneider, J. A., The Minority Aging Research Study: ongoing efforts to obtain brain donation from African Americans without dementia. *Curr Alzheimer Res* **2012,** *9* (6), 734-745.
31. Williams, M. M.; Meisel, M. M.; Williams, J.; Morris, J. C., An interdisciplinary outreach model of African American recruitment for Alzheimer's disease research. *Gerontologist* **2011,** *51* (Suppl 1), S134-S141.
32. Ferguson, S. A.; Panos, J. J.; Sloper, D.; Varma, V., Neurodegenerative markers are increased in postmortem BA21 tissue from African Americans with Alzheimer's disease. *J Alzheimers Dis* **2017,** *59*, 57-66.
33. Ferguson, S. A.; Varma, V.; Sloper, D.; Panos, J. J.; Sarkar, S., Increased inflammation in BA21 brain tissue from African Americans with Alzheimer’s disease. *Metab Brain Dis* **2020,** *35* (1), 121-133.

34. Kelchtermans, P.; Bittremieux, W.; De Grave, K.; Degroeve, S.; Ramon, J.; Laukens, K.; Valkenborg, D.; Barsnes, H.; Martens, L., Machine learning applications in proteomics research: How the past can boost the future. *PROTEOMICS* **2014,** *14* (4-5), 353-366.
35. Swan, A. L.; Mobasheri, A.; Allaway, D.; Liddell, S.; Bacardit, J., Application of machine learning to proteomics data: Classification and biomarker identification in postgenomics biology. *Omics* **2013,** *17* (12), 595-610.
36. Hua, D.; Desaire, H., Improved discrimination of disease states using proteomics data with the updated Aristotle Classifier. *J Proteome Res* **2021,** *20* (5), 2823-2829.
37. Khan, M. J.; Desaire, H.; Lopez, O. L.; Kamboh, M. I.; Robinson, R. A. S., Why inclusion matters for Alzheimer's disease biomarker discovery in plasma. *J Alzheimers Dis* **2021,** *79* (3), 1327-1344.
38. Chen, T.; Guestrin, C., XGBoost: A scalable tree boosting system. In *Proceedings of the 22nd ACM SIGKDD International Conference on Knowledge Discovery and Data Mining*, Association for Computing Machinery: San Francisco, California, USA, **2016**, 10.1145/2939672.2939785pp 785–794.
39. Boser, B. E.; Guyon, I. M.; Vapnik, V. N., A training algorithm for optimal margin classifiers. In *Proceedings of the Fifth Annual Workshop on Computational Learning Theory*, Association for Computing Machinery: Pittsburgh, Pennsylvania, USA, **1992**, 10.1145/130385.130401pp 144–152.
40. Hua, D.; Patabandige, M. W.; Go, E. P.; Desaire, H., The Aristotle Classifier: Using the whole glycomic profile to indicate a disease state. *Anal Chem* **2019,** *91* (17), 11070-11077.
41. Stamate, D.; Kim, M.; Proitsi, P.; Westwood, S.; Baird, A.; Nevado-Holgado, A.; Hye, A.; Bos, I.; Vos, S. J. B.; Vandenberghe, R., et al., A metabolite-based machine learning approach to diagnose Alzheimer-type dementia in blood: Results from the European Medical Information Framework for Alzheimer disease biomarker discovery cohort. *Alzheimers Dement* **2019,** *5*, 933-938.
42. Sun, X., Application and comparison of artificial neural networks and XGBoost on Alzheimer's disease. In *Proceedings of the 2021 International Conference on Bioinformatics and Intelligent Computing*, Association for Computing Machinery: Harbin, China, **2021**, 10.1145/3448748.3448765pp 101–105.
43. Akter, L.; Ferdib Al, I. In *Dementia identification for diagnosing Alzheimer's disease using XGBoost algorithm*, 2021 International Conference on Information and Communication Technology for Sustainable Development (ICICT4SD), 27-28 Feb. 2021; **2021**; pp 205-209.
44. AD Knowledge Portal. https://www.synapse.org/#!Synapse:syn21347564 (accessed 06/03/2021).
45. Viner, R.; Bomgarden, R.; Blank, M.; Rogers, J. *Increasing the multiplexing of protein quantitation from 6- to 10-plex with reporter ion isotopologues*; Thermo Scientific: **2013**.
46. Li, J.; Cai, Z.; Bomgarden, R. D.; Pike, I.; Kuhn, K.; Rogers, J. C.; Roberts, T. M.; Gygi, S. P.; Paulo, J. A., TMTpro-18plex: The expanded and complete set of TMTpro reagents for sample multiplexing. *J Proteome Res* **2021,** *20* (5), 2964-2972.
47. Robin, X.; Turck, N.; Hainard, A.; Tiberti, N.; Lisacek, F.; Sanchez, J.-C.; Müller, M. pROC: An open-source package for R and S+ to analyze and compare ROC curves. *BMC Bioinformatics* [Online], **2011**. https://doi.org/10.1186/1471-2105-12-77 (accessed 2011/03/17).
48. Mu, Y.; Gage, F. H. Adult hippocampal neurogenesis and its role in Alzheimer's disease. *Mol Neurodegener* [Online], **2011**. https://www.ncbi.nlm.nih.gov/pmc/articles/PMC3261815/pdf/1750-1326-6-85.pdf.

49. Xu, J.; Patassini, S.; Rustogi, N.; Riba-Garcia, I.; Hale, B. D.; Phillips, A. M.; Waldvogel, H.; Haines, R.; Bradbury, P.; Stevens, A., et al. Regional protein expression in human Alzheimer's brain correlates with disease severity. *Commun Biol* [Online], **2019**. https://www.nature.com/articles/s42003-018-0254-9.pdf.
50. Hondius, D. C.; van Nierop, P.; Li, K. W.; Hoozemans, J. J. M.; van der Schors, R. C.; van Haastert, E. S.; van der Vies, S. M.; Rozemuller, A. J. M.; Smit, A. B., Profiling the human hippocampal proteome at all pathologic stages of Alzheimer's disease. *Alzheimers Dement* **2016,** *12* (6), 654-668.
51. Smith, A. D., Imaging the progression of Alzheimer pathology through the brain. *Proc Natl Acad Sci U S A* **2002,** *99* (7), 4135-4137.
52. Scahill, R. I.; Schott, J. M.; Stevens, J. M.; Rossor, M. N.; Fox, N. C., Mapping the evolution of regional atrophy in Alzheimer's disease: unbiased analysis of fluid-registered serial MRI. *Proc Natl Acad Sci U S A* **2002,** *99* (7), 4703-4707.
53. Zahid, S.; Oellerich, M.; Asif, A. R.; Ahmed, N., Differential expression of proteins in brain regions of Alzheimer's disease patients. *Neurochem Res* **2014,** *39* (1), 208-215.
54. Schrotter, A.; Oberhaus, A.; Kolbe, K.; Seger, S.; Mastalski, T.; El Magraoui, F.; Hoffmann-Posorske, E.; Bohnert, M.; Deckert, J.; Braun, C., et al., LMD proteomics provides evidence for hippocampus field-specific motor protein abundance changes with relevance to Alzheimer's disease. *Biochim Biophys Acta, Proteins Proteomics* **2017,** *1865* (6), 703-714.
55. O'Connor, A. R.; Han, S.; Dobbins, I. G., The inferior parietal lobule and recognition memory: Expectancy violation or successful retrieval? *J Neurosci* **2010,** *30* (8), 2924-2934.
56. Alain, C.; He, Y.; Grady, C., The contribution of the inferior parietal lobe to auditory spatial working memory. *J Cogn Neurosci* **2008,** *20* (2), 285-295.
57. Igelström, K. M.; Graziano, M. S. A., The inferior parietal lobule and temporoparietal junction: A network perspective. *Neuropsychologia* **2017,** *105*, 70-83.
58. Friedman, H.; Goldman-Rakic, P., Coactivation of prefrontal cortex and inferior parietal cortex in working memory tasks revealed by 2DG functional mapping in the rhesus monkey. *J Neurosci* **1994,** *14* (5), 2775-2788.
59. Markesbery, W. R.; Schmitt, F. A.; Kryscio, R. J.; Davis, D. G.; Smith, C. D.; Wekstein, D. R., Neuropathologic substrate of mild cognitive impairment. *Arch Neurol* **2006,** *63* (1), 38-46.
60. Nelson, P. T.; Abner, E. L.; Scheff, S. W.; Schmitt, F. A.; Kryscio, R. J.; Jicha, G. A.; Smith, C. D.; Patel, E.; Markesbery, W. R., Alzheimer's-type neuropathology in the precuneus is not increased relative to other areas of neocortex across a range of cognitive impairment. *Neurosci Lett* **2009,** *450* (3), 336-339.
61. Köhler, S.; Black, S. E.; Sinden, M.; Szekely, C.; Kidron, D.; Parker, J. L.; Foster, J. K.; Moscovitch, M.; Winocour, G.; Szalai, J. P., et al., Memory impairments associated with hippocampal versus parahippocampal-gyrus atrophy: an MR volumetry study in Alzheimer's disease. *Neuropsychologia* **1998,** *36* (9), 901-914.
62. LaFlamme, E. M.; Waguespack, H. F.; Forcelli, P. A.; Malkova, L., The parahippocampal cortex and its functional connection with the hippocampus are critical for nonnavigational spatial memory in macaques. *Cereb* **2020,** *31* (4), 2251-2267.
63. Higginbotham, L.; Ping, L.; Dammer, E. B.; Duong, D. M.; Zhou, M.; Gearing, M.; Hurst, C.; Glass, J. D.; Factor, S. A.; Johnson, E. C. B., et al., Integrated proteomics reveals brain-based cerebrospinal fluid biomarkers in asymptomatic and symptomatic Alzheimer's disease. *Sci Adv* **2020,** *6* (43).

CHAPTER 6

Conclusions & Future Directions

6.1 Conclusions

In this dissertation, proteomics techniques were applied in a human cell line and postmortem brain tissue to study racial disparities in Alzheimer's disease (AD), specifically in African American/Black adults. In **Chapter 2**, we used discovery-based proteomics to investigate the impact of a mutation in the phospholipid-transporting ATPase ABCA7 (*ABCA7*) gene that is associated with AD risk in African American/Black adults. An empty vector, wild-type ABCA7, and *ABCA7* variant rs3752232, which encodes a threonine to alanine substitution at amino acid 319 (T319A), were expressed in human embryonic kidney (HEK) 293 cells and analyzed using proteomics, in order to determine the impact of this mutation on the cellular proteome. The results from our proteomics experiments, in combination with other structural and localization analyses, show that the T319A mutation has subtle structural and downstream proteomic effects and highlight the importance of such studies for understanding the functional impacts of genetic variants associated with AD.

In **Chapters 3-4**, we used discovery-based proteomics to study postmortem brain tissue from African American/Black and non-Hispanic White adults who were cognitively normal (CN) or diagnosed with AD. Our analysis of three brain regions (hippocampus, inferior parietal lobule (IPL), and globus pallidus (GP)) from a pilot cohort in **Chapter 3** revealed that proteomic changes in AD were mostly brain region-specific. Many novel protein changes in AD were identified as these studies included IPL and GP regions, about which previous studies have been

limited. Furthermore, racial background was significantly associated with protein levels for a smaller subset of proteins that were differentially expressed in AD in at least one racial group. This pilot study highlights the need to include diverse groups in AD research to better understand AD pathogenesis at the molecular level. To further investigate these changes in a slightly larger cohort, we utilized an improved discovery-based proteomics workflow in **Chapter 4** in a second, independent biracial cohort to analyze the IPL region. Analytical improvements in our proteomics analysis of this cohort yielded approximately four times the brain proteome coverage compared to the analysis in **Chapter 3**. We also identified many novel differentially-expressed proteins in AD in this study, likely related to the cohort diversity and prior proteomics studies of this region being few. As in **Chapter 3**, we observed a subset of proteins significantly associated with race and diagnosis of AD and race-specific patterns of change, most of which were unique to this cohort. Importantly, we found that covariates beyond race such as education are also associated with protein changes in AD, highlighting the importance of diversity across racial background and other factors in future studies of AD. In **Chapter 5**, machine learning was used across existing brain proteomics datasets, containing mostly non-Hispanic White adults, to test whether a small subset of proteins that best distinguished AD and CN groups in non-Hispanic White adults performed as well in a diverse cohort described in **Chapter 3**. These analyses showed that the selected proteins were able to differentiate between AD and CN groups across cohorts and brain regions, although with inconsistencies in performance outcomes across racial groups that require additional investigation. Taken together, this dissertation work emphasizes that diversity and inclusion in all types of AD studies is essential to further understand the disease at the molecular level and to particularly further our understanding of racial disparities.

6.2 Future Directions

6.2.1 Studying genetic risk factors in AD

In **Chapter 2** of this dissertation, we described the structural and functional impact of an *ABCA7* mutation associated with African American/Black adults in a HEK 293 cell model system, which provided insight into general downstream effects of this mutation in cells. Further study of this mutation in other cell models that may be more representative of the brain environment such as neuronal cell lines and under conditions similar to AD (i.e., in the presence and absence of amyloid-beta (Aβ) peptides) can provide additional information specific to brain that may be more informative for AD pathogenesis. Furthermore, a recent study developed induced pluripotent stem cells from the blood of African American/Black adults with AD that had an *ABCA7* mutation and from matched CN individuals, which were then differentiated into cortical neurons and microglia.[1-2] This strategy provided insights into the effects of this mutation in a cell model specifically with African American/Black background in AD, and allowed the impact of this mutation on Aβ production in neurons and on Aβ clearance and phagocytic functions in microglia to be probed, a benefit of producing both neurons and microglia from the iPSCs. A similar approach could be valuable to study the T319A variant since this variant is also particularly associated with AD risk in African American/Black adults.

Our findings also suggest the importance of monitoring lipid levels in future studies of this *ABCA7* variant, specifically phosphatidylinositol (4,5)-bisphosphate (PIP_2) and other lipids in the PIP_2 pathway such as phosphatidylinositol 5-phosphate (PI5P) and diacylglycerol (see **Chapter 2 Figure 2.10**). Potential differences in the PIP_2 pathway between wild-type ABCA7 and the T319A variant were implicated by both structural and proteomics analyses. These lipid

levels could be measured using either targeted or untargeted lipidomics approaches, both of which are effective to measure these lipid classes as shown by our laboratory previously.[3] Lipidomics approaches would complement proteomics analyses and be useful to determine if ABCA7's lipid metabolism and transport functions are affected by this mutation. These types of studies are also necessary to determine the downstream impact of other *ABCA7* mutations at the molecular level that may contribute to AD risk in African American/Black adults and to racial disparities in AD.

6.2.2 Racial disparities and the AD brain

In **Chapters 3-4** of this dissertation, discovery-based proteomics was applied to study postmortem brain tissue in diverse cohorts composed of African American/Black and non-Hispanic White adults who were CN or whom had AD. From these studies, we identified groups of differentially-expressed proteins in AD and additional subsets of proteins that had race-specific changes in AD. Further proteomic characterization of AD brain across larger diverse cohorts is necessary to determine whether the protein changes observed in these initial analyses are robust and generalizable to other cohorts. Increased sample sizes are required to account for differences in demographic factors such as education and comorbidities that may differ across sample groups. In our studies, there were differences across groups that we could not account for due to the limited statistical power of our small sample sizes, which could impact the protein differences observed across groups in AD. We showed in **Chapter 4** that covariates such as education (measured by years of education) and body mass index (BMI) were associated with protein changes in AD in a subset of proteins. Others have shown that accounting for measures of education quality attenuated racial differences in cognitive performance between African

American/Black and non-Hispanic White adults, beyond accounting for years of education.[4-6] In addition to education quality, early-life measures of socioeconomic status[7] and education,[8] parental education levels,[9] and measures related to lifetime experience of stress and adversity[10-11] may additionally contribute to racial differences and should be considered across groups. Including covariates such as these that may differ across groups will be important when determining differentially-expressed proteins in future studies to ensure that the identified proteomic differences in AD are robust and reproducible across cohorts.

Studies that focus on characterizing proteomic changes in AD solely within African American/Black groups could be valuable to further understanding of AD pathogenesis within this racial group. Though comparison studies between African American/Black and non-Hispanic White adults can be informative, they do not consider the variability within either group and can be limited in statistical power when the number of samples is not the same across groups.[12] Characterization of proteomic changes in AD across multiple brain regions in African American/Black adults would be extremely beneficial to provide insight into molecular changes in AD brain. Previous studies have inconsistently observed neuropathological differences including white matter hyperintensities, Lewy bodies, and presentation of AD in combination with these pathologies between African American/Black and non-Hispanic White adults across different cohorts.[13-18] These findings suggest that heterogeneity in AD-related changes within racial groups may affect observed differences across groups and highlight the importance of investigations focusing within a specific racial group. Additional brain regions of interest for future studies include middle temporal gyrus (Brodmann area 21), which is involved in language, semantic memory processing, and visual perception including facial recognition. Racial differences in markers of inflammation and neurodegeneration have been previously identified in

this brain region using immunoassays,[19-20] suggesting that analysis of this brain region using discovery-based proteomics could reveal other proteins with different changes in AD across racial groups. The dorsolateral prefrontal cortex (DLPFC) could also be interesting to study given its roles in executive functions such as working memory and decision making, which are affected later in AD. Furthermore, the DLPFC has been shown to be affected by severe stress,[21] relating this brain region to some of the psychosocial factors that contribute to racial disparities in AD, particularly among African American/Black adults.[22-25]

By comprehensively characterizing proteomic changes across multiple brain regions in African American/Black adults, this ideal study would advance understanding of molecular contributions to AD risk in African American/Black adults and racial disparities. The findings from this study could later be compared to the plentiful existing research in primarily non-Hispanic White adults. It is important to note that the work throughout this dissertation has focused on AD risk in African American/Black adults, but characterization of molecular changes within other racial groups that have been underrepresented in AD research, such as individuals of various Hispanic/Latino, Asian, and Native American backgrounds,[26-29] are also necessary for more complete understanding of AD pathogenesis across the entire population.

Machine learning can be used to evaluate classification of AD and CN individuals across racial groups using data derived from AD brain proteomics datasets. In **Chapter 5**, we have demonstrated that brain proteins that distinguish AD and CN groups in proteomics datasets containing mostly non-Hispanic White participants were also able to classify these groups in a more diverse cohort, our dataset from **Chapter 3**. We also observed that classification was not consistent across racial groups, likely due to the small sample size and relatively low number of proteins identified in the test dataset from **Chapter 3**, which may have limited the protein

features that were identified during the feature selection step. Therefore, testing machine learning model performance on additional diverse datasets will be important to determine whether the trends observed in our initial machine learning analyses are consistent and generalizable across cohorts. The dataset from **Chapter 4** is currently the only additional brain proteomics dataset from a diverse cohort to our knowledge that could be incorporated as an additional test dataset. In the future, our laboratory will also be analyzing other brain regions from the same cohort, which could be useful for machine learning analyses as well, given our results showing successful classification of AD and CN groups across brain regions.

Furthermore, it will also be important to understand whether protein changes in AD brain are associated with other factors contributing to racial disparities. Molecular differences in plasma proteins have been previously identified between African American/Black and non-Hispanic White adults that may be related to allostatic load, to which various psychosocial risk factors contribute (**Chapter 1 Section 1.1.1**). Connections between the small groups of proteins with significant race x diagnosis interactions and race-specific changes in AD identified in **Chapters 3-4** and other contributors to racial disparities could be investigated. Factors of interest that have been previously implicated in racial disparities include education, comorbidities including hypertension and diabetes, and BMI. Furthermore, including the additional factors that have been linked to AD risk in African American/Black adults beyond simply years of education would also be important in such studies where this information is available, as discussed above. Analyses such as these could identify potential links between different contributors to racial disparities, i.e. between molecular contributors and comorbidity or socioeconomic contributors.

Finally, all of the studies described in **Chapters 3-5** of this dissertation have used proteomics to understand the impact of AD in postmortem brain tissue. While these studies are

important to fundamental understanding of AD pathogenesis, particularly given that proteomic changes within various racial groups and brain regions in AD have not yet been well characterized, the eventual translation of findings from these studies into more accessible biological samples such as cerebrospinal fluid (CSF), plasma, or urine that can be analyzed antemortem would be essential for clinical relevance. Measuring potential target brain proteins from these studies would be particularly useful in CSF given the ability of CSF to provide information about conditions in the brain. Racial differences in various tau[17, 30-32] and other[33-34] markers have also been recently reported, suggesting the potential utility in this biofluid for further investigation of racial disparities. However, acquiring CSF from diverse cohorts has known obstacles stemming from fear and negative perceptions of the lumbar puncture procedure and potential adverse effects, historical mistreatment in research, and mistrust of the research community.[35-36] Various research centers have been working to overcome these barriers and increase diverse representation in CSF sample collection for these studies through community relationships, education, and communication,[37] which have successfully more than doubled the rates of CSF donation amongst diverse participants in some cases.[38]

6.3 References

1. Cukier, H. N.; Mehta, N.; Ramirez, J.; Rolati, S.; Whitehead, P. L.; Adams, L. D.; Celis, K.; Carney, R.; Vance, J. M.; Cuccaro, M. L., et al., Patient-derived iPSC model of an *ABCA7* frameshift deletion associated with Alzheimer's disease in African Americans. *Alzheimers Dement* **2017,** *13* (7), P650.
2. Cukier, H. N.; Laverde-Paz, J.; Ramirez, J.; Adams, L. D.; Starks, T. D.; Vance, J. M.; Cuccaro, M. L.; Blurton-Jones, M.; Haines, J. L.; Byrd, G. S., et al. iPSC-derived neurons and microglia with an African-specific ABCA7 frameshift deletion have impaired function. *Alzheimers Dement* [Online], **2020**. https://alz-journals.onlinelibrary.wiley.com/doi/abs/10.1002/alz.046109.
3. Khan, M. J.; Codreanu, S. G.; Goyal, S.; Wages, P. A.; Gorti, S. K. K.; Pearson, M. J.; Uribe, I.; Sherrod, S. D.; McLean, J. A.; Porter, N. A., et al. Evaluating a targeted multiple reaction monitoring approach to global untargeted lipidomic analyses of human plasma. *Rapid*

Commun Mass Spectrom [Online], **2020**. PubMed. http://europepmc.org/abstract/MED/32738001.
4. Chin, A. L.; Negash, S.; Xie, S.; Arnold, S. E.; Hamilton, R., Quality, and not just quantity, of education accounts for differences in psychometric performance between African Americans and White Non-Hispanics with Alzheimer's disease. *J Int Neuropsychol Soc* **2012,** *18* (2), 277-285.
5. Manly, J. J.; Jacobs, D. M.; Sano, M.; Bell, K.; Merchant, C. A.; Small, S. A.; Stern, Y., Cognitive test performance among nondemented elderly African Americans and whites. *Neurology* **1998,** *50* (5), 1238-1245.
6. Fyffe, D. C.; Mukherjee, S.; Barnes, L. L.; Manly, J. J.; Bennett, D. A.; Crane, P. K., Explaining differences in episodic memory performance among older African Americans and Whites: The roles of factors related to cognitive reserve and test bias. *J Int Neuropsychol Soc* **2011,** *17* (4), 625-638.
7. Wilson, R. S.; Scherr, P. A.; Hoganson, G.; Bienias, J. L.; Evans, D. A.; Bennett, D. A., Early life socioeconomic status and late life risk of Alzheimer's disease. *Neuroepidemiology* **2005,** *25* (1), 8-14.
8. Sisco, S.; Gross, A. L.; Shih, R. A.; Sachs, B. C.; Glymour, M. M.; Bangen, K. J.; Benitez, A.; Skinner, J.; Schneider, B. C.; Manly, J. J., The role of early-life educational quality and literacy in explaining racial disparities in cognition in late life. *J Gerontol B Psychol Sci Soc Sci* **2015,** *70* (4), 557-567.
9. Melrose, R. J.; Brewster, P.; Marquine, M. J.; MacKay-Brandt, A.; Reed, B.; Farias, S. T.; Mungas, D., Early life development in a multiethnic sample and the relation to late life cognition. *J Gerontol B Psychol Sci Soc Sci* **2015,** *70* (4), 519-531.
10. Barnes, L. L.; Wilson, R. S.; Mendes de Leon, C. F.; Bennett, D. A., The relation of lifetime cognitive activity and lifetime access to resources to late-life cognitive function in older African Americans. *Neuropsychol Dev Cogn B Aging Neuropsychol Cogn* **2006,** *13* (3-4), 516-528.
11. Barnes, L. L.; Wilson, R. S.; Everson-Rose, S. A.; Hayward, M. D.; Evans, D. A.; Mendes de Leon, C. F., Effects of early-life adversity on cognitive decline in older African Americans and whites. *Neurology* **2012,** *79* (24), 2321-2327.
12. Whitfield, K. E.; Allaire, J. C.; Belue, R.; Edwards, C. L., Are comparisons the answer to understanding behavioral aspects of aging in racial and ethnic groups? *J Gerontol B Psychol Sci Soc Sci* **2008,** *63* (5), P301-P308.
13. Barnes, L. L.; Leurgans, S.; Aggarwal, N. T.; Shah, R. C.; Arvanitakis, Z.; James, B. D.; Buchman, A. S.; Bennett, D. A.; Schneider, J. A., Mixed pathology is more likely in black than white decedents with Alzheimer dementia. *Neurology* **2015,** *85* (6), 528-534.
14. Graff-Radford, N. R.; Besser, L. M.; Crook, J. E.; Kukull, W. A.; Dickson, D. W., Neuropathological differences by race from the National Alzheimer's Coordinating Center. *Alzheimers Dement* **2016,** *12* (6), 669-677.
15. Gottesman, R. F.; Fornage, M.; Knopman, D. S.; Mosley, T. H., Brain aging in African-Americans: the Atherosclerosis Risk in Communities (ARIC) experience. *Curr Alzheimer Res* **2015,** *12* (7), 607-613.
16. Brickman, A. M.; Schupf, N.; Manly, J. J.; Luchsinger, J. A.; Andrews, H.; Tang, M. X.; Reitz, C.; Small, S. A.; Mayeux, R.; DeCarli, C., et al., Brain morphology in older African Americans, Caribbean Hispanics, and whites from northern Manhattan. *Arch Neurol* **2008,** *65* (8), 1053-61.

17. Morris, J. C.; Schindler, S. E.; McCue, L. M.; Moulder, K. L.; Benzinger, T. L. S.; Cruchaga, C.; Fagan, A. M.; Grant, E.; Gordon, B. A.; Holtzman, D. M., et al., Assessment of racial disparities in biomarkers for Alzheimer disease. *JAMA Neurol* **2019,** *76* (3), 264-273.
18. Barnes, L. L., Biomarkers for Alzheimer dementia in diverse racial and ethnic minorities—a public health priority. *JAMA Neurol* **2019,** *76* (3), 251-253.
19. Ferguson, S. A.; Panos, J. J.; Sloper, D.; Varma, V., Neurodegenerative markers are increased in postmortem BA21 tissue from African Americans with Alzheimer's disease. *J Alzheimers Dis* **2017,** *59*, 57-66.
20. Ferguson, S. A.; Varma, V.; Sloper, D.; Panos, J. J.; Sarkar, S., Increased inflammation in BA21 brain tissue from African Americans with Alzheimer's disease. *Metab Brain Dis* **2020,** *35* (1), 121-133.
21. Qin, S.; Hermans, E. J.; van Marle, H. J. F.; Luo, J.; Fernández, G., Acute psychological stress reduces working memory-related activity in the dorsolateral prefrontal cortex. *Biol Psychiatry* **2009,** *66* (1), 25-32.
22. Wilkins, C. H.; Schindler, S. E.; Morris, J. C., Addressing health disparities among minority populations: Why clinical trial recruitment is not enough. *JAMA Neurol* **2020,** *77* (9), 1063-1064.
23. Chen, R.; Weuve, J.; Misra, S.; Cuevas, A.; Kubzansky, L. D.; Williams, D. R., Racial disparities in cognitive function among middle-aged and older adults: the roles of cumulative stress exposures across the life course. *J Gerontol A* **2021**, 10.1093/gerona/glab099.
24. Trammell, A. R.; McDaniel, D. J.; Obideen, M.; Okafor, M.; Thomas, T. L.; Goldstein, F. C.; Shaw, L. M.; Hajjar, I. M., Perceived stress is associated with Alzheimer's disease cerebrospinal fluid biomarkers in African Americans with mild cognitive impairment. *J Alzheimers Dis* **2020,** *77*, 843-853.
25. Geronimus, A. T.; Hicken, M.; Keene, D.; Bound, J., "Weathering" and age patterns of allostatic load scores among blacks and whites in the United States. *Am J Public Health* **2006,** *96* (5), 826-833.
26. Gilmore-Bykovskyi, A. L.; Jin, Y.; Gleason, C.; Flowers-Benton, S.; Block, L. M.; Dilworth-Anderson, P.; Barnes, L. L.; Shah, M. N.; Zuelsdorff, M., Recruitment and retention of underrepresented populations in Alzheimer's disease research: A systematic review. *Alzheimers Dement (N Y)* **2019,** *5*, 751-770.
27. Raman, R.; Quiroz, Y. T.; Langford, O.; Choi, J.; Ritchie, M.; Baumgartner, M.; Rentz, D.; Aggarwal, N. T.; Aisen, P.; Sperling, R., et al. Disparities by race and ethnicity among adults recruited for a preclinical Alzheimer disease trial. *JAMA Netw Open* [Online], **2021**. https://doi.org/10.1001/jamanetworkopen.2021.14364.
28. Olson, N. L.; Albensi, B. C., Race- and sex-based disparities in Alzheimer's disease clinical trial enrollment in the United States and Canada: An indigenous perspective. *J Alzheimers Dis Rep* **2020,** *4*, 325-344.
29. Manly, J. J.; Gilmore-Bykovskyi, A.; Deters, K. D. Inclusion of underrepresented groups in preclinical Alzheimer disease trials—Opportunities abound. *JAMA Netw Open* [Online], **2021**. https://doi.org/10.1001/jamanetworkopen.2021.14606.
30. Howell, J. C.; Watts, K. D.; Parker, M. W.; Wu, J.; Kollhoff, A.; Wingo, T. S.; Dorbin, C. D.; Qiu, D.; Hu, W. T. Race modifies the relationship between cognition and Alzheimer's disease cerebrospinal fluid biomarkers. *Alzheimers Res Ther* [Online], **2017**. https://doi.org/10.1186/s13195-017-0315-1.

31. Garrett, S. L.; McDaniel, D.; Obideen, M.; Trammell, A. R.; Shaw, L. M.; Goldstein, F. C.; Hajjar, I. Racial disparity in cerebrospinal fluid amyloid and tau biomarkers and associated cutoffs for mild cognitive impairment. *JAMA Netw Open* [Online], **2019**. https://doi.org/10.1001/jamanetworkopen.2019.17363.
32. Chaudhry, A.; Rizig, M. Comparing fluid biomarkers of Alzheimer's disease between African American or Black African and white groups: A systematic review and meta-analysis. *J Neurol Sci* [Online], **2021**. https://www.sciencedirect.com/science/article/pii/S0022510X20306067?via%3Dihub.
33. Wharton, W.; Kollhoff, A. L.; Gangishetti, U.; Verble, D. D.; Upadhya, S.; Zetterberg, H.; Kumar, V.; Watts, K. D.; Kippels, A. J.; Gearing, M., et al., Interleukin 9 alterations linked to Alzheimer disease in African Americans. *Ann Neurol* **2019,** *86*, 407-418.
34. Schindler, S. E.; Cruchaga, C.; Joseph, A.; McCue, L.; Farias, F. H. G.; Wilkins, C. H.; Deming, Y.; Henson, R. L.; Mikesell, R. J.; Piccio, L., et al. African Americans have differences in CSF soluble TREM2 and associated genetic variants. *Neurol Genet* [Online], **2021**. https://ng.neurology.org/content/nng/7/2/e571.full.pdf.
35. Howell, J. C.; Parker, M. W.; Watts, K. D.; Kollhoff, A.; Tsvetkova, D. Z.; Hu, W. T. Research lumbar punctures among African Americans and Caucasians: Perception predicts experience. *Front Aging Neurosci* [Online], **2016**. https://www.ncbi.nlm.nih.gov/pmc/articles/PMC5133251/pdf/fnagi-08-00296.pdf.
36. Blazel, M. M.; Lazar, K. K.; Van Hulle, C. A.; Ma, Y.; Cole, A.; Spalitta, A.; Davenport-Sis, N.; Bendlin, B. B.; Wahoske, M.; Illingworth, C., et al., Factors associated with lumbar puncture participation in Alzheimer's disease research. *J Alzheimers Dis* **2020,** *77*, 1559-1567.
37. Williams, M. M.; Scharff, D. P.; Mathews, K. J.; Hoffsuemmer, J. S.; Jackson, P.; Morris, J. C.; Edwards, D. F., Barriers and facilitators of African American participation in Alzheimer disease biomarker research. *Alzheimer Dis Assoc Disord* **2010,** *24 Suppl* (Suppl), S24-S29.
38. Williams, M. M.; Meisel, M. M.; Williams, J.; Morris, J. C., An interdisciplinary outreach model of African American recruitment for Alzheimer's disease research. *Gerontologist* **2011,** *51* (Suppl 1), S134-S141.

APPENDIX A

References for Adaptation of Chapters

Chapters published in this dissertation were previously published in the following articles:

Chapter 1. **Stepler, K. E.** and Robinson, R. A. S. The potential of 'omics to link lipid metabolism and genetic and comorbidity risk factors of Alzheimer's disease in African Americans. *In Reviews on Biomarker Studies in Psychiatric and Neurodegenerative Disorders*, Guest, P. C., Ed. Springer International Publishing: Cham, **2019**; Vol. 1118, pp 1-28.

Chapter 3. **Stepler, K. E.**; Mahoney, E. R.; Kofler, J.; Hohman, T. J.; Lopez, O. L.; Robinson, R. A. S. Inclusion of African American/Black adults in a pilot brain proteomics study of Alzheimer's disease, *Neurobiol. Dis*. **2020**, 146, doi: 10.1016/j.nbd.2020.105129.

APPENDIX B

Supplementary Information for Chapter 2

Data B2.1. Processing of proteomics data. This appendix data file can be accessed in the supplementary material in the online version of this dissertation, in the Excel file Supplementary Data B2.1.

Table B2.1. TMT^{10}-plex channel assignments.

TMT Channel	Sample
126	WT1
127N	T319A1
127C	EV1
128N	WT2
128C	--
129N	Pool
129C	--
130N	--
130C	T319A2
131	EV2

Table B2.2. Differentially-expressed proteins in EV, WT, and T319A cells.

Accession Number[a]	Protein Name	PSMs	Average Reporter Ion Intensities[b]			EV vs. WT		EV vs. T319A		WT vs. T319A	
			EV	WT	T319A	WT/EV[c]	p-Value[d]	T319A/EV[c]	p-Value[d]	T319A/ WT[c]	p-Value[d]
O00469	Procollagen-lysine,2-oxoglutarate 5-dioxygenase 2	7	265814	389082	299772	**1.46**	**0.040**	1.13	0.29	**0.77**	0.085
O00541	Pescadillo homolog	39	2171222	2631201	2108376	**1.21**	**0.046**	0.97	0.60	**0.80**	**0.017**
O14654	Insulin receptor substrate 4	180	28387952	34213935	27727388	1.21	**0.0079**	0.98	0.34	**0.81**	**0.0012**
O14879	Interferon-induced protein with tetratricopeptide repeats 3	234	19248458	50355833	22066102	**2.62**	**0.0029**	1.15	**0.045**	**0.44**	**0.0031**
O14933	Ubiquitin/ISG15-conjugating enzyme E2 L6	9	524824	1180179	526361	**2.25**	**0.0077**	1.00	0.97	**0.45**	**0.010**
O15162	Phospholipid scramblase 1	6	374079	506902	399412	**1.36**	0.065	1.07	0.54	**0.79**	**0.012**
O15182	Centrin-3	7	424335	541574	415666	**1.28**	**0.0079**	0.98	0.68	**0.77**	**0.015**
O43617	Trafficking protein particle complex subunit 3	52	2534455	3102133	2533517	**1.22**	**0.0090**	1.00	0.99	**0.82**	**0.0019**
O60637	Tetraspanin-3	34	24339138	31591470	24414275	**1.30**	**0.010**	1.00	0.75	**0.77**	**0.010**
O60828	Polyglutamine-binding protein 1	10	3926191	4974132	4149268	**1.27**	**0.0079**	1.06	0.076	0.83	**0.0076**
O75475	PC4 and SFRS1-interacting protein	193	28982143	23639192	23291462	**0.82**	**0.039**	**0.80**	0.072	**0.81**	0.99
O75794	Cell division cycle protein 123 homolog	8	952422	1557067	1204876	**1.63**	**0.00067**	**1.27**	**0.0086**	**0.77**	**0.0060**
O76071	Probable cytosolic iron-sulfur protein assembly protein CIAO1	8	480583	585078	482474	**1.22**	**0.013**	1.00	0.94	**0.82**	0.050
O95786	Antiviral innate immune response receptor RIG-I	72	2384191	4658088	2504299	**1.95**	**0.0035**	1.05	0.41	**0.54**	**0.0037**
P01889	HLA class I histocompatibility antigen, B alpha chain	69	2680576	3710899	2978494	**1.38**	**0.043**	1.11	0.31	**0.80**	0.059

Table B2.2 (continued)

P03243	E1B 55 kDa protein	579	258997818	183743720	258429462	**0.71**	0.10	1.00	0.99	**1.41**	**0.030**
P04439	HLA class I histocompatibility antigen, A alpha chain	74	8595346	14821952	9156932	**1.72**	**0.0050**	1.07	0.18	**0.62**	**0.0040**
P04818	Thymidylate synthase	22	1586050	2271072	1660072	**1.43**	**0.011**	1.05	0.15	**0.73**	**0.011**
P05161	Ubiquitin-like protein ISG15	172	52229448	95983145	56403357	**1.84**	**0.011**	1.08	0.28	**0.59**	**0.0081**
P07951	Tropomyosin beta chain	505	2594274	2124258	2617818	**0.82**	**0.014**	1.01	0.87	**1.23**	0.058
P08243	Asparagine synthetase [glutamine-hydrolyzing]	168	15203035	19774300	16493136	**1.30**	**0.00036**	1.08	**0.0015**	0.83	**0.00066**
P08962	CD63 antigen	34	13608045	18694789	14152063	**1.37**	**0.0086**	1.04	0.073	**0.76**	**0.011**
P09104	Gamma-enolase	474	5638356	6529154	5289904	1.16	0.061	0.94	0.25	**0.81**	**0.022**
P09543	2',3'-cyclic-nucleotide 3'-phosphodiesterase	146	11852881	14567803	12113051	**1.23**	**0.028**	1.02	0.38	0.83	**0.030**
P09651	Heterogeneous nuclear ribonucleoprotein A1	932	236020846	195272768	209214914	**0.83**	**0.0044**	0.89	**0.012**	1.07	**0.037**
P09913	Interferon-induced protein with tetratricopeptide repeats 2	174	10635851	34695976	11771546	**3.26**	**0.0025**	1.11	0.094	**0.34**	**0.0025**
P09914	Interferon-induced protein with tetratricopeptide repeats 1	193	14445646	40948534	16869138	**2.83**	**0.0020**	1.17	**0.041**	**0.41**	**0.0019**
P0DJ07	Protein PET100 homolog, mitochondrial	2	630796	783705	662707	**1.24**	**0.014**	1.05	0.53	0.85	0.12
P10109	Adrenodoxin, mitochondrial	18	1612254	1957764	1694816	**1.21**	**0.0071**	1.05	0.13	0.87	**0.011**
P10321	HLA class I histocompatibility antigen, C alpha chain	84	877612	1421364	971409	**1.62**	**0.0026**	1.11	**0.010**	**0.68**	**0.0036**
P12004	Proliferating cell nuclear antigen	477	185111671	293525308	214313786	**1.59**	**0.015**	1.16	**0.031**	**0.73**	**0.025**
P13987	CD59 glycoprotein	10	1892139	2422236	2037805	**1.28**	**0.016**	1.08	0.23	0.84	0.071

Table B2.2 (continued)

P15104	Glutamine synthetase	16	817208	1191254	812672	**1.46**	**0.011**	0.99	0.30	**0.68**	**0.011**
P15880	40S ribosomal protein S2	639	369526710	459991009	406236394	**1.24**	**0.010**	1.10	**0.009**	0.88	**0.026**
P15924	Desmoplakin	125	4726920	5941083	4610970	**1.26**	**0.039**	0.98	0.65	**0.78**	**0.019**
P16278	Beta-galactosidase	23	1589877	1963570	1585157	**1.24**	0.10	1.00	0.97	**0.81**	**0.015**
P16401	Histone H1.5	419	506167	1046421	460562	**2.07**	**0.00057**	0.91	0.16	**0.44**	**0.0011**
P18077	60S ribosomal protein L35a	239	121951663	160286542	130745603	**1.31**	**0.00066**	1.07	0.20	**0.82**	**0.024**
P18124	60S ribosomal protein L7	585	340933976	448112827	376586380	**1.31**	**0.0012**	1.10	**0.050**	0.84	**0.013**
P18621	60S ribosomal protein L17	420	263549253	332748724	281819668	**1.26**	**0.0033**	1.07	0.082	0.85	**0.016**
P19474	E3 ubiquitin-protein ligase TRIM21	26	519348	730076	549655	**1.41**	**0.017**	1.06	0.30	**0.75**	**0.025**
P19525	Interferon-induced, double-stranded RNA-activated protein kinase	163	7415881	10089692	7521380	**1.36**	**0.00060**	1.01	0.27	**0.75**	**0.00010**
P20591	Interferon-induced GTP-binding protein Mx1	102	6093209	14933945	6048078	**2.45**	**0.0014**	0.99	0.91	**0.40**	**0.0010**
P21333	Filamin-A	5063	2090337170	1819658970	2214552673	0.87	**0.024**	1.06	0.10	**1.22**	**0.0043**
P22626	Heterogeneous nuclear ribonucleoproteins A2/B1	1218	1352258335	1085170565	1203983296	**0.80**	**0.033**	0.89	**0.0059**	1.05	0.067
P23381	Tryptophan--tRNA ligase, cytoplasmic	300	36996826	63207811	37116679	**1.71**	**0.0019**	1.00	0.90	**0.59**	**0.0010**
P23396	40S ribosomal protein S3	1128	447090494	586702039	490781900	**1.31**	**0.0017**	1.10	**0.042**	0.84	**0.0094**
P23921	Ribonucleoside-diphosphate reductase large subunit	193	12119415	15596485	12360616	**1.29**	**0.019**	1.02	0.34	**0.79**	**0.021**
P24666	Low molecular weight phosphotyrosine protein phosphatase	68	9820670	12756708	9561422	**1.30**	**0.0015**	0.97	0.22	**0.75**	**0.0015**
P26373	60S ribosomal protein L13	375	251306589	333604607	272568144	**1.33**	**0.0050**	1.08	0.11	**0.82**	**0.015**

Table B2.2 (continued)

P28340	DNA polymerase delta catalytic subunit	41	82002	96232	76108	1.17	0.12	0.93	0.24	**0.79**	**0.048**
P29590	Protein PML	57	4538625	7199023	4784243	**1.59**	**0.0091**	1.05	0.23	**0.66**	**0.011**
P29728	2'-5'-oligoadenylate synthase 2	31	1807021	3758712	1823134	**2.08**	**0.0018**	1.01	0.89	**0.49**	**0.0022**
P29966	Myristoylated alanine-rich C-kinase substrate	154	98139404	130907389	110078756	**1.33**	**0.016**	1.12	**0.013**	0.84	**0.037**
P30876	DNA-directed RNA polymerase II subunit RPB2	19	661046	823318	648326	**1.25**	**0.042**	0.98	0.55	**0.79**	**0.045**
P32189	Glycerol kinase	59	2739232	3069148	2530434	1.12	0.061	0.92	0.080	**0.82**	**0.027**
P33316	Deoxyuridine 5'-triphosphate nucleotidohydrolase, mitochondrial	131	20646992	25586800	21645617	**1.24**	**0.038**	1.05	0.45	0.85	**0.018**
P33552	Cyclin-dependent kinases regulatory subunit 2	7	1870701	2334140	1898740	**1.25**	**0.032**	1.01	0.76	**0.81**	0.058
P35221	Catenin alpha-1	155	6250780	7743999	6343272	**1.24**	**0.012**	1.01	0.59	**0.82**	**0.0075**
P36578	60S ribosomal protein L4	774	340826255	433556582	378988863	**1.27**	**0.0064**	1.11	**0.047**	0.87	**0.0085**
P37268	Squalene synthase	43	2302175	2808883	2495911	**1.22**	**0.018**	1.08	**0.044**	0.89	**0.044**
P39019	40S ribosomal protein S19	560	223755765	325625525	257475088	**1.46**	**0.00066**	1.15	**0.020**	**0.79**	**0.0054**
P40429	60S ribosomal protein L13a	379	138923747	180454754	151873954	**1.30**	**0.00091**	1.09	**0.034**	0.84	**0.0091**
P40763	Signal transducer and activator of transcription 3	18	624201	897003	671953	**1.44**	**0.013**	1.08	0.20	**0.75**	**0.012**
P42224	Signal transducer and activator of transcription 1-alpha/beta	486	39103346	70105116	44526353	**1.79**	**0.0034**	1.14	**0.017**	**0.64**	**0.0050**
P42766	60S ribosomal protein L35	143	208715830	275195260	227914301	**1.32**	**0.0029**	1.09	0.050	**0.83**	**0.0084**
P43155	Carnitine O-acetyltransferase	4	106537	120317	96382	1.13	0.23	0.90	0.32	**0.80**	**0.050**

Table B2.2 (continued)

P45954	Short/branched chain specific acyl-CoA dehydrogenase, mitochondrial	39	2224654	2457870	2009941	1.10	0.14	0.90	**0.035**	**0.82**	**0.038**
P45984	Mitogen-activated protein kinase 9	17	3870267	4728581	4021956	**1.22**	**0.0041**	1.04	0.42	0.85	**0.049**
P46013	Proliferation marker protein Ki-67	154	10246023	11407252	9245271	1.11	0.086	0.90	0.12	**0.81**	**0.010**
P46778	60S ribosomal protein L21	262	166290731	220479635	185886638	**1.33**	**0.0074**	1.12	0.064	0.84	**0.012**
P46779	60S ribosomal protein L28	197	157066056	202604102	174144925	**1.29**	**0.0073**	1.11	**0.037**	0.86	**0.010**
P46781	40S ribosomal protein S9	657	410069923	562155163	444040434	**1.37**	**0.0011**	1.08	0.092	**0.79**	**0.010**
P46783	40S ribosomal protein S10	291	90210132	115294284	98623565	**1.28**	**0.0086**	1.09	**0.0050**	0.86	**0.019**
P49207	60S ribosomal protein L34	225	165648491	220071769	180953500	**1.33**	**0.0064**	1.09	0.11	**0.82**	**0.013**
P49643	DNA primase large subunit	33	608983	713485	590058	1.17	0.050	0.97	0.60	**0.83**	**0.038**
P49750	YLP motif-containing protein 1	10	951711	1106550	911203	1.16	0.23	0.96	0.70	**0.82**	**0.013**
P50225	Sulfotransferase 1A1	62	4608369	5569565	4227174	1.21	**0.0047**	0.92	**0.048**	**0.76**	**0.0063**
P51153	Ras-related protein Rab-13	91	200105	251172	204494	**1.26**	**0.037**	1.02	0.38	**0.81**	**0.041**
P51617	Interleukin-1 receptor-associated kinase 1	7	216168	178775	189227	**0.83**	**0.028**	0.88	**0.048**	1.01	0.069
P51784	Ubiquitin carboxyl-terminal hydrolase 11	10	117984	170808	130436	**1.45**	**0.015**	1.11	0.18	**0.76**	**0.0028**
P52630	Signal transducer and activator of transcription 2	6	95651	175487	84928	**1.83**	**0.020**	0.89	0.17	**0.48**	**0.014**
P54920	Alpha-soluble NSF attachment protein	84	3715585	5118615	3734730	**1.38**	**0.037**	1.01	0.87	**0.73**	**0.033**
P61247	40S ribosomal protein S3a	661	272383354	375692797	302178144	**1.38**	**0.000042**	1.11	**0.010**	**0.80**	**0.0016**
P61254	60S ribosomal protein L26	151	177735338	216325188	190491745	**1.22**	**0.0033**	1.07	0.097	0.88	**0.021**

Table B2.2 (continued)

P61313	60S ribosomal protein L15	187	79136484	96191972	83073383	**1.22**	**0.020**	1.05	0.066	0.86	**0.033**
P61353	60S ribosomal protein L27	212	150452612	197328084	167426355	**1.31**	**0.0059**	1.11	0.052	0.85	**0.0083**
P61768	Major prion protein	7	439738	569543	435173	**1.30**	**0.0013**	0.99	0.85	**0.76**	**0.025**
P61927	60S ribosomal protein L37	28	38930140	53668617	43185190	**1.38**	**0.0021**	1.11	0.082	**0.80**	**0.012**
P62081	40S ribosomal protein S7	400	232682359	302328533	250827886	**1.30**	**0.0012**	1.08	0.081	**0.83**	**0.013**
P62241	40S ribosomal protein S8	616	100012960	136487147	110294740	**1.36**	**0.0047**	1.10	0.062	**0.81**	**0.019**
P62244	40S ribosomal protein S15a	221	211237340	283295616	238342396	**1.34**	**0.0032**	1.13	**0.025**	0.84	**0.013**
P62249	40S ribosomal protein S16	430	190604458	246893088	204473242	**1.30**	**0.00067**	1.07	0.077	**0.83**	**0.010**
P62263	40S ribosomal protein S14	313	103554944	134931621	112197325	**1.30**	**0.00054**	1.08	**0.016**	0.83	**0.0017**
P62266	40S ribosomal protein S23	193	141804930	177423862	152991067	**1.25**	**0.0044**	1.08	**0.025**	0.86	**0.011**
P62269	40S ribosomal protein S18	518	277272928	362860852	298961983	**1.31**	**0.00073**	1.08	**0.049**	**0.82**	**0.0056**
P62277	40S ribosomal protein S13	318	198680897	265651935	214721755	**1.34**	**0.0066**	1.08	0.11	**0.81**	**0.0073**
P62280	40S ribosomal protein S11	399	225677353	297041636	248005011	**1.32**	**0.0087**	1.10	**0.017**	0.83	**0.015**
P62424	60S ribosomal protein L7a	645	272188330	333000108	297075486	**1.22**	**0.021**	1.09	**0.017**	1.06	0.12
P62701	40S ribosomal protein S4, X isoform	547	311323588	426079532	341908085	**1.37**	**0.00023**	1.10	**0.017**	**0.80**	**0.0023**
P62750	60S ribosomal protein L23a	463	176575250	217513962	192387205	**1.23**	**0.0016**	1.09	**0.016**	0.88	**0.0085**
P62753	40S ribosomal protein S6	467	217015052	269118427	234748632	**1.24**	**0.0092**	1.08	0.084	0.87	**0.0053**
P62805	Histone H4	323	225916896	195045131	261151254	0.86	**0.0079**	1.16	**0.0059**	**1.34**	**0.0017**
P62829	60S ribosomal protein L23	366	78801164	96023982	84503081	**1.22**	**0.019**	1.07	0.062	0.88	**0.050**
P62841	40S ribosomal protein S15	36	6342018	7962794	7063438	**1.26**	**0.026**	1.11	**0.0055**	0.89	0.063

Table B2.2 (continued)

P62847	40S ribosomal protein S24	245	170359248	223867180	185544466	**1.31**	**0.00011**	1.09	**0.0013**	**0.83**	**0.00028**
P62851	40S ribosomal protein S25	395	245775680	302779817	261169838	**1.23**	**0.0019**	1.06	0.094	0.86	**0.018**
P62857	40S ribosomal protein S28	261	82871289	111741620	93064949	**1.35**	**0.013**	1.12	0.16	0.83	**0.045**
P62861	40S ribosomal protein S30	45	21298092	29888004	23710233	**1.40**	**0.020**	1.11	0.066	**0.79**	**0.028**
P62899	60S ribosomal protein L31	290	220230337	274581413	234317564	**1.25**	**0.00054**	1.06	0.22	0.85	**0.037**
P62906	60S ribosomal protein L10a	309	121896896	154273263	131211425	**1.27**	**0.00046**	1.08	0.093	0.85	**0.016**
P62910	60S ribosomal protein L32	149	49051443	61320208	53234435	**1.25**	**0.011**	1.09	**0.039**	0.87	**0.017**
P62913	60S ribosomal protein L11	212	115718173	146136969	124923915	**1.26**	**0.0012**	1.08	**0.012**	0.85	**0.0015**
P62917	60S ribosomal protein L8	270	130364316	164916048	141215193	**1.27**	**0.0012**	1.08	0.077	0.86	**0.019**
P63173	60S ribosomal protein L38	145	47467145	60544116	51593409	**1.28**	**0.0013**	1.09	**0.012**	0.85	**0.0045**
P63208	S-phase kinase-associated protein 1	173	22213402	27796376	23606095	**1.25**	**0.021**	1.06	**0.041**	0.85	**0.032**
P63220	40S ribosomal protein S21	145	113590601	139443704	120015062	**1.23**	**0.0093**	1.06	0.059	0.86	**0.014**
P63244	Receptor of activated protein C kinase 1	891	471888413	587926342	508593161	**1.25**	**0.013**	1.08	0.17	0.87	**0.019**
P67809	Y-box-binding protein 1	289	24157083	18343491	23591737	**0.76**	**0.015**	0.98	0.45	**1.29**	**0.015**
P83731	60S ribosomal protein L24	245	207066868	264881977	228457014	**1.28**	**0.00084**	1.10	**0.020**	0.86	**0.0074**
P83881	60S ribosomal protein L36a	116	69899737	89018147	76887957	**1.27**	**0.011**	1.10	0.083	0.86	**0.0044**
P84098	60S ribosomal protein L19	317	113304562	151145061	122445554	**1.33**	**0.0070**	1.08	0.060	**0.81**	**0.0059**
P84243	Histone H3.3	131	147082738	122965270	178056273	0.84	**0.0016**	1.21	**0.045**	**1.45**	**0.015**
Q00341	Vigilin	278	14693489	18204141	15287298	**1.24**	**0.0025**	1.04	**0.0077**	0.84	**0.0037**
Q01581	Hydroxymethylglutaryl-CoA synthase, cytoplasmic	366	53848725	85534561	58991800	**1.59**	**0.0030**	1.10	**0.011**	**0.69**	**0.0042**

Table B2.2 (continued)

Q02543	60S ribosomal protein L18a	254	127014903	161552519	139859446	**1.27**	**0.0034**	1.10	**0.023**	0.87	**0.00023**
Q02878	60S ribosomal protein L6	525	244258270	309934919	274164834	**1.27**	**0.00066**	1.12	**0.010**	0.88	**0.0057**
Q03135	Caveolin-1	8	195648	243008	202320	**1.24**	**0.022**	1.03	0.35	0.83	**0.044**
Q03519	Antigen peptide transporter 2	8	544631	877793	538053	**1.61**	**0.015**	0.99	0.78	**0.61**	**0.017**
Q07021	Complement component 1 Q subcomponent-binding protein, mitochondrial	865	14878561	10616439	13696354	**0.71**	**0.044**	0.92	**0.037**	0.99	0.11
Q08380	Galectin-3-binding protein	250	41359518	65114791	42316861	**1.57**	**0.0063**	1.02	0.64	**0.65**	**0.0018**
Q08945	FACT complex subunit SSRP1	91	18256401	15641875	19348250	0.86	0.21	1.06	0.52	**1.24**	**0.0041**
Q10589	Bone marrow stromal antigen 2	12	491001	809172	495789	**1.65**	**0.0043**	1.01	0.89	**0.61**	**0.0078**
Q13151	Heterogeneous nuclear ribonucleoprotein A0	230	100581766	77952342	84817326	**0.78**	**0.0080**	0.84	**0.014**	1.09	**0.045**
Q13428	Treacle protein	223	49624790	64671277	59062323	**1.30**	**0.0042**	1.19	0.13	0.91	0.26
Q13895	Bystin	83	2340551	2909882	2401059	**1.24**	**0.0058**	1.03	0.23	**0.83**	**0.0072**
Q13907	Isopentenyl-diphosphate Delta-isomerase 1	149	24999227	32011820	24743462	**1.28**	**0.0047**	0.99	0.77	**0.77**	**0.0081**
Q14258	E3 ubiquitin/ISG15 ligase TRIM25	213	15903542	21182325	16748064	**1.33**	**0.014**	1.05	0.18	**0.79**	**0.020**
Q14BN4	Sarcolemmal membrane-associated protein	2	42486	38145	32260	0.90	0.25	**0.76**	**0.034**	0.85	0.10
Q14318	Peptidyl-prolyl cis-trans isomerase FKBP8	83	594101	873485	629662	**1.47**	**0.032**	1.06	0.46	**0.72**	**0.018**
Q14978	Nucleolar and coiled-body phosphoprotein 1	75	16641784	35626661	17157714	**2.14**	**0.00018**	1.03	0.33	**0.48**	**0.00029**
Q15149	Plectin	84	6788459	8222967	7262267	**1.21**	**0.047**	1.07	0.12	0.88	0.12
Q16666	Gamma-interferon-inducible protein 16	63	1177154	1807235	1186933	**1.54**	**0.0023**	1.01	0.81	**0.66**	**0.0011**

Table B2.2 (continued)

Q4KWH8	1-phosphatidylinositol 4,5-bisphosphate phosphodiesterase eta-1	2	1683961	2121504	1750474	**1.26**	**0.0079**	1.04	0.18	**0.83**	**0.0084**
Q53EL6	Programmed cell death protein 4	4	67441	93966	62167	**1.39**	**0.020**	0.92	**0.016**	**0.66**	**0.014**
Q5EBL4	RILP-like protein 1	3	87012	113169	86015	**1.30**	0.05	0.99	0.83	**0.76**	**0.032**
Q5EBM0	UMP-CMP kinase 2, mitochondrial	7	33925	55884	30291	**1.65**	**0.020**	0.89	0.11	**0.54**	**0.013**
Q5IFJ7	60S ribosomal protein L9	243	43289927	54434507	46375530	**1.26**	**0.012**	1.07	0.14	0.85	**0.042**
Q5K651	Sterile alpha motif domain-containing protein 9	36	526359	670424	520961	**1.27**	**0.0010**	0.99	0.65	**0.78**	**0.0038**
Q5TAX3	Terminal uridylyltransferase 4	2	48138	45700	38511	0.95	0.12	**0.80**	**0.0060**	0.84	**0.0055**
Q5TBB1	Ribonuclease H2 subunit B	13	219524	255625	210447	1.16	**0.050**	0.96	0.45	**0.82**	**0.014**
Q5TC12	ATP synthase mitochondrial F1 complex assembly factor 1	8	480745	566060	458465	1.18	**0.034**	0.95	0.14	**0.81**	**0.015**
Q63HN8	E3 ubiquitin-protein ligase RNF213	20	160002	196930	139296	**1.23**	0.14	0.87	0.26	**0.71**	**0.032**
Q6DKI1	60S ribosomal protein L7-like 1	3	754822	1031619	933131	**1.37**	**0.031**	**1.24**	0.085	0.90	0.19
Q6NZI2	Caveolae-associated protein 1	13	448599	612585	479036	**1.37**	**0.014**	1.07	0.069	**0.78**	**0.025**
Q6PJG6	BRCA1-associated ATM activator 1	7	1050597	1500420	1100528	**1.43**	**0.002**	1.05	0.18	**0.73**	**0.0019**
Q7L592	Protein arginine methyltransferase NDUFAF7, mitochondrial	7	145399	92621	77663	**0.64**	**0.031**	**0.53**	**0.019**	0.84	0.19
Q7L9L4	MOB kinase activator 1B	68	5472020	7667773	5764479	**1.40**	**0.0076**	1.05	0.095	**0.75**	**0.0093**

Table B2.2 (continued)

Q7LBC6	Lysine-specific demethylase 3B	10	603775	732961	604310	**1.21**	0.13	1.00	0.99	**0.82**	**0.027**
Q86UV5	Ubiquitin carboxyl-terminal hydrolase 48	9	99699	90035	81368	0.90	0.20	**0.82**	**0.021**	0.90	0.27
Q8IUR0	Trafficking protein particle complex subunit 5	6	798422	967434	847399	**1.21**	**0.012**	1.06	0.22	0.88	**0.038**
Q8IV08	5'-3' exonuclease PLD3	91	7252137	10014971	7833166	**1.38**	**0.0051**	1.08	**0.0052**	**0.78**	**0.0078**
Q8IYM9	E3 ubiquitin-protein ligase TRIM22	5	266822	607143	296103	**2.28**	**0.0011**	1.11	0.11	**0.49**	**0.0020**
Q8IZY2	ATP-binding cassette sub-family A member 7	208	11982623	24801709	11320275	**2.07**	**0.0018**	0.94	0.12	**0.46**	**0.0015**
Q8NBT2	Kinetochore protein Spc24	26	637718	785122	653072	**1.23**	**0.018**	1.02	0.42	0.83	**0.011**
Q8TCB0	Interferon-induced protein 44	5	287386	470325	329058	**1.64**	**0.011**	1.15	0.14	**0.70**	**0.011**
Q8TDB6	E3 ubiquitin-protein ligase DTX3L	4	938572	1270336	1032225	**1.35**	**0.011**	1.10	0.15	**0.81**	**0.028**
Q8WXG1	Radical S-adenosyl methionine domain-containing protein 2	17	634193	1173935	659097	**1.85**	**0.00060**	1.04	0.17	**0.56**	**0.00068**
Q92522	Histone H1x	119	38509662	54279752	41060672	**1.41**	**0.014**	1.07	0.45	**0.76**	**0.026**
Q969Z3	Mitochondrial amidoxime reducing component 2	3	738561	968727	802614	**1.31**	**0.020**	1.09	0.29	**0.83**	**0.042**
Q96B36	Proline-rich AKT1 substrate 1	24	1729601	2111449	1780506	**1.22**	**0.016**	1.03	0.51	0.84	0.054
Q96C36	Pyrroline-5-carboxylate reductase 2	11	736739	989240	777854	**1.34**	**0.0093**	1.06	**0.047**	**0.79**	**0.012**
Q96GX2	Ataxin-7-like protein 3B	4	519511	671491	547412	**1.29**	**0.0035**	1.05	0.15	**0.82**	**0.014**
Q9BQE5	Apolipoprotein L2	37	4608958	6110312	4477678	**1.33**	0.056	0.97	0.61	**0.73**	**0.040**
Q9BTE3	Mini-chromosome maintenance complex-binding protein	40	2923397	3347644	2720525	1.15	0.325	0.93	0.57	**0.81**	**0.038**
Q9BTZ2	Dehydrogenase/reductase SDR family member 4	3	2207276	3221206	2331582	**1.46**	**0.015**	1.06	0.51	**0.72**	**0.012**

Table B2.2 (continued)

Q9BUP0	EF-hand domain-containing protein D1	40	383782	567517	417408	**1.48**	**0.0073**	1.09	0.17	**0.74**	**0.00059**
Q9BZL1	Ubiquitin-like protein 5	6	1943432	3414068	2417254	**1.76**	**0.024**	**1.24**	**0.034**	**0.71**	**0.044**
Q9H6T3	RNA polymerase II-associated protein 3	69	327751	414856	336425	**1.27**	**0.013**	1.03	0.49	**0.81**	**0.0048**
Q9HA77	Probable cysteine--tRNA ligase, mitochondrial	9	378506	439500	341485	1.16	0.13	0.90	0.20	**0.78**	**0.030**
Q9HB40	Retinoid-inducible serine carboxypeptidase	8	685811	819240	659912	1.19	**0.013**	0.96	0.11	**0.81**	**0.0060**
Q9HBM1	Kinetochore protein Spc25	12	1262055	1547904	1283256	**1.23**	**0.0018**	1.02	0.61	**0.83**	**0.017**
Q9HBM6	Transcription initiation factor TFIID subunit 9B	5	89141	99641	82398	1.12	0.20	0.92	0.35	**0.83**	**0.0027**
Q9NPQ8	Synembryn-A	58	40867036	57063734	45175289	**1.40**	**0.0059**	1.11	0.077	**0.79**	**0.00029**
Q9NRV9	Heme-binding protein 1	19	1187883	1341960	1106115	1.13	0.14	0.93	0.29	**0.82**	**0.046**
Q9NYF8	Bcl-2-associated transcription factor 1	210	49556731	39886943	48646124	**0.80**	**0.028**	0.98	0.68	**1.22**	**0.012**
Q9NZT2	Opioid growth factor receptor	28	344816	420733	339510	**1.22**	**0.00062**	0.98	0.77	**0.81**	**0.035**
Q9NZZ3	Charged multivesicular body protein 5	119	17612764	22410996	18105757	**1.27**	**0.0072**	1.03	0.45	**0.81**	**0.0075**
Q9P2E9	Ribosome-binding protein 1	203	98053243	146635214	112279204	**1.50**	**0.00022**	1.15	**0.0065**	**0.77**	**0.00088**
Q9UBB4	Ataxin-10	59	3229111	4568163	3352047	**1.41**	**0.00023**	1.04	0.22	**0.73**	**0.0036**
Q9UBS8	E3 ubiquitin-protein ligase RNF14	2	160467	175325	145304	1.09	0.051	0.91	0.11	**0.83**	**0.030**
Q9UII4	E3 ISG15--protein ligase HERC5	51	2005353	3571038	2127477	**1.78**	**0.0092**	1.06	**0.0085**	**0.60**	**0.011**
Q9ULC4	Malignant T-cell-amplified sequence 1	58	305445	242956	297223	**0.80**	0.11	0.97	0.75	**1.22**	**0.0038**
Q9UNF1	Melanoma-associated antigen D2	99	14158513	17704583	13633656	**1.25**	**0.0044**	0.96	0.29	**0.77**	**0.0049**
Q9Y314	Nitric oxide synthase-interacting protein	9	452401	573978	483111	**1.27**	**0.024**	1.07	0.077	0.84	**0.035**

Table B2.2 (continued)

Q9Y3E1	Hepatoma-derived growth factor-related protein 3	27	2937308	2135487	2146961	**0.73**	**0.049**	**0.73**	0.078	1.01	0.95
Q9Y3P9	Rab GTPase-activating protein 1	25	68370	89804	73633	**1.31**	**0.015**	1.08	0.22	**0.82**	**0.026**
Q9Y3U8	60S ribosomal protein L36	108	35052414	44043740	36740936	**1.26**	**0.000076**	1.05	0.26	0.83	**0.022**
Q9Y3Z3	Deoxynucleoside triphosphate triphosphohydrolase SAMHD1	101	8505997	11088104	8536619	**1.30**	**0.019**	1.00	0.95	**0.77**	**0.0044**
Q9Y5B9	FACT complex subunit SPT16	167	11093029	9118592	11357891	**0.82**	0.19	1.02	0.82	**1.25**	**0.0066**
Q9Y617	Phosphoserine aminotransferase	289	68393388	85016683	70074406	**1.24**	**0.00065**	1.02	0.16	**0.82**	**0.0021**
Q9Y6K5	2'-5'-oligoadenylate synthase 3	51	1860112	3566766	2059505	**1.92**	**0.0028**	1.11	0.23	**0.58**	**0.0027**

[a]The accession number from the UniProt human database. [b]TMT reporter ion intensities averaged from workflow replicates of each cell type, [c]Fold changes calculated using average TMT reporter ion intensities for each cell type. Bold indicates fold changes < 0.83 and > 1.21. [d]Bold indicates p-value < 0.05. Abbreviations: PSMs, peptide spectral matches; EV, empty vector; WT, wild-type; T319A, Thr to Ala mutation at amino acid 319.

APPENDIX C

Supplementary Information for Chapter 3

Data C3.1. Processing of hippocampus data. This appendix data can be accessed in the supplementary material in the online version of this dissertation, in the Excel file Supplementary Data C3.1.

Data C3.2. Processing of IPL data. This appendix data can be accessed in the supplementary material in the online version of this dissertation, in the Excel file Supplementary Data C3.2.

Data C3.3. Processing of GP data. This appendix data can be accessed in the supplementary material in the online version of this dissertation, in the Excel file Supplementary Data C3.3.

Data C3.4. Protein list corresponding to hippocampus heatmap of differentially-expressed proteins. This appendix data can be accessed in the supplementary material in the online version of this dissertation, in the Excel file Supplementary Data C3.4.

In-batch	126	Pool A
Protein 1	i_1	i_1
Protein 2	i_2	i_2
Protein n	i_n	i_n
Sum Intensity	I_{126}	I_{Pool}
Scaling Factor ($SF_{channel}$)	I_{Pool}/I_{126}	N/A

↓

Across-batch	126	Pool A	Geometric Mean of Pools (GM_x)	Scaling Factor (SF_x)
Protein 1	j_1	i_1	$\sqrt{i_{1A} \times i_{1B}}$	GM_1/i_1
Protein 2	j_2	i_2	$\sqrt{i_{2A} \times i_{2B}}$	GM_2/i_2
Protein n	j_n	i_n	$\sqrt{i_{nA} \times i_{nB}}$	GM_n/i_n

↓

Final	126
Protein 1	k_1
Protein 2	k_2
Protein n	k_n

Figure C3.1. Normalization workflow. This internal reference scaling normalization workflow was used for all analyses (modified from Plubell, D. L., et al. *Mol. Cell Proteomics*, 2017). TMT reporter ion intensities were normalized within each batch to the total summed intensity for all of the proteins in the pooled channel. These intensities were then normalized across the two batches to the geometric mean of the pooled channels at the protein level. Only quantified proteins underwent normalization. j_x = in-batch normalized protein intensity = $i_x \times SF_{channel}$; k_x = final normalized protein intensity = $j_x \times SF_x$. Figure reprinted from Neurobiol. Dis., Vol 146, Stepler, K. E., et al., Inclusion of African American/Black adults in a pilot brain proteomics study of Alzheimer's disease, Article No. 105129, Copyright (2020), with permission from Elsevier.[74]

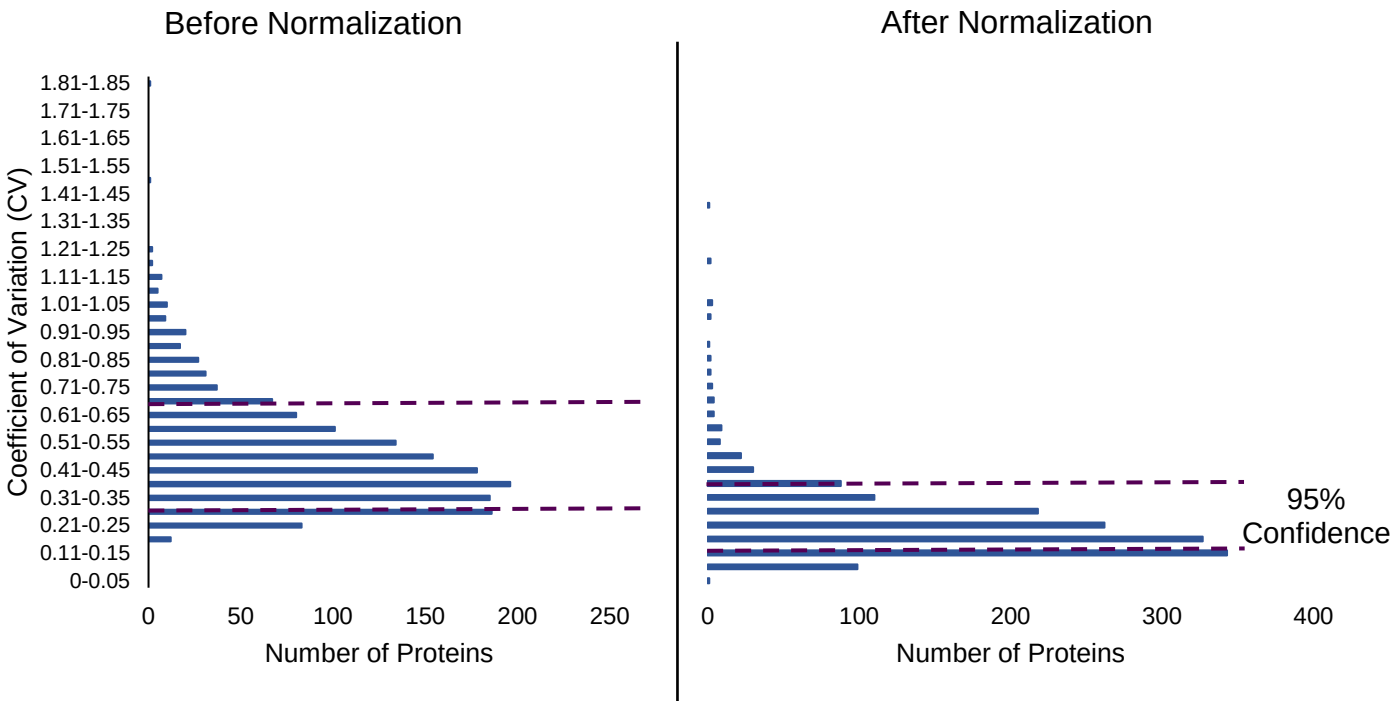

Figure C3.2. Results of normalization. Change in hippocampal reporter ion intensities before and after normalization. Coefficients of variation (CVs) were calculated as standard deviation divided by average, across all TMT channels. Dashed lines indicate 95% confidence range. These results are representative of the results of normalization from IPL and GP. Figure reprinted from Neurobiol. Dis., Vol 146, Stepler, K. E., et al., Inclusion of African American/Black adults in a pilot brain proteomics study of Alzheimer's disease, Article No. 105129, Copyright (2020), with permission from Elsevier.[74]

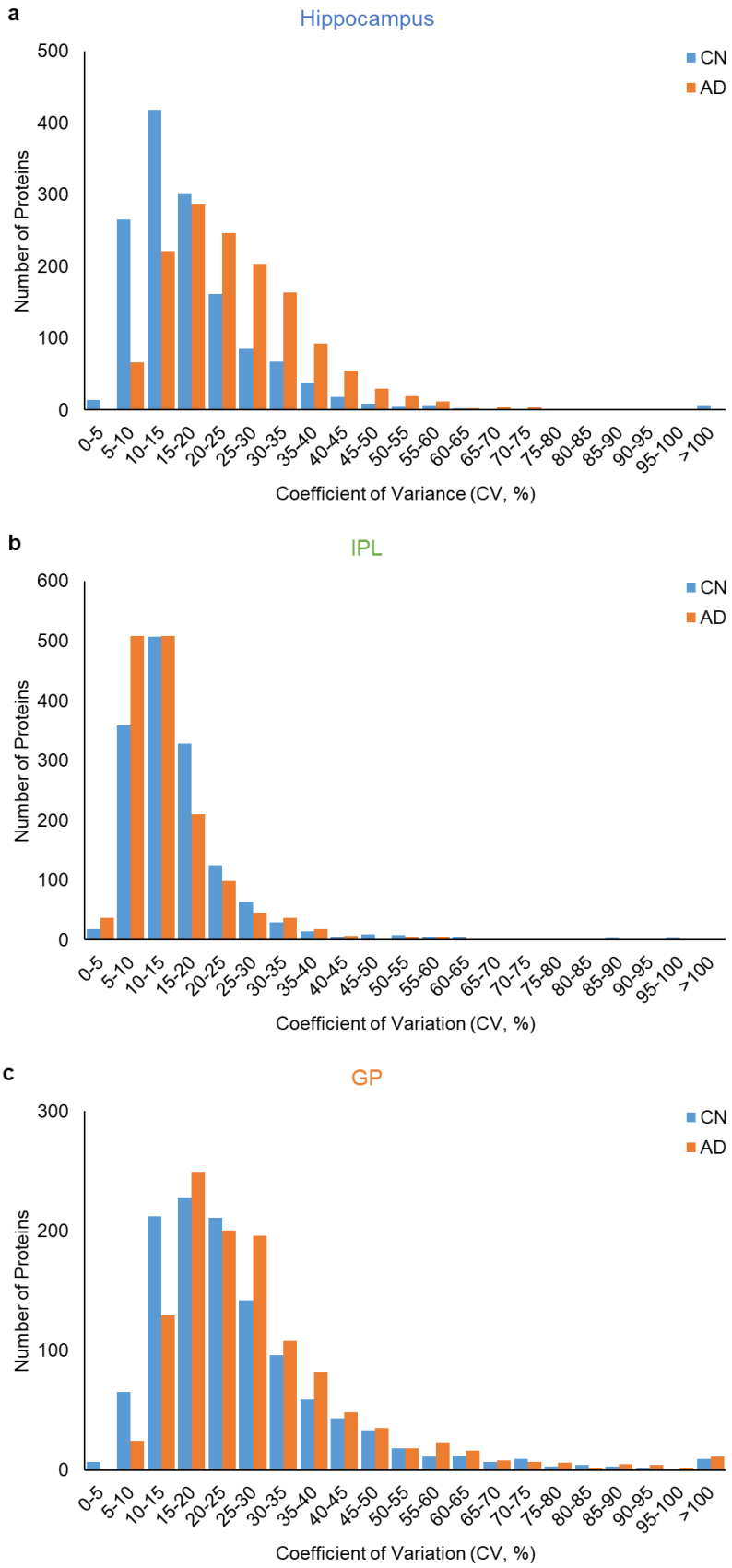
a
Hippocampus
CN
AD
Number of Proteins
0
100
200
300
400
500
0-5
5-10
10-15
15-20
20-25
25-30
30-35
35-40
40-45
45-50
50-55
55-60
60-65
65-70
70-75
75-80
80-85
85-90
90-95
95-100
>100
Coefficient of Variance (CV, %)
b
IPL
CN
AD
Number of Proteins
0
100
200
300
400
500
600
0-5
5-10
10-15
15-20
20-25
25-30
30-35
35-40
40-45
45-50
50-55
55-60
60-65
65-70
70-75
75-80
80-85
85-90
90-95
95-100
>100
Coefficient of Variation (CV, %)
c
GP
CN
AD
Number of Proteins
0
100
200
300
0-5
5-10
10-15
15-20
20-25
25-30
30-35
35-40
40-45
45-50
50-55
55-60
60-65
65-70
70-75
75-80
80-85
85-90
90-95
95-100
>100
Coefficient of Variation (CV, %)

Figure C3.3. Protein variance distributions in each region. Histograms show the coefficients of variation (CVs) in protein reporter ion intensities within the CN and AD groups for **a**, hippocampus, **b**, IPL, and **c**, GP. All quantified proteins are shown for each region (N = 1,414, 1,487, and 1,173 for hippocampus, IPL, and GP, respectively), and each protein is shown for both the CN and AD groups. CV percentages were calculated as standard deviation of summed total reporter ion intensities for each protein across the CN or AD group/mean summed total reporter ion intensities in the CN or AD group x 100%. CN groups are shown in blue bars; AD groups are shown in orange bars. Proteins with CVs larger than two standard deviations from the mean (i.e., CV > 0.49, 0.34, and 0.61 for hippocampus, IPL, and GP, respectively) were excluded from further analysis. Abbreviations: CN, cognitively normal; AD, Alzheimer's disease; CV, coefficient of variation; IPL, inferior parietal lobule; GP, globus pallidus. Figure reprinted from Neurobiol. Dis., Vol 146, Stepler, K. E., et al., Inclusion of African American/Black adults in a pilot brain proteomics study of Alzheimer's disease, Article No. 105129, Copyright (2020), with permission from Elsevier.[74]

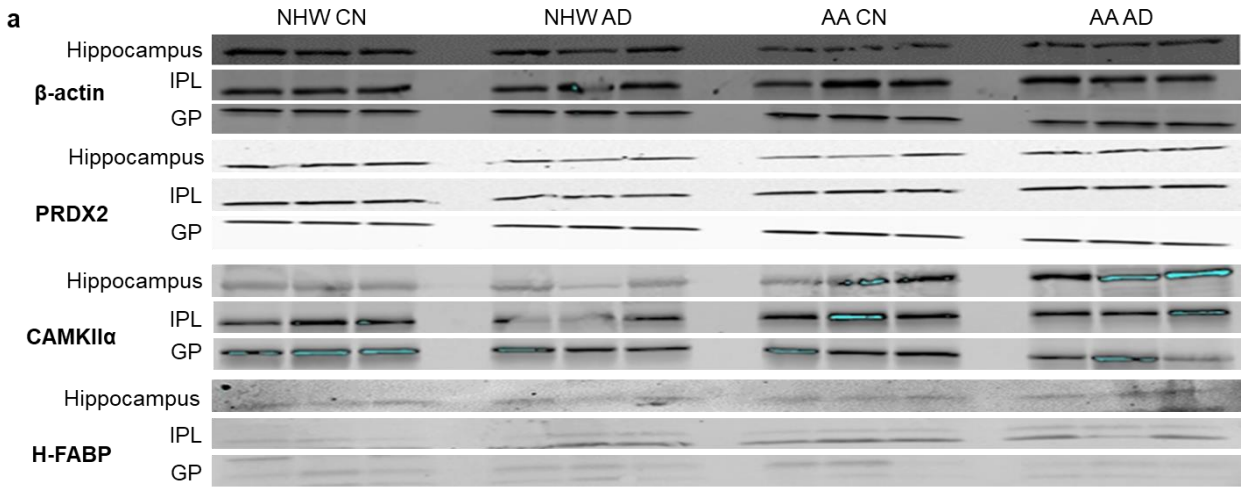
a
NHW CN
NHW AD
AA CN
AA AD
Hippocampus
β-actin
IPL
GP
Hippocampus
PRDX2
IPL
GP
Hippocampus
CAMKIIα
IPL
GP
Hippocampus
H-FABP
IPL
GP

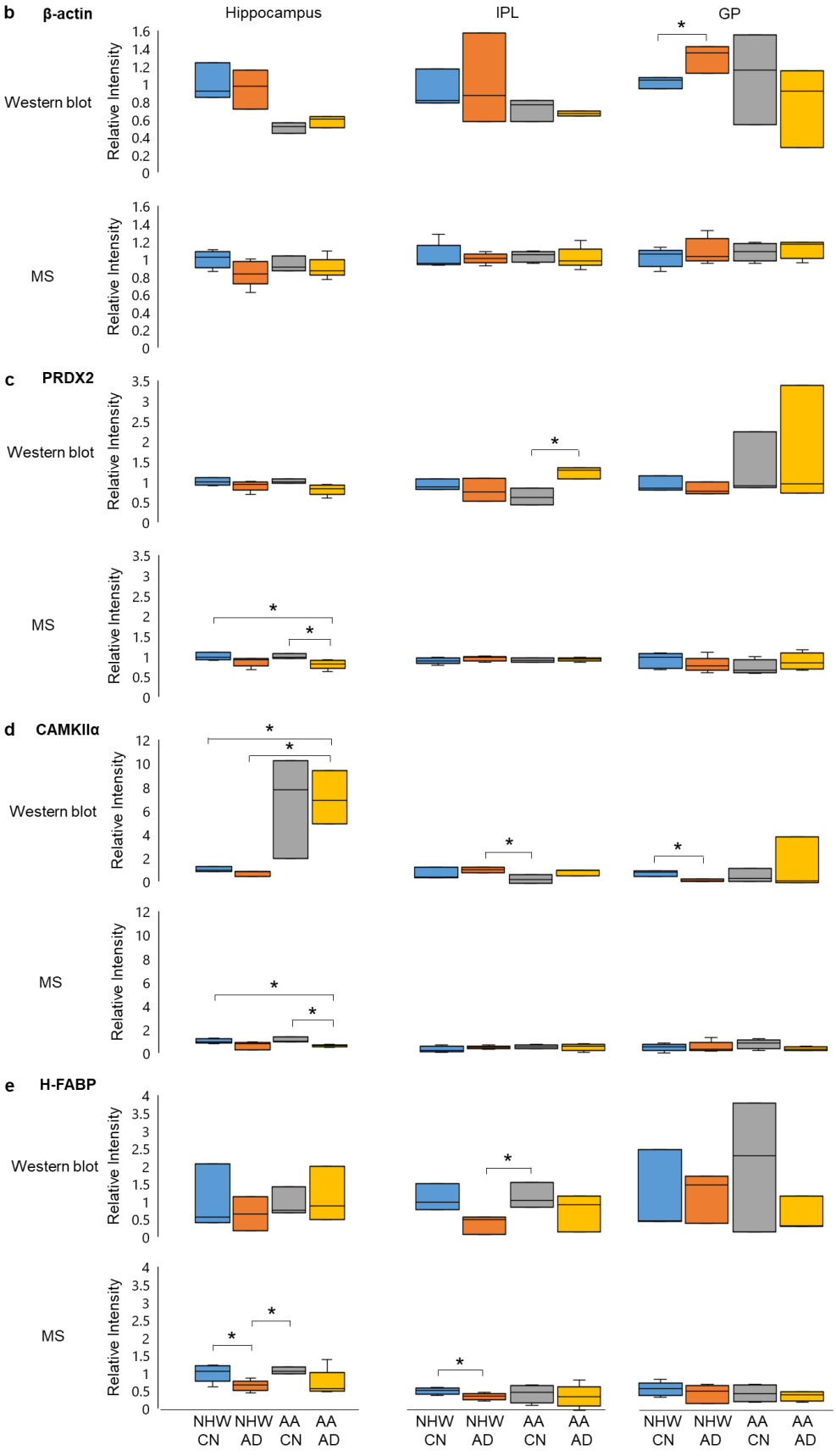
b β-actin
Hippocampus
IPL
GP
Western blot
MS
Relative Intensity
c PRDX2
d CAMKIIα
e H-FABP
NHW CN
NHW AD
AA CN
AA AD

Figure C3.4. Comparison of Western blot and MS results. a, Western blot images of β-actin, PRDX2, CAMKIIα, and H-FABP from all three regions (N = 3 per group), and box plots showing Western blot and TMT MS intensities for **b**, β-actin, **c**, PRDX2, **d**, CAMKIIα, and **e**, H-FABP from the three regions. The center line of each box is the median. The upper and lower limits of the box are the upper and lower quartiles, respectively, and the whiskers reflect the minimum and maximum values where present. There are no whiskers on the Western blot box plots because N = 3 samples per group. Western blot intensities were normalized to β-actin intensities and all intensities are shown relative to the non-Hispanic White CN group. * indicates $p < 0.05$ using two-tailed t-tests. Trends in protein expression from MS data were generally supported by Western blots. Generally, MS data had less variability than Western blot data, likely due to small sample sizes (N = 3) and other methodological limitations (see Aebersold, R.; Burlingame, A. L.; Bradshaw, R. A. *Mol. Cell. Proteomics*, 2013). Abbreviations: NHW, non-Hispanic White; CN, cognitively normal; AD, Alzheimer's disease; AA, African American/Black; IPL, inferior parietal lobule; GP, globus pallidus; PRDX2, peroxiredoxin-2; CAMKIIα, calcium/calmodulin dependent protein kinase IIα; H-FABP, fatty acid-binding protein, heart type. Figure reprinted from Neurobiol. Dis., Vol 146, Stepler, K. E., et al., Inclusion of African American/Black adults in a pilot brain proteomics study of Alzheimer's disease, Article No. 105129, Copyright (2020), with permission from Elsevier.[74]

Table C3.1. TMT batch assignments for all regions

TMT Channel	Hippocampus		IPL		GP	
	Batch 1	Batch 2	Batch 1	Batch 2	Batch 1	Batch 2
126	AA CN	Pool	NHW AD	NHW AD	Pool	AA AD
127N	NHW CN	NHW CN	AA AD	Pool	NHW AD	NHW AD
127C	NHW AD	AA AD	NHW AD	AA CN	NHW CN	AA AD
128N	NHW AD	NHW AD	AA AD	NHW CN	AA CN	NHW CN
128C	AA AD	NHW CN	NHW CN	Pool	NHW AD	NHW AD
129N	Pool	AA CN	Pool	AA AD	NHW AD	Pool
129C	AA AD	AA AD	AA CN	NHW CN	AA CN	AA CN
130N	NHW CN	AA CN	AA AD	NHW AD	NHW CN	AA AD
130C	NHW AD	NHW AD	AA CN	NHW AD	AA CN	NHW CN
131	NHW CN	AA AD	NHW CN	AA CN	AA AD	NHW CN
131C	--	--	NHW CN	AA AD	--	--

Abbreviations: AA, African American/Black; CN, cognitively normal; NHW, non-Hispanic White; AD, Alzheimer's disease; IPL, inferior parietal lobule; GP, globus pallidus.

Table C3.2. Differentially-expressed proteins in AD postmortem hippocampus.

Accession Number[a]	Protein Name	PSMs[b]	Average Reporter Ion Intensities[c]		AD/CN[d]	p-Value[e]	Corrected p-value[e]	Significant in ROSMAP[f]
			All CN	All AD				
Q04917	14-3-3 protein eta	69	2432508 ± 454518	3020511 ± 380973	**1.24**	0.000083	0.057	No
Q9UHD8	Septin-9	79	1371640 ± 324701	1982483 ± 637863	**1.45**	0.00018	0.068	No
Q96F85	CB1 cannabinoid receptor-interacting protein 1	598	29532317 ± 4975967	18717800 ± 8107358	**0.63**	0.00020	0.057	No
P04216	Thy-1 membrane glycoprotein	5	47888 ± 9839	38531 ± 7403	**0.80**	0.00036	0.057	No
O95865	N(G),N(G)-dimethylarginine dimethylaminohydrolase 2	24	72703 ± 23349	47498 ± 16687	**0.65**	0.00040	0.074	Yes
Q9NTK5	Obg-like ATPase 1	27	636172 ± 50052	553834 ± 96863	0.87	0.00046	0.090	No
P27348	14-3-3 protein theta	389	18249467 ± 1919605	14078884 ± 4443870	**0.77**	0.00059	0.057	Yes
Q9UM19	Hippocalcin-like protein 4	296	9442182 ± 785533	10974635 ± 1780588	1.16	0.00066	0.057	No
P31946	14-3-3 protein beta/alpha	59	1595805 ± 286375	1183366 ± 356490	**0.74**	0.00074	0.057	No
P20337	Ras-related protein Rab-3B	13	145060 ± 34091	103437 ± 36647	**0.71**	0.00076	0.057	Yes
P42262	Glutamate receptor 2	65	1370877 ± 71768	1088801 ± 255780	**0.79**	0.00079	0.12	Yes
P61204	ADP-ribosylation factor 3	686	75888674 ± 5250141	63420693 ± 11979882	0.84	0.00081	0.072	No
Q9H9B4	Sideroflexin-1	122	3192685 ± 288888	2598842 ± 597192	0.81	0.00086	0.095	Yes
Q13557	Calcium/calmodulin-dependent protein kinase type II subunit delta	141	3560418 ± 493759	2448334 ± 980610	**0.69**	0.00087	0.057	No
O43426	Synaptojanin-1	7	10020 ± 4031	6657 ± 2106	**0.66**	0.00093	0.057	No
Q9BW30	Tubulin polymerization-promoting protein family member 3	48	2373529 ± 546807	1293076 ± 551913	**0.54**	0.0010	0.068	No
P84085	ADP-ribosylation factor 5	15	1301902 ± 409370	2175844 ± 1052416	**1.67**	0.0010	0.057	Yes
O00154	Cytosolic acyl coenzyme A thioester hydrolase	155	4689231 ± 694916	3326966 ± 736289	**0.71**	0.0010	0.057	Yes
P67775	Serine/threonine-protein phosphatase 2A catalytic subunit alpha isoform	16	732389 ± 179643	1285413 ± 423457	**1.76**	0.0010	0.057	No

Table C3.2 (continued)

Q9UQM7	Calcium/calmodulin-dependent protein kinase type II subunit alpha	17	223678 ± 29396	259331 ± 38731	1.16	0.0011	0.13	No
Q13554	Calcium/calmodulin-dependent protein kinase type II subunit beta	55	3017638 ± 291883	2339552 ± 435311	**0.78**	0.0012	0.057	No
Q13630	GDP-L-fucose synthase	176	7270014 ± 812283	5953577 ± 1436087	0.82	0.0012	0.074	Yes
Q8NI08	Nuclear receptor coactivator 7	219	6062868 ± 761390	7645828 ± 1105108	**1.26**	0.0013	0.057	No
O14561	Acyl carrier protein, mitochondrial	28	113615 ± 17626	156031 ± 34918	**1.37**	0.0013	0.073	Yes
O75489	NADH dehydrogenase [ubiquinone] iron-sulfur protein 3, mitochondrial	10	91583 ± 16721	67593 ± 12674	**0.74**	0.0013	0.057	Yes
Q8IUD2	ELKS/Rab6-interacting/CAST family member 1	219	6199824 ± 873269	5399250 ± 643696	0.87	0.0013	0.073	No
P04908	Histone H2A type 1-B/E	327	4960561 ± 1049415	7392737 ± 2127652	**1.49**	0.0014	0.057	No
Q4KMQ2	Anoctamin-6	964	59091052 ± 5747189	46654427 ± 12668836	**0.79**	0.0014	0.057	Yes
Q9HB71	Calcyclin-binding protein	89	1109248 ± 307657	1663106 ± 426251	**1.50**	0.0014	0.057	No
P08238	Heat shock protein HSP 90-beta	40	540246 ± 35346	429738 ± 135098	**0.80**	0.0014	0.057	No
O15083	ERC protein 2	4	29355 ± 10701	19788 ± 5821	**0.67**	0.0014	0.057	Yes
Q14254	Flotillin-2	14	25573 ± 8429	16495 ± 5594	**0.65**	0.0015	0.057	No
Q13555	Calcium/calmodulin-dependent protein kinase type II subunit gamma	28	138130 ± 26671	109480 ± 24277	**0.79**	0.0015	0.083	No
P08670	Vimentin	23	435893 ± 37110	319843 ± 92454	**0.73**	0.0015	0.057	No
Q9H115	Beta-soluble NSF attachment protein	50	1299310 ± 257714	2002742 ± 549774	**1.54**	0.0015	0.068	No
O60641	Clathrin coat assembly protein AP180	48	623209 ± 55979	486688 ± 113104	**0.78**	0.0016	0.057	No
P31942	Heterogeneous nuclear ribonucleoprotein H3	9	226666 ± 35040	163741 ± 49780	**0.72**	0.0016	0.080	Yes
P07900	Heat shock protein HSP 90-alpha	98	1660082 ± 111107	1956866 ± 247704	1.18	0.0016	0.057	No
Q96E17	Ras-related protein Rab-3C	11	164434 ± 35986	118874 ± 47248	**0.72**	0.0016	0.057	No

Table C3.2 (continued)

Q92930	Ras-related protein Rab-8B	127	1940752 ± 296745	2778666 ± 569682	**1.43**	0.0017	0.073	No
P16402	Histone H1.3	18	52201 ± 7401	64150 ± 12848	1.23	0.0017	0.057	No
Q15019	Septin-2	41	813878 ± 209119	593084 ± 144885	**0.73**	0.0018	0.057	Yes
P04083	Annexin A1	84	1314047 ± 126273	1052087 ± 223208	**0.80**	0.0018	0.057	No
O60664	Perilipin-3	11	418965 ± 49729	312348 ± 63414	**0.75**	0.0020	0.057	Yes
Q14315	Filamin-C	990	73103523 ± 5047307	61989054 ± 8931098	0.85	0.0020	0.094	No
Q15555	Microtubule-associated protein RP/EB family member 2	57	2912077 ± 546141	2053085 ± 496970	**0.71**	0.0020	0.068	No
P61981	14-3-3 protein gamma	1006	165148800 ± 20432250	139119335 ± 27100658	0.84	0.0021	0.057	No
P08727	Keratin, type I cytoskeletal 19	106	2161795 ± 210141	1924200 ± 208831	0.89	0.0021	0.057	No
P61026	Ras-related protein Rab-10	333	120070987 ± 42351148	84842743 ± 26501760	**0.71**	0.0021	0.057	No
P61916	NPC intracellular cholesterol transporter 2	17	1094664 ± 196993	658018 ± 209607	**0.60**	0.0022	0.069	No
Q96A26	Protein FAM162A	18	170643 ± 18803	148060 ± 22692	0.87	0.0022	0.057	No
P61006	Ras-related protein Rab-8A	35	895425 ± 245711	706513 ± 116353	**0.79**	0.0023	0.12	No
P26038	Moesin	32	313708 ± 30079	251222 ± 70122	**0.80**	0.0024	0.091	No
Q15286	Ras-related protein Rab-35	9	81430 ± 12776	115252 ± 28490	**1.42**	0.0024	0.057	No
P40121	Macrophage-capping protein	164	3133017 ± 259218	2563178 ± 637104	0.82	0.0024	0.057	Yes
Q12959	Disks large homolog 1	9	71434 ± 6445	55494 ± 12307	**0.78**	0.0025	0.057	No
Q9ULU8	Calcium-dependent secretion activator 1	70	754103 ± 123667	1027540 ± 200274	**1.36**	0.0025	0.064	Yes
Q15700	Disks large homolog 2	34	962811 ± 137403	714023 ± 160743	**0.74**	0.0025	0.069	No
P61086	Ubiquitin-conjugating enzyme E2 K	152	2267264 ± 342571	3464806 ± 930030	**1.53**	0.0025	0.057	No
O95299	NADH dehydrogenase [ubiquinone] 1 alpha subcomplex subunit 10, mitochondrial	9	209255 ± 23113	170540 ± 42343	0.81	0.0026	0.057	Yes
Q8TDJ6	DmX-like protein 2	31	439114 ± 165671	814934 ± 264591	**1.86**	0.0026	0.083	Yes
P09211	Glutathione S-transferase P	44	1948801 ± 261131	1516812 ± 375467	**0.78**	0.0026	0.095	Yes

Table C3.2 (continued)

P11766	Alcohol dehydrogenase class-3	95	2719443 ± 405275	2012274 ± 645643	**0.74**	0.0026	0.14	No
Q9UJY1	Heat shock protein beta-8	154	1027407 ± 198884	1467975 ± 366323	**1.43**	0.0028	0.069	Yes
Q99536	Synaptic vesicle membrane protein VAT-1 homolog	43	2320351 ± 306371	1890863 ± 479981	0.81	0.0029	0.064	No
Q09666	Neuroblast differentiation-associated protein AHNAK	776	68103093 ± 29991887	201916109 ± 94693354	**2.96**	0.0030	0.091	Yes
Q15223	Nectin-1	16	57928 ± 7331	48008 ± 9555	0.83	0.0030	0.12	Yes
P16104	Histone H2AX	397	22320547 ± 3058881	16529132 ± 4337195	**0.74**	0.0030	0.057	Yes
P34932	Heat shock 70 kDa protein 4	6	29492 ± 3730	25086 ± 4178	0.85	0.0030	0.057	No
Q96FJ2	Dynein light chain 2, cytoplasmic	264	18134095 ± 4789936	11904390 ± 5330343	**0.66**	0.0030	0.057	Yes
Q96FW1	Ubiquitin thioesterase OTUB1	124	2107850 ± 246566	1817601 ± 167629	0.86	0.0031	0.057	No
P45985	Dual specificity mitogen-activated protein kinase kinase 4	5	44806 ± 4455	36819 ± 4157	0.82	0.0032	0.057	Yes
Q86YM7	Homer protein homolog 1	58	706358 ± 101200	938974 ± 202938	**1.33**	0.0032	0.057	Yes
O95817	BAG family molecular chaperone regulator 3	59	823211 ± 143218	1050279 ± 179916	**1.28**	0.0033	0.057	Yes
P02545	Prelamin-A/C	10	40895 ± 8421	29138 ± 9606	**0.71**	0.0033	0.086	No
P15311	Ezrin	26	537756 ± 92878	364850 ± 97947	**0.68**	0.0034	0.057	No
P05230	Fibroblast growth factor 1	129	4067261 ± 530418	3368015 ± 798551	0.83	0.0034	0.12	No
P18085	ADP-ribosylation factor 4	7	110556 ± 16671	80433 ± 36249	**0.73**	0.0034	0.120	No
Q06830	Peroxiredoxin-1	478	23998653 ± 1818264	19472426 ± 2884935	0.81	0.0034	0.057	Yes
O60502	Protein O-GlcNAcase	654	61545781 ± 5293368	43131209 ± 15838494	**0.70**	0.0035	0.071	No
P09382	Galectin-1	12	70943 ± 21376	50236 ± 16163	**0.71**	0.0035	0.064	Yes
P20336	Ras-related protein Rab-3A	13	28558 ± 3109	24263 ± 4035	0.85	0.0036	0.057	No
O00408	cGMP-dependent 3',5'-cyclic phosphodiesterase	11	47142 ± 6659	40676 ± 6168	0.86	0.0036	0.073	No
Q14696	LRP chaperone MESD	23	629510 ± 61238	452685 ± 144877	**0.72**	0.0037	0.11	No
P14406	Cytochrome c oxidase subunit 7A2, mitochondrial	143	6797256 ± 640947	5453486 ± 1183397	**0.80**	0.0037	0.057	No

Table C3.2 (continued)

P14854	Cytochrome c oxidase subunit 6B1	182	7625369 ± 860239	5588615 ± 1518204	**0.73**	0.0037	0.057	Yes
Q00610	Clathrin heavy chain 1	539	34740201 ± 4101304	26503286 ± 7930865	**0.76**	0.0038	0.073	No
Q13404	Ubiquitin-conjugating enzyme E2 variant 1	5	45738 ± 14110	31436 ± 12598	**0.69**	0.004	0.068	No
Q99447	Ethanolamine-phosphate cytidylyltransferase	12	1080504 ± 227397	1350245 ± 284875	**1.25**	0.0039	0.073	No
P63010	AP-2 complex subunit beta	794	36444263 ± 3676943	29400801 ± 7619905	**0.81**	0.0039	0.057	Yes
P28838	Cytosol aminopeptidase	36	295905 ± 32200	225996 ± 52395	**0.76**	0.0039	0.057	No
Q9H008	Phospholysine phosphohistidine inorganic pyrophosphate phosphatase	33	823820 ± 170565	639112 ± 181272	**0.78**	0.0039	0.070	Yes
P22626	Heterogeneous nuclear ribonucleoproteins A2/B1	8	30938 ± 4065	23223 ± 6669	**0.75**	0.0040	0.097	Yes
P08758	Annexin A5	15	388800 ± 38333	328120 ± 69393	0.84	0.0040	0.057	No
Q5JSH3	WD repeat-containing protein 44	4	17057 ± 5353	12274 ± 3704	**0.72**	0.0040	0.068	No
Q13642	Four and a half LIM domains protein 1	429	56169752 ± 3995790	43951439 ± 11607676	**0.78**	0.0041	0.075	No
P46459	Vesicle-fusing ATPase	117	4480579 ± 646020	3410547 ± 1011510	**0.76**	0.0041	0.075	No
P12532	Creatine kinase U-type, mitochondrial	512	32447998 ± 4840524	24831697 ± 8891407	**0.77**	0.0041	0.073	No
Q15819	Ubiquitin-conjugating enzyme E2 variant 2	91	3033204 ± 442034	2443212 ± 404953	**0.81**	0.0042	0.12	No
P60903	Protein S100-A10	5	52004 ± 10210	37924 ± 9773	**0.73**	0.0042	0.057	No
O43678	NADH dehydrogenase [ubiquinone] 1 alpha subcomplex subunit 2	185	4762038 ± 678427	3781445 ± 1062741	**0.79**	0.0043	0.057	Yes
P21266	Glutathione S-transferase Mu 3	23	423434 ± 48944	311911 ± 92857	**0.74**	0.0043	0.057	No
Q14103	Heterogeneous nuclear ribonucleoprotein D0	912	48629850 ± 5161699	40105610 ± 10026348	0.82	0.0043	0.071	No

Table C3.2 (continued)

Q13885	Tubulin beta-2A chain	88	1757598 ± 213903	1331511 ± 376249	**0.76**	0.0043	0.057	No
P61421	V-type proton ATPase subunit d 1	36	77755 ± 29934	218219 ± 102573	**2.81**	0.0044	0.057	No
Q14240	Eukaryotic initiation factor 4A-II	16	447793 ± 46577	367571 ± 66651	0.82	0.0044	0.057	No
Q9GZP4	PITH domain-containing protein 1	24	96182 ± 11068	121162 ± 20405	**1.26**	0.0044	0.057	No
Q8N461	F-box/LRR-repeat protein 16	272	52785810 ± 9674218	40713068 ± 8640450	**0.77**	0.0045	0.11	Yes
Q92598	Heat shock protein 105 kDa	45	2058387 ± 782630	1185972 ± 540254	**0.58**	0.0045	0.057	No
P17600	Synapsin-1	11	16099 ± 1795	13016 ± 2287	**0.81**	0.0045	0.080	No
O94826	Mitochondrial import receptor subunit TOM70	134	4627093 ± 544567	5417935 ± 648713	1.17	0.0045	0.057	Yes
Q9BVA1	Tubulin beta-2B chain	138	8571554 ± 1364517	5277024 ± 2430999	**0.62**	0.0046	0.057	No
Q9NVD7	Alpha-parvin	52	1434466 ± 330179	1901286 ± 260593	**1.33**	0.0049	0.060	No
Q15334	Lethal(2) giant larvae protein homolog 1	128	8427790 ± 1033473	5827725 ± 1987981	**0.69**	0.0049	0.081	Yes
P04792	Heat shock protein beta-1	43	896352 ± 62242	792086 ± 112661	0.88	0.0050	0.10	Yes
P11169	Solute carrier family 2, facilitated glucose transporter member 3	36	2575794 ± 510459	1695439 ± 398151	**0.66**	0.0054	0.057	Yes
Q99798	Aconitate hydratase, mitochondrial	50	1240208 ± 120496	998714 ± 140419	**0.81**	0.0056	0.057	Yes
P35241	Radixin	35	420353 ± 25372	313428 ± 81170	**0.75**	0.0056	0.12	Yes
P62140	Serine/threonine-protein phosphatase PP1-beta catalytic subunit	11	32045 ± 6423	23354 ± 8666	**0.73**	0.0056	0.095	Yes
P51858	Hepatoma-derived growth factor	69	1303052 ± 183608	977905 ± 303222	**0.75**	0.0056	0.078	No
Q8IXS6	Paralemmin-2	49	1286269 ± 234398	912509 ± 230780	**0.71**	0.0056	0.069	No
Q96KP4	Cytosolic non-specific dipeptidase	8	150820 ± 39512	96676 ± 27334	**0.64**	0.0057	0.057	Yes
P63104	14-3-3 protein zeta/delta	76	1539993 ± 261557	1085174 ± 375876	**0.70**	0.0057	0.057	No

Table C3.2 (continued)

Q9Y2J0	Rabphilin-3A	52	707178 ± 144454	1082847 ± 422164	**1.53**	0.0059	0.064	Yes
O43615	Mitochondrial import inner membrane translocase subunit TIM44	111	4110047 ± 320581	3263846 ± 761203	**0.79**	0.0060	0.081	Yes
Q13409	Cytoplasmic dynein 1 intermediate chain 2	175	5118020 ± 573254	3762178 ± 1036793	**0.74**	0.0060	0.057	No
P31930	Cytochrome b-c1 complex subunit 1, mitochondrial	29	713319 ± 62296	548139 ± 117095	**0.77**	0.0063	0.057	Yes
Q99685	Monoglyceride lipase	44	1902874 ± 332664	1446403 ± 422568	**0.76**	0.0064	0.12	Yes
P40926	Malate dehydrogenase, mitochondrial	8	66076 ± 6805	77065 ± 11133	1.17	0.0064	0.057	No
O43491	Band 4.1-like protein 2	152	4963929 ± 950338	3971345 ± 980691	**0.80**	0.0064	0.057	No
P11142	Heat shock cognate 71 kDa protein	85	3184294 ± 338468	2649887 ± 562934	0.83	0.0065	0.074	No
P54920	Alpha-soluble NSF attachment protein	46	3141288 ± 322881	2653830 ± 239913	0.84	0.0065	0.057	Yes
O00299	Chloride intracellular channel protein 1	10	106628 ± 14937	86600 ± 19886	0.81	0.0066	0.057	No
O60861	Growth arrest-specific protein 7	33	276625 ± 50129	160248 ± 65831	**0.58**	0.0067	0.057	Yes
O14531	Dihydropyrimidinase-related protein 4	49	949324 ± 111969	1218993 ± 269601	**1.28**	0.0067	0.057	No
P00568	Adenylate kinase isoenzyme 1	59	422900 ± 67598	272527 ± 92506	**0.64**	0.0068	0.064	Yes
Q96F07	Cytoplasmic FMR1-interacting protein 2	107	5399924 ± 484933	4300774 ± 927149	**0.80**	0.0068	0.091	Yes
Q9NTX5	Ethylmalonyl-CoA decarboxylase	29	82481 ± 9203	98965 ± 19516	1.20	0.0068	0.057	No
P12268	Inosine-5'-monophosphate dehydrogenase 2	30	299500 ± 28080	219018 ± 61175	**0.73**	0.0068	0.13	Yes
Q9Y490	Talin-1	60	533526 ± 55824	480080 ± 46324	0.90	0.0069	0.097	No
Q10567	AP-1 complex subunit beta-1	6	76838 ± 19059	50154 ± 11667	**0.65**	0.0070	0.081	Yes

Table C3.2 (continued)

P53779	Mitogen-activated protein kinase 10	52	2935708 ± 293341	2292977 ± 430035	**0.78**	0.0071	0.057	No
Q01813	ATP-dependent 6-phosphofructokinase, platelet type	1000	119550965 ± 12824875	97769611 ± 21140162	0.82	0.0071	0.057	No
P21333	Filamin-A	60	1594911 ± 173936	1201070 ± 345405	**0.75**	0.0072	0.085	No
P11177	Pyruvate dehydrogenase E1 component subunit beta, mitochondrial	35	1180204 ± 174678	912005 ± 276980	**0.77**	0.0074	0.057	Yes
Q9H3Z4	DnaJ homolog subfamily C member 5	184	10303530 ± 1229294	7786074 ± 2402370	**0.76**	0.0075	0.057	No
O75380	NADH dehydrogenase [ubiquinone] iron-sulfur protein 6, mitochondrial	101	2259460 ± 122885	1961833 ± 271179	0.87	0.0075	0.069	Yes
Q86VP6	Cullin-associated NEDD8-dissociated protein 1	41	1374018 ± 123436	971182 ± 315375	**0.71**	0.0075	0.057	No
P51178	1-phosphatidylinositol 4,5-bisphosphate phosphodiesterase delta-1	60	1122212 ± 99748	915069 ± 232317	0.82	0.0076	0.10	No
Q9NQX3	Gephyrin	11	57768 ± 12902	40676 ± 14885	**0.70**	0.0076	0.057	Yes
P38606	V-type proton ATPase catalytic subunit A	67	1737284 ± 284303	1388839 ± 334243	**0.80**	0.0076	0.071	No
P27816	Microtubule-associated protein 4	38	1015705 ± 273606	659869 ± 302384	**0.65**	0.0077	0.057	No
Q07955	Serine/arginine-rich splicing factor 1	33	570452 ± 89533	430396 ± 128846	**0.75**	0.0077	0.068	No
Q14019	Coactosin-like protein	104	2537565 ± 301214	3189419 ± 610427	**1.26**	0.0080	0.060	No
Q9H0U4	Ras-related protein Rab-1B	20	506908 ± 119848	350203 ± 164449	**0.69**	0.0080	0.073	No
Q9C0C9	(E3-independent) E2 ubiquitin-conjugating enzyme	98	3358729 ± 325286	2693985 ± 315144	**0.80**	0.0082	0.073	No
Q9NRW1	Ras-related protein Rab-6B	252	8505792 ± 1104838	6369047 ± 2219772	**0.75**	0.0082	0.084	No
O94967	WD repeat-containing protein 47	41	189536 ± 32305	160474 ± 15642	0.85	0.0082	0.12	No

Table C3.2 (continued)

P63027	Vesicle-associated membrane protein 2	220	11169857 ± 1428592	8869221 ± 2645793	**0.79**	0.0082	0.057	No
O95757	Heat shock 70 kDa protein 4L	7	22533 ± 7156	14558 ± 5462	**0.65**	0.0083	0.073	No
P60174	Triosephosphate isomerase	21	502164 ± 48754	413262 ± 75490	0.82	0.0086	0.057	No
P07910	Heterogeneous nuclear ribonucleoproteins C1/C2 4	4	38096 ± 4304	31193 ± 4810	0.82	0.0087	0.091	No
Q9NQ66	1-phosphatidylinositol 4,5-bisphosphate phosphodiesterase beta-1	71	1364219 ± 105646	1127866 ± 290760	0.83	0.0087	0.057	Yes
Q13424	Alpha-1-syntrophin	81	6428617 ± 910515	11077696 ± 3736141	**1.72**	0.0088	0.057	No
P00846	ATP synthase subunit a	30	331440 ± 39272	419237 ± 68990	**1.26**	0.0089	0.068	No
Q8N987	N-terminal EF-hand calcium-binding protein 1	1204	135544299 ± 12472506	106916745 ± 21834626	**0.79**	0.0089	0.12	Yes
Q9UIW2	Plexin-A1	266	9380777 ± 905869	7619388 ± 842086	0.81	0.0090	0.14	Yes
Q01469	Fatty acid-binding protein, epidermal	9	62859 ± 7001	50144 ± 13303	**0.80**	0.0090	0.081	No
P17987	T-complex protein 1 subunit alpha	41	1254000 ± 70978	1121112 ± 137278	0.89	0.0090	0.11	No
P05413	Fatty acid-binding protein, heart	117	1752789 ± 155359	1338056 ± 253371	**0.76**	0.0092	0.12	No
Q9NX40	OCIA domain-containing protein 1	101	2082851 ± 190614	1614503 ± 413199	**0.78**	0.0092	0.068	No
P68366	Tubulin alpha-4A chain	120	9483327 ± 1848829	6273945 ± 2570859	**0.66**	0.0092	0.078	No
Q9BZV1	UBX domain-containing protein 6	21	167213 ± 26941	131191 ± 30290	**0.78**	0.0092	0.089	No
Q9NUQ9	Protein FAM49B	26	336223 ± 51012	502549 ± 164469	**1.49**	0.0093	0.083	No
O15394	Neural cell adhesion molecule 2	11	225438 ± 28982	297346 ± 46634	**1.32**	0.0094	0.085	No
Q9UI12	V-type proton ATPase subunit H	58	431274 ± 40262	308118 ± 89926	**0.71**	0.0094	0.073	No
Q96GW7	Brevican core protein	165	8811184 ± 724961	5939596 ± 2013995	**0.67**	0.0094	0.12	No

Table C3.2 (continued)

P14621	Acylphosphatase-2	120	2833014 ± 411234	2252036 ± 601128	**0.79**	0.0094	0.11	No
Q9NR46	Endophilin-B2	301	9701067 ± 857588	7635449 ± 2369897	**0.79**	0.0095	0.073	No
O43175	D-3-phosphoglycerate dehydrogenase	19	190496 ± 48629	295851 ± 123612	**1.55**	0.0095	0.091	Yes
Q16643	Drebrin	33	334431 ± 44570	253055 ± 89995	**0.76**	0.0096	0.14	No
P32119	Peroxiredoxin-2	91	955837 ± 110649	1220959 ± 238525	**1.28**	0.0098	0.067	No
Q03252	Lamin-B2	730	53963927 ± 2778938	44506761 ± 6564257	0.82	0.0098	0.065	No
P35232	Prohibitin	12	235946 ± 22728	189133 ± 43425	**0.80**	0.0098	0.13	No
O75914	Serine/threonine-protein kinase PAK 3	667	38831692 ± 4811557	26481430 ± 9481344	**0.68**	0.0098	0.057	No
Q9UBB4	Ataxin-10	666	30798747 ± 3049678	24007117 ± 6744571	**0.78**	0.0099	0.12	Yes
Q9Y2Z0	Protein SGT1 homolog	19	234186 ± 52513	290025 ± 41385	1.24	0.010	0.13	No
Q7L5N1	COP9 signalosome complex subunit 6	14	772973 ± 101940	615072 ± 124799	**0.80**	0.010	0.083	No
Q9NY65	Tubulin alpha-8 chain	108	5572303 ± 429315	4449946 ± 1295317	**0.80**	0.010	0.12	No
Q93050	V-type proton ATPase 116 kDa subunit a isoform 1	52	2327765 ± 664632	3669695 ± 1301576	**1.58**	0.010	0.13	No
P62258	14-3-3 protein epsilon	21	177037 ± 41142	229450 ± 36502	**1.30**	0.010	0.088	No
O14979	Heterogeneous nuclear ribonucleoprotein D-like	13	180010 ± 23164	124076 ± 41328	**0.69**	0.010	0.057	No
Q9BPX5	Actin-related protein 2/3 complex subunit 5-like protein	27	301811 ± 30494	220479 ± 69896	**0.73**	0.010	0.068	No
P05129	Protein kinase C gamma type	98	1292264 ± 67109	1440107 ± 145244	1.11	0.010	0.11	No
P31321	cAMP-dependent protein kinase type I-beta regulatory subunit	30	411857 ± 79621	311121 ± 68331	**0.76**	0.011	0.14	No
Q13228	Selenium-binding protein 1	266	8362216 ± 1066344	10963033 ± 1824952	**1.31**	0.011	0.11	Yes
Q12931	Heat shock protein 75 kDa, mitochondrial	71	1176523 ± 288365	2051487 ± 687248	**1.74**	0.011	0.11	No

Table C3.2 (continued)

Q9BPW8	Protein NipSnap homolog 1	180	3129334 ± 355502	2662843 ± 370385	0.85	0.011	0.069	Yes
Q969P0	Immunoglobulin superfamily member 8	37	1289290 ± 233797	1730199 ± 305304	**1.34**	0.011	0.057	No
P62820	Ras-related protein Rab-1A	7	16997 ± 5885	32774 ± 10254	**1.93**	0.011	0.073	No
Q15843	NEDD8	192	5982120 ± 528186	7502045 ± 1254902	**1.25**	0.011	0.076	No
P12956	X-ray repair cross-complementing protein 6	21	202512 ± 48566	315602 ± 75796	**1.56**	0.011	0.12	No
P45974	Ubiquitin carboxyl-terminal hydrolase 5	133	16977558 ± 3784775	10022317 ± 3438685	**0.59**	0.011	0.11	No
O75955	Flotillin-1	9	392263 ± 80543	490389 ± 99043	**1.25**	0.011	0.096	No
Q1KMD3	Heterogeneous nuclear ribonucleoprotein U-like protein 2	6	82923 ± 19879	55735 ± 16929	**0.67**	0.011	0.057	No
Q9Y6V0	Protein piccolo	46	340984 ± 40907	252877 ± 78694	**0.74**	0.011	0.12	No
Q02156	Protein kinase C epsilon type	35	269503 ± 61209	160164 ± 58083	**0.59**	0.012	0.099	Yes
P62942	Peptidyl-prolyl cis-trans isomerase FKBP1A	38	264903 ± 41783	201474 ± 58144	**0.76**	0.012	0.071	No
P10515	Dihydrolipoyllysine-residue acetyltransferase component of pyruvate dehydrogenase complex, mitochondrial	6	31207 ± 8452	20433 ± 4043	**0.65**	0.012	0.091	Yes
O95970	Leucine-rich glioma-inactivated protein 1	119	2855820 ± 278185	3096984 ± 194817	1.08	0.012	0.12	No
P09936	Ubiquitin carboxyl-terminal hydrolase isozyme L1	20	252502 ± 32180	217058 ± 21356	0.86	0.012	0.057	No
O14576	Cytoplasmic dynein 1 intermediate chain 1	24	600304 ± 226863	407093 ± 146638	**0.68**	0.012	0.120	No
Q71U36	Tubulin alpha-1A chain	125	3022811 ± 121252	2505662 ± 522107	0.83	0.012	0.078	No
Q9Y277	Voltage-dependent anion-selective channel protein 3	9	36113 ± 13835	23634 ± 7077	**0.65**	0.012	0.12	No

Table C3.2 (continued)

Q9NP72	Ras-related protein Rab-18	24	493494 ± 42800	402829 ± 94804	0.82	0.013	0.091	No
Q13177	Serine/threonine-protein kinase PAK 2	8	195772 ± 31524	143466 ± 40820	**0.73**	0.013	0.13	No
P61081	NEDD8-conjugating enzyme Ubc12	61	895418 ± 178630	624983 ± 230167	**0.70**	0.013	0.073	No
Q15149	Plectin	61	1707278 ± 186783	2113319 ± 275560	1.24	0.013	0.14	Yes
P16298	Serine/threonine-protein phosphatase 2B catalytic subunit beta isoform	47	450117 ± 58228	625466 ± 123383	**1.39**	0.013	0.14	No
Q9BUF5	Tubulin beta-6 chain	172	4207371 ± 496760	3159832 ± 1104348	**0.75**	0.013	0.085	No
Q9UMF0	Intercellular adhesion molecule 5	10	131882 ± 14468	156422 ± 27946	1.19	0.013	0.13	No
P08574	Cytochrome c1, heme protein, mitochondrial	195	6799347 ± 1033101	5768686 ± 952568	0.85	0.013	0.060	Yes
Q8N8N7	Prostaglandin reductase 2	84	2836261 ± 324290	2215955 ± 661747	**0.78**	0.013	0.12	Yes
O00429	Dynamin-1-like protein	131	5161978 ± 364181	4276975 ± 1047734	0.83	0.013	0.13	Yes
Q00325	Phosphate carrier protein, mitochondrial	93	1907283 ± 267880	1604030 ± 220493	0.84	0.013	0.12	No
Q16658	Fascin	45	443049 ± 44229	503657 ± 44783	1.14	0.013	0.13	No
P55786	Puromycin-sensitive aminopeptidase	43	1003667 ± 62392	762286 ± 181402	**0.76**	0.014	0.091	No
P78559	Microtubule-associated protein 1A	22	203761 ± 18229	168647 ± 38241	0.83	0.014	0.11	No
O14617	AP-3 complex subunit delta-1	18	137669 ± 14566	98312 ± 35989	**0.71**	0.014	0.098	No
O43837	Isocitrate dehydrogenase [NAD] subunit beta, mitochondrial	363	36196560 ± 4572527	25258898 ± 11339120	**0.70**	0.014	0.095	Yes
P49189	4-trimethylaminobutyraldehyde dehydrogenase	47	655696 ± 106743	960839 ± 230149	**1.47**	0.014	0.081	No
P10768	S-formylglutathione hydrolase	36	660238 ± 100773	477177 ± 216430	**0.72**	0.014	0.12	Yes
Q13332	Receptor-type tyrosine-protein phosphatase S	33	359055 ± 34953	252221 ± 78415	**0.70**	0.014	0.12	No
P30519	Heme oxygenase 2	6	32090 ± 5565	22760 ± 8917	**0.71**	0.014	0.078	No
P10915	Hyaluronan and proteoglycan link protein 1	52	983568 ± 77450	852343 ± 146672	0.87	0.014	0.077	No

Table C3.2 (continued)

Q9UDY2	Tight junction protein ZO-2	71	3078717 ± 762489	2404719 ± 515053	**0.78**	0.014	0.13	Yes
P04075	Fructose-bisphosphate aldolase A	100	1034728 ± 97985	872709 ± 175317	0.84	0.015	0.084	No
P13804	Electron transfer flavoprotein subunit alpha, mitochondrial	40	1018027 ± 52829	906717 ± 123042	0.89	0.015	0.067	Yes
Q16623	Syntaxin-1A	53	426417 ± 21037	358211 ± 82481	0.84	0.015	0.064	Yes
P78352	Disks large homolog 4	18	159286 ± 49116	106110 ± 37721	**0.67**	0.015	0.069	Yes
Q9BX66	Sorbin and SH3 domain-containing protein 1	26	488937 ± 44755	419411 ± 81080	0.86	0.015	0.091	No
O15294	UDP-N-acetylglucosamine--peptide N-acetylglucosaminyltransferase 110 kDa subunit	105	3516403 ± 400706	2628257 ± 712161	**0.75**	0.015	0.11	Yes
Q05193	Dynamin-1	26	191711 ± 20835	138477 ± 43071	**0.72**	0.015	0.057	Yes
P61978	Heterogeneous nuclear ribonucleoprotein K	25	145377 ± 23189	122449 ± 21106	0.84	0.015	0.076	No
Q9NQC3	Reticulon-4	77	4123047 ± 242622	3619679 ± 579408	0.88	0.016	0.12	Yes
Q9UPV7	PHD finger protein 24	9	113255 ± 17380	78786 ± 35593	**0.70**	0.016	0.097	Yes
P48147	Prolyl endopeptidase	54	2285472 ± 414162	3133923 ± 698185	**1.37**	0.016	0.13	No
O60313	Dynamin-like 120 kDa protein, mitochondrial	153	2508409 ± 258017	2198434 ± 315592	0.88	0.016	0.10	No
Q14289	Protein-tyrosine kinase 2-beta	13	39836 ± 7226	25643 ± 8884	**0.64**	0.016	0.11	No
O14594	Neurocan core protein	435	24177391 ± 1787403	21524883 ± 2420511	0.89	0.016	0.085	No
P21281	V-type proton ATPase subunit B, brain isoform	38	736319 ± 83616	575296 ± 145172	**0.78**	0.016	0.057	No
P50991	T-complex protein 1 subunit delta	168	7752572 ± 1193685	10081183 ± 1400386	**1.30**	0.017	0.073	No
Q13367	AP-3 complex subunit beta-2	15	224409 ± 43415	166887 ± 63368	**0.74**	0.017	0.13	Yes

Table C3.2 (continued)

O14994	Synapsin-3	125	2995620 ± 337363	2303360 ± 633340	**0.77**	0.017	0.057	No
Q13363	C-terminal-binding protein 1	19	34973 ± 3818	30435 ± 4303	0.87	0.017	0.11	No
Q99962	Endophilin-A1	41	2357217 ± 192499	1931929 ± 521130	0.82	0.017	0.057	No
Q96PU8	Protein quaking	11	23006 ± 3300	18824 ± 3706	0.82	0.017	0.12	No
P00492	Hypoxanthine-guanine phosphoribosyltransferase	84	1346304 ± 162434	1121089 ± 188254	0.83	0.017	0.091	No
P06576	ATP synthase subunit beta, mitochondrial	57	1235997 ± 172688	1037044 ± 131907	0.84	0.017	0.13	No
O94973	AP-2 complex subunit alpha-2	8	121399 ± 14523	92770 ± 32747	**0.76**	0.017	0.097	No
O43237	Cytoplasmic dynein 1 light intermediate chain 2	265	26873009 ± 2098075	22792783 ± 3445476	0.85	0.017	0.10	Yes
P11182	Lipoamide acyltransferase component of branched-chain alpha-keto acid dehydrogenase complex, mitochondrial	244	10878026 ± 1241630	8423767 ± 3027532	**0.77**	0.018	0.13	Yes
Q9UKK9	ADP-sugar pyrophosphatase	104	2192230 ± 265416	1705213 ± 462313	**0.78**	0.018	0.12	No
P56385	ATP synthase subunit e, mitochondrial	72	862204 ± 143882	681734 ± 83528	**0.79**	0.018	0.11	No
P17302	Gap junction alpha-1 protein	221	12228443 ± 1608549	13749070 ± 1176234	1.12	0.018	0.11	Yes
P52209	6-phosphogluconate dehydrogenase, decarboxylating	147	7125764 ± 797257	5810243 ± 1542843	0.82	0.018	0.14	No
P28331	NADH-ubiquinone oxidoreductase 75 kDa subunit, mitochondrial	53	1435415 ± 217028	1725967 ± 202384	1.20	0.018	0.13	Yes
P30626	Sorcin	48	1433113 ± 281614	1029885 ± 369420	**0.72**	0.018	0.089	No
P50213	Isocitrate dehydrogenase [NAD] subunit alpha, mitochondrial	75	2636392 ± 657171	1849367 ± 693213	**0.70**	0.018	0.097	Yes
Q7L099	Protein RUFY3	78	2671582 ± 467089	1908557 ± 760291	**0.71**	0.018	0.11	No
Q9NSE4	Isoleucine--tRNA ligase, mitochondrial	8	164605 ± 21555	135451 ± 20564	0.82	0.018	0.13	Yes
Q9Y5J7	Mitochondrial import inner membrane translocase subunit Tim9	11	158715 ± 26469	122492 ± 30887	**0.77**	0.018	0.13	No

Table C3.2 (continued)

P25705	ATP synthase subunit alpha, mitochondrial	109	2627704 ± 305703	2061231 ± 601160	**0.78**	0.018	0.12	No
Q99961	Endophilin-A2	33	532436 ± 68941	450754 ± 54532	0.85	0.018	0.091	Yes
P21291	Cysteine and glycine-rich protein 1	30	369511 ± 63982	237713 ± 76891	**0.64**	0.019	0.13	Yes
P08559	Pyruvate dehydrogenase E1 component subunit alpha, somatic form, mitochondrial	34	466735 ± 99641	989948 ± 432586	**2.12**	0.019	0.11	Yes
P61088	Ubiquitin-conjugating enzyme E2 N	60	1938659 ± 305384	1355610 ± 487622	**0.70**	0.019	0.091	No
Q6PCE3	Glucose 1,6-bisphosphate synthase	20	129937 ± 21249	183375 ± 57447	**1.41**	0.019	0.13	Yes
Q9UPX8	SH3 and multiple ankyrin repeat domains protein 2	60	430885 ± 56707	332948 ± 112788	**0.77**	0.019	0.13	Yes
P42658	Dipeptidyl aminopeptidase-like protein 6	70	1958489 ± 324342	1548272 ± 443966	**0.79**	0.020	0.11	Yes
O95782	AP-2 complex subunit alpha-1	14	225754 ± 53560	156056 ± 52873	**0.69**	0.020	0.12	Yes
Q4V328	GRIP1-associated protein 1	10	51515 ± 13097	35117 ± 13774	**0.68**	0.020	0.084	Yes
P49418	Amphiphysin	20	102231 ± 18458	145687 ± 22075	**1.43**	0.020	0.12	No
O94772	Lymphocyte antigen 6H	154	3948346 ± 297515	3446300 ± 512251	0.87	0.020	0.13	No
Q00535	Cyclin-dependent-like kinase 5	18	244769 ± 18643	213691 ± 24988	0.87	0.020	0.096	Yes
P31150	Rab GDP dissociation inhibitor alpha	10	81643 ± 18834	97288 ± 9183	1.19	0.020	0.075	No
Q08174	Protocadherin-1	12	177494 ± 17920	133214 ± 41818	**0.75**	0.020	0.067	No
P17677	Neuromodulin	1154	136920741 ± 15189191	113897266 ± 22541731	0.83	0.020	0.099	No
P21283	V-type proton ATPase subunit C 1	18	630109 ± 65334	513622 ± 112836	0.82	0.021	0.12	No
P69905	Hemoglobin subunit alpha	11	253249 ± 16916	218003 ± 42612	0.86	0.021	0.073	No
Q99784	Noelin	50	1212852 ± 255991	913711 ± 251353	**0.75**	0.021	0.14	Yes
Q9P1U1	Actin-related protein 3B	19	126829 ± 16016	152523 ± 23356	1.20	0.021	0.073	No

Table C3.2 (continued)

P13637	Sodium/potassium-transporting ATPase subunit alpha-3	316	27575152 ± 2175084	21087335 ± 4587834	**0.76**	0.021	0.13	No
P37840	Alpha-synuclein	25	180747 ± 32361	239109 ± 43263	**1.32**	0.021	0.12	No
P07437	Tubulin beta chain	525	37151679 ± 3488784	31371328 ± 4469742	0.84	0.021	0.12	No
Q92796	Disks large homolog 3	5	19897 ± 2106	16145 ± 2958	0.81	0.021	0.098	No
O94925	Glutaminase kidney isoform, mitochondrial	16	181436 ± 38119	148030 ± 28224	0.82	0.022	0.057	Yes
P62316	Small nuclear ribonucleoprotein Sm D2	26	287942 ± 22632	232567 ± 66613	**0.81**	0.022	0.13	No
Q16720	Plasma membrane calcium-transporting ATPase 3	18	97954 ± 15454	77921 ± 9623	**0.80**	0.022	0.067	No
P54727	UV excision repair protein RAD23 homolog B	19	193484 ± 21531	234586 ± 29940	1.21	0.022	0.13	No
P31948	Stress-induced-phosphoprotein 1	69	2181829 ± 392035	1671914 ± 507733	**0.77**	0.022	0.095	No
Q9Y6M9	NADH dehydrogenase [ubiquinone] 1 beta subcomplex subunit 9	25	335343 ± 29435	258120 ± 81718	**0.77**	0.022	0.13	Yes
Q9Y3A5	Ribosome maturation protein SBDS	129	902101 ± 99479	1046083 ± 96845	1.16	0.022	0.12	No
Q02218	2-oxoglutarate dehydrogenase, mitochondrial	12	38314 ± 7490	27997 ± 10873	**0.73**	0.022	0.076	No
P49591	Serine--tRNA ligase, cytoplasmic	48	691356 ± 42361	549744 ± 96753	**0.80**	0.023	0.057	No
P13716	Delta-aminolevulinic acid dehydratase	511	35806672 ± 4445329	30207100 ± 3740354	0.84	0.023	0.12	Yes
Q16798	NADP-dependent malic enzyme, mitochondrial	74	1289746 ± 173879	1490616 ± 194914	1.16	0.024	0.12	Yes
Q9UPW8	Protein unc-13 homolog A	6	147160 ± 64171	93886 ± 10644	**0.64**	0.024	0.088	No
Q16143	Beta-synuclein	22	224803 ± 25992	286290 ± 60786	**1.27**	0.024	0.11	No
Q9NX63	MICOS complex subunit MIC19	10	60719 ± 7289	46471 ± 11843	**0.77**	0.024	0.14	No
Q99623	Prohibitin-2	29	932344 ± 93608	658437 ± 169223	**0.71**	0.024	0.10	No

Table C3.2 (continued)

P18433	Receptor-type tyrosine-protein phosphatase alpha	918	340630637 ± 125063243	234991738 ± 74139754	**0.69**	0.024	0.12	No
Q9HAV0	Guanine nucleotide-binding protein subunit beta-4	159	3421416 ± 988783	5264121 ± 1781319	**1.54**	0.024	0.12	No
P19404	NADH dehydrogenase [ubiquinone] flavoprotein 2, mitochondrial	41	1246512 ± 307058	811542 ± 358039	**0.65**	0.024	0.12	No
Q9Y2A7	Nck-associated protein 1	9	93548 ± 23248	60451 ± 20963	**0.65**	0.024	0.091	No
P13798	Acylamino-acid-releasing enzyme	9	56874 ± 9032	68034 ± 9410	1.20	0.024	0.11	No
Q99963	Endophilin-A3	83	640135 ± 95352	490924 ± 112559	**0.77**	0.025	0.090	No
P20020	Plasma membrane calcium-transporting ATPase 1	392	13867661 ± 2259467	10416400 ± 2886192	**0.75**	0.025	0.12	No
P21796	Voltage-dependent anion-selective channel protein 1	359	11126912 ± 916864	8244680 ± 2253358	**0.74**	0.025	0.12	No
O60884	DnaJ homolog subfamily A member 2	15	50865 ± 5975	56169 ± 4374	1.10	0.025	0.12	No
O75044	SLIT-ROBO Rho GTPase-activating protein 2	44	196248 ± 29422	159157 ± 39007	0.81	0.025	0.12	Yes
Q9UPA5	Protein bassoon	28	760656 ± 133247	526260 ± 239841	**0.69**	0.025	0.068	Yes
P50570	Dynamin-2	27	197086 ± 40876	249027 ± 56532	**1.26**	0.025	0.099	No
O43143	Pre-mRNA-splicing factor ATP-dependent RNA helicase DHX15	144	4945737 ± 416645	4273776 ± 647408	0.86	0.025	0.067	Yes
O75145	Liprin-alpha-3	63	764368 ± 53975	611051 ± 179839	**0.80**	0.025	0.081	No
P68371	Tubulin beta-4B chain	201	14960073 ± 3108365	20857925 ± 6564117	**1.39**	0.025	0.091	No
Q9UPR5	Sodium/calcium exchanger 2	20	155488 ± 26367	110514 ± 40701	**0.71**	0.025	0.073	No
Q5T0D9	Tumor protein p63-regulated gene 1-like protein	485	21303577 ± 1945760	16663057 ± 3697811	**0.78**	0.025	0.13	No
O76070	Gamma-synuclein	9	46659 ± 5796	36894 ± 8802	**0.79**	0.025	0.080	No
P27338	Amine oxidase [flavin-containing] B	72	925128 ± 60813	760995 ± 174536	0.82	0.026	0.095	Yes

Table C3.2 (continued)

P48643	T-complex protein 1 subunit epsilon	73	1064714 ± 173602	1388116 ± 226747	**1.30**	0.026	0.12	No
Q14982	Opioid-binding protein/cell adhesion molecule	193	10966951 ± 1582719	7989367 ± 2349028	**0.73**	0.026	0.12	No
Q13451	Peptidyl-prolyl cis-trans isomerase FKBP5	89	1652447 ± 205387	1372976 ± 307040	0.83	0.027	0.12	Yes
Q16795	NADH dehydrogenase [ubiquinone] 1 alpha subcomplex subunit 9, mitochondrial	7	186641 ± 79254	121279 ± 46771	**0.65**	0.027	0.14	Yes
P07311	Acylphosphatase-1	33	938805 ± 138085	713624 ± 206095	**0.76**	0.027	0.14	No
P30084	Enoyl-CoA hydratase, mitochondrial	352	26435840 ± 4568233	38161344 ± 8707359	**1.44**	0.027	0.064	Yes
Q9UJU6	Drebrin-like protein	43	402638 ± 34277	283627 ± 73353	**0.70**	0.027	0.074	Yes
O14490	Disks large-associated protein 1	13	147126 ± 21080	120876 ± 19427	0.82	0.028	0.099	No
P14927	Cytochrome b-c1 complex subunit 7	79	1929969 ± 258171	1269444 ± 571745	**0.66**	0.028	0.075	Yes
P12081	Histidine--tRNA ligase, cytoplasmic	55	1742316 ± 242129	1194242 ± 412821	**0.69**	0.028	0.077	No
Q01814	Plasma membrane calcium-transporting ATPase 2	36	296825 ± 39258	211043 ± 60484	**0.71**	0.028	0.12	Yes
Q13303	Voltage-gated potassium channel subunit beta-2	9	17125 ± 3072	11526 ± 2998	**0.67**	0.028	0.13	No
Q9NX14	NADH dehydrogenase [ubiquinone] 1 beta subcomplex subunit 11, mitochondrial	46	1661473 ± 189728	2108646 ± 198399	**1.27**	0.028	0.12	Yes
Q9Y2J8	Protein-arginine deiminase type-2	75	960230 ± 244528	684310 ± 265030	**0.71**	0.029	0.097	Yes
O43707	Alpha-actinin-4	48	850946 ± 76442	769964 ± 74561	0.90	0.029	0.085	Yes
P05023	Sodium/potassium-transporting ATPase subunit alpha-1	11	257418 ± 55557	185854 ± 42971	**0.72**	0.029	0.083	Yes
Q93009	Ubiquitin carboxyl-terminal hydrolase 7	15	512275 ± 115302	360496 ± 79170	**0.70**	0.030	0.13	No

Table C3.2 (continued)

Q6ZVM7	TOM1-like protein 2	233	18557407 ± 2585602	13590754 ± 4712466	**0.73**	0.030	0.081	No
P61225	Ras-related protein Rap-2b	57	1242821 ± 93409	1090962 ± 176456	0.88	0.030	0.096	No
Q15274	Nicotinate-nucleotide pyrophosphorylase [carboxylating]	49	1706328 ± 301776	1139374 ± 200812	**0.67**	0.030	0.14	Yes
P62745	Rho-related GTP-binding protein RhoB	115	3024845 ± 928391	4890789 ± 1390050	**1.62**	0.030	0.11	No
Q13509	Tubulin beta-3 chain	114	3768675 ± 210200	2910823 ± 1007314	**0.77**	0.031	0.077	No
Q9UEY8	Gamma-adducin	135	3399629 ± 450289	4621423 ± 866268	**1.36**	0.031	0.10	No
Q13423	NAD(P) transhydrogenase, mitochondrial	19	882579 ± 266511	653914 ± 191072	**0.74**	0.031	0.085	Yes
Q9BY11	Protein kinase C and casein kinase substrate in neurons protein 1	10	161841 ± 27322	130312 ± 16769	**0.81**	0.031	0.12	No
Q9ULC3	Ras-related protein Rab-23	40	330037 ± 87861	215141 ± 86210	**0.65**	0.031	0.057	No
P69891	Hemoglobin subunit gamma-1	6	32527 ± 8027	42514 ± 9816	**1.31**	0.031	0.12	No
O00217	NADH dehydrogenase [ubiquinone] iron-sulfur protein 8, mitochondrial	288	14329629 ± 2872875	17548418 ± 3003862	1.22	0.031	0.080	Yes
Q17R89	Rho GTPase-activating protein 44	58	1476517 ± 98779	1194990 ± 304819	**0.81**	0.031	0.11	Yes
P61160	Actin-related protein 2	78	1488274 ± 217813	1132217 ± 343538	**0.76**	0.031	0.083	No
P52597	Heterogeneous nuclear ribonucleoprotein F	6	26310 ± 3358	19387 ± 4713	**0.74**	0.032	0.090	Yes
P09497	Clathrin light chain B	44	2857218 ± 297097	2222850 ± 417853	**0.78**	0.032	0.090	No
O94856	Neurofascin	144	9022947 ± 1506004	6502861 ± 2391287	**0.72**	0.032	0.057	No
P30531	Sodium- and chloride-dependent GABA transporter 1	667	9836898 ± 2144011	16373904 ± 4902346	**1.66**	0.032	0.065	No
O95741	Copine-6	79	2515292 ± 462948	1974354 ± 406630	**0.78**	0.032	0.12	No
O43920	NADH dehydrogenase [ubiquinone] iron-sulfur protein 5	244	7260182 ± 1054143	5459698 ± 1372992	**0.75**	0.032	0.11	Yes

Table C3.2 (continued)

O96000	NADH dehydrogenase [ubiquinone] 1 beta subcomplex subunit 10	137	6780289 ± 552275	5232500 ± 1691610	**0.77**	0.032	0.13	Yes
O75964	ATP synthase subunit g, mitochondrial	30	431709 ± 118079	305435 ± 116246	**0.71**	0.032	0.057	No
P53396	ATP-citrate synthase	9	198527 ± 51453	283953 ± 90190	**1.43**	0.033	0.057	No
P22695	Cytochrome b-c1 complex subunit 2, mitochondrial	121	3958881 ± 340518	3292838 ± 527721	0.83	0.033	0.057	Yes
Q8WVM8	Sec1 family domain-containing protein 1	198	7003234 ± 1011231	8852615 ± 2093936	**1.26**	0.033	0.057	Yes
Q9P2R7	Succinate--CoA ligase [ADP-forming] subunit beta, mitochondrial	35	264598 ± 28245	311501 ± 49965	1.18	0.033	0.089	Yes
Q13153	Serine/threonine-protein kinase PAK 1	34	295014 ± 41926	394827 ± 93825	**1.34**	0.033	0.13	Yes
O60825	6-phosphofructo-2-kinase/fructose-2,6-bisphosphatase 2	45	357799 ± 33004	283482 ± 67885	**0.79**	0.033	0.14	No
P06396	Gelsolin	143	3052199 ± 423012	2472489 ± 363547	0.81	0.033	0.12	Yes
P52306	Rap1 GTPase-GDP dissociation stimulator 1	1009	22163875 ± 3952901	30281699 ± 7367496	**1.37**	0.033	0.057	No
Q99250	Sodium channel protein type 2 subunit alpha	4	15505 ± 2208	11938 ± 4225	**0.77**	0.033	0.057	No
O95219	Sorting nexin-4	8	74615 ± 27557	50278 ± 16776	**0.67**	0.033	0.057	Yes
P37837	Transaldolase	57	1006284 ± 159169	800930 ± 97420	**0.80**	0.033	0.075	No
P62879	Guanine nucleotide-binding protein G(I)/G(S)/G(T) subunit beta-2	28	667645 ± 212780	1217535 ± 352790	**1.82**	0.033	0.10	No
Q6IQ23	Pleckstrin homology domain-containing family A member 7	10	112503 ± 13515	136929 ± 24661	1.22	0.034	0.085	No
P68104	Elongation factor 1-alpha 1	22	34380 ± 3634	27505 ± 4792	**0.80**	0.034	0.073	No
Q12905	Interleukin enhancer-binding factor 2	62	1508248 ± 197419	1165448 ± 406215	**0.77**	0.034	0.099	No

Table C3.2 (continued)

Q9BT78	COP9 signalosome complex subunit 4	22	202846 ± 25958	155288 ± 39156	**0.77**	0.034	0.13	No
P43304	Glycerol-3-phosphate dehydrogenase, mitochondrial	180	22082264 ± 3885755	14103814 ± 4740925	**0.64**	0.034	0.11	No
P49802	Regulator of G-protein signaling 7	17	114169 ± 13037	183607 ± 51727	**1.61**	0.034	0.12	Yes
P49840	Glycogen synthase kinase-3 alpha	10	217313 ± 38287	270081 ± 27671	**1.24**	0.034	0.076	No
Q9UNF0	Protein kinase C and casein kinase substrate in neurons protein 2	37	532492 ± 27657	400014 ± 148515	**0.75**	0.034	0.13	No
P19367	Hexokinase-1	268	70182886 ± 24958146	46228687 ± 14205116	**0.66**	0.035	0.095	No
Q9H936	Mitochondrial glutamate carrier 1	8	61948 ± 8686	49110 ± 9471	**0.79**	0.035	0.11	No
O15511	Actin-related protein 2/3 complex subunit 5	236	18913436 ± 1778287	13893438 ± 3011226	**0.73**	0.035	0.13	No
P09622	Dihydrolipoyl dehydrogenase, mitochondrial	51	2793619 ± 294734	2169008 ± 404341	**0.78**	0.035	0.12	Yes
P55263	Adenosine kinase	138	2411777 ± 458516	3414818 ± 811820	**1.42**	0.035	0.091	No
P29966	Myristoylated alanine-rich C-kinase substrate	84	944167 ± 121496	807102 ± 123783	0.85	0.035	0.073	No
Q9P0L0	Vesicle-associated membrane protein-associated protein A	23	296477 ± 53711	533087 ± 182586	**1.80**	0.036	0.12	No
P49757	Protein numb homolog	29	202647 ± 33737	145269 ± 52118	**0.72**	0.036	0.13	Yes
O14523	Phospholipid transfer protein C2CD2L	7	82503 ± 19997	58917 ± 22066	**0.71**	0.036	0.057	Yes
P16152	Carbonyl reductase [NADPH] 1	25	367717 ± 42623	272074 ± 55845	**0.74**	0.036	0.073	Yes
P51970	NADH dehydrogenase [ubiquinone] 1 alpha subcomplex subunit 8	25	142442 ± 12770	121738 ± 24735	0.85	0.036	0.13	Yes
P61106	Ras-related protein Rab-14	98	1553038 ± 80043	1326967 ± 217518	0.85	0.037	0.12	No
Q8IWQ3	Serine/threonine-protein kinase BRSK2	40	614933 ± 95802	438973 ± 148101	**0.71**	0.037	0.14	No
P13489	Ribonuclease inhibitor	75	3477110 ± 421171	3897900 ± 228802	1.12	0.037	0.13	Yes

Table C3.2 (continued)

Q9Y570	Protein phosphatase methylesterase 1	33	359247 ± 36172	305492 ± 58208	0.85	0.037	0.099	No
P47985	Cytochrome b-c1 complex subunit Rieske, mitochondrial	1249	138804815 ± 12669230	109168401 ± 22466102	**0.79**	0.037	0.12	Yes
Q8WZA2	Rap guanine nucleotide exchange factor 4	13	92521 ± 17520	124820 ± 29564	**1.35**	0.037	0.075	Yes
P30153	Serine/threonine-protein phosphatase 2A 65 kDa regulatory subunit A alpha isoform	16	321749 ± 71611	403782 ± 41805	**1.25**	0.037	0.057	Yes
Q9Y2Q0	Phospholipid-transporting ATPase IA	43	430419 ± 39370	372679 ± 43388	0.87	0.037	0.068	Yes
Q96QK1	Vacuolar protein sorting-associated protein 35	21	1684073 ± 442715	1035824 ± 449149	**0.62**	0.038	0.073	No
P36969	Phospholipid hydroperoxide glutathione peroxidase	38	338644 ± 43261	268319 ± 63304	**0.79**	0.038	0.12	No
P31949	Protein S100-A11	44	1149895 ± 133605	936984 ± 177474	0.81	0.038	0.12	No
P46976	Glycogenin-1	41	1716233 ± 199341	2292948 ± 451122	**1.34**	0.038	0.057	No
P36543	V-type proton ATPase subunit E 1	23	320715 ± 68040	232525 ± 70894	**0.73**	0.038	0.13	No
Q9H0Q0	Protein FAM49A	7	74575 ± 11225	62287 ± 6208	0.84	0.038	0.10	Yes
P29401	Transketolase	272	12351024 ± 1468894	8425658 ± 1665150	**0.68**	0.039	0.067	Yes
Q9NV96	Cell cycle control protein 50A	96	1950569 ± 363209	2611447 ± 716266	**1.34**	0.039	0.064	No
P17540	Creatine kinase S-type, mitochondrial	726	158671193 ± 11918593	130745730 ± 24327723	0.82	0.039	0.092	No
P04350	Tubulin beta-4A chain	5	108247 ± 17698	124492 ± 9906	1.15	0.039	0.090	No
Q9UMR2	ATP-dependent RNA helicase DDX19B	17	144878 ± 13466	124457 ± 21785	0.86	0.039	0.11	No
P14625	Endoplasmin	25	1426048 ± 343059	994675 ± 299980	**0.70**	0.039	0.075	Yes
P13645	Keratin, type I cytoskeletal 10	23	487112 ± 63618	379933 ± 75625	**0.78**	0.040	0.074	No
O43676	NADH dehydrogenase [ubiquinone] 1 beta subcomplex subunit 3	191	4145320 ± 595544	5488107 ± 1056245	**1.32**	0.040	0.12	Yes

Table C3.2 (continued)

P40227	T-complex protein 1 subunit zeta	81	1171218 ± 168959	1584846 ± 359994	**1.35**	0.040	0.12	No
Q2M2I8	AP2-associated protein kinase 1	12	301237 ± 64260	242570 ± 47937	**0.81**	0.040	0.073	Yes
P25713	Metallothionein-3	30	263404 ± 32779	209150 ± 45101	**0.79**	0.040	0.071	No
P68871	Hemoglobin subunit beta	23	395983 ± 51754	295134 ± 105495	**0.75**	0.040	0.057	No
Q9UQB8	Brain-specific angiogenesis inhibitor 1-associated protein 2	313	26696810 ± 5406221	15793066 ± 6075252	**0.59**	0.040	0.13	No
P42704	Leucine-rich PPR motif-containing protein, mitochondrial	234	23507673 ± 4136809	14764000 ± 5074225	**0.63**	0.041	0.071	Yes
P29692	Elongation factor 1-delta	302	13927786 ± 2286961	10127434 ± 3370640	**0.73**	0.041	0.14	No
Q99714	3-hydroxyacyl-CoA dehydrogenase type-2	273	8674091 ± 1128725	6710192 ± 2173841	**0.77**	0.041	0.13	No
O43765	Small glutamine-rich tetratricopeptide repeat-containing protein alpha	115	2867672 ± 452710	3773732 ± 1018146	**1.32**	0.042	0.12	No
P06454	Prothymosin alpha	18	74569 ± 9991	84442 ± 8212	1.13	0.042	0.080	No
P05026	Sodium/potassium-transporting ATPase subunit beta-1	60	1100584 ± 119572	932734 ± 153034	0.85	0.042	0.13	Yes
P80723	Brain acid soluble protein 1	1216	221069734 ± 13959283	186980263 ± 31577759	0.85	0.042	0.073	No
P20674	Cytochrome c oxidase subunit 5A, mitochondrial	23	340648 ± 50817	246547 ± 48255	**0.72**	0.043	0.088	Yes
Q92752	Tenascin-R	13	101491 ± 15313	73628 ± 22759	**0.73**	0.043	0.069	No
O60268	Uncharacterized protein KIAA0513	39	231959 ± 48902	360924 ± 91296	**1.56**	0.043	0.073	No
P60981	Destrin	239	27012917 ± 4085560	19588926 ± 7529699	**0.73**	0.043	0.091	No
Q6NVY1	3-hydroxyisobutyryl-CoA hydrolase, mitochondrial	139	3926022 ± 373488	3036947 ± 893818	**0.77**	0.043	0.073	Yes
P04264	Keratin, type II cytoskeletal 1	18	132086 ± 20179	167832 ± 38779	**1.27**	0.043	0.13	No
P22033	Methylmalonyl-CoA mutase, mitochondrial	176	3954471 ± 944669	6171006 ± 1924010	**1.56**	0.043	0.11	No

Table C3.2 (continued)

Q16775	Hydroxyacylglutathione hydrolase, mitochondrial	28	237790 ± 38205	307961 ± 44996	**1.30**	0.044	0.073	No
P18859	ATP synthase-coupling factor 6, mitochondrial	48	4662535 ± 2150286	2780647 ± 1192889	**0.60**	0.044	0.10	Yes
Q9Y617	Phosphoserine aminotransferase	107	2489660 ± 461428	3226252 ± 853648	**1.30**	0.044	0.13	Yes
P31146	Coronin-1A	61	2444471 ± 291597	1835676 ± 490143	**0.75**	0.044	0.12	Yes
Q99622	Protein C10	31	1059020 ± 446756	663681 ± 276797	**0.63**	0.044	0.097	Yes
Q8WY54	Protein phosphatase 1E	122	3681368 ± 860163	6187544 ± 1577597	**1.68**	0.044	0.12	Yes
Q13526	Peptidyl-prolyl cis-trans isomerase NIMA-interacting 1	11	66283 ± 10606	52749 ± 11633	**0.80**	0.044	0.073	No
Q9NPJ3	Acyl-coenzyme A thioesterase 13	412	122524349 ± 6289658	104325954 ± 16628898	0.85	0.044	0.11	No
P00505	Aspartate aminotransferase, mitochondrial	18	87533 ± 20659	142381 ± 47062	**1.63**	0.044	0.12	No
Q8N111	Cell cycle exit and neuronal differentiation protein 1	15	406618 ± 66640	340621 ± 54371	0.84	0.045	0.081	No
Q14CZ8	Hepatocyte cell adhesion molecule	85	3699150 ± 836721	2102648 ± 926868	**0.57**	0.045	0.13	Yes
P42566	Epidermal growth factor receptor substrate 15	822	105763812 ± 12272326	87796042 ± 18371384	0.83	0.045	0.12	No
Q9H8H3	Methyltransferase-like protein 7A	19	279500 ± 38586	217958 ± 63232	**0.78**	0.045	0.11	No
P10809	60 kDa heat shock protein, mitochondrial	52	1792166 ± 223253	1535811 ± 194476	0.86	0.045	0.11	Yes
Q9NZN3	EH domain-containing protein 3	40	516955 ± 53742	446660 ± 66242	0.86	0.045	0.088	No
P21912	Succinate dehydrogenase [ubiquinone] iron-sulfur subunit, mitochondrial	16	100817 ± 19808	125054 ± 26916	1.24	0.045	0.10	Yes
P61764	Syntaxin-binding protein 1	24	381489 ± 148375	237519 ± 95013	**0.62**	0.045	0.095	No
P20339	Ras-related protein Rab-5A	407	30296983 ± 4625091	22440440 ± 9141638	**0.74**	0.046	0.13	No
O60939	Sodium channel subunit beta-2	46	1512593 ± 281548	1025441 ± 465932	**0.68**	0.046	0.057	No
P50502	Hsc70-interacting protein	17	131157 ± 15772	100983 ± 26523	**0.77**	0.046	0.14	No
P35080	Profilin-2	20	803199 ± 107963	644750 ± 157789	**0.80**	0.046	0.078	No

Table C3.2 (continued)

P02042	Hemoglobin subunit delta	118	2285231 ± 185908	2552174 ± 231908	1.12	0.046	0.11	No
P01023	Alpha-2-macroglobulin	17	1607264 ± 195669	1223534 ± 439699	**0.76**	0.046	0.065	No
Q9H7Z7	Prostaglandin E synthase 2	13	118156 ± 18287	155942 ± 28297	**1.32**	0.047	0.12	No
Q9Y265	RuvB-like 1	82	2913760 ± 375546	2139971 ± 695431	**0.73**	0.047	0.12	No
P61266	Syntaxin-1B	38	611492 ± 165056	432769 ± 145876	**0.71**	0.048	0.073	No
Q15056	Eukaryotic translation initiation factor 4H	30	369447 ± 24715	294539 ± 64158	**0.80**	0.048	0.10	No
P49441	Inositol polyphosphate 1-phosphatase	39	446761 ± 69434	334949 ± 72519	**0.75**	0.048	0.12	No
O00232	26S proteasome non-ATPase regulatory subunit 12	191	12057388 ± 2069038	9523958 ± 2290181	**0.79**	0.049	0.091	No
O43301	Heat shock 70 kDa protein 12A	232	6348826 ± 368183	5171543 ± 889660	0.81	0.050	0.13	No
Q00839	Heterogeneous nuclear ribonucleoprotein U	148	3166346 ± 196175	2686642 ± 405229	0.85	0.050	0.10	No
Q92747	Actin-related protein 2/3 complex subunit 1A	207	9301810 ± 1366652	6800202 ± 2721340	**0.73**	0.050	0.076	No

[a]The accession number from the UniProt human database. [b]PSMs are summed from both batches of samples. [c]Average ± standard deviation calculated from TMT reporter ion intensities, N = 8-10 per group.[d]Bold indicates fold changes < 0.81 and > 1.24. [e]p-values from linear regression model for main effects of diagnosis. [f]Proteins were significant with uncorrected $p < 0.05$ and with same direction of change in ROSMAP TMT dataset. Abbreviations: PSMs, peptide spectral matches; CN, cognitively normal; AD, Alzheimer's disease; ROSMAP, Religious Orders Study and Rush Memory and Aging Project.

Table C3.3. Differentially-expressed proteins in AD postmortem IPL.

Accession Number[a]	Protein Name	PSMs[b]	Average Reporter Ion Intensities[c]		AD/CN[d]	p-Value[e]	Corrected p-value[e]	Significant in ROSMAP[f]
			All CN	All AD				
P21397	Amine oxidase [flavin-containing] A	28	60949 ± 7171	69846 ± 8227	1.15	0.00061	0.16	No
Q13642	Four and a half LIM domains protein 1	2084	89730456 ± 7168060	97444864 ± 8239575	1.09	0.0006	0.16	No
P17844	Probable ATP-dependent RNA helicase DDX5	18	32630 ± 4994	40784 ± 6244	**1.25**	0.0013	0.22	No
Q7Z3D6	D-glutamate cyclase, mitochondrial	45	60477 ± 4946	69712 ± 5426	1.15	0.0013	0.22	No
P11766	Alcohol dehydrogenase class-3	136	1511258 ± 337570	1950481 ± 449297	**1.29**	0.0020	0.30	No
P48739	Phosphatidylinositol transfer protein beta isoform	335	2308029 ± 166224	2170569 ± 103854	0.94	0.0034	0.30	No
Q00839	Heterogeneous nuclear ribonucleoprotein U	64	479076 ± 60771	554735 ± 68059	1.16	0.0037	0.30	No
P51812	Ribosomal protein S6 kinase alpha-3	5244	164587867 ± 10046621	174753443 ± 9713166	1.06	0.004	0.30	No
O75891	Cytosolic 10-formyltetrahydrofolate dehydrogenase	291	1558177 ± 237904	2004294 ± 474731	**1.29**	0.0042	0.30	No
P49189	4-trimethylaminobutyraldehyde dehydrogenase	105	346152 ± 33018	386812 ± 23564	1.12	0.0044	0.30	No
Q15847	Adipogenesis regulatory factor	251	1539504 ± 167848	1758720 ± 142885	1.14	0.0046	0.30	No
P08670	Vimentin	192	2958616 ± 482266	3560947 ± 575369	1.20	0.0055	0.31	No
Q14019	Coactosin-like protein	752	8100481 ± 1358741	9121796 ± 531055	1.13	0.0056	0.31	No
O60749	Sorting nexin-2	127	1016190 ± 194605	1381491 ± 415733	**1.36**	0.0063	0.31	No
P51452	Dual specificity protein phosphatase 3	370	2409826 ± 199924	2684346 ± 164361	1.11	0.0073	0.32	No
P49588	Alanine--tRNA ligase, cytoplasmic	44	195612 ± 33102	225962 ± 27449	1.16	0.0077	0.32	No
Q9NQW7	Xaa-Pro aminopeptidase 1	340	3904149 ± 369721	4394478 ± 300262	1.13	0.0078	0.32	No
O43396	Thioredoxin-like protein 1	264	1817146 ± 110635	1919912 ± 99838	1.06	0.0080	0.32	No
P41208	Centrin-2	102	584908 ± 24894	629623 ± 37806	1.08	0.0082	0.32	No
P06744	Glucose-6-phosphate isomerase	216	4244112 ± 331301	3831243 ± 410893	0.90	0.0092	0.33	No
P48163	NADP-dependent malic enzyme	357	3745092 ± 270909	3975326 ± 140448	1.06	0.0092	0.33	No

Table C3.3 (continued)

P00558	Phosphoglycerate kinase 1	1196	50399800 ± 4702440	55481217 ± 3376705	1.10	0.0093	0.33	No
P21266	Glutathione S-transferase Mu 3	129	598168 ± 71647	776152 ± 217726	**1.30**	0.0095	0.33	No
P30041	Peroxiredoxin-6	648	4937008 ± 759517	5715165 ± 446324	1.16	0.010	0.33	No
Q9ULP0	Protein NDRG4	394	5079631 ± 362979	4604717 ± 433764	0.91	0.010	0.34	No
P16402	Histone H1.3	250	567710 ± 90888	855546 ± 249781	**1.51**	0.011	0.35	No
Q9NR45	Sialic acid synthase	20	47179 ± 5150	52529 ± 5206	1.11	0.011	0.35	No
Q8N335	Glycerol-3-phosphate dehydrogenase 1-like protein	192	1756632 ± 222646	2127147 ± 160893	1.21	0.012	0.35	No
Q9UHD8	Septin-9	641	6765056 ± 985447	7520282 ± 421071	1.11	0.012	0.35	No
P49407	Beta-arrestin-1	16	31454 ± 2806	34758 ± 3230	1.11	0.013	0.36	No
P62937	Peptidyl-prolyl cis-trans isomerase A	341	3531531 ± 334146	3851904 ± 285975	1.09	0.014	0.37	No
P01023	Alpha-2-macroglobulin	108	508955 ± 41644	552108 ± 38271	1.08	0.016	0.40	No
Q14195	Dihydropyrimidinase-related protein 3	122	658810 ± 120345	776331 ± 75997	1.18	0.017	0.41	No
P52565	Rho GDP-dissociation inhibitor 1	12	66111 ± 7538	73365 ± 7315	1.11	0.020	0.43	No
Q8N608	Inactive dipeptidyl peptidase 10	32	652479 ± 59343	579099 ± 77985	0.89	0.020	0.43	No
Q99536	Synaptic vesicle membrane protein VAT-1 homolog	342	3312850 ± 290571	3613253 ± 270143	1.09	0.021	0.43	No
O00186	Syntaxin-binding protein 3	61	112430 ± 17890	136349 ± 29257	1.21	0.023	0.44	No
P17252	Protein kinase C alpha type	174	873977 ± 68462	1085985 ± 105715	**1.24**	0.023	0.44	No
P22307	Non-specific lipid-transfer protein	85	762119 ± 74249	920983 ± 89418	1.21	0.024	0.44	No
O00487	26S proteasome non-ATPase regulatory subunit 14	136	632192 ± 110911	537678 ± 70352	0.85	0.024	0.44	No
P07108	Acyl-CoA-binding protein	125	649208 ± 31099	694380 ± 52679	1.07	0.024	0.44	No
P42025	Beta-centractin	476	2600795 ± 356982	2196764 ± 227337	0.84	0.025	0.46	No
Q13424	Alpha-1-syntrophin	1000	12007385 ± 746185	13423690 ± 1536795	1.12	0.026	0.47	No
Q9NVD7	Alpha-parvin	111	1637240 ± 219318	1922091 ± 210363	1.17	0.026	0.47	No
P08758	Annexin A5	155	1330731 ± 387941	1772117 ± 264716	**1.33**	0.028	0.47	No

Table C3.3 (continued)

P62805	Histone H4	720	4344720 ± 391311	4765140 ± 192116	1.10	0.029	0.47	No
P30085	UMP-CMP kinase	116	430123 ± 27509	477717 ± 43305	1.11	0.029	0.47	No
O94979	Protein transport protein Sec31A	55	604241 ± 54611	660065 ± 46692	1.09	0.030	0.47	No
P52209	6-phosphogluconate dehydrogenase, decarboxylating	28	73575 ± 8822	83028 ± 9025	1.13	0.032	0.49	No
Q9UQ80	Proliferation-associated protein 2G4	52	1340237 ± 198218	1651597 ± 394363	1.23	0.032	0.49	No
P55263	Adenosine kinase	45	310100 ± 41375	279859 ± 13593	0.90	0.033	0.49	No
O43390	Heterogeneous nuclear ribonucleoprotein R	534	5294807 ± 337126	6066164 ± 725763	1.15	0.034	0.49	No
P05198	Eukaryotic translation initiation factor 2 subunit 1	74	417355 ± 46100	508670 ± 68623	1.22	0.034	0.49	No
Q9Y230	RuvB-like 2	254	849684 ± 113075	1005078 ± 107190	1.18	0.034	0.49	No
Q9H492	Microtubule-associated proteins 1A/1B light chain 3A	67	532287 ± 70052	628908 ± 54232	1.18	0.035	0.50	No
P11310	Medium-chain specific acyl-CoA dehydrogenase, mitochondrial	98	665428 ± 82150	735757 ± 51842	1.11	0.035	0.50	No
Q12906	Interleukin enhancer-binding factor 3	282	8192618 ± 648448	8963606 ± 609525	1.09	0.037	0.51	No
P05771	Protein kinase C beta type	155	276292 ± 6447	299846 ± 19913	1.09	0.038	0.51	No
Q03252	Lamin-B2	931	15631900 ± 1001708	17335032 ± 1454581	1.11	0.039	0.51	No
Q9Y570	Protein phosphatase methylesterase 1	180	665758 ± 30114	706002 ± 45900	1.06	0.039	0.52	No
P24752	Acetyl-CoA acetyltransferase, mitochondrial	218	3145236 ± 250747	3683143 ± 449232	1.17	0.041	0.52	No
Q16531	DNA damage-binding protein 1	54	330525 ± 73973	271793 ± 37536	0.82	0.041	0.52	No
P11216	Glycogen phosphorylase, brain form	175	1755816 ± 237368	2226344 ± 270901	**1.27**	0.042	0.52	No
Q9NUP9	Protein lin-7 homolog C	377	5837852 ± 558768	6531336 ± 518302	1.12	0.042	0.52	No
Q92905	COP9 signalosome complex subunit 5	70	270448 ± 51241	322608 ± 32435	1.19	0.043	0.52	No
P07339	Cathepsin D	125	2146170 ± 162919	2331818 ± 170602	1.09	0.045	0.53	No
P28066	Proteasome subunit alpha type-5	481	6765229 ± 501339	7375554 ± 500949	1.09	0.047	0.53	No
P55786	Puromycin-sensitive aminopeptidase	31	101257 ± 10070	90617 ± 11633	0.89	0.048	0.53	No

Table C3.3 (continued)

Q86Y82	Syntaxin-12	89	281115 ± 28542	321406 ± 33349	1.14	0.048	0.53	No
P52306	Rap1 GTPase-GDP dissociation stimulator 1	44	91864 ± 8327	103927 ± 11810	1.13	0.049	0.53	No
P22033	Methylmalonyl-CoA mutase, mitochondrial	287	2196307 ± 409471	2578904 ± 266388	1.17	0.049	0.53	No
Q92974	Rho guanine nucleotide exchange factor 2	454	2329473 ± 320411	2024281 ± 139620	0.87	0.049	0.53	No
P62745	Rho-related GTP-binding protein RhoB	106	1007141 ± 151667	892238 ± 65682	0.89	0.049	0.53	No
P52788	Spermine synthase	141	1481926 ± 204451	1720950 ± 164163	1.16	0.049	0.53	No
P51553	Isocitrate dehydrogenase [NAD] subunit gamma, mitochondrial	66	333526 ± 39917	377276 ± 43387	1.13	0.050	0.53	No
Q15149	Plectin	255	2155758 ± 624008	1591405 ± 224665	**0.74**	0.000049	0.063	Yes
Q6GMV3	Putative peptidyl-tRNA hydrolase PTRHD1	1851	34746379 ± 11400387	51193134 ± 11158378	**1.47**	0.000085	0.063	Yes
P36871	Phosphoglucomutase-1	545	3286767 ± 668566	4358507 ± 736811	**1.33**	0.00066	0.16	Yes
P14136	Glial fibrillary acidic protein	88	228392 ± 62257	285219 ± 44406	**1.25**	0.00066	0.16	Yes
P27338	Amine oxidase [flavin-containing] B	224	1612901 ± 127773	1740616 ± 100984	1.08	0.00092	0.19	Yes
O15540	Fatty acid-binding protein, brain	240	2381276 ± 169487	2612908 ± 189886	1.10	0.003	0.30	Yes
Q09666	Neuroblast differentiation-associated protein AHNAK	1544	40482456 ± 2957837	43492168 ± 2460925	1.07	0.0030	0.30	Yes
P06733	Alpha-enolase	280	1141028 ± 213542	1492459 ± 222162	**1.31**	0.0032	0.30	Yes
Q03001	Dystonin	5201	148476767 ± 9353860	165621968 ± 12079733	1.12	0.0035	0.30	Yes
Q9NV96	Cell cycle control protein 50A	292	1734583 ± 79596	1652094 ± 88610	0.95	0.0035	0.30	Yes
Q13126	S-methyl-5'-thioadenosine phosphorylase	1166	29938813 ± 2870937	33019871 ± 3277896	1.10	0.0042	0.30	Yes
Q15121	Astrocytic phosphoprotein PEA-15	213	3953716 ± 406962	4499238 ± 232274	1.14	0.0048	0.30	Yes
P22626	Heterogeneous nuclear ribonucleoproteins A2/B1	67	330399 ± 26872	357912 ± 21416	1.08	0.0054	0.31	Yes
P16930	Fumarylacetoacetase	46	122572 ± 17825	146044 ± 13065	1.19	0.0061	0.31	Yes

Table C3.3 (continued)

O43741	5'-AMP-activated protein kinase subunit beta-2	296	3099251 ± 191064	3398935 ± 329899	1.10	0.0062	0.31	Yes
P15121	Aldose reductase	1915	14815517 ± 1007996	18724034 ± 1952545	**1.26**	0.0069	0.32	Yes
Q9Y2Q0	Phospholipid-transporting ATPase IA	129	923287 ± 89056	1008285 ± 83859	1.09	0.0069	0.32	Yes
P31153	S-adenosylmethionine synthase isoform type-2	55	93320 ± 5909	102525 ± 5894	1.10	0.0073	0.32	Yes
Q16623	Syntaxin-1A	64	663671 ± 112941	752975 ± 68464	1.13	0.0085	0.32	Yes
Q16204	Coiled-coil domain-containing protein 6	50	297838 ± 26567	264776 ± 20691	0.89	0.012	0.35	Yes
Q9H008	Phospholysine phosphohistidine inorganic pyrophosphate phosphatase	63	158260 ± 13215	175839 ± 20424	1.11	0.012	0.35	Yes
P29218	Inositol monophosphatase 1	444	6563261 ± 484859	7580015 ± 819158	1.15	0.013	0.36	Yes
P22314	Ubiquitin-like modifier-activating enzyme 1	93	325631 ± 26303	364630 ± 31050	1.12	0.013	0.36	Yes
O43175	D-3-phosphoglycerate dehydrogenase	57	155476 ± 15202	173518 ± 18354	1.12	0.013	0.36	Yes
Q9NQ66	1-phosphatidylinositol 4,5-bisphosphate phosphodiesterase beta-1	36	153300 ± 21398	175418 ± 18245	1.14	0.014	0.37	Yes
Q9HCJ6	Synaptic vesicle membrane protein VAT-1 homolog-like	864	9175771 ± 760814	10091152 ± 673190	1.10	0.016	0.40	Yes
P49773	Histidine triad nucleotide-binding protein 1	3804	86527375 ± 6924695	93953633 ± 3837248	1.09	0.016	0.40	Yes
Q15019	Septin-2	93	766050 ± 75279	845275 ± 75510	1.10	0.017	0.41	Yes
P17302	Gap junction alpha-1 protein	131	424443 ± 96485	629501 ± 131405	**1.48**	0.018	0.42	Yes
P00568	Adenylate kinase isoenzyme 1	3548	58540435 ± 19895424	120944512 ± 40827869	**2.07**	0.018	0.43	Yes
P50897	Palmitoyl-protein thioesterase 1	388	3250039 ± 317276	3628079 ± 314481	1.12	0.020	0.43	Yes
Q12765	Secernin-1	68	211066 ± 30688	249581 ± 44661	1.18	0.020	0.43	Yes
Q68DH5	LMBR1 domain-containing protein 2	210	1478975 ± 140853	1628662 ± 120886	1.10	0.021	0.43	Yes

Table C3.3 (continued)

P10645	Chromogranin-A	852	17874629 ± 1565337	19655697 ± 1468364	1.10	0.021	0.43	Yes
Q06830	Peroxiredoxin-1	399	10371157 ± 1222402	12546195 ± 2355919	1.21	0.021	0.43	Yes
Q96DG6	Carboxymethylenebutenolidase homolog	64	123260 ± 34895	151456 ± 22313	1.23	0.022	0.44	Yes
P09211	Glutathione S-transferase P	1217	31399893 ± 1874828	34171498 ± 2747054	1.09	0.023	0.44	Yes
O14818	Proteasome subunit alpha type-7	799	8127324 ± 427719	8567588 ± 461181	1.05	0.026	0.47	Yes
P07195	L-lactate dehydrogenase B chain	21	60326 ± 10577	80477 ± 16493	**1.33**	0.027	0.47	Yes
Q04760	Lactoylglutathione lyase	19	39364 ± 7827	48263 ± 8800	1.23	0.027	0.47	Yes
P60520	Gamma-aminobutyric acid receptor-associated protein-like 2	30	149697 ± 11762	163037 ± 11262	1.09	0.028	0.47	Yes
P40123	Adenylyl cyclase-associated protein 2	82	286181 ± 27432	319635 ± 37093	1.12	0.029	0.47	Yes
Q99497	Protein/nucleic acid deglycase DJ-1	67	403092 ± 59767	460080 ± 39218	1.14	0.029	0.47	Yes
Q16851	UTP--glucose-1-phosphate uridylyltransferase	378	2393515 ± 235354	2833610 ± 402176	1.18	0.030	0.47	Yes
P63151	Serine/threonine-protein phosphatase 2A 55 kDa regulatory subunit B alpha isoform	1397	31336560 ± 2972437	34651264 ± 3063349	1.11	0.031	0.48	Yes
P06756	Integrin alpha-V	47	337043 ± 33541	379101 ± 27757	1.12	0.033	0.49	Yes
Q5T0D9	Tumor protein p63-regulated gene 1-like protein	191	1115777 ± 88880	1224636 ± 129172	1.10	0.036	0.50	Yes
Q9P035	Very-long-chain (3R)-3-hydroxyacyl-CoA dehydratase 3	60	204668 ± 18095	226749 ± 23068	1.11	0.038	0.51	Yes
P52943	Cysteine-rich protein 2	84	253595 ± 20460	274288 ± 11273	1.08	0.038	0.51	Yes
P04406	Glyceraldehyde-3-phosphate dehydrogenase	302	4225870 ± 400360	5026451 ± 434914	1.19	0.039	0.51	Yes
Q99685	Monoglyceride lipase	41	132360 ± 7673	144725 ± 9920	1.09	0.040	0.52	Yes
O60282	Kinesin heavy chain isoform 5C	58	250468 ± 9731	272589 ± 19712	1.09	0.043	0.52	Yes
Q96EQ0	Small glutamine-rich tetratricopeptide repeat-containing protein beta	12	74129 ± 7404	84172 ± 5811	1.14	0.043	0.52	Yes

Table C3.3 (continued)

O95817	BAG family molecular chaperone regulator 3	147	1636592 ± 215683	1452056 ± 162836	0.89	0.043	0.52	Yes
P09936	Ubiquitin carboxyl-terminal hydrolase isozyme L1	1013	5815775 ± 656475	6927292 ± 737505	1.19	0.045	0.53	Yes
P07305	Histone H1.0	131	2493749 ± 579509	3298898 ± 737073	**1.32**	0.045	0.53	Yes
P55072	Transitional endoplasmic reticulum ATPase	10	49552 ± 6105	43235 ± 4621	0.87	0.046	0.53	Yes
P27361	Mitogen-activated protein kinase 3	1893	52416099 ± 1581403	54755543 ± 2193245	1.04	0.048	0.53	Yes
Q9BWD1	Acetyl-CoA acetyltransferase, cytosolic	75	506885 ± 59008	587654 ± 63994	1.16	0.050	0.53	Yes

[a]The accession number from the UniProt human database. [b]PSMs are summed from both batches of samples. [c]Average ± standard deviation calculated from TMT reporter ion intensities, N = 9-10 per group.[d]Bold indicates fold changes < 0.81 and > 1.24. [e]p-values from linear regression model for main effects of diagnosis. [f]Proteins were significant with uncorrected $p < 0.05$ and with same direction of change in ROSMAP TMT dataset. Abbreviations: PSMs, peptide spectral matches; CN, cognitively normal; AD, Alzheimer's disease; ROSMAP, Religious Orders Study and Rush Memory and Aging Project.

Table C3.4. Differentially-expressed proteins in AD postmortem GP.

Accession Number[a]	Protein Name	PSMs[b]	Average Reporter Ion Intensities[c]		AD/CN[d]	p-Value[e]	Corrected p-value[e]	Significant in ROSMAP[f]
			All CN	All AD				
P13639	Elongation factor 2	45	185581 ± 17540	206230 ± 16107	1.11	0.019	1.00	No
P14136	Glial fibrillary acidic protein	2838	63396301 ± 27158255	93361259 ± 30466990	**1.47**	0.043	1.00	Yes
P25788	Proteasome subunit alpha type-3	15	26375 ± 2745	31263 ± 5981	1.19	0.041	1.00	No
Q13228	Methanethiol oxidase	72	525537 ± 55187	616283 ± 110974	1.17	0.043	1.00	Yes
Q14764	Major vault protein	17	57722 ± 16988	39419 ± 15318	**0.68**	0.029	1.00	No
Q9H0Q0	Protein FAM49A	9	109890 ± 16975	92070 ± 16972	0.84	0.041	1.00	Yes

[a]The accession number from the UniProt human database. [b]PSMs are summed from both batches of samples. [c]Average ± standard deviation calculated from TMT reporter ion intensities, N = 9-10 per group.[d]Bold indicates fold changes < 0.81 and > 1.24. [e]p-values from linear regression model for main effects of diagnosis. [f]Proteins were significant with uncorrected $p < 0.05$ and with same direction of change in ROSMAP TMT dataset. Abbreviations: PSMs, peptide spectral matches; CN, cognitively normal; AD, Alzheimer's disease; ROSMAP, Religious Orders Study and Rush Memory and Aging Project.

Table C3.5. IPA significant pathways across regions.

Pathway Name	Hippocampus		IPL		GP	
	-log(p-value)[a]	Proteins in Pathway	-log(p-value)[a]	Proteins in Pathway	-log(p-value)[a]	Proteins in Pathway
Mitochondrial Dysfunction	32.4	ACO2,ATP5F1A, ATP5F1B,ATP5ME, ATP5MG,ATP5PF, COX5A,COX6B1, COX7A2,CYC1,GPD2, GPX4,HSD17B10, MAOB,MAP2K4, MAPK10, MTATP6, NDUFA10,NDUFA2, NDUFA8,NDUFA9, NDUFAB1,NDUFB10, NDUFB11,NDUFB3, NDUFB9,NDUFS1, NDUFS3,NDUFS5, NDUFS6, NDUFS8, NDUFV2,OGDH, PDHA1,SDHB,SNCA, UQCRB,UQCRC1, UQCRC2,UQCRFS1, VDAC1, VDAC3				
Oxidative Phosphorylation	24.8	ATP5F1A,ATP5F1B, ATP5ME,ATP5MG, ATP5PF,COX5A,COX6B1,COX7A2,CYC1, MT-ATP6,NDUFA10, NDUFA2,NDUFA8, NDUFA9, NDUFAB1, NDUFB10,NDUFB11, NDUFB3, NDUFB9, NDUFS1, NDUFS3, NDUFS5,NDUFS6, NDUFS8,NDUFV2, SDHB,UQCRB, UQCRC1, UQCRC2, UQCRFS1				

Table C3.5 (continued)

Synaptogenesis Signaling Pathway	19.6	ACTR2,AP1B1,AP2A1, AP2A2,AP2B1, ARPC1A, ARPC5, ARPC5L,CAMK2A, CAMK2B,CAMK2D, CAMK2G,CDK5,DLG4, DNAJC5,GRIA2, HSPA8, MARCKS, NAPA,NAPB,NECTIN, NSF,PAK1, PRKAR1B, PRKCE,RAB3A, RAB5A,RAP2B,SGTA, SNCA,SNCB,SNCG, STX1A,STX1B, STXBP1,SYN1,SYN3, TLN1,UNC13A, VAMP2		
Sirtuin Signaling Pathway	18.1	ACLY,ATP5F1A, ATP5F1B,ATP5PF, CYC1,GLS, GOT2, H1-3, MT-ATP6, NDUFA10, NDUFA2, NDUFA8,NDUFA9, NDUFAB1,NDUFB10, NDUFB11,NDUFB3, NDUFB9,NDUFS1, NDUFS3,NDUFS5, NDUFS6,NDUFS8, NDUFV2,PDHA1, SDHB, TIMM44, TIMM9,TOMM70, TUBA1A,TUBA4A, TUBA8,UQCRC2, UQCRFS1,VDAC1, VDAC3, XRCC6	2.78	GABARAPL2,H1-0, H1-3, LDHB, MAP1LC3A, MAPK3,PGK1

Table C3.5 (continued)

14-3-3-mediated Signaling	18.0	GSK3A,MAP2K4, MAPK10,PLCB1, PLCD1,PRKCE, PRKCG,RAP2B,SNCA, TUBA1A,TUBA4A, TUBA8,TUBB,TUBB2 A,TUBB2B,TUBB3, TUBB4A, TUBB4B, TUBB6,VIM,YWHAB, YWHAE,YWHAG, YWHAH,YWHAQ, YWHAZ	3.98	GFAP,MAPK3,PLCB1, PRKCA,PRKCB,VIM	1.48	GFAP
Remodeling of Epithelial Adherens Junctions	17.4	ACTN4,ACTR2, ARPC1A,ARPC5, ARPC5L, DNM1, DNM1L,DNM2, MAPRE2,RAB5A, TUBA1A, TUBA4A, TUBA8,TUBB, TUBB2A,TUBB2B, TUBB3,TUBB4A, TUBB4B,TUBB6				
Phagosome Maturation	17.1	ATP6V0A1, ATP6V0D1,ATP6V1A, ATP6V1B2,ATP6V1C1, ATP6V1E1,ATP6V1H, DYNC1I1, DYNC1I2, DYNC1LI2,NAPA, NAPB,NSF,PRDX1, PRDX2,RAB5A, TUBA1A,TUBA4A, TUBA8, TUBB, TUBB2A,TUBB2B, TUBB3,TUBB4A, TUBB4B,TUBB6, VAMP2				

Table C3.5 (continued)

Huntington's Disease Signaling	16.4	AP2A2,ATP5F1A, ATP5F1B,ATP5PF, CDK5,CLTB,CLTC, DLG4,DNAJC5,DNM1, DNM1L,DNM2, DYNC1I2,GLS,GNB2, GNB4,HSPA4,HSPA8, MAP2K4,NAPA,NAPB, NSF,PACSIN1,PLCB1, PRKCE,PRKCG, RPH3A,SDHB, SH3GL3,SNCA, STX1A,VAMP2	2.56	CTSD,MAPK3,PLCB1, PRKCA,PRKCB, STX1A
Clathrin-mediated Endocytosis Signaling	14.3	AAK1,ACTR2,AMPH, AP1B1,AP2A1,AP2A2, AP2B1,ARPC1A, ARPC5,ARPC5L,CLTB, CLTC, DNM1, DNM1L, DNM2,EPS15,FGF1,HS PA8, NUMB, PPP3CB, RAB5A,SH3GL1, SH3GL2,SH3GL3, SH3GLB2,SNAP91, SYNJ1		
Germ Cell-Sertoli Cell Junction Signaling	11.1	A2M,ACTN4,GSN, MAP2K4,MAPK10, PAK1, PAK2,PAK3, RAB8B,RAP2B,RHOB, SORBS1, TUBA1A, TUBA4A,TUBA8, TUBB,TUBB2A, TUBB2B,TUBB3, TUBB4A,TUBB4B, TUBB6		

Table C3.5 (continued)

Sertoli Cell-Sertoli Cell Junction Signaling	10.4	A2M,ACTN4,DLG1, GSK3A,MAP2K4, MAPK10, NECTIN1, PRKAR1B,RAB8B, RAP2B,SORBS1,TJP2, TUBA1A,TUBA4A, TUBA8,TUBB, TUBB2A, TUBB2B, TUBB3,TUBB4A, TUBB4B,TUBB6		
Epithelial Adherens Junction Signaling	10.3	ACTN4,ACTR2, ARPC1A,ARPC5, ARPC5L, BAIAP2, FGF1, NECTIN1, RAP2B,SORBS1, TUBA1A,TUBA4A, TUBA8,TUBB, TUBB2A, TUBB2B, TUBB3,TUBB4A, TUBB4B,TUBB6		
HIPPO signaling	9.69	DLG1,DLG2,DLG3, DLG4,LLGL1,PPP1CB, PPP2CA, PPP2R1A, TJP2,YWHAB, YWHAE,YWHAG, YWHAH,YWHAQ, YWHAZ		
Gap Junction Signaling	9.00	DBN1,GJA1,GRIA2, PLCB1,PLCD1, PPP3CB, PRKAR1B, PRKCE,PRKCG, RAP2B,TJP2,TUBA1A, TUBA4A,TUBA8, TUBB,TUBB2A, TUBB2B, TUBB3, TUBB4A,TUBB4B, TUBB6	2.20	GJA1,MAPK3,PLCB1, PRKCA,PRKCB

Table C3.5 (continued)

Axonal Guidance Signaling	8.63	ACTR2,ARPC1A, ARPC5,ARPC5L, BAIAP2,CDK5,GNB2, GNB4,PAK1,PAK2, PAK3,PFN2,PLCB1, PLCD1,PLXNA1, PPP3CB,PRKAR1B, PRKCE, PRKCG, RAP2B,RTN4, SHANK2,SRGAP2, TUBA1A,TUBA4A, TUBA8,TUBB, TUBB2A,TUBB2B, TUBB3,TUBB4A, TUBB4B,TUBB6		
Protein Ubiquitination Pathway	8.53	DNAJC5,HSP90AA1, HSP90AB1,HSP90B1, HSPA12A,HSPA4, HSPA4L,HSPA8, HSPB1,HSPB8,HSPD1, HSPH1,PSMD12, SUGT1,TRAP1,UBE2K, UBE2M, UBE2N, UBE2O, UBE2V1, UBE2V2,UCHL1,USP5, USP7	1.65	PSMA5,PSMA7, PSMD14,UBA1,UCHL1

Table C3.5 (continued)

Protein Kinase A Signaling	8.29	ADD3,CAMK2A, CAMK2B,CAMK2D, CAMK2G, FLNA, FLNC, GNB2,GNB4, GSK3A,H1-3, PALM2AKAP2,PDE2A, PLCB1,PLCD1, PPP1CB, PPP3CB, PRKAR1B,PRKCE, PRKCG,PTK2B, PTPRA,PTPRS, YWHAB,YWHAE, YWHAG,YWHAH, YWHAQ,YWHAZ	2.61	DUSP3,H1-0,H1-3, MAPK3,PLCB1, PRKCA,PRKCB,PYGB
Actin Cytoskeleton Signaling	8.24	ACTN4,ACTR2, ARPC1A,ARPC5, ARPC5L, BAIAP2, CYFIP2,EZR,FGF1, FLNA,GSN,MSN, NCKAP1,PAK1,PAK2, PAK3,PFN2,PPP1CB, RAP2B,RDX,TLN1		
TCA Cycle II (Eukaryotic)	7.76	ACO2,DLD,IDH3A, IDH3B,MDH2,OGDH, SDHB, SUCLA2		
ERK/MAPK Signaling	7.67	HSPB1,PAK1,PAK2, PAK3,PPP1CB, PPP2CA, PPP2R1A,PRKAR1B, PRKCE,PRKCG, PTK2B, RAP2B, RAPGEF4,TLN1, YWHAB,YWHAG, YWHAH,YWHAQ, YWHAZ	1.57	MAPK3,PPP2R2A, PRKCA,PRKCB

Table C3.5 (continued)

Aldosterone Signaling in Epithelial Cells	7.49	DNAJC5,HSP90AA1, HSP90AB1,HSP90B1, HSPA12A,HSPA4, HSPA4L,HSPA8, HSPB1,HSPB8,HSPD1, HSPH1,PLCB1,PLCD1, PRKCE,PRKCG, TRAP1	1.85	MAPK3,PLCB1, PRKCA,PRKCB
Acetyl-CoA Biosynthesis I (Pyruvate Dehydrogenase Complex)	7.13	DBT,DLAT,DLD,PDH A1,PDHB		
Integrin Signaling	6.98	ACTN4,ACTR2,ARF3, ARF4,ARF5,ARPC1A, ARPC5,ARPC5L,GSN, MAP2K4,PAK1,PAK2, PAK3,PARVA,PFN2, PPP1CB,RAP2B,RHOB, TLN1	1.43	ITGAV,MAPK3, PARVA,RHOB
Signaling by Rho Family GTPases	6.71	ACTR2,ARPC1A, ARPC5,ARPC5L, BAIAP2,EZR, GNB2, GNB4,MAP2K4, MAPK10,MSN,PAK1, PAK2,PAK3,PTK2B, RDX,RHOB,SEPTIN2, SEPTIN9, VIM	3.22	ARHGEF2,GFAP, MAPK3,RHOB, SEPTIN2, SEPTIN9,VIM
RhoA Signaling	6.58	ACTR2,ARPC1A, ARPC5,ARPC5L, BAIAP2,EZR, MSN, PFN2,PLXNA1, PPP1CB,PTK2B,RDX, SEPTIN2,SEPTIN9		

Table C3.5 (continued)

Virus Entry via Endocytic Pathways	6.49	AP1B1,AP2A1,AP2A2, AP2B1,CLTB,CLTC, DNM1,DNM2,FLNA, FLNC,PRKCE,PRKCG, RAP2B		
Regulation of Actin-based Motility by Rho	6.27	ACTR2,ARPC1A, ARPC5,ARPC5L, BAIAP2,GSN, PAK1, PAK2,PAK3,PFN2, PPP1CB,RHOB		
Xenobiotic Metabolism PXR Signaling Pathway	6.26	ALDH9A1,CAMK2A, CAMK2B,CAMK2D, CAMK2G,CDK5,ESD, GSTM3,GSTP1, HSP90AA1, HSP90AB1,HSP90B1, MAOB,PPP1CB, PRKAR1B, PRKCE, PRKCG	4.74	ALDH1L1,ALDH9A1, GSTM3,GSTP1,MAOA, MAOB,PRKCA,PRKCB
Rac Signaling	6.25	ACTR2,ARPC1A, ARPC5,ARPC5L, BAIAP2, CYFIP2, MAP2K4,NCKAP1, PAK1,PAK2,PAK3, PTK2B,RAP2B		
Melatonin Signaling	5.66	CAMK2A,CAMK2B, CAMK2D,CAMK2G, MAP2K4,PLCB1, PLCD1,PRKAR1B, PRKCE, PRKCG	3.07	MAPK3,PLCB1, PRKCA,PRKCB
Synaptic Long Term Potentiation	5.55	CAMK2A,CAMK2B, CAMK2D,CAMK2G, GRIA2, PLCB1, PLCD1,PPP1CB, PPP3CB,PRKAR1B, PRKCE,PRKCG, RAP2B	2.15	MAPK3,PLCB1, PRKCA,PRKCB

Table C3.5 (continued)

p70S6K Signaling	5.55	PLCB1,PLCD1, PPP2CA,PPP2R1A, PRKCE,PRKCG, RAP2B,YWHAB, YWHAE,YWHAG, YWHAH, YWHAQ, YWHAZ	3.01	MAPK3,PLCB1, PPP2R2A,PRKCA, PRKCB	1.47	EEF2
GNRH Signaling	5.48	CAMK2A,CAMK2B, CAMK2D,CAMK2G, MAP2K4,MAPK10, PAK1,PAK2,PAK3, PLCB1, PRKAR1B, PRKCE,PRKCG, PTK2B,RAP2B	1.72	MAPK3,PLCB1, PRKCA,PRKCB		
Opioid Signaling Pathway	5.37	AP1B1,AP2A1,AP2A2, AP2B1,CAMK2A, CAMK2B,CAMK2D, CAMK2G,CLTB,CLTC, MAP2K4,PLCB1, PPP3CB,PRKAR1B, PRKCE, PRKCG, RAP2B,RGS7	2.47	ARRB1,MAPK3, PLCB1,PRKCA, PRKCB,RPS6KA3		
Role of NFAT in Cardiac Hypertrophy	4.98	CAMK2A,CAMK2B, CAMK2D,CAMK2G, GNB2, GNB4, MAP2K4,MAPK10, PLCB1,PLCD1, PPP3CB, PRKAR1B, PRKCE,PRKCG, RAP2B,SLC8A2	1.43	MAPK3,PLCB1, PRKCA,PRKCB		
PI3K/AKT Signaling	4.76	GSK3A,HSP90AA1, HSP90AB1,HSP90B1, PPP2CA,PPP2R1A, RAP2B,SYNJ1, YWHAB,YWHAE, YWHAG,YWHAH, YWHAQ,YWHAZ				

Table C3.5 (continued)

Estrogen Receptor Signaling	4.74	ATP5F1A,CTBP1, CYC1,DLG4,GSK3A, HNRNPD, HSP90AA1, HSP90AB1,HSP90B1, MT-ATP6,PAK1, PLCB1,PLCD1, PPP1CB,PRKAR1B, PRKCE,PRKCG, RAP2B,UQCRC2, UQCRFS1	1.89	DDX5,MAPK3,PLCB1, PRKAB2,PRKCA, PRKCB
Mechanisms of Viral Exit from Host Cells	4.73	LMNB2,PRKCE, PRKCG,SH3GL1, SH3GL2,SH3GL3, SH3GLB2	2.75	LMNB2,PRKCA, PRKCB
Hypoxia Signaling in the Cardiovascular System	4.67	HSP90AA1,HSP90AB1, HSP90B1,UBE2K, UBE2M,UBE2N, UBE2O,UBE2V1, UBE2V2		
Necroptosis Signaling Pathway	4.62	CAMK2A,CAMK2B, CAMK2D,CAMK2G, DNM1L,FKBP1A, PPP3CB,SLC25A3, TIMM44,TIMM9, TOMM70,VDAC1, VDAC3		
Fcγ Receptor-mediated Phagocytosis in Macrophages and Monocytes	4.61	ACTR2,ARPC1A, ARPC5,ARPC5L,EZR, PAK1, PRKCE, PRKCG,PTK2B,TLN1	1.75	MAPK3,PRKCA, PRKCB
Iron homeostasis signaling pathway	4.55	ACO2,ATP6V0A1, ATP6V0D1,ATP6V1A, ATP6V1B2,ATP6V1C1, ATP6V1E1,ATP6V1H, HBB,HBD,HBG1, HMOX2		

Table C3.5 (continued)

fMLP Signaling in Neutrophils	4.54	ACTR2,ARPC1A, ARPC5,ARPC5L, GNB2,GNB4, PLCB1,PPP3CB, PRKCE,PRKCG, RAP2B	2.31	MAPK3,PLCB1, PRKCA,PRKCB
Xenobiotic Metabolism Signaling	4.49	ALDH9A1,CAMK2A, CAMK2B,CAMK2D, CAMK2G,ESD,GSTM3, GSTP1,HSP90AA1, HSP90AB1,HSP90B1, MAOB,MAP2K4, PPP2CA, PPP2R1A, PRKCE,PRKCG, RAP2B	5.12	ALDH1L1,ALDH9A1, GSTM3,GSTP1,MAOA, MAOB,MAPK3, PPP2R2A,PRKCA, PRKCB
Calcium Transport I	4.47	ANXA5,ATP2B1, ATP2B2,ATP2B3		
NRF2-mediated Oxidative Stress Response	4.39	CBR1,DNAJA2, DNAJC5,FKBP5, GSTM3,GSTP1, HSPB8,MAP2K4, PRDX1,PRKCE, PRKCG,RAP2B, STIP1,UBE2K	4.80	GSTM3,GSTP1, HACD3,MAPK3, PRDX1,PRKCA, PRKCB,VCP
Neuropathic Pain Signaling In Dorsal Horn Neurons	4.34	CAMK2A,CAMK2B, CAMK2D,CAMK2G, GRIA2, PLCB1, PLCD1,PRKAR1B, PRKCE,PRKCG	2.53	MAPK3,PLCB1, PRKCA,PRKCB
Reelin Signaling in Neurons	4.11	ACTR2,ARPC1A, ARPC5,ARPC5L, CAMK2A, CAMK2B, CAMK2D,CAMK2G, CDK5,MAP2K4, MAPK10		

Table C3.5 (continued)

Paxillin Signaling	4.09	ACTN4,MAP2K4, MAPK10,PAK1,PAK2, PAK3, PARVA,PTK2B, RAP2B,TLN1		
RhoGDI Signaling	4.00	ACTR2,ARPC1A, ARPC5,ARPC5L,EZR, GNB2, GNB4,MSN, PAK1,PAK2,PAK3, RDX,RHOB	1.67	ARHGDIA,ARHGEF2, PRKCA,RHOB
GABA Receptor Signaling	3.81	ALDH9A1,AP1B1, AP2A1,AP2A2,AP2B1, DNM1, GPHN, NSF, SLC6A1		
Renin-Angiotensin Signaling	3.77	MAP2K4,MAPK10, PAK1,PAK2,PAK3, PRKAR1B,PRKCE, PRKCG,PTK2B,RAP2B	1.49	MAPK3,PRKCA, PRKCB
CXCR4 Signaling	3.72	GNB2,GNB4,MAP2K4, MAPK10,PAK1,PAK2, PAK3,PLCB1,PRKCE, PRKCG,RAP2B,RHOB	2.51	MAPK3,PLCB1, PRKCA,PRKCB,RHOB
Cdc42 Signaling	3.72	ACTR2,ARPC1A, ARPC5,ARPC5L, BAIAP2,LLGL1, MAP2K4,MAPK10, PAK1,PAK2,PAK3, PPP1CB		
Semaphorin Signaling in Neurons	3.64	CDK5,DPYSL4,PAK1, PAK2,PAK3,PLXNA1, RHOB	2.28	DPYSL3,MAPK3, RHOB
Chemokine Signaling	3.61	CAMK2A,CAMK2B, CAMK2D,CAMK2G, PLCB1, PPP1CB, PTK2B,RAP2B	2.90	MAPK3,PLCB1, PRKCA,PRKCB
CCR3 Signaling in Eosinophils	3.59	GNB2,GNB4,PAK1, PAK2,PAK3,PLCB1, PPP1CB, PRKCE, PRKCG,RAP2B	2.21	MAPK3,PLCB1, PRKCA,PRKCB

Table C3.5 (continued)

Ephrin Receptor Signaling	3.42	ACTR2,ARPC1A, ARPC5,ARPC5L, FGF1,GNB2, GNB4, PAK1,PAK2,PAK3, RAP2B,SORBS1		
CREB Signaling in Neurons	3.41	CAMK2A,CAMK2B, CAMK2D,CAMK2G, GNB2, GNB4, GRIA2, PLCB1,PLCD1, PRKAR1B,PRKCE, PRKCG,RAP2B	1.47	MAPK3,PLCB1, PRKCA,PRKCB
nNOS Signaling in Neurons	3.40	CAMK2A,DLG2,DLG4, PPP3CB,PRKCE, PRKCG	1.51	PRKCA,PRKCB
Thrombin Signaling	3.39	CAMK2A,CAMK2B, CAMK2D,CAMK2G, GNB2, GNB4,PLCB1, PLCD1,PPP1CB, PRKCE,PRKCG, RAP2B,RHOB	2.84	ARHGEF2,MAPK3, PLCB1,PRKCA, PRKCB,RHOB
Formaldehyde Oxidation II (Glutathione-dependent)	3.37	ADH5,ESD	1.93	ADH5
Valine Degradation I	3.36	DBT,DLD,ECHS1, HIBCH		
Cell Cycle: G2/M DNA Damage Checkpoint Regulation	3.31	YWHAB,YWHAE, YWHAG,YWHAH, YWHAQ, YWHAZ		
CTLA4 Signaling in Cytotoxic T Lymphocytes	3.29	AP1B1,AP2A1,AP2A2, AP2B1,CLTB,CLTC, PPP2CA,PPP2R1A		

Table C3.5 (continued)

PPARα/RXRα Activation	3.21	AP2A2,CAND1,GOT2, GPD2,HSP90AA1, HSP90AB1,HSP90B1, MAP2K4,PLCB1, PLCD1, PRKAR1B, RAP2B	2.28	MAPK3,PLCB1, PRKAB2,PRKCA, PRKCB
Breast Cancer Regulation by Stathmin1	3.20	CAMK2A,CAMK2B, CAMK2D,CAMK2G, GNB2, GNB4,PAK1, PLCB1,PPP1CB, PPP2CA,PPP2R1A, PRKAR1B,PRKCE, PRKCG,RAP2B, TUBA1A, TUBA4A, TUBA8,TUBB, TUBB2A,TUBB2B, TUBB3,TUBB4A, TUBB4B,TUBB6		
Tec Kinase Signaling	3.20	GNB2,GNB4,MAP2K4, MAPK10,PAK1,PAK2, PAK3,PRKCE,PRKCG, PTK2B,RHOB		
ERK5 Signaling	3.15	RAP2B,YWHAB, YWHAE,YWHAG, YWHAH, YWHAQ, YWHAZ		
Actin Nucleation by ARP-WASP Complex	3.15	ACTR2,ARPC1A, ARPC5,ARPC5L, BAIAP2, RAP2B,RHOB		
ErbB Signaling	3.13	MAP2K4,MAPK10, PAK1,PAK2,PAK3, PRKCE, PRKCG, RAP2B	1.75	MAPK3,PRKCA, PRKCB
Tight Junction Signaling	3.12	LLGL1,NAPA,NAPB, NECTIN1,NSF, PPP2CA, PPP2R1A, PRKAR1B,TJP2, VAMP2,VAPA		

Table C3.5 (continued)

Neuregulin Signaling	3.07	CDK5,DLG4,HSP90AA 1,HSP90AB1,HSP90B1, PRKCE,PRKCG, RAP2B	1.72	MAPK3,PRKCA, PRKCB
Pentose Phosphate Pathway	3.03	PGD,TALDO1,TKT		
Inhibition of ARE-Mediated mRNA Degradation Pathway	3.01	PPP2CA,PPP2R1A, PRKAR1B,YWHAB, YWHAE, YWHAG, YWHAH,YWHAQ, YWHAZ		
Factors Promoting Cardiogenesis in Vertebrates	2.94	CAMK2A,CAMK2B, CAMK2D,CAMK2G, MAP2K4,MAPK10, PLCB1,PLCD1,PRKCE, PRKCG		
Calcium Signaling	2.90	ATP2B1,ATP2B2, ATP2B3,CAMK2A, CAMK2B, CAMK2D, CAMK2G,GRIA2, PPP3CB,PRKAR1B, RAP2B,SLC8A2		
IGF-1 Signaling	2.85	PRKAR1B,RAP2B, YWHAB,YWHAE, YWHAG, YWHAH, YWHAQ,YWHAZ		
Glucocorticoid Receptor Signaling	2.74	A2M,ANXA1,FKBP5, HSP90AA1,HSP90AB1, HSP90B1,HSPA4, HSPA8,KRT1,KRT10, KRT19, MAP2K4, MAPK10,PPP3CB, RAP2B,YWHAH		
Lipid Antigen Presentation by CD1	2.73	AP1B1,AP2A1,AP2A2, AP2B1		

Table C3.5 (continued)

Xenobiotic Metabolism CAR Signaling Pathway	2.70	ALDH9A1,GSTM3, GSTP1,HSP90AA1, HSP90AB1,HSP90B1, MAP2K4,PPP2CA, PPP2R1A,PRKCE, PRKCG	4.80	ALDH1L1,ALDH9A1, GSTM3,GSTP1, MAPK3, PPP2R2A, PRKCA,PRKCB
Glioma Signaling	2.69	CAMK2A,CAMK2B, CAMK2D,CAMK2G, IDH3B,PRKCE, PRKCG,RAP2B	3.32	IDH3G,MAPK3,PA2G4, PRKCA,PRKCB
ILK Signaling	2.68	ACTN4,FLNA,FLNC, GSK3A,MAP2K4, MAPK10, PARVA, PPP2CA,PPP2R1A, RHOB,VIM	2.28	MAPK3,PARVA, PPP2R2A,RHOB,VIM
Dopamine-DARPP32 Feedback in cAMP Signaling	2.67	CDK5,PLCB1,PLCD1, PPP1CB,PPP2CA, PPP2R1A, PPP3CB,PRKAR1B, PRKCE,PRKCG	1.81	PLCB1,PPP2R2A, PRKCA,PRKCB
Pyridoxal 5'-phosphate Salvage Pathway	2.65	CDK5,MAP2K4,PAK1, PAK2,PAK3,PRKCE		
Branched-chain α-keto acid Dehydrogenase Complex	2.61	DBT,DLD		
Cardiac β-adrenergic Signaling	2.57	GNB2,GNB4, PALM2AKAP2,PDE2A, PPP1CB, PPP2CA, PPP2R1A,PRKAR1B, SLC8A2		
Leukocyte Extravasation Signaling	2.56	ACTN4,EZR,MAP2K4, MAPK10,MSN,PRKCE, PRKCG,PTK2B, RAPGEF4,RDX,THY1		

Table C3.5 (continued)

Aryl Hydrocarbon Receptor Signaling	2.53	ALDH9A1,GSTM3, GSTP1,HSP90AA1, HSP90AB1,HSP90B1, HSPB1,NCOA7,NEDD8	3.70	ALDH1L1,ALDH9A1, CTSD,GSTM3,GSTP1, MAPK3
GM-CSF Signaling	2.49	CAMK2A,CAMK2B, CAMK2D,CAMK2G, PPP3CB,RAP2B		
Isoleucine Degradation I	2.48	DLD,ECHS1, HSD17B10	2.47	ACAT1,ACAT2
Cholecystokinin/ Gastrin-mediated Signaling	2.48	MAP2K4,MAPK10, PLCB1,PRKCE, PRKCG,PTK2B, RAP2B,RHOB	3.16	MAPK3,PLCB1, PRKCA,PRKCB,RHOB
CCR5 Signaling in Macrophages	2.47	GNB2,GNB4,MAP2K4, MAPK10,PRKCE, PRKCG, PTK2B		
Molecular Mechanisms of Cancer	2.47	CAMK2A,CAMK2B, CAMK2D,CAMK2G, CDK5, GSK3A, MAP2K4,MAPK10, PAK1,PAK2,PAK3, PLCB1,PRKAR1B, PRKCE,PRKCG, RAP2B,RHOB	2.08	ARHGEF2,MAPK3, PA2G4,PLCB1,PRKCA, PRKCB,RHOB
CD28 Signaling in T Helper Cells	2.46	ACTR2,ARPC1A, ARPC5,ARPC5L, MAP2K4, MAPK10, PAK1,PPP3CB		
α-Adrenergic Signaling	2.42	GNB2,GNB4, PRKAR1B,PRKCE, PRKCG,RAP2B, SLC8A2	2.61	MAPK3,PRKCA, PRKCB,PYGB
G Beta Gamma Signaling	2.41	DNM2,GNB2,GNB4, PAK1,PRKAR1B, PRKCE, PRKCG, RAP2B	1.46	MAPK3,PRKCA, PRKCB

Table C3.5 (continued)

UVC-Induced MAPK Signaling	2.40	MAP2K4,MAPK10, PRKCE,PRKCG, RAP2B	2.48	MAPK3,PRKCA, PRKCB
Caveolar-mediated Endocytosis Signaling	2.40	DNM2,FLNA,FLNC, FLOT1,FLOT2,RAB5A		
PAK Signaling	2.40	MAP2K4,MAPK10, PAK1,PAK2,PAK3, PTK2B, RAP2B		
Salvage Pathways of Pyrimidine Ribonucleotides	2.40	AK1,CDK5,MAP2K4, PAK1,PAK2,PAK3, PRKCE	1.71	AK1,CMPK1,MAPK3
2-ketoglutarate Dehydrogenase Complex	2.39	DLD,OGDH		
Serine Biosynthesis	2.39	PHGDH,PSAT1	1.54	PHGDH
2-oxobutanoate Degradation I	2.39	DLD,MMUT	1.54	MMUT
Nitric Oxide Signaling in the Cardiovascular System	2.35	HSP90AA1,HSP90AB1, HSP90B1,PDE2A, PRKAR1B,PRKCE, PRKCG	1.69	MAPK3,PRKCA, PRKCB
G-Protein Coupled Receptor Signaling	2.34	CAMK2A,CAMK2B, CAMK2D,CAMK2G, PDE2A,PLCB1, PRKAR1B,PRKCE, PRKCG,PTK2B, RAP2B,RAPGEF4, RGS7		
Macropinocytosis Signaling	2.31	ACTN4,PAK1,PRKCE, PRKCG,RAB5A, RAP2B		
P2Y Purigenic Receptor Signaling Pathway	2.31	GNB2,GNB4,PLCB1, PLCD1,PRKAR1B, PRKCE, PRKCG, RAP2B	2.18	MAPK3,PLCB1, PRKCA,PRKCB

Table C3.5 (continued)

B Cell Receptor Signaling	2.28	CAMK2A,CAMK2B, CAMK2D,CAMK2G, GSK3A,MAP2K4,PPP3 CB,PTK2B,RAP2B, SYNJ1		
Gαq Signaling	2.25	GNB2,GNB4,PLCB1, PPP3CB,PRKCE, PRKCG, PTK2B,RGS7, RHOB	2.62	MAPK3,PLCB1, PRKCA,PRKCB,RHOB
Agrin Interactions at Neuromuscular Junction	2.23	MAP2K4,MAPK10, PAK1,PAK2,PAK3, RAP2B		
eNOS Signaling	2.23	DNM2,HSP90AA1, HSP90AB1,HSP90B1, HSPA4, HSPA8, PRKAR1B,PRKCE, PRKCG		
Unfolded protein response	2.23	DNAJA2,HSP90B1, HSPA4,HSPA8,HSPH1		
Pentose Phosphate Pathway (Non-oxidative Branch)	2.22	TALDO1,TKT		
LPS-stimulated MAPK Signaling	2.15	MAP2K4,MAPK10, PAK1,PRKCE,PRKCG, RAP2B	1.91	MAPK3,PRKCA, PRKCB
CDK5 Signaling	2.15	CDK5,MAPK10, PPP1CB,PPP2CA, PPP2R1A, PRKAR1B, RAP2B		
Phospholipase C Signaling	2.13	AHNAK,GNB2,GNB4, MARCKS,PLCB1, PLCD1, PPP1CB, PPP3CB,PRKCE, PRKCG,RAP2B,RHOB	3.85	AHNAK,ARHGEF2, MAPK3,PLCB1, PRKCA, PRKCB, RHOB,RPS6KA3

Table C3.5 (continued)

PI3K Signaling in B Lymphocytes	2.10	CAMK2A,CAMK2B, CAMK2D,CAMK2G, PLCB1,PLCD1, PPP3CB,RAP2B	1.32	MAPK3,PLCB1, PRKCB
Superpathway of Serine and Glycine Biosynthesis I	2.08	PHGDH,PSAT1	1.39	PHGDH
Aspartate Degradation II	2.08	GOT2,MDH2		
IL-8 Signaling	2.05	GNB2,GNB4,MAP2K4, MAPK10,PAK2, PRKCE, PRKCG, PTK2B,RAP2B,RHOB	2.19	ITGAV,MAPK3, PRKCA,PRKCB,RHOB
Crosstalk between Dendritic Cells and Natural Killer Cells	1.99	CAMK2A,CAMK2B, CAMK2D,CAMK2G, FSCN1,TLN1		
Role of PKR in Interferon Induction and Antiviral Response	1.96	HSP90AA1,HSP90AB1, HSP90B1,HSPA4, HSPA8,MAP2K4, MAPK10		
Cardiac Hypertrophy Signaling	1.94	GNB2,GNB4,HSPB1, MAP2K4,MAPK10, PLCB1, PLCD1, PPP3CB,PRKAR1B, RAP2B,RHOB		
Mitotic Roles of Polo-Like Kinase	1.93	HSP90AA1,HSP90AB1, HSP90B1,PPP2CA, PPP2R1A		

Table C3.5 (continued)

Cardiac Hypertrophy Signaling (Enhanced)	1.88	CAMK2A,CAMK2B, CAMK2D,CAMK2G, DLG1, FGF1,GSK3A, HSPB1,MAP2K4, MAPK10,PDE2A, PLCB1,PLCD1, PPP3CB,PRKAR1B, PRKCE,PRKCG, RAP2B		
AMPK Signaling	1.86	AK1,PFKFB2,PFKP, PPM1E,PPP2CA, PPP2R1A, PRKAR1B, RAB1A, RAB3A, RAB8A		
Sucrose Degradation V (Mammalian)	1.86	ALDOA,TPI1		
PFKFB4 Signaling Pathway	1.83	HK1,MAP2K4,PRKAR 1B,TKT	1.53	GPI,MAPK3
ATM Signaling	1.82	H2AX,MAP2K4, MAPK10,PPP2CA, PPP2R1A, USP7		
Glycolysis I	1.80	ALDOA,PFKP,TPI1	4.82	ENO1,GAPDH,GPI, PGK1
Gluconeogenesis I	1.80	ALDOA,MDH2,ME3	6.42	ENO1,GAPDH,GPI, ME1,PGK1
Apelin Liver Signaling Pathway	1.80	GSK3A,MAP2K4, MAPK10		
Apelin Cardiomyocyte Signaling Pathway	1.77	MAPK10,PLCB1,PLCD 1,PRKCE,PRKCG,SLC8 A2	2.56	MAPK3,PLCB1, PRKCA,PRKCB
Endocannabinoid Neuronal Synapse Pathway	1.77	GRIA2,MAPK10, MGLL,PLCB1,PLCD1, PPP3CB, PRKAR1B	1.40	MAPK3,MGLL,PLCB1

Table C3.5 (continued)

TNFR1 Signaling	1.71	MAP2K4,PAK1,PAK2, PAK3		
NER Pathway	1.70	COPS4,COPS6,NEDD8, RAD23B,UBE2N,USP7	1.64	CETN2,COPS5,DDB1
cAMP-mediated signaling	1.69	CAMK2A,CAMK2B, CAMK2D,CAMK2G, PALM2AKAP2,PDE2A, PPP3CB,PRKAR1B, RAPGEF4, RGS7		
Acetyl-CoA Biosynthesis III (from Citrate)	1.68	ACLY		
Adenine and Adenosine Salvage VI	1.68	ADK	2.23	ADK
Dopamine Receptor Signaling	1.67	MAOB,PPP1CB, PPP2CA,PPP2R1A, PRKAR1B	1.98	MAOA,MAOB, PPP2R2A
UVB-Induced MAPK Signaling	1.65	MAP2K4,MAPK10, PRKCE,PRKCG	3.61	MAPK3,PRKCA, PRKCB,RPS6KA3
Androgen Signaling	1.64	GNB2,GNB4, HSP90AA1,HSPA4, PRKAR1B, PRKCE,PRKCG	1.34	MAPK3,PRKCA, PRKCB
Telomerase Signaling	1.63	HSP90AA1,HSP90AB1, HSP90B1,PPP2CA, PPP2R1A,RAP2B		
IL-3 Signaling	1.62	PAK1,PPP3CB,PRKCE, PRKCG,RAP2B	1.95	MAPK3,PRKCA, PRKCB
BEX2 Signaling Pathway	1.62	LGALS1,MAP2K4, MAPK10,PPP2CA, PPP2R1A		
G Protein Signaling Mediated by Tubby	1.59	GNB2,GNB4,PLCB1		

Table C3.5 (continued)

Insulin Receptor Signaling	1.58	ACLY,GSK3A, PPP1CB,PRKAR1B, RAP2B,SYNJ1,VAMP2		
HGF Signaling	1.56	MAP2K4,MAPK10, PAK1,PRKCE,PRKCG, RAP2B	1.56	MAPK3,PRKCA, PRKCB
GPCR-Mediated Nutrient Sensing in Enteroendocrine Cells	1.54	PLCB1,PLCD1, PRKAR1B,PRKCE, PRKCG, RAPGEF4	1.55	PLCB1,PRKCA,PRKCB
Glutamate Receptor Signaling	1.52	DLG4,GLS,GRIA2,HO MER1		
Apelin Endothelial Signaling Pathway	1.49	MAP2K4,MAPK10, PLCB1,PRKCE, PRKCG,RAP2B	3.23	MAPK3,PLCB1, PRKAB2,PRKCA, PRKCB
Phenylalanine Degradation IV (Mammalian, via Side Chain)	1.48	GOT2,MAOB	2.53	MAOA,MAOB
Fc Epsilon RI Signaling	1.46	MAP2K4,MAPK10, PRKCE,PRKCG, RAP2B,SYNJ1	1.50	MAPK3,PRKCA, PRKCB
Noradrenaline and Adrenaline Degradation	1.45	ADH5,ALDH9A1, MAOB	4.29	ADH5,ALDH9A1, MAOA,MAOB
RANK Signaling in Osteoclasts	1.45	GSN,MAP2K4, MAPK10,PPP3CB, PTK2B		
Telomere Extension by Telomerase	1.43	HNRNPA2B1,XRCC6		
Prostate Cancer Signaling	1.39	GSTP1,HSP90AA1, HSP90AB1,HSP90B1, RAP2B	1.79	GSTP1,MAPK3,PA2G4

Table C3.5 (continued)

IL-1 Signaling	1.39	GNB2,GNB4,MAP2K4, MAPK10,PRKAR1B		
Superpathway of Methionine Degradation	1.39	DLD,GOT2,MMUT	1.70	MAT2A,MMUT
Guanine and Guanosine Salvage I	1.39	HPRT1		
GDP-L-fucose Biosynthesis I (from GDP-D-mannose)	1.39	TSTA3		
Glutamine Degradation I	1.39	GLS		
Production of Nitric Oxide and Reactive Oxygen Species in Macrophages	1.38	MAP2K4,MAPK10, PPP1CB,PPP2CA, PPP2R1A, PRKCE, PRKCG,RHOB	2.30	MAPK3,PPP2R2A, PRKCA,PRKCB,RHOB
Parkinson's Signaling	1.37	SNCA,UCHL1	2.41	PARK7,UCHL1
PKCθ Signaling in T Lymphocytes	1.37	CAMK2A,CAMK2B, CAMK2D,CAMK2G, MAP2K4,PPP3CB, RAP2B		
Synaptic Long Term Depression	1.37	GRIA2,PLCB1,PLCD1, PPP2CA,PPP2R1A, PRKCE, PRKCG, RAP2B	2.29	MAPK3,PLCB1, PPP2R2A,PRKCA, PRKCB
Regulation of Cellular Mechanics by Calpain Protease	1.34	ACTN4,EZR,RAP2B, TLN1		
Phagosome Formation	1.34	MARCKS,PLCB1, PLCD1,PRKCE, PRKCG,RHOB	2.20	PLCB1,PRKCA, PRKCB,RHOB
tRNA Charging	1.34	HARS1,IARS2,SARS1		

Table C3.5 (continued)

FAK Signaling	1.33	PAK1,PAK2,PAK3, RAP2B,TLN1		
D-myo-inositol (1,4,5)-trisphosphate Degradation	1.33	INPP1,SYNJ1		
Glycogen Degradation II			4.38	MTAP,PGM1,PYGB
Growth Hormone Signaling			4.21	A2M,MAPK3,PRKCA, PRKCB,RPS6KA3
Role of Tissue Factor in Cancer			4.18	ARRB1,ITGAV, MAPK3,PLCB1, PRKCA,RPS6KA3
Glycogen Degradation III			4.17	MTAP,PGM1,PYGB
Glutaryl-CoA Degradation			3.98	ACAT1,ACAT2,PARK7
Triacylglycerol Degradation			3.78	AARS1,MGLL,PPME1, PRDX6
Melatonin Degradation II			3.69	MAOA,MAOB
Putrescine Degradation III			3.62	ALDH9A1,MAOA, MAOB
mTOR Signaling			3.61	MAPK3,PPP2R2A, PRKAB2,PRKCA, PRKCB, RHOB, RPS6KA3
Tryptophan Degradation III (Eukaryotic)			3.50	ACAT1,ACAT2,PARK7
LPS/IL-1 Mediated Inhibition of RXR Function			3.44	ALDH1L1,ALDH9A1, FABP7,GSTM3,GSTP1, MAOA,MAOB
Tryptophan Degradation X (Mammalian, via Tryptamine)			3.39	ALDH9A1,MAOA, MAOB

Table C3.5 (continued)

Serotonin Degradation	3.19	ADH5,ALDH9A1, MAOA,MAOB
Dopamine Degradation	3.15	ALDH9A1,MAOA, MAOB
NF-κB Activation by Viruses	2.86	ITGAV,MAPK3, PRKCA,PRKCB
Apelin Adipocyte Signaling Pathway	2.86	GSTP1,MAPK3,PRDX6 ,PRKAB2
Ketolysis	2.83	ACAT1,ACAT2
Xenobiotic Metabolism General Signaling Pathway	2.81	GSTM3,GSTP1, MAPK3,PRKCA, PRKCB
Ketogenesis	2.74	ACAT1,ACAT2
UVA-Induced MAPK Signaling	2.58	MAPK3,PLCB1, PRKCA,RPS6KA3
VEGF Signaling	2.56	EIF2S1,MAPK3, PRKCA,PRKCB
Mevalonate Pathway I	2.53	ACAT1,ACAT2
Colanic Acid Building Blocks Biosynthesis	2.53	GPI,UGP2
Superpathway of Geranylgeranyl-diphosphate Biosynthesis I (via Mevalonate)	2.31	ACAT1,ACAT2
Granzyme A Signaling	2.26	H1-0,H1-3
Thrombopoietin Signaling	2.22	MAPK3,PRKCA, PRKCB
ErbB4 Signaling	2.15	MAPK3,PRKCA, PRKCB

Table C3.5 (continued)

Pyrimidine Deoxyribonucleo-tides De Novo Biosynthesis I	2.14	AK1,CMPK1
Heparan Sulfate Biosynthesis (Late Stages)	2.08	AARS1,PPME1,PRDX6
Glutathione Redox Reactions I	2.06	GSTP1,PRDX6
Non-Small Cell Lung Cancer Signaling	2.04	MAPK3,PA2G4, PRKCA
Ovarian Cancer Signaling	2.04	ARRB1,GJA1,MAPK3, PA2G4
Glioma Invasiveness Signaling	2.03	ITGAV,MAPK3,RHOB
Type II Diabetes Mellitus Signaling	2.01	MAPK3,PRKAB2, PRKCA,PRKCB
Erythropoietin Signaling	2.00	MAPK3,PRKCA, PRKCB
Heparan Sulfate Biosynthesis	1.96	AARS1,PPME1,PRDX6
Spermine Biosynthesis	1.93	SMS
S-methyl-5'-thioadenosine Degradation II	1.93	MTAP
Prolactin Signaling	1.92	MAPK3,PRKCA, PRKCB
Superpathway of Cholesterol Biosynthesis	1.90	ACAT1,ACAT2

Table C3.5 (continued)

Role of Pattern Recognition Receptors in Recognition of Bacteria and Viruses	1.89	EIF2S1,MAPK3, PRKCA,PRKCB
VEGF Family Ligand-Receptor Interactions	1.88	MAPK3,PRKCA, PRKCB
PDGF Signaling	1.85	MAPK3,PRKCA, PRKCB
Ceramide Signaling	1.82	CTSD,MAPK3, PPP2R2A
Glutathione-mediated Detoxification	1.82	GSTM3,GSTP1
Ethanol Degradation II	1.82	ADH5,ALDH9A1
Fatty Acid β-oxidation I	1.82	ACADM,SCP2
L-carnitine Biosynthesis	1.76	ALDH9A1
NADH Repair	1.76	GAPDH
Methylglyoxal Degradation I	1.76	GLO1
Thyroid Hormone Biosynthesis	1.76	CTSD
Oxidized GTP and dGTP Detoxification	1.76	RUVBL2
S-adenosyl-L-methionine Biosynthesis	1.76	MAT2A
Pentose Phosphate Pathway (Oxidative Branch)	1.63	PGD

Table C3.5 (continued)

Methylmalonyl Pathway	1.63	MMUT
Pyrimidine Ribonucleotides Interconversion	1.62	AK1,CMPK1
Endothelin-1 Signaling	1.61	MAPK3,PLCB1, PRKCA,PRKCB
Role of IL-17F in Allergic Inflammatory Airway Diseases	1.60	MAPK3,RPS6KA3
Pyrimidine Ribonucleotides De Novo Biosynthesis	1.58	AK1,CMPK1
Serotonin Receptor Signaling	1.58	MAOA,MAOB
HIF1α Signaling	1.54	COPS5,LDHB,MAPK3
CMP-N-acetylneuraminate Biosynthesis I (Eukaryotes)	1.54	NANS
Myo-inositol Biosynthesis	1.54	IMPA1
Tyrosine Degradation I	1.54	FAH
Sphingosine-1-phosphate Signaling	1.50	MAPK3,PLCB1,RHOB
Pyruvate Fermentation to Lactate	1.46	LDHB
GDP-mannose Biosynthesis	1.46	GPI

Table C3.5 (continued)

Glycogen Biosynthesis II (from UDP-D-Glucose)	1.39	UGP2		
EGF Signaling	1.38	MAPK3,PRKCA		
IL-12 Signaling and Production in Macrophages	1.37	MAPK3,PRKCA, PRKCB		
CNTF Signaling	1.36	MAPK3,RPS6KA3		
Diphthamide Biosynthesis			3.10	EEF2

[a]IPA calculated -log(p-value) for each pathway. Only pathways with $p < 0.05$ are shown. Abbreviations: IPL, inferior parietal lobule; GP, globus pallidus.

Table C3.6. Proteins with significant race x diagnosis interactions in AD postmortem hippocampus. These appendix tables can be accessed in the supplementary material in the online version of this dissertation, in the Excel file Supplementary Tables C3.6-3.8.

Table C3.7. Proteins with significant race x diagnosis interactions in AD postmortem IPL. These appendix tables can be accessed in the supplementary material in the online version of this dissertation, in the Excel file Supplementary Tables C3.6-3.8.

Table C3.8. Proteins with significant race x diagnosis interactions in AD postmortem GP. These appendix tables can be accessed in the supplementary material in the online version of this dissertation, in the Excel file Supplementary Tables C3.6-3.8.

APPENDIX D

Supplementary Information for Chapter 4

Data D4.1. Processing of data. This appendix data can be accessed in the supplementary material in the online version of this dissertation, in the Excel file Supplementary Data D4.1.

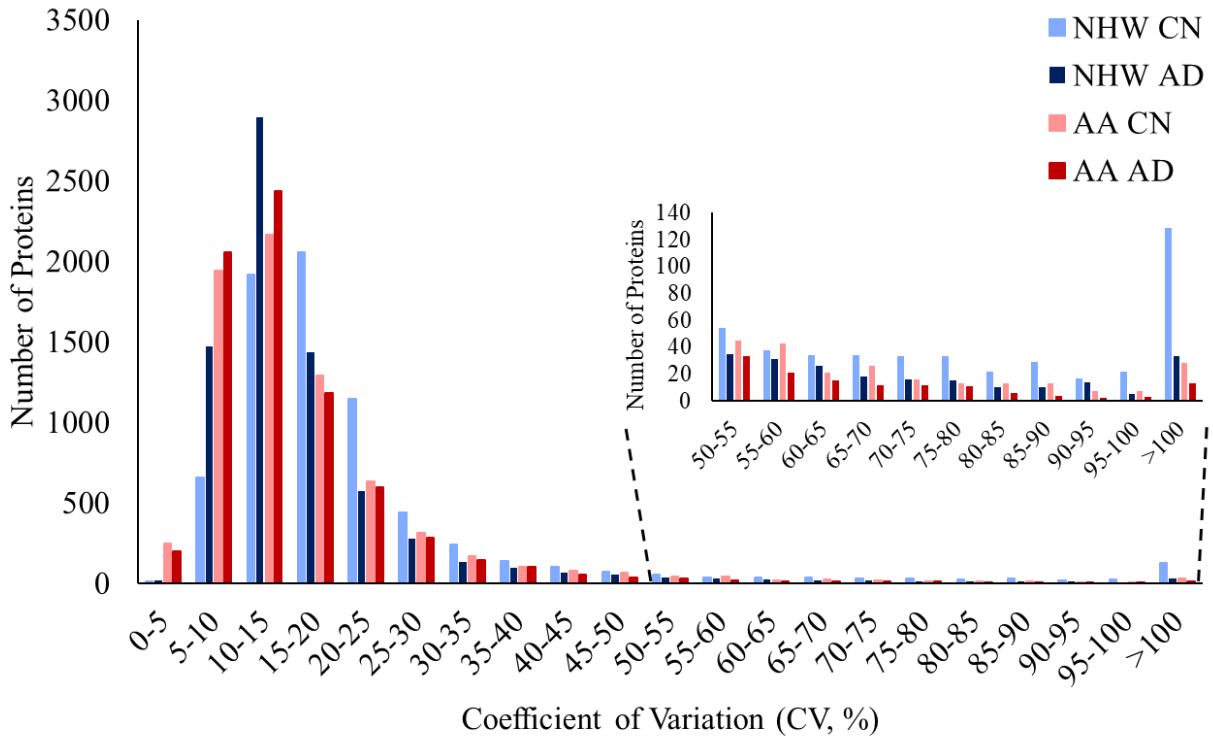

Figure D4.1. Within-group variation across groups. Coefficients of variation (CVs) were calculated within each group using normalized TMT reporter ion intensities. Inset shows a zoomed view of proteins with CVs > 50%. Proteins with CVs greater than two standard deviations from the mean CV in any group (CV > 0.49) were excluded from all groups of differentially-expressed or statistically significant proteins.

Table D4.2. Differentially-expressed proteins in AD.

Accession Number[a]	Protein Name	PSMs[b]	Average Reporter Ion Intensities[c]		AD/CN[d]	p-Value[e]	Corrected p-value[e]	Significant in Pitt[f]
			All CN	All AD				
Q9BVA1	Tubulin beta-2B chain	12863	800556 ± 186152	944290 ± 219460	1.18	0.00081	0.37	No
P14136	Glial fibrillary acidic protein	8316	10319361967 ± 323280262	1348729823 ± 511173545	**1.31**	0.013	0.59	Yes
P07197	Neurofilament medium polypeptide	5072	389453061 ± 131607432	471482584 ± 12677532	1.21	0.023	0.61	No
P07196	Neurofilament light polypeptide	4604	237001916 ± 96157773	299331670 ± 87766332	**1.26**	0.025	0.62	No
P07900	Heat shock protein HSP 90-alpha	4091	141753494 ± 27747913	159743057 ± 18329336	1.13	0.040	0.65	No
P46459	Vesicle-fusing ATPase	3014	99665664 ± 20912637	109477727 ± 15571002	1.10	0.049	0.65	No
P31946	14-3-3 protein beta/alpha	2992	7351918 ± 1480746	7712796 ± 1377747	1.05	0.036	0.65	No
Q9Y4G6	Talin-2	2644	33565900 ± 3461677	30682214 ± 2476061	0.91	0.0011	0.38	No
Q02952	A-kinase anchor protein 12	2541	30121146 ± 2910918	32754401 ± 4241553	1.09	0.038	0.65	No
P06744	Glucose-6-phosphate isomerase	1638	99708978 ± 21115181	113079732 ± 19872529	1.13	0.044	0.65	Yes
P14625	Endoplasmin	1555	31789401 ± 4683898	29961030 ± 3757922	0.94	0.042	0.65	No
P49327	Fatty acid synthase	1487	12804504 ± 1842400	14627900 ± 2197384	1.14	0.019	0.61	No
P32004	Neural cell adhesion molecule L1	1464	24367000 ± 4055358	26333080 ± 3191766	1.08	0.028	0.62	No
P22314	Ubiquitin-like modifier-activating enzyme 1	1449	37991968 ± 5236864	41261451 ± 4871769	1.09	0.040	0.65	Yes
P31948	Stress-induced-phosphoprotein 1	1430	31923776 ± 2990350	34363858 ± 2608291	1.08	0.030	0.64	No

Table D4.2 (continued)

P06753	Tropomyosin alpha-3 chain	1257	21909017 ± 2224903	22656194 ± 2281355	1.03	0.023	0.61	No
Q03252	Lamin-B2	1201	19991850 ± 3616944	18727349 ± 2651368	0.94	0.045	0.65	Yes
P27816	Microtubule-associated protein 4	1196	15346106 ± 2087764	14313928 ± 1617630	0.93	0.017	0.61	No
Q12765	Secernin-1	1142	35411241 ± 3709456	38200593 ± 4176990	1.08	0.027	0.62	Yes
P48735	Isocitrate dehydrogenase [NADP], mitochondrial	1116	36754340 ± 6413218	32547089 ± 4026235	0.89	0.034	0.65	No
P68104	Elongation factor 1-alpha 1	1101	44215739 ± 2949539	47416353 ± 4526338	1.07	0.012	0.59	No
Q13555	Calcium/calmodulin-dependent protein kinase type II subunit gamma	1093	4115626 ± 675914	4630898 ± 667555	1.13	0.0051	0.59	No
Q02790	Peptidyl-prolyl cis-trans isomerase FKBP4	1081	16385173 ± 2263714	18075253 ± 2154378	1.10	0.038	0.65	No
Q05639	Elongation factor 1-alpha 2	1080	28938924 ± 6276252	33129595 ± 3903631	1.14	0.0076	0.59	No
P15104	Glutamine synthetase	1061	68390698 ± 14338682	74967570 ± 15649938	1.10	0.040	0.65	No
Q15843	NEDD8	993	5820828 ± 473870	5462818 ± 422127	0.94	0.0057	0.59	No
Q14697	Neutral alpha-glucosidase AB	970	10626734 ± 959786	9814227 ± 667445	0.92	0.0016	0.44	No
P22626	Heterogeneous nuclear ribonucleoproteins A2/B1	923	35347961 ± 5153337	39492650 ± 3999623	1.12	0.0029	0.54	Yes
P40939	Trifunctional enzyme subunit alpha, mitochondrial	907	23027356 ± 3124150	20275710 ± 2587804	0.88	0.00017	0.20	No
O15394	Neural cell adhesion molecule 2	873	13465726 ± 2877030	14996530 ± 2269074	1.11	0.021	0.61	No
P38117	Electron transfer flavoprotein subunit beta	809	16490108 ± 2013760	15400249 ± 1687270	0.93	0.0026	0.54	No

Table D4.2 (continued)

P30038	Delta-1-pyrroline-5-carboxylate dehydrogenase, mitochondrial	809	17255459 ± 3746873	15999795 ± 2114147	0.93	0.044	0.65	No
Q14980	Nuclear mitotic apparatus protein 1	797	4710444 ± 574756	4494595 ± 458660	0.95	0.039	0.65	No
Q9Y2Q0	Phospholipid-transporting ATPase IA	780	5946521 ± 1370907	6976949 ± 1316090	1.17	0.031	0.64	Yes
P07237	Protein disulfide-isomerase	776	22777403 ± 2729072	21046358 ± 1546144	0.92	0.041	0.65	No
P55084	Trifunctional enzyme subunit beta, mitochondrial	740	15780003 ± 1964896	14066032 ± 1464158	0.89	0.00043	0.33	No
P09382	Galectin-1	727	41050426 ± 8982692	37325009 ± 4114513	0.91	0.031	0.64	No
Q15019	Septin-2	717	21877507 ± 1353617	23134871 ± 2303139	1.06	0.0076	0.59	Yes
Q07157	Tight junction protein ZO-1	707	4749713 ± 728923	4399369 ± 352652	0.93	0.018	0.61	No
Q01518	Adenylyl cyclase-associated protein 1	704	14257164 ± 1518143	13187305 ± 977809	0.92	0.037	0.65	No
P02511	Alpha-crystallin B chain	662	17128371 ± 4230511	19219650 ± 4910736	1.12	0.023	0.61	No
P52565	Rho GDP-dissociation inhibitor 1	631	16662834 ± 2258019	14996990 ± 1886837	0.90	0.0086	0.59	Yes
O15240	Neurosecretory protein VGF	619	4187845 ± 1220009	2943053 ± 805892	0.70	0.0074	0.59	No
P04275	von Willebrand factor	617	3830089 ± 1390176	2911186 ± 611501	**0.76**	0.013	0.60	No
Q02750	Dual specificity mitogen-activated protein kinase kinase 1	614	13345764 ± 1992604	14270780 ± 1612549	1.07	0.048	0.65	No
P28482	Mitogen-activated protein kinase 1	611	25581791 ± 4978937	29760811 ± 4567535	1.16	0.025	0.62	No

Table D4.2 (continued)

Q14847	LIM and SH3 domain protein 1	601	8881480 ± 812584	8339255 ± 811549	0.94	0.022	0.61	No
Q7KZF4	Staphylococcal nuclease domain-containing protein 1	588	5704047 ± 606442	5435996 ± 315545	0.95	0.036	0.65	No
Q9UNF0	Protein kinase C and casein kinase substrate in neurons protein 2	587	2907241 ± 247936	2829985 ± 248442	0.97	0.035	0.65	No
P15259	Phosphoglycerate mutase 2	584	66709 ± 16678	82352 ± 24098	**1.23**	0.038	0.65	No
P10645	Chromogranin-A	578	4464781 ± 902038	5346376 ± 982005	1.20	0.010	0.59	Yes
P30044	Peroxiredoxin-5, mitochondrial	564	21938210 ± 3075303	23705143 ± 2938991	1.08	0.047	0.65	No
P49748	Very long-chain specific acyl-CoA dehydrogenase, mitochondrial	561	7956141 ± 1195093	7105531 ± 846895	0.89	0.034	0.65	No
O00533	Neural cell adhesion molecule L1-like protein	544	5474546 ± 505319	5106882 ± 679891	0.93	0.047	0.65	No
Q9NRW1	Ras-related protein Rab-6B	542	2817949 ± 453055	3221691 ± 427793	1.14	0.040	0.65	No
Q9UIJ7	GTP:AMP phosphotransferase AK3, mitochondrial	536	11132877 ± 1404031	10073461 ± 1009151	0.90	0.027	0.62	No
P21266	Glutathione S-transferase Mu 3	535	11398503 ± 2759655	13330335 ± 3074443	1.17	0.0071	0.59	Yes
P05165	Propionyl-CoA carboxylase alpha chain, mitochondrial	524	5183617 ± 605866	5001826 ± 424661	0.96	0.033	0.65	No
Q9P2E9	Ribosome-binding protein 1	516	2822948 ± 580106	2588860 ± 256981	0.92	0.045	0.65	No
O95433	Activator of 90 kDa heat shock protein ATPase homolog 1	496	8319337 ± 1268630	9218180 ± 933959	1.11	0.0073	0.59	No

Table D4.2 (continued)

P48637	Glutathione synthetase	486	7824344 ± 979264	6816012 ± 990062	0.87	0.024	0.62	No
Q01433	AMP deaminase 2	472	3751399 ± 513452	4168213 ± 507578	1.11	0.021	0.61	No
P13489	Ribonuclease inhibitor	467	11051338 ± 1087669	11574221 ± 1485639	1.05	0.036	0.65	No
P05166	Propionyl-CoA carboxylase beta chain, mitochondrial	459	5028761 ± 507813	4766076 ± 435174	0.95	0.0053	0.59	No
O60716	Catenin delta-1	455	3970652 ± 469218	3563060 ± 280725	0.90	0.0064	0.59	No
Q9Y2J8	Protein-arginine deiminase type-2	446	4486661 ± 647193	5390513 ± 1441683	1.20	0.022	0.61	No
P27361	Mitogen-activated protein kinase 3	432	6350199 ± 1112946	7401385 ± 1199111	1.17	0.0068	0.59	Yes
Q13177	Serine/threonine-protein kinase PAK 2	432	1277135 ± 92511	1227549 ± 84895	0.96	0.015	0.61	No
P20700	Lamin-B1	428	2444848 ± 495471	2189169 ± 212999	0.90	0.026	0.62	No
Q9HCJ6	Synaptic vesicle membrane protein VAT-1 homolog-like	419	3313192 ± 697856	3763728 ± 574586	1.14	0.048	0.65	Yes
O60884	DnaJ homolog subfamily A member 2	416	4933699 ± 499094	5205351 ± 320856	1.06	0.0073	0.59	No
Q96AE4	Far upstream element-binding protein 1	408	2578024 ± 213269	2399702 ± 197467	0.93	0.014	0.60	No
Q969E4	Transcription elongation factor A protein-like 3	406	1084737 ± 221098	1160356 ± 222271	1.07	0.018	0.61	No
Q4J6C6	Prolyl endopeptidase-like	399	6033924 ± 990478	6870102 ± 807920	1.14	0.010	0.59	No
O43157	Plexin-B1	389	1830983 ± 189502	2038176 ± 253808	1.11	0.0070	0.59	No
O75475	PC4 and SFRS1-interacting protein	381	5580844 ± 834464	5092131 ± 941057	0.91	0.0094	0.59	No
P42765	3-ketoacyl-CoA thiolase, mitochondrial	378	8146288 ± 1162077	7403595 ± 850415	0.91	0.00060	0.37	No

Table D4.2 (continued)

P00390	Glutathione reductase, mitochondrial	360	7189316 ± 565831	6514343 ± 581598	0.91	0.012	0.59	No
Q02818	Nucleobindin-1	360	2269002 ± 193450	2131577 ± 213732	0.94	0.026	0.62	No
O43488	Aflatoxin B1 aldehyde reductase member 2	358	9374245 ± 1392419	9163995 ± 1056794	0.98	0.021	0.61	No
Q16698	2,4-dienoyl-CoA reductase [(3E)-enoyl-CoA-producing], mitochondrial	354	9102073 ± 1439692	8342901 ± 917938	0.92	0.017	0.61	No
Q9BZL4	Protein phosphatase 1 regulatory subunit 12C	354	1241504 ± 75292	1178490 ± 83129	0.95	0.023	0.61	No
P00352	Retinal dehydrogenase 1	351	4262838 ± 1575074	3287691 ± 674315	**0.77**	0.012	0.59	No
P62834	Ras-related protein Rap-1A	349	669095 ± 103195	725305 ± 95479	1.08	0.018	0.61	No
Q07065	Cytoskeleton-associated protein 4	348	2463811 ± 500678	2202814 ± 411231	0.89	0.014	0.60	No
P11182	Lipoamide acyltransferase component of branched-chain alpha-keto acid dehydrogenase complex, mitochondrial	346	4722679 ± 532258	4008887 ± 505680	0.85	0.00012	0.19	No
Q13011	Delta(3,5)-Delta(2,4)-dienoyl-CoA isomerase, mitochondrial	346	5854666 ± 1042991	5160945 ± 784922	0.88	0.0095	0.59	No
P20073	Annexin A7	346	3668038 ± 555103	3322296 ± 311840	0.91	0.027	0.62	No
Q15349	Ribosomal protein S6 kinase alpha-2	340	2678758 ± 473939	3129602 ± 527733	1.17	0.010	0.59	No
Q6YN16	Hydroxysteroid dehydrogenase-like protein 2	335	4437672 ± 550817	4007691 ± 370060	0.90	0.00079	0.37	No
Q9NV96	Cell cycle control protein 50A	329	2913637 ± 571613	3425569 ± 648183	1.18	0.042	0.65	Yes

Table D4.2 (continued)

P05455	Lupus La protein	328	3665419 ± 563631	3518509 ± 435211	0.96	0.048	0.65	No
Q96AQ6	Pre-B-cell leukemia transcription factor-interacting protein 1	325	2139039 ± 429979	2406882 ± 359093	1.13	0.049	0.65	No
O43719	HIV Tat-specific factor 1	318	1399748 ± 177014	1519974 ± 196446	1.09	0.0020	0.44	No
P13716	Delta-aminolevulinic acid dehydratase	315	2052567 ± 143513	2216985 ± 188082	1.08	0.034	0.65	No
P51148	Ras-related protein Rab-5C	314	2292145 ± 367147	2138188 ± 317325	0.93	0.027	0.62	No
Q9UK22	F-box only protein 2	311	2307218 ± 298095	2392557 ± 281832	1.04	0.044	0.65	No
P17302	Gap junction alpha-1 protein	307	5620265 ± 1340410	7381224 ± 1991913	**1.31**	0.0064	0.59	Yes
P55010	Eukaryotic translation initiation factor 5	304	2660205 ± 361504	2978398 ± 334834	1.12	0.0060	0.59	No
P26440	Isovaleryl-CoA dehydrogenase, mitochondrial	302	4264461 ± 653853	3767089 ± 542389	0.88	0.0032	0.56	No
P12694	2-oxoisovalerate dehydrogenase subunit alpha, mitochondrial	301	2168688 ± 243827	1906372 ± 185531	0.88	0.00046	0.33	No
Q9UMS4	Pre-mRNA-processing factor 19	297	3498892 ± 299692	3209857 ± 394653	0.92	0.025	0.62	No
P46060	Ran GTPase-activating protein 1	297	2483968 ± 333735	2703152 ± 222607	1.09	0.031	0.64	No
Q8TCS8	Polyribonucleotide nucleotidyltransferase 1, mitochondrial	297	2476688 ± 465856	2232634 ± 224106	0.90	0.040	0.65	No
P23786	Carnitine O-palmitoyltransferase 2, mitochondrial	292	3540951 ± 363191	3121077 ± 450932	0.88	0.015	0.61	No
P51805	Plexin-A3	292	91483 ± 18300	84006 ± 13728	0.92	0.030	0.63	No

Table D4.2 (continued)

Q9HCC0	Methylcrotonoyl-CoA carboxylase beta chain, mitochondrial	288	2389456 ± 342759	2220352 ± 224622	0.93	0.044	0.65	No
Q99784	Noelin	286	3250107 ± 704425	2766038 ± 378263	0.85	0.027	0.62	No
Q96I99	Succinate--CoA ligase [GDP-forming] subunit beta, mitochondrial	284	2945325 ± 609746	2772147 ± 338377	0.94	0.042	0.65	No
P31689	DnaJ homolog subfamily A member 1	281	1485452 ± 217352	1671011 ± 197592	1.12	0.00032	0.29	No
Q9UHW9	Solute carrier family 12 member 6	279	890086 ± 155232	952925 ± 112512	1.07	0.029	0.63	No
P58546	Myotrophin	277	3385462 ± 336278	3596704 ± 425057	1.06	0.020	0.61	No
Q9Y6R0	Numb-like protein	275	2764911 ± 562102	2531928 ± 374185	0.92	0.049	0.65	No
P48739	Phosphatidylinositol transfer protein beta isoform	261	1267073 ± 206029	1302504 ± 160952	1.03	0.027	0.62	Yes
P56545	C-terminal-binding protein 2	261	393880 ± 51063	362835 ± 38292	0.92	0.038	0.65	No
O15018	PDZ domain-containing protein 2	261	786450 ± 133288	710383 ± 79178	0.90	0.041	0.65	No
P56211	cAMP-regulated phosphoprotein 19	256	700114 ± 89600	656397 ± 82239	0.94	0.048	0.65	No
P21695	Glycerol-3-phosphate dehydrogenase [NAD(+)], cytoplasmic	254	1829703 ± 504944	2239218 ± 609483	1.22	0.017	0.61	No
Q5JPE7	Nodal modulator 2	253	1652608 ± 162462	1583151 ± 140519	0.96	0.024	0.61	No
P23381	Tryptophan--tRNA ligase, cytoplasmic	253	3371810 ± 330208	3012710 ± 453604	0.89	0.029	0.63	No
Q06481	Amyloid-like protein 2	253	1011578 ± 43821	1044966 ± 74652	1.03	0.038	0.65	No
Q13492	Phosphatidylinositol-binding clathrin assembly protein	251	1342518 ± 121311	1270668 ± 135728	0.95	0.010	0.59	No

Table D4.2 (continued)

P13987	CD59 glycoprotein	251	8794901 ± 962400	9132280 ± 929753	1.04	0.030	0.64	No
Q9BXM9	FSD1-like protein	251	2558152 ± 372344	2734495 ± 284076	1.07	0.031	0.64	No
Q9BWD1	Acetyl-CoA acetyltransferase, cytosolic	248	3440667 ± 693785	3896395 ± 625488	1.13	0.013	0.60	Yes
Q7L266	Isoaspartyl peptidase/L-asparaginase	245	3616428 ± 487598	3980055 ± 412814	1.10	0.0017	0.44	No
Q9ULP0	Protein NDRG4	240	4279802 ± 825844	4917469 ± 600897	1.15	0.041	0.65	Yes
Q9BY89	Uncharacterized protein KIAA1671	238	765875 ± 73903	724304 ± 52574	0.95	0.010	0.59	No
Q16836	Hydroxyacyl-coenzyme A dehydrogenase, mitochondrial	235	8221487 ± 981240	7828652 ± 817199	0.95	0.028	0.62	No
P26012	Integrin beta-8	233	1532293 ± 274839	1677349 ± 197243	1.09	0.028	0.62	No
O43795	Unconventional myosin-Ib	231	1624887 ± 301083	1428454 ± 139505	0.88	0.039	0.65	No
Q9NZ72	Stathmin-3	230	1298850 ± 271691	1122773 ± 161096	0.86	0.025	0.62	No
P45954	Short/branched chain specific acyl-CoA dehydrogenase, mitochondrial	228	2734117 ± 276153	2245628 ± 390396	0.82	0.00094	0.37	No
Q96MM6	Heat shock 70 kDa protein 12B	227	546961 ± 151359	481360 ± 52422	0.88	0.045	0.65	No
Q99714	3-hydroxyacyl-CoA dehydrogenase type-2	226	2158760 ± 207543	1996355 ± 142480	0.92	0.037	0.65	No
O75326	Semaphorin-7A	223	1022295 ± 181974	1180943 ± 151765	1.16	0.0048	0.59	No
P12429	Annexin A3	220	3079925 ± 1251073	2357267 ± 339645	**0.77**	0.024	0.61	No
Q9HA64	Ketosamine-3-kinase	220	1894649 ± 270636	1751002 ± 228231	0.92	0.034	0.65	No
P49757	Protein numb homolog	218	941110 ± 99765	865126 ± 73114	0.92	0.011	0.59	No

Table D4.2 (continued)

Q96I24	Far upstream element-binding protein 3	215	968140 ± 97738	912371 ± 71264	0.94	0.042	0.65	No
P34897	Serine hydroxymethyltransferase, mitochondrial	211	2120161 ± 428295	1898084 ± 240442	0.90	0.019	0.61	No
Q9NRY5	Protein FAM114A2	210	1263255 ± 120654	1374505 ± 138963	1.09	0.0060	0.59	No
P51610	Host cell factor 1	210	1085622 ± 93740	1033575 ± 92615	0.95	0.018	0.61	No
P42566	Epidermal growth factor receptor substrate 15	210	1089904 ± 66678	1129885 ± 144197	1.04	0.034	0.65	No
P07947	Tyrosine-protein kinase Yes	210	1097435 ± 102867	1162089 ± 110644	1.06	0.036	0.65	No
Q9BQI7	PH and SEC7 domain-containing protein 2	207	1268623 ± 217231	1435333 ± 225618	1.13	0.022	0.61	No
P31937	3-hydroxyisobutyrate dehydrogenase, mitochondrial	205	1288586 ± 160749	1173747 ± 122871	0.91	0.0011	0.37	No
Q9GZV4	Eukaryotic translation initiation factor 5A-2	202	46973 ± 11039	53941 ± 17811	1.15	0.019	0.61	No
Q5JTZ9	Alanine--tRNA ligase, mitochondrial	201	1048727 ± 150198	961050 ± 149124	0.92	0.046	0.65	No
Q6ZWB6	BTB/POZ domain-containing protein KCTD8	200	1117515 ± 96519	1159941 ± 88211	1.04	0.013	0.60	No
Q15052	Rho guanine nucleotide exchange factor 6	199	961850 ± 76439	1019926 ± 96237	1.06	0.029	0.63	No
Q13162	Peroxiredoxin-4	197	360545 ± 110693	300142 ± 46649	0.83	0.044	0.65	No
P30531	Sodium- and chloride-dependent GABA transporter 1	193	1020887 ± 207511	1109990 ± 226825	1.09	0.026	0.62	No
Q6P2I3	Fumarylacetoacetate hydrolase domain-containing protein 2B	189	48765 ± 7842	43484 ± 6165	0.89	0.0038	0.59	No
Q86XP3	ATP-dependent RNA helicase DDX42	189	913005 ± 76436	885021 ± 79261	0.97	0.022	0.61	No

Table D4.2 (continued)

P25787	Proteasome subunit alpha type-2	187	1800142 ± 116910	1738034 ± 134718	0.97	0.036	0.65	No
O75936	Gamma-butyrobetaine dioxygenase	185	1576444 ± 296771	1669693 ± 415733	1.06	0.017	0.61	No
Q5JTV8	Torsin-1A-interacting protein 1	185	1028814 ± 203157	951921 ± 101173	0.93	0.036	0.65	No
P51687	Sulfite oxidase, mitochondrial	184	1774920 ± 176542	1587023 ± 174868	0.89	0.0019	0.44	No
P07686	Beta-hexosaminidase subunit beta	182	2099647 ± 444115	1816904 ± 187624	0.87	0.010	0.59	No
Q9P266	Junctional protein associated with coronary artery disease	181	715553 ± 124212	645467 ± 87256	0.90	0.011	0.59	No
Q09028	Histone-binding protein RBBP4	181	203099 ± 29266	224019 ± 39906	1.10	0.015	0.61	No
Q92947	Glutaryl-CoA dehydrogenase, mitochondrial	178	2087177 ± 330421	1791326 ± 262619	0.86	0.0089	0.59	No
Q86T65	Disheveled-associated activator of morphogenesis 2	176	608596 ± 105458	668041 ± 105448	1.10	0.035	0.65	No
O60547	GDP-mannose 4,6 dehydratase	175	1303018 ± 176230	1210066 ± 82085	0.93	0.016	0.61	No
Q9P0J1	[Pyruvate dehydrogenase [acetyl-transferring]]-phosphatase 1, mitochondrial	175	1221281 ± 144070	1098065 ± 169332	0.90	0.024	0.61	No
Q9UHL4	Dipeptidyl peptidase 2	175	1061294 ± 185426	961329 ± 184985	0.91	0.046	0.65	No
Q13255	Metabotropic glutamate receptor 1	172	661387 ± 115002	755242 ± 130167	1.14	0.037	0.65	No
Q5JTJ3	Cytochrome c oxidase assembly factor 6 homolog	171	1831969 ± 216773	1645251 ± 249871	0.90	0.022	0.61	No
P49674	Casein kinase I isoform epsilon	171	695960 ± 103467	773037 ± 108446	1.11	0.047	0.65	No

Table D4.2 (continued)

O14618	Copper chaperone for superoxide dismutase	168	2208962 ± 381235	2019238 ± 170011	0.91	0.037	0.65	No
Q5T6V5	Queuosine salvage protein	167	1724603 ± 191313	1566651 ± 107876	0.91	0.0055	0.59	No
Q12904	Aminoacyl tRNA synthase complex-interacting multifunctional protein 1	167	2028639 ± 203401	1912960 ± 213167	0.94	0.044	0.65	No
Q9Y2Q3	Glutathione S-transferase kappa 1	165	1271189 ± 160024	1126624 ± 127592	0.89	0.0036	0.59	No
P85037	Forkhead box protein K1	165	726351 ± 50860	685564 ± 66606	0.94	0.012	0.59	No
Q8NBS9	Thioredoxin domain-containing protein 5	165	1232816 ± 465158	1042318 ± 169322	0.85	0.044	0.65	No
P54819	Adenylate kinase 2, mitochondrial	164	1586778 ± 291411	1467190 ± 163182	0.92	0.025	0.62	No
Q2TAA2	Isoamyl acetate-hydrolyzing esterase 1 homolog	162	1834859 ± 236024	1678272 ± 276583	0.91	0.0010	0.37	No
Q6NY19	KN motif and ankyrin repeat domain-containing protein 3	161	643218 ± 95519	586359 ± 45128	0.91	0.044	0.65	No
Q8N4Q0	Prostaglandin reductase 3	158	2285467 ± 261421	2117012 ± 220581	0.93	0.026	0.62	No
P43007	Neutral amino acid transporter A	158	1870577 ± 670871	2160601 ± 616175	1.16	0.034	0.65	No
P32856	Syntaxin-2	158	115367 ± 25858	127589 ± 31638	1.11	0.035	0.65	No
P16333	Cytoplasmic protein NCK1	158	646316 ± 78829	663300 ± 79963	1.03	0.041	0.65	No
O95861	3'(2'),5'-bisphosphate nucleotidase 1	158	1047926 ± 76127	982394 ± 96569	0.94	0.050	0.65	No
P62495	Eukaryotic peptide chain release factor subunit 1	157	693898 ± 61507	728841 ± 79195	1.05	0.045	0.65	No
P52564	Dual specificity mitogen-activated protein kinase kinase 6	156	1221747 ± 167331	1354902 ± 179365	1.11	0.040	0.65	No

Table D4.2 (continued)

Q15154	Pericentriolar material 1 protein	154	696434 ± 71533	643137 ± 50246	0.92	0.020	0.61	No
Q03113	Guanine nucleotide-binding protein subunit alpha-12	153	377110 ± 56845	400944 ± 51426	1.06	0.050	0.65	No
P50453	Serpin B9	152	677961 ± 178421	544160 ± 122711	**0.80**	0.0067	0.59	No
Q9NVH6	Trimethyllysine dioxygenase, mitochondrial	152	1547708 ± 228539	1327770 ± 237090	0.86	0.0068	0.59	No
Q86WA6	Valacyclovir hydrolase	152	1914970 ± 546842	1746567 ± 562450	0.91	0.017	0.61	No
Q96CM8	Medium-chain acyl-CoA ligase ACSF2, mitochondrial	152	892504 ± 322332	788640 ± 112851	0.88	0.045	0.65	No
P51153	Ras-related protein Rab-13	152	470997 ± 76627	426471 ± 56598	0.91	0.050	0.65	No
Q99471	Prefoldin subunit 5	151	3045963 ± 594430	2759891 ± 677053	0.91	0.044	0.65	No
Q9UL12	Sarcosine dehydrogenase, mitochondrial	149	748541 ± 45833	633913 ± 137436	0.85	0.0019	0.44	No
Q7Z408	CUB and sushi domain-containing protein 2	145	505828 ± 55254	472999 ± 48452	0.94	0.049	0.65	No
O00148	ATP-dependent RNA helicase DDX39A	144	143187 ± 24220	162268 ± 39174	1.13	0.022	0.61	No
Q02108	Guanylate cyclase soluble subunit alpha-1	142	645238 ± 92572	712010 ± 72506	1.10	0.015	0.61	No
Q6NUK1	Calcium-binding mitochondrial carrier protein SCaMC-1	142	1764172 ± 460127	1591356 ± 295887	0.90	0.035	0.65	No
Q8TBB6	Probable cationic amino acid transporter	142	562479 ± 77444	634121 ± 72486	1.13	0.042	0.65	No
O75521	Enoyl-CoA delta isomerase 2	141	1078600 ± 273470	921515 ± 129112	0.85	0.0051	0.59	No
Q9BX68	Histidine triad nucleotide-binding protein 2, mitochondrial	141	3368101 ± 482203	3140144 ± 435821	0.93	0.034	0.65	No

Table D4.2 (continued)

Q5VWZ2	Lysophospholipase-like protein 1	135	1655185 ± 142148	1492375 ± 183329	0.90	0.0058	0.59	No
P30740	Leukocyte elastase inhibitor	135	1509892 ± 635731	1236668 ± 384185	0.82	0.041	0.65	No
Q9HC35	Echinoderm microtubule-associated protein-like 4	134	739153 ± 60833	688812 ± 56373	0.93	0.0079	0.59	No
P49790	Nuclear pore complex protein Nup153	133	532979 ± 79796	494615 ± 78302	0.93	0.012	0.59	No
Q8IVF5	T-lymphoma invasion and metastasis-inducing protein 2	131	862712 ± 154692	961255 ± 150319	1.11	0.012	0.59	No
O95897	Noelin-2	130	1435578 ± 271157	1270519 ± 220413	0.89	0.026	0.62	No
Q9Y5L4	Mitochondrial import inner membrane translocase subunit Tim13	129	1503025 ± 191221	1344122 ± 198013	0.89	0.0055	0.59	No
O00244	Copper transport protein ATOX1	128	1894404 ± 253871	1772081 ± 293124	0.94	0.021	0.61	No
Q53TN4	Plasma membrane ascorbate-dependent reductase CYBRD1	127	632133 ± 322714	467233 ± 93561	**0.74**	0.011	0.59	No
Q8TBG9	Synaptoporin	127	1826047 ± 375505	2126860 ± 372285	1.16	0.012	0.59	No
Q16630	Cleavage and polyadenylation specificity factor subunit 6	127	413200 ± 45170	387132 ± 48779	0.94	0.029	0.62	No
P35914	Hydroxymethylglutaryl-CoA lyase, mitochondrial	126	2435170 ± 501141	2228497 ± 266195	0.92	0.019	0.61	No
P42126	Enoyl-CoA delta isomerase 1, mitochondrial	125	1210729 ± 130913	1030353 ± 174885	0.85	0.0031	0.54	No
P49619	Diacylglycerol kinase gamma	125	581580 ± 114260	684739 ± 135886	1.18	0.013	0.60	No
Q9HCG7	Non-lysosomal glucosylceramidase	125	423740 ± 62077	462613 ± 83837	1.09	0.023	0.61	No

Table D4.2 (continued)

Q92520	Protein FAM3C	124	981596 ± 208118	867822 ± 103336	0.88	0.011	0.59	No
P23434	Glycine cleavage system H protein, mitochondrial	124	1297493 ± 200404	1177667 ± 98391	0.91	0.019	0.61	No
Q8TCZ2	CD99 antigen-like protein 2	123	799515 ± 173812	942542 ± 189869	1.18	0.011	0.59	No
Q8N0X4	Citramalyl-CoA lyase, mitochondrial	122	1009829 ± 356824	803787 ± 230074	**0.80**	0.019	0.61	No
Q8NBN7	Retinol dehydrogenase 13	121	803396 ± 158363	706984 ± 94637	0.88	0.011	0.59	No
Q13242	Serine/arginine-rich splicing factor 9	120	816766 ± 96598	746147 ± 80189	0.91	0.0010	0.37	No
Q15126	Phosphomevalonate kinase	119	1321878 ± 253045	1211333 ± 232703	0.92	0.010	0.59	No
Q9NRG7	Epimerase family protein SDR39U1	118	712932 ± 100069	629675 ± 72900	0.88	0.0013	0.40	No
Q9P016	Thymocyte nuclear protein 1	118	1332703 ± 156744	1226254 ± 149339	0.92	0.0092	0.59	No
O00422	Histone deacetylase complex subunit SAP18	118	1848924 ± 165735	1755352 ± 138592	0.95	0.019	0.61	No
Q8NCN5	Pyruvate dehydrogenase phosphatase regulatory subunit, mitochondrial	117	1122801 ± 153004	1023055 ± 107934	0.91	0.0039	0.59	No
P06865	Beta-hexosaminidase subunit alpha	117	794307 ± 160438	692233 ± 83785	0.87	0.019	0.61	No
Q9BTU6	Phosphatidylinositol 4-kinase type 2-alpha	114	468863 ± 51469	507679 ± 49123	1.08	0.012	0.59	No
Q5HYI8	Rab-like protein 3	113	723602 ± 104411	672936 ± 76541	0.93	0.025	0.62	No
O75582	Ribosomal protein S6 kinase alpha-5	112	435164 ± 89786	535352 ± 89177	**1.23**	0.0054	0.59	No
Q9BV79	Enoyl-[acyl-carrier-protein] reductase, mitochondrial	112	3188392 ± 544931	2961784 ± 403539	0.93	0.045	0.65	No

Table D4.2 (continued)

Q9NQ29	Putative RNA-binding protein Luc7-like 1	111	153531 ± 25860	171828 ± 21286	1.12	0.015	0.61	No
P23919	Thymidylate kinase	111	714815 ± 108335	674637 ± 81593	0.94	0.034	0.65	No
Q99729	Heterogeneous nuclear ribonucleoprotein A/B	110	1044027 ± 207453	9544812 ± 187154	0.91	0.023	0.61	No
Q96QE2	Proton myo-inositol cotransporter	110	680665 ± 150163	761421 ± 141468	1.12	0.046	0.65	No
Q6IQ20	N-acyl-phosphatidylethanolamine-hydrolyzing phospholipase D	109	1221924 ± 244250	1403204 ± 197364	1.15	0.016	0.61	No
Q9NPJ3	Acyl-coenzyme A thioesterase 13	109	1335068 ± 235873	1240735 ± 233411	0.93	0.045	0.65	No
P33240	Cleavage stimulation factor subunit 2	108	150445 ± 19282	138910 ± 18093	0.92	0.019	0.61	No
Q99567	Nuclear pore complex protein Nup88	108	449875 ± 31596	433150 ± 46587	0.96	0.020	0.61	No
P47972	Neuronal pentraxin-2	108	1085196 ± 340999	788204 ± 272193	**0.73**	0.021	0.61	No
P58400	Neurexin-1-beta	107	64249 ± 10692	69711 ± 11024	1.09	0.042	0.65	No
Q6ZMT1	SH3 and cysteine-rich domain-containing protein 2	107	433767 ± 73671	404624 ± 61588	0.93	0.049	0.65	No
O95848	Uridine diphosphate glucose pyrophosphatase NUDT14	106	628461 ± 93483	562818 ± 69653	0.90	0.011	0.59	No
Q96IJ6	Mannose-1-phosphate guanyltransferase alpha	106	500604 ± 39810	488915 ± 41606	0.98	0.027	0.62	No
Q07021	Complement component 1 Q subcomponent-binding protein, mitochondrial	105	1118963 ± 224714	1218244 ± 275332	1.09	0.020	0.61	No

Table D4.2 (continued)

P62857	40S ribosomal protein S28	104	2146209 ± 313408	1925278 ± 301382	0.90	0.014	0.60	No
O75608	Acyl-protein thioesterase 1	104	1015213 ± 83621	932593 ± 90221	0.92	0.016	0.61	No
Q6UWP2	Dehydrogenase/reductase SDR family member 11	104	607794 ± 127863	532728 ± 73032	0.88	0.031	0.64	No
Q6PL24	Protein TMED8	104	673452 ± 97221	702431 ± 116228	1.04	0.038	0.65	No
O43314	Inositol hexakisphosphate and diphosphoinositol-pentakisphosphate kinase 2	104	264218 ± 29397	241774 ± 28104	0.92	0.047	0.65	No
P21953	2-oxoisovalerate dehydrogenase subunit beta, mitochondrial	103	1343194 ± 193452	1157820 ± 119851	0.86	0.00072	0.37	No
Q9Y2K5	R3H domain-containing protein 2	103	517700 ± 89216	446177 ± 70884	0.86	0.017	0.61	No
Q8NBF2	NHL repeat-containing protein 2	102	620378 ± 83108	592812 ± 48723	0.96	0.039	0.65	No
Q8WXE0	Caskin-2	101	903270 ± 107001	835821 ± 70888	0.93	0.0015	0.44	No
Q4VC31	Protein MIX23	101	919582 ± 116190	832848 ± 105369	0.91	0.0068	0.59	No
P22607	Fibroblast growth factor receptor 3	99	368338 ± 69277	331326 ± 50616	0.90	0.042	0.65	No
Q96JB5	CDK5 regulatory subunit-associated protein 3	98	621129 ± 50882	583494 ± 52510	0.94	0.019	0.61	No
Q8NC56	LEM domain-containing protein 2	98	448227 ± 51458	421359 ± 35367	0.94	0.028	0.62	No
Q8WUH6	Transmembrane protein 263	96	188325 ± 19095	173834 ± 18770	0.92	0.0011	0.37	No
Q5T440	Putative transferase CAF17, mitochondrial	96	536335 ± 63373	490907 ± 42574	0.92	0.0061	0.59	No
P56962	Syntaxin-17	96	569929 ± 68229	533350 ± 61498	0.94	0.036	0.65	No

Table D4.2 (continued)

Q9GZT3	SRA stem-loop-interacting RNA-binding protein, mitochondrial	96	1023280 ± 150387	927686 ± 146865	0.91	0.040	0.65	No
O94779	Contactin-5	96	269026 ± 44779	284945 ± 35342	1.06	0.050	0.65	No
Q15637	Splicing factor 1	95	622914 ± 104976	581042 ± 108847	0.93	0.024	0.61	No
Q9Y2Q5	Ragulator complex protein LAMTOR2	95	491403 ± 63016	454751 ± 44836	0.93	0.027	0.62	No
Q9BRA2	Thioredoxin domain-containing protein 17	94	918697 ± 120981	853013 ± 83184	0.93	0.0092	0.59	No
O95396	Adenylyltransferase and sulfurtransferase MOCS3	93	458294 ± 43986	419880 ± 55421	0.92	0.034	0.65	No
Q8N4T8	Carbonyl reductase family member 4	92	637403 ± 83833	563916 ± 62213	0.88	0.00013	0.19	No
Q9BVV7	Mitochondrial import inner membrane translocase subunit Tim21	91	462218 ± 73323	484134 ± 57626	1.05	0.036	0.65	No
P11172	Uridine 5'-monophosphate synthase	89	663686 ± 77435	623801 ± 83972	0.94	0.019	0.61	No
Q9BW83	Intraflagellar transport protein 27 homolog	87	343877 ± 38073	323710 ± 32520	0.94	0.021	0.61	No
P06132	Uroporphyrinogen decarboxylase	87	419600 ± 34973	395715 ± 23968	0.94	0.024	0.62	No
P05204	Non-histone chromosomal protein HMG-17	87	1044774 ± 328566	914173 ± 242746	0.87	0.040	0.65	No
O94813	Slit homolog 2 protein	86	361208 ± 74745	474610 ± 79578	**1.31**	0.00062	0.37	No
Q9NWT6	Hypoxia-inducible factor 1-alpha inhibitor	86	404879 ± 55086	451841 ± 42833	1.12	0.0082	0.59	No
P45381	Aspartoacylase	86	534348 ± 95500	585980 ± 145876	1.10	0.014	0.61	No
Q5VV63	Attractin-like protein 1	86	384944 ± 51497	427899 ± 55355	1.11	0.022	0.61	No
Q13043	Serine/threonine-protein kinase 4	86	382139 ± 39854	361352 ± 23562	0.95	0.028	0.62	No

Table D4.2 (continued)

Q8NFU3	Thiosulfate:glutathione sulfurtransferase	86	1720060 ± 229667	1572287 ± 193416	0.91	0.031	0.64	No
Q9Y6W3	Calpain-7	86	421884 ± 37066	431592 ± 29215	1.02	0.046	0.65	No
Q9UBR2	Cathepsin Z	85	789743 ± 314575	677172 ± 147191	0.86	0.041	0.65	No
Q92563	Testican-2	84	966146 ± 168898	1099049 ± 149346	1.14	0.0018	0.44	No
Q7Z6J0	E3 ubiquitin-protein ligase SH3RF1	84	290552 ± 31899	263966 ± 27024	0.91	0.029	0.62	No
O75312	Zinc finger protein ZPR1	84	458535 ± 55749	426647 ± 42941	0.93	0.044	0.65	No
Q96AQ8	Mitochondrial calcium uniporter regulator 1	84	872314 ± 98137	815279 ± 120972	0.93	0.049	0.65	No
Q16348	Solute carrier family 15 member 2	83	636856 ± 153329	749657 ± 155406	1.18	0.0090	0.59	No
Q8ND56	Protein LSM14 homolog A	83	500126 ± 54918	470560 ± 55837	0.94	0.041	0.65	No
Q9NR19	Acetyl-coenzyme A synthetase, cytoplasmic	81	701407 ± 135212	776711 ± 136723	1.11	0.044	0.65	No
P07093	Glia-derived nexin	80	620357 ± 138592	474604 ± 95280	**0.77**	0.0013	0.40	No
Q96T23	Remodeling and spacing factor 1	80	140626 ± 23851	129468 ± 13703	0.92	0.0078	0.59	No
Q6JBY9	CapZ-interacting protein	79	425684 ± 57565	390524 ± 69612	0.92	0.023	0.61	No
O14832	Phytanoyl-CoA dioxygenase, peroxisomal	79	486040 ± 64929	432283 ± 52526	0.89	0.044	0.65	No
Q13685	Angio-associated migratory cell protein	78	480501 ± 64633	537814 ± 67525	1.12	0.0030	0.54	No
P17081	Rho-related GTP-binding protein RhoQ	78	52310 ± 7390	58020 ± 8586	1.11	0.032	0.65	No
Q96JM3	Chromosome alignment-maintaining phosphoprotein 1	78	236363 ± 39067	224442 ± 16121	0.95	0.041	0.65	No
Q8NC44	Reticulophagy regulator 2	77	196161 ± 26426	174685 ± 31411	0.89	0.011	0.59	No

Table D4.2 (continued)

Q96CN9	GRIP and coiled-coil domain-containing protein 1	77	335183 ± 49378	304924 ± 29547	0.91	0.019	0.61	No
Q92506	Estradiol 17-beta-dehydrogenase 8	76	703371 ± 151785	615900 72937±	0.88	0.0069	0.59	No
O75175	CCR4-NOT transcription complex subunit 3	76	552844 ± 33197	526580 ± 32098	0.95	0.011	0.59	No
Q9UN70	Protocadherin gamma-C3	76	335510 ± 37993	303321 ± 37982	0.90	0.044	0.65	No
P05186	Alkaline phosphatase, tissue-nonspecific isozyme	75	731070 ± 222096	587530 ± 103779	**0.80**	0.0071	0.59	No
P05114	Non-histone chromosomal protein HMG-14	75	358312 ± 119423	300769 ± 65110	0.84	0.034	0.65	No
Q96PE7	Methylmalonyl-CoA epimerase, mitochondrial	74	1466416 ± 264531	1261775 ± 249295	0.86	0.0075	0.59	No
Q6P1X6	UPF0598 protein C8orf82	74	569751 ± 80786	516568 ± 64836	0.91	0.0076	0.59	No
Q8N135	Leucine-rich repeat LGI family member 4	74	712949 ± 121721	832142 ± 111061	1.17	0.023	0.61	No
Q6UVY6	DBH-like monooxygenase protein 1	74	538686 ± 117087	606007 ± 206517	1.12	0.031	0.64	No
Q9UNP9	Peptidyl-prolyl cis-trans isomerase E	74	212933 ± 34736	185060 ± 24039	0.87	0.031	0.64	No
O00560	Syntenin-1	73	459633 ± 122599	378191 ± 122988	0.82	0.0084	0.59	No
P14384	Carboxypeptidase M	72	388518 ± 86166	448021 ± 115928	1.15	0.030	0.64	No
O60220	Mitochondrial import inner membrane translocase subunit Tim8 A	72	793665 ± 138186	704785 ± 100276	0.89	0.046	0.65	No
O95232	Luc7-like protein 3	70	366339 ± 53555	398722 ± 69503	1.09	0.017	0.61	No
Q9BQI9	Nuclear receptor-interacting protein 2	70	332862 ± 63412	391156 ± 64661	1.18	0.023	0.61	No

Table D4.2 (continued)

Q9Y3L3	SH3 domain-binding protein 1	70	379201 ± 54944	345272 ± 44175	0.91	0.033	0.65	No
P32929	Cystathionine gamma-lyase	69	373716 ± 54064	344319 ± 32707	0.92	0.0085	0.59	No
O76071	Probable cytosolic iron-sulfur protein assembly protein CIAO1	69	242465 ± 32553	255476 ± 27962	1.05	0.021	0.61	No
Q8IVS2	Malonyl-CoA-acyl carrier protein transacylase, mitochondrial	69	356068 ± 43381	329983 ± 40019	0.93	0.027	0.62	No
O95302	Peptidyl-prolyl cis-trans isomerase FKBP9	69	496391 ± 116636	436711 ± 45812	0.88	0.029	0.63	No
Q0JRZ9	F-BAR domain only protein 2	68	323621 ± 79770	280781 ± 19084	0.87	0.013	0.60	No
O60234	Glia maturation factor gamma	68	75106 ± 14691	68226 ± 11035	0.91	0.049	0.65	No
P09661	U2 small nuclear ribonucleoprotein A'	67	381308 ± 65469	352908 ± 65485	0.93	0.018	0.61	No
P50607	Tubby protein homolog	67	317598 ± 35782	303225 ± 31024	0.95	0.028	0.62	No
O43741	5'-AMP-activated protein kinase subunit beta-2	65	138118 ± 21935	158968 ± 26498	1.15	0.0037	0.59	Yes
Q13243	Serine/arginine-rich splicing factor 5	65	455190 ± 141951	363003 ± 87172	**0.80**	0.025	0.62	No
Q6GMV3	Putative peptidyl-tRNA hydrolase PTRHD1	64	814570 ± 89210	958141 ± 125078	1.18	0.000040	0.19	Yes
Q96T83	Sodium/hydrogen exchanger 7	64	348013 ± 64886	385681 ± 48216	1.11	0.0060	0.59	No
P02753	Retinol-binding protein 4	64	172779 ± 50964	143811 ± 30144	0.83	0.022	0.61	No
Q9H2J4	Phosducin-like protein 3	64	234458 ± 36853	252901 ± 21764	1.08	0.022	0.61	No

Table D4.2 (continued)

Q9UIG0	Tyrosine-protein kinase BAZ1B	64	385139 ± 101664	337340 ± 57813	0.88	0.044	0.65	No
Q9NXD2	Myotubularin-related protein 10	63	242301 ± 38027	264907 ± 36078	1.09	0.0052	0.59	No
P27815	cAMP-specific 3',5'-cyclic phosphodiesterase 4A	63	75217 ± 7673	68133 ± 8501	0.91	0.010	0.59	No
Q5TAQ9	DDB1- and CUL4-associated factor 8	63	326828 ± 27345	295030 ± 36535	0.90	0.018	0.61	No
Q8WV93	AFG1-like ATPase	63	309884 ± 51674	285779 ± 32671	0.92	0.046	0.65	No
O14786	Neuropilin-1	62	226599 ± 55621	198992 ± 26051	0.88	0.019	0.61	No
Q9BXR0	Queuine tRNA-ribosyltransferase catalytic subunit 1	62	198022 ± 16908	182130 ± 22437	0.92	0.024	0.61	No
Q9UQF2	C-Jun-amino-terminal kinase-interacting protein 1	62	229269 ± 30388	241795 ± 25030	1.05	0.027	0.62	No
Q96M27	Protein PRRC1	61	571799 ± 75540	530821 ± 34399	0.93	0.010	0.59	No
Q9BRK5	45 kDa calcium-binding protein	61	307173 ± 36553	275014 ± 33099	0.90	0.011	0.59	No
O95271	Poly [ADP-ribose] polymerase tankyrase-1	61	206158 ± 28620	224105 ± 19803	1.09	0.023	0.61	No
Q9UKB3	DnaJ homolog subfamily C member 12	61	471773 ± 88200	534687 ± 66544	1.13	0.046	0.65	No
P61278	Somatostatin	60	846500 ± 256332	624380 ± 200114	**0.74**	0.021	0.61	No
Q15007	Pre-mRNA-splicing regulator WTAP	60	218545 ± 19685	207934 ± 12675	0.95	0.024	0.61	No
Q9UBL0	cAMP-regulated phosphoprotein 21	60	442216 ± 85637	391241 ± 75669	0.88	0.032	0.65	No
Q9BTE7	DCN1-like protein 5	58	524997 ± 83299	496694 ± 75032	0.95	0.031	0.64	No
Q9UGR2	Zinc finger CCCH domain-containing protein 7B	58	249448 ± 23554	238181 ± 21107	0.95	0.042	0.65	No

Table D4.2 (continued)

Q9UF11	Pleckstrin homology domain-containing family B member 1	57	356700 ± 121555	398051 ± 118126	1.12	0.0093	0.59	No
Q6P4Q7	Metal transporter CNNM4	57	67095 ± 16609	77421 ± 15223	1.15	0.018	0.61	No
Q12974	Protein tyrosine phosphatase type IVA 2	57	216660 ± 38324	244865 ± 40513	1.13	0.019	0.61	No
Q9UEE9	Craniofacial development protein 1	57	304342 ± 47998	358633 ± 45080	1.18	0.021	0.61	No
P62312	U6 snRNA-associated Sm-like protein LSm6	57	1536994 ± 130443	1499297 ± 106028	0.98	0.038	0.65	No
Q9Y4C2	TRPM8 channel-associated factor 1	57	175195 ± 34775	193956 ± 31695	1.11	0.041	0.65	No
Q7Z407	CUB and sushi domain-containing protein 3	55	156734 ± 15235	144713 ± 14524	0.92	0.0055	0.59	No
P24593	Insulin-like growth factor-binding protein 5	54	309224 ± 54024	387354 ± 104736	**1.25**	0.0093	0.59	No
Q9P2F8	Signal-induced proliferation-associated 1-like protein 2	54	70393 ± 12010	62730 ± 7004	0.89	0.027	0.62	No
Q9Y237	Peptidyl-prolyl cis-trans isomerase NIMA-interacting 4	53	282979 ± 73381	252544 ± 65733	0.89	0.040	0.65	No
Q99417	c-Myc-binding protein	52	257304 ± 30836	239411 ± 20482	0.93	0.011	0.59	No
O75376	Nuclear receptor corepressor 1	52	130527 ± 19362	120669 ± 12284	0.92	0.041	0.65	No
Q9BQ16	Testican-3	51	165528 ± 27705	212144 ± 37327	**1.28**	0.00012	0.19	No
P07711	Procathepsin L	51	606377 ± 192141	489929 ± 95266	**0.81**	0.022	0.61	No
P61925	cAMP-dependent protein kinase inhibitor alpha	51	208353 ± 62164	178743 ± 57273	0.86	0.023	0.61	No
Q9UIK5	Tomoregulin-2	50	156850 ± 20006	190671 ± 25379	1.22	0.000080	0.19	No
Q5RKV6	Exosome complex component MTR3	50	190113 ± 27453	172716 ± 15191	0.91	0.021	0.61	No

Table D4.2 (continued)

P53370	Nucleoside diphosphate-linked moiety X motif 6	50	204530 ± 52544	181196 ± 39923	0.89	0.025	0.62	No
Q9BY42	Replication termination factor 2	50	196273 ± 25846	213260 ± 24232	1.09	0.041	0.65	No
Q96DM3	Regulator of MON1-CCZ1 complex	49	304224 ± 53741	335875 ± 48297	1.10	0.016	0.61	No
Q9Y5H0	Protocadherin gamma-A3	49	60485 ± 7738	53939 ± 9697	0.89	0.030	0.64	No
Q9Y653	Adhesion G-protein coupled receptor G1	48	267434 ± 67538	328872 ± 64568	1.23	0.0024	0.53	No
P62256	Ubiquitin-conjugating enzyme E2 H	48	541222 ± 53635	603146 ± 64523	1.11	0.012	0.59	No
O00584	Ribonuclease T2	48	180513 ± 59394	156351 ± 24222	0.87	0.042	0.65	No
Q08117	TLE family member 5	48	122091 ± 21019	110920 ± 17312	0.91	0.042	0.65	No
Q99689	Fasciculation and elongation protein zeta-1	46	459244 ± 87818	530413 ± 84321	1.15	0.0057	0.59	No
Q9BYD3	39S ribosomal protein L4, mitochondrial	46	141977 ± 23315	124076 ± 19119	0.87	0.018	0.61	No
Q9BTT0	Acidic leucine-rich nuclear phosphoprotein 32 family member E	46	167609 ± 33298	149339 ± 35103	0.89	0.049	0.65	No
Q9BPY8	Homeodomain-only protein	45	583745 ± 118066	510444 ± 115712	0.87	0.0059	0.59	No
Q9P0T7	Proton-transporting V-type ATPase complex assembly regulator TMEM9	45	55980 ± 8859	61059 ± 9611	1.09	0.032	0.64	No
Q8N983	39S ribosomal protein L43, mitochondrial	44	346344 ± 39918	304109 ± 41005	0.88	0.0011	0.37	No

Table D4.2 (continued)

Q9H2J7	Sodium-dependent neutral amino acid transporter B(0)AT2	44	117363 ± 26404	142161 ± 34015	1.21	0.0051	0.59	No
Q9UKV0	Histone deacetylase 9	44	62675 ± 14210	52772 ± 7477	0.84	0.015	0.61	No
Q8TB45	DEP domain-containing mTOR-interacting protein	44	151606 ± 23029	140908 ± 21061	0.93	0.028	0.62	No
Q01167	Forkhead box protein K2	44	120911 ± 15271	115296 ± 10431	0.95	0.049	0.65	No
Q9ULC5	Long-chain-fatty-acid--CoA ligase 5	44	15322 ± 3806	13023 ± 2300	0.85	0.049	0.65	No
O75711	Scrapie-responsive protein 1	43	722825 ± 145828	595215 ± 119807	0.82	0.013	0.60	No
O43665	Regulator of G-protein signaling 10	43	116495 ± 36074	102537 ± 17851	0.88	0.015	0.61	No
Q96B36	Proline-rich AKT1 substrate 1	43	333638 ± 44546	304541 ± 36566	0.91	0.036	0.65	No
Q9Y6H1	Coiled-coil-helix-coiled-coil-helix domain-containing protein 2	42	350248 ± 126374	274325 ± 105228	**0.78**	0.030	0.63	No
P48547	Potassium voltage-gated channel subfamily C member 1	41	93878 ± 22154	117510 ± 30085	**1.25**	0.0027	0.54	No
P17050	Alpha-N-acetylgalactosaminidase	41	207737 ± 52751	178336 ± 18552	0.86	0.017	0.61	No
Q9H1B7	Probable E3 ubiquitin-protein ligase IRF2BPL	41	172632 ± 13909	162911 ± 12537	0.94	0.022	0.61	No
P51397	Death-associated protein 1	41	738017 ± 138178	678360 ± 70170	0.92	0.026	0.62	No
P47914	60S ribosomal protein L29	41	262257 ± 79784	232176 ± 55400	0.89	0.034	0.65	No
P15151	Poliovirus receptor	41	181384 ± 51972	156719 ± 22527	0.86	0.039	0.65	No

Table D4.2 (continued)

P22304	Iduronate 2-sulfatase	41	305313 ± 44609	284911 ± 30611	0.93	0.045	0.65	No
Q9BV57	1,2-dihydroxy-3-keto-5-methylthiopentene dioxygenase	40	94378 ± 30699	67087 ± 11630	**0.71**	0.0089	0.59	No
Q9NPA8	Transcription and mRNA export factor ENY2	40	536711 ± 60352	501349 ± 54760	0.93	0.010	0.59	No
Q9ULX7	Carbonic anhydrase 14	40	127870 ± 32585	146563 ± 21192	1.15	0.011	0.59	No
Q03519	Antigen peptide transporter 2	40	190752 ± 48112	167097 ± 27141	0.88	0.033	0.65	No
Q9UKJ3	G patch domain-containing protein 8	40	102823 ± 11253	95867 ± 9558	0.93	0.039	0.65	No
Q9Y2D0	Carbonic anhydrase 5B, mitochondrial	39	131163 ± 25680	111694 ± 21928	0.85	0.022	0.61	No
Q9BZG1	Ras-related protein Rab-34	39	116810 ± 24952	105166 ± 15549	0.90	0.030	0.64	No
P08913	Alpha-2A adrenergic receptor	39	84070 ± 13121	88900 ± 11628	1.06	0.041	0.65	No
P50914	60S ribosomal protein L14	39	272843 ± 53730	254834 ± 57267	0.93	0.046	0.65	No
Q9C037	E3 ubiquitin-protein ligase TRIM4	38	159744 ± 22651	146407 ± 14313	0.92	0.032	0.65	No
Q96AY3	Peptidyl-prolyl cis-trans isomerase FKBP10	37	151244 ± 48268	121554 ± 20198	**0.80**	0.012	0.59	No
P52630	Signal transducer and activator of transcription 2	37	107896 ± 11827	99964 ± 13755	0.93	0.027	0.62	No
Q9UI47	Catenin alpha-3	37	107337 ± 21858	120312 ± 20183	1.12	0.031	0.64	No
Q69YN2	CWF19-like protein 1	37	134404 ± 17845	124767 ± 12826	0.93	0.037	0.65	No
Q99624	Sodium-coupled neutral amino acid transporter 3	36	346020 ± 63573	404725 ± 89251	1.17	0.015	0.61	No
Q13237	cGMP-dependent protein kinase 2	36	191025 ± 54875	163565 ± 40087	0.86	0.026	0.62	No

Table D4.2 (continued)

P0DI82	Trafficking protein particle complex subunit 2B	36	85164 ± 16602	89348 ± 19961	1.05	0.048	0.65	No
Q9Y6P5	Sestrin-1	35	73061 ± 13471	88406 ± 16116	1.21	0.0030	0.54	No
P35659	Protein DEK	35	94093 ± 11989	106725 ± 18890	1.13	0.010	0.59	No
Q9BTC0	Death-inducer obliterator 1	35	77834 ± 8509	72710 ± 6998	0.93	0.050	0.65	No
O14683	Tumor protein p53-inducible protein 11	34	286080 ± 118513	225544 ± 61069	**0.79**	0.0042	0.59	No
Q9NYR9	NF-kappa-B inhibitor-interacting Ras-like protein 2	34	178954 ± 20003	162718 ± 14363	0.91	0.010	0.59	No
Q6PJG9	Leucine-rich repeat and fibronectin type-III domain-containing protein 4	34	132795 ± 21860	120254 ± 14870	0.91	0.018	0.61	No
O95858	Tetraspanin-15	34	122202 ± 41222	135644 ± 49912	1.11	0.033	0.65	No
P61077	Ubiquitin-conjugating enzyme E2 D3	33	465794 ± 133311	398694 ± 171606	0.86	0.012	0.59	No
O14641	Segment polarity protein dishevelled homolog DVL-2	33	29798 ± 7905	26094 ± 4081	0.88	0.020	0.61	No
A6NHX0	Cytosolic arginine sensor for mTORC1 subunit 2	33	317856 ± 44415	281317 ± 27930	0.89	0.023	0.61	No
O95486	Protein transport protein Sec24A	33	102902 ± 9954	97393 ± 10583	0.95	0.047	0.65	No
Q15853	Upstream stimulatory factor 2	32	74895 ± 9519	69149 ± 6571	0.92	0.017	0.61	No
Q9NP66	High mobility group protein 20A	32	143269 ± 17310	131610 ± 18305	0.92	0.018	0.61	No
P0DJ93	Small integral membrane protein 13	32	179708 ± 27309	169042 ± 19141	0.94	0.021	0.61	No

Table D4.2 (continued)

O60266	Adenylate cyclase type 3	32	156765 ± 32205	144305 ± 14179	0.92	0.047	0.65	No
O95452	Gap junction beta-6 protein	31	114921 ± 47121	89186 ± 27743	**0.78**	0.0070	0.59	No
P32321	Deoxycytidylate deaminase	31	65466 ± 15217	57524 ± 11169	0.88	0.010	0.59	No
Q9BQ52	Zinc phosphodiesterase ELAC protein 2	31	61412 ± 7289	55992 ± 6548	0.91	0.012	0.59	No
Q99933	BAG family molecular chaperone regulator 1	31	88495 ± 11489	82127 ± 5970	0.93	0.041	0.65	No
Q9UKV5	E3 ubiquitin-protein ligase AMFR	31	106435 ± 18893	94088 ± 18986	0.88	0.044	0.65	No
A5D8V6	Vacuolar protein sorting-associated protein 37C	30	138967 ± 11990	129208 ± 15978	0.93	0.023	0.61	No
Q8N9B8	Ras-GEF domain-containing family member 1A	30	118151 ± 15444	109996 ± 13413	0.93	0.032	0.64	No
P48067	Sodium- and chloride-dependent glycine transporter 1	29	53702 ± 10144	61542 ± 12065	1.15	0.0028	0.54	No
Q9NZU0	Leucine-rich repeat transmembrane protein FLRT3	29	94984 ± 12986	100575 ± 15515	1.06	0.024	0.61	No
P01213	Proenkephalin-B	29	119764 ± 35073	165945 ± 65457	**1.39**	0.028	0.62	No
Q8WUF8	Cotranscriptional regulator FAM172A	29	120638 ± 14659	112384 ± 11384	0.93	0.034	0.65	No
Q86YL5	Testis development-related protein	29	109475 ± 12401	117032 ± 12744	1.07	0.036	0.65	No
Q9NU23	LYR motif-containing protein 2	28	170618 ± 33983	152291 ± 20767	0.89	0.011	0.59	No
Q9BU89	Deoxyhypusine hydroxylase	28	47279 ± 4692	44744 ± 6464	0.95	0.027	0.62	No

Table D4.2 (continued)

Q5BKU9	Oxidoreductase-like domain-containing protein 1	28	178575 ± 26346	163913 ± 24917	0.92	0.031	0.64	No
Q6UXH1	Protein disulfide isomerase CRELD2	28	136100 ± 30634	118142 ± 15853	0.87	0.033	0.65	No
P78540	Arginase-2, mitochondrial	28	76212 ± 23687	86196 ± 24401	1.13	0.034	0.65	No
O95347	Structural maintenance of chromosomes protein 2	28	76909 ± 10201	72587 ± 7647	0.94	0.037	0.65	No
P63218	Guanine nucleotide-binding protein G(I)/G(S)/G(O) subunit gamma-5	27	2718335 ± 645994	2290506 ± 333510	0.84	0.0036	0.59	No
Q05823	2-5A-dependent ribonuclease	27	72249 ± 10566	62942 ± 9794	0.87	0.013	0.60	No
Q04864	Proto-oncogene c-Rel	27	84858 ± 10625	77068 ± 10578	0.91	0.019	0.61	No
Q9UKW4	Guanine nucleotide exchange factor VAV3	27	54992 ± 8256	58223 ± 9142	1.06	0.020	0.61	No
P42702	Leukemia inhibitory factor receptor	27	90424 ± 14527	84178 ± 9783	0.93	0.040	0.65	No
P52569	Cationic amino acid transporter 2	27	98363 ± 26390	117738 ± 38004	1.20	0.042	0.65	No
Q9Y5W8	Sorting nexin-13	27	66540 ± 13700	66286 ± 16080	1.00	0.044	0.65	No
Q16854	Deoxyguanosine kinase, mitochondrial	26	211309 ± 29681	182022 ± 22701	0.86	0.0026	0.54	No
P20309	Muscarinic acetylcholine receptor M3	26	63385 ± 15314	73537 ± 14240	1.16	0.013	0.60	No
P78508	ATP-sensitive inward rectifier potassium channel 10	26	121862 ± 35425	143721 ± 40957	1.18	0.034	0.65	No
Q8NHZ8	Anaphase-promoting complex subunit CDC26	26	86746 ± 10679	83272 ± 8509	0.96	0.039	0.65	No

Table D4.2 (continued)

Q9Y3R5	Protein dopey-2	26	83080 ± 9888	77351 ± 10439	0.93	0.040	0.65	No
Q9BRK3	Matrix remodeling-associated protein 8	26	59601 ± 22701	50564 ± 7152	0.85	0.041	0.65	No
Q04656	Copper-transporting ATPase 1	26	78441 ± 11590	72914 ± 6728	0.93	0.049	0.65	No
Q96C90	Protein phosphatase 1 regulatory subunit 14B	25	38075 ± 10004	32779 ± 6855	0.86	0.0019	0.44	No
O94952	F-box only protein 21	25	102911 ± 18536	111125 ± 15808	1.08	0.014	0.60	No
Q12778	Forkhead box protein O1	24	25249 ± 3423	28121 ± 4439	1.11	0.012	0.59	No
P52657	Transcription initiation factor IIA subunit 2	24	316602 ± 33818	286161 ± 31081	0.90	0.039	0.65	No
Q16270	Insulin-like growth factor-binding protein 7	24	180712 ± 76258	144468 ± 40181	**0.80**	0.047	0.65	No
Q7Z5H3	Rho GTPase-activating protein 22	23	40791 ± 10240	47080 ± 14000	1.15	0.018	0.61	No
Q9H773	dCTP pyrophosphatase 1	23	58645 ± 9766	51400 ± 9521	0.88	0.027	0.62	No
P31152	Mitogen-activated protein kinase 4	22	58166 ± 6721	51026 ± 9165	0.88	0.039	0.65	No
P50749	Ras association domain-containing protein 2	22	45687 ± 8549	41686 ± 4470	0.91	0.049	0.65	No
O15379	Histone deacetylase 3	21	73488 ± 7747	67262 ± 7941	0.92	0.0076	0.59	No
Q15043	Metal cation symporter ZIP14	21	51418 ± 6731	58194 ± 9728	1.13	0.0087	0.59	No
Q96B18	Dapper homolog 3	21	55687 ± 10923	50154 ± 10405	0.90	0.017	0.61	No
Q9HCN8	Stromal cell-derived factor 2-like protein 1	21	108715 ± 21008	93393 ± 17167	0.86	0.026	0.62	No
Q96IZ7	Serine/Arginine-related protein 53	21	65554 ± 9258	71345 ± 11958	1.09	0.034	0.65	No

Table D4.2 (continued)

Q16540	39S ribosomal protein L23, mitochondrial	21	379058 ± 65299	327882 ± 81038	0.86	0.044	0.65	No
P17707	S-adenosylmethionine decarboxylase proenzyme	20	21481 ± 8295	27530 ± 6732	**1.28**	0.033	0.65	No
Q9BQE4	Selenoprotein S	20	41179 ± 10294	36943 ± 6923	0.90	0.034	0.65	No
O00268	Transcription initiation factor TFIID subunit 4	20	39078 ± 6140	35822 ± 4692	0.92	0.037	0.65	No
Q9HA72	Calcium homeostasis modulator protein 2	20	121361 ± 36484	108548 ± 16066	0.89	0.049	0.65	No
Q9Y6G3	39S ribosomal protein L42, mitochondrial	19	106195 ± 15043	90528 ± 13955	0.85	0.0065	0.59	No
Q15048	Leucine-rich repeat-containing protein 14	19	172997 ± 32341	146234 ± 43070	0.85	0.015	0.61	No
Q8N357	Solute carrier family 35 member F6	19	70708 ± 9631	63977 ± 11392	0.90	0.018	0.61	No
P16455	Methylated-DNA--protein-cysteine methyltransferase	19	127987 ± 45791	109009 ± 26583	0.85	0.026	0.62	No
Q32P41	tRNA (guanine(37)-N1)-methyltransferase	19	35889 ± 5730	31970 ± 5387	0.89	0.033	0.65	No
Q6ZSJ9	Protein shisa-6	19	65114 ± 11536	56217 ± 9755	0.86	0.043	0.65	No
Q01780	Exosome component 10	18	78085 ± 11448	66470 ± 7090	0.85	0.00020	0.21	No
Q63HQ0	AP-1 complex-associated regulatory protein	18	77081 ± 12427	83411 ± 7705	1.08	0.024	0.62	No
Q9H9Q4	Non-homologous end-joining factor 1	18	31423 ± 6686	35563 ± 8003	1.13	0.026	0.62	No
Q15059	Bromodomain-containing protein 3	17	13165 ± 2532	11511 ± 1918	0.87	0.014	0.61	No
Q6ZMK1	Cysteine and histidine-rich protein 1	17	48337 ± 8170	42007 ± 7562	0.87	0.018	0.61	No

Table D4.2 (continued)

Q86VU5	Catechol O-methyltransferase domain-containing protein 1	17	68357 ± 17136	79192 ± 23879	1.16	0.024	0.62	No
A8MXV4	Nucleoside diphosphate-linked moiety X motif 19	17	130067 ± 20470	124037 ± 20555	0.95	0.029	0.62	No
Q9ULW5	Ras-related protein Rab-26	17	36403 ± 11174	43709. ± 7926	1.20	0.044	0.65	No
F8WBI6	Golgin subfamily A member 8N	17	179304 ± 32948	164932 ± 28046	0.92	0.049	0.65	No
P51811	Membrane transport protein XK	17	93906 ± 21778	106911 ± 22903	1.14	0.049	0.65	No
P61009	Signal peptidase complex subunit 3	16	252473 ± 28037	239771 ± 27909	0.95	0.010	0.59	No
Q5MNZ9	WD repeat domain phosphoinositide-interacting protein 1	16	53177 ± 7893	46397 ± 5320	0.87	0.020	0.61	No
Q9NP73	Putative bifunctional UDP-N-acetylglucosamine transferase and deubiquitinase ALG13	16	86417 ± 12669	82739 ± 13918	0.96	0.026	0.62	No
O95715	C-X-C motif chemokine 14	16	50788 ± 11107	57210 ± 9997	1.13	0.032	0.65	No
Q9UK08	Guanine nucleotide-binding protein G(I)/G(S)/G(O) subunit gamma-8	16	61168 ± 19527	70811 ± 18813	1.16	0.047	0.65	No
Q96C36	Pyrroline-5-carboxylate reductase 2	15	142463 ± 28282	117414 ± 24859	0.82	0.0088	0.59	No
Q7Z5A7	Chemokine-like protein TAFA-5	15	48274 ± 6751	43761 ± 6563	0.91	0.013	0.60	No
Q9NX74	tRNA-dihydrouridine(20) synthase [NAD(P)+]-like	15	18627 ± 3898	16118 ± 3766	0.87	0.016	0.61	No

Table D4.2 (continued)

O95931	Chromobox protein homolog 7	15	70553 ± 8088	67259 ± 6351	0.95	0.044	0.65	No
Q8WV24	Pleckstrin homology-like domain family A member 1	15	119463 ± 42904	102332 ± 8423	0.86	0.046	0.65	No
Q9H1D9	DNA-directed RNA polymerase III subunit RPC6	14	59397 ± 8652	52697 ± 6269	0.89	0.0064	0.59	No
Q52LW3	Rho GTPase-activating protein 29	14	27795 ± 9078	22715 ± 5373	0.82	0.012	0.59	No
Q8NDX5	Polyhomeotic-like protein 3	14	56419 ± 8034	53651 ± 5380	0.95	0.013	0.60	No
P62314	Small nuclear ribonucleoprotein Sm D1	14	126294 ± 38019	108324 ± 23424	0.86	0.036	0.65	No
Q14596	Next to BRCA1 gene 1 protein	14	16597 ± 2441	18172 ± 4417	1.09	0.050	0.65	No
Q96BZ8	Leukocyte receptor cluster member 1	13	37733 ± 8923	33060 ± 10995	0.88	0.013	0.60	No
Q6JQN1	Acyl-CoA dehydrogenase family member 10	13	38222 ± 16000	30599 ± 7751	0.80	0.020	0.61	No
P55210	Caspase-7	13	22400 ± 6585	25095 ± 7843	1.12	0.022	0.61	No
Q86Y79	Probable peptidyl-tRNA hydrolase	11	21500 ± 5025	17951 ± 5604	0.83	0.0055	0.59	No
Q8TCF1	AN1-type zinc finger protein 1	11	47569 ± 6272	41784 ± 7448	0.88	0.010	0.59	No
P18509	Pituitary adenylate cyclase-activating polypeptide	10	45406 ± 17011	32873 ± 10053	**0.72**	0.010	0.59	No
P40261	Nicotinamide N-methyltransferase	10	72546 ± 26010	57679 ± 9741	**0.80**	0.034	0.65	No

Table D4.2 (continued)

O15427	Monocarboxylate transporter 4	10	47050 ± 17283	38041 ± 11563	**0.81**	0.038	0.65	No
Q9NX76	CKLF-like MARVEL transmembrane domain-containing protein 6	9	54918 ± 13593	65240 ± 14935	1.19	0.028	0.62	No
Q8TAA5	GrpE protein homolog 2, mitochondrial	9	44055 ± 8825	37314 ± 7268	0.85	0.043	0.65	No
Q5T2D3	OTU domain-containing protein 3	9	13656 ± 3287	14710 ± 2735	1.08	0.048	0.65	No
O15116	U6 snRNA-associated Sm-like protein LSm1	8	255458 ± 70247	222747 ± 72564	0.87	0.010	0.59	No
Q9HB20	Pleckstrin homology domain-containing family A member 3	8	24475 ± 3858	22399 ± 3884	0.92	0.040	0.65	No
P78560	Death domain-containing protein CRADD	8	87532 ± 14414	79968 ± 10928	0.91	0.047	0.65	No

[a]The accession number from the UniProt human database. [b]PSMs are summed across all batches. [c]Average ± standard deviation calculated from normalized TMT reporter ion intensities, N = 19-21 per group. [d]Bold indicates fold changes < 0.81 and > 1.23. [e]p-values from linear regression model for main effects of diagnosis covaried for age and sex. [f]Proteins were significant with uncorrected $p < 0.05$ in the Pitt ADRC IPL dataset. Abbreviations: PSMs, peptide spectral matches; CN, cognitively normal; AD, Alzheimer's disease.

Table D4.3. Significant IPA pathways in AD.

Pathway Name	-log(p-value)[a]	Proteins in Pathway[b]
Glutaryl-CoA Degradation	8.89	ACAA2,ACAT2,GCDH,HADH,HADHA,HADHB, HSD17B10,HSD17B8
Fatty Acid β-oxidation I	8.60	ACAA2,ACSL5,ECI1,ECI2,HADH,HADHA,HADHB, HSD17B10,HSD17B8,IVD
Tryptophan Degradation III (Eukaryotic)	7.47	ACAA2,ACAT2,GCDH,HADH,HADHA,HADHB, HSD17B10,HSD17B8
Valine Degradation I	6.76	ACADSB,BCKDHA,BCKDHB,DBT,HADHA,HADHB, HIBADH
Isoleucine Degradation I	5.89	ACAA2,ACADSB,ACAT2,HADHA,HADHB, HSD17B10
Ketogenesis	5.63	ACAA2,ACAT2,HADHA,HADHB,HMGCL
Mevalonate Pathway I	5.01	ACAA2,ACAT2,HADHA,HADHB,PMVK
Superpathway of Geranylgeranyldiphosphate Biosynthesis I (via Mevalonate)	4.41	ACAA2,ACAT2,HADHA,HADHB,PMVK
Branched-chain α-keto acid Dehydrogenase Complex	4.35	BCKDHA,BCKDHB,DBT
Methylmalonyl Pathway	4.35	MCEE,PCCA,PCCB
Ketolysis	4.32	ACAA2,ACAT2,HADHA,HADHB
Semaphorin Signaling in Neurons	4.13	MAPK1,MAPK3,NRP1,PAK2,PLXNA3,PLXNB1, RHOQ,SEMA7A
2-oxobutanoate Degradation I	3.95	MCEE,PCCA,PCCB
Superpathway of Methionine Degradation	3.78	CTH,MCEE,MGMT,PCCA,PCCB,SUOX
Relaxin Signaling	3.72	ADCY3,CTH,GNA12,GNG5,GUCY1A1,MAP2K1, MAPK1,MAPK3,NAPEPLD,PDE4A,RAP1A,REL
Prostate Cancer Signaling	3.64	FOXO1,HDAC3,HDAC9,HSP90AA1,HSP90B1, MAP2K1,MAPK1,MAPK3,RAP1A,REL
CNTF Signaling	3.54	LIFR,MAP2K1,MAPK1,MAPK3,RAP1A,RPS6KA2, RPS6KA5
NRF2-mediated Oxidative Stress Response	3.46	AKR7A2,DNAJA1,DNAJA2,DNAJC12,GSR,GSTK1, GSTM3,HSP90AA1,HSP90B1,MAP2K1,MAP2K6, MAPK1,MAPK3,RAP1A,STIP1
Antiproliferative Role of Somatostatin Receptor 2	3.46	CTH,GNG5,GUCY1A1,MAP2K1,MAPK1,MAPK3, RAP1A,SST
Superpathway of Cholesterol Biosynthesis	3.36	ACAA2,ACAT2,HADHA,HADHB,PMVK
PPARα/RXRα Activation	3.33	ADCY3,FASN,GPD1,HSP90AA1,HSP90B1,MAP2K1, MAP2K6,MAPK1,MAPK3,NCOR1,PRKAB2,RAP1A, REL
Role of IL-17F in Allergic Inflammatory Airway Diseases	3.30	MAP2K1,MAPK1,MAPK3,REL,RPS6KA2,RPS6KA5
PFKFB4 Signaling Pathway	3.25	GPI,MAP2K1,MAP2K6,MAPK1,MAPK3,RPS6KA5

Table D4.3 (continued)

Gap Junction Signaling	3.23	ADCY3,CSNK1E,CTH,GJA1,GJB6,GUCY1A1, MAP2K1,MAPK1,MAPK3,PRKG2,RAP1A,TJP1, TUBB2B
Leucine Degradation I	3.06	HMGCL,IVD,MCCC2
ErbB Signaling	2.89	FOXO1,MAP2K1,MAP2K6,MAPK1,MAPK3,NCK1, PAK2,RAP1A
FAK Signaling	2.87	ARHGEF6,CAPN7,ITGB8,MAP2K1,MAPK1,MAPK3, PAK2,RAP1A,TLN2
L-carnitine Biosynthesis	2.82	BBOX1,TMLHE
Opioid Signaling Pathway	2.79	ADCY3,CAMK2G,GNA12,GNG5,MAP2K1,MAP2K6, MAPK1,MAPK3,MAPK4,PDYN,RAP1A,RGS10, RPS6KA2,RPS6KA5,YES1
Endocannabinoid Developing Neuron Pathway	2.71	ADCY3,AKT1S1,GNG5,MAP2K1,MAP2K6,MAPK1, MAPK3,MAPK4,RAP1A
Estrogen-Dependent Breast Cancer Signaling	2.69	DHRS11,HSD17B10,HSD17B8,MAPK1,MAPK3, RAP1A,REL
FLT3 Signaling in Hematopoietic Progenitor Cells	2.66	MAP2K1,MAPK1,MAPK3,RAP1A,RPS6KA2, RPS6KA5,STAT2
cAMP-mediated signaling	2.65	ADCY3,ADRA2A,AKAP12,CAMK2G,CHRM3, MAP2K1,MAPK1,MAPK3,NAPEPLD,PDE4A,PKIA, RAP1A,RGS10
Reelin Signaling in Neurons	2.64	ARHGEF6,CAMK2G,MAP2K1,MAP2K6,MAPK1, MAPK3,MAPK8IP1,RAP1A,YES1
Semaphorin Neuronal Repulsive Signaling Pathway	2.63	GUCY1A1,ITGB8,MAP2K1,MAP2K6,NRP1,PAK2, PDE4A,PLXNA3,PLXNB1,PRKG2
14-3-3-mediated Signaling	2.62	AKT1S1,FOXO1,GFAP,MAP2K1,MAPK1,MAPK3, RAP1A,TUBB2B,YWHAB
IGF-1 Signaling	2.61	FOXO1,IGFBP5,IGFBP7,MAP2K1,MAPK1,MAPK3, RAP1A,YWHAB
α-Adrenergic Signaling	2.55	ADCY3,ADRA2A,GNA12,GNG5,MAP2K1,MAPK1, MAPK3,RAP1A
Chronic Myeloid Leukemia Signaling	2.53	CTBP2,HDAC3,HDAC9,MAP2K1,MAPK1,MAPK3, RAP1A,REL
Telomerase Signaling	2.53	HDAC3,HDAC9,HSP90AA1,HSP90B1,MAP2K1, MAPK1,MAPK3,RAP1A
Arginine Degradation I (Arginase Pathway)	2.53	ALDH4A1,ARG2
Fatty Acid β-oxidation III (Unsaturated, Odd Number)	2.53	ECI1,ECI2
PPAR Signaling	2.53	HSP90AA1,HSP90B1,MAP2K1,MAPK1,MAPK3, NCOR1,RAP1A,REL
Aryl Hydrocarbon Receptor Signaling	2.47	ALDH1A1,ALDH4A1,GSTK1,GSTM3,HSP90AA1, HSP90B1,MAPK1,MAPK3,NEDD8,REL
Colanic Acid Building Blocks Biosynthesis	2.46	GMDS,GMPPA,GPI
Xenobiotic Metabolism AHR Signaling Pathway	2.45	ALDH1A1,ALDH4A1,GSTK1,GSTM3,HSP90AA1, HSP90B1,REL

Table D4.3 (continued)

White Adipose Tissue Browning Pathway	2.42	ADCY3,CTBP2,FGFR3,GUCY1A1,HIF1AN,MAPK1, PRKAB2,PRKG2,VGF
Unfolded protein response	2.37	AMFR,CD82,DNAJA1,DNAJA2,DNAJC12,HSP90B1, P4HB
Apelin Endothelial Signaling Pathway	2.36	ADCY3,GNA12,GNG5,MAP2K1,MAPK1,MAPK3, PRKAB2,RAP1A,REL
Acute Myeloid Leukemia Signaling	2.34	IDH2,MAP2K1,MAP2K6,MAPK1,MAPK3,RAP1A, REL
Bladder Cancer Signaling	2.32	FGFR3,HDAC3,HDAC9,MAP2K1,MAPK1,MAPK3, RAP1A,RPS6KA5
Role of Tissue Factor in Cancer	2.32	GNA12,MAPK1,MAPK3,P4HB,RAP1A,RPS6KA2, RPS6KA5,YES1
Neuregulin Signaling	2.29	HSP90AA1,HSP90B1,ITGB8,MAP2K1,MAPK1, MAPK3,RAP1A,TMEFF2
Granzyme B Signaling	2.29	LMNB1,LMNB2,NUMA1
PAK Signaling	2.27	ARHGEF6,ITGB8,MAP2K1,MAPK1,MAPK3,NCK1, PAK2,RAP1A
Gαq Signaling	2.27	CHRM3,GNA12,GNG5,GRM1,MAP2K1,MAPK1, MAPK3,NAPEPLD,REL,RHOQ
Fcγ Receptor-mediated Phagocytosis in Macrophages and Monocytes	2.27	MAPK1,MAPK3,NAPEPLD,NCK1,TLN2,VAV3,YES1
Melanocyte Development and Pigmentation Signaling	2.27	ADCY3,MAP2K1,MAPK1,MAPK3,RAP1A,RPS6KA2, RPS6KA5
Non-Small Cell Lung Cancer Signaling	2.27	HDAC3,HDAC9,MAP2K1,MAPK1,MAPK3,RAP1A,S TK4
Germ Cell-Sertoli Cell Junction Signaling	2.25	CTNND1,MAP2K1,MAP2K6,MAPK1,MAPK3,PAK2, RAP1A,RHOQ,TJP1,TUBB2B
Cholecystokinin/Gastrin-mediated Signaling	2.25	GNA12,MAP2K1,MAP2K6,MAPK1,MAPK3,RAP1A, RHOQ,SST
Nitric Oxide Signaling in the Cardiovascular System	2.25	ARG2,GUCY1A1,HSP90AA1,HSP90B1,MAP2K1, MAPK1,MAPK3,PRKG2
Ephrin B Signaling	2.24	CAP1,GNA12,GNG5,MAPK1,MAPK3,VAV3
PI3K/AKT Signaling	2.24	FOXO1,HSP90AA1,HSP90B1,ITGB8,MAP2K1, MAPK1,MAPK3,MAPK8IP1,RAP1A,REL,YWHAB
Adrenomedullin signaling pathway	2.24	ADCY3,CTH,GUCY1A1,MAP2K1,MAP2K6,MAPK1, MAPK3,MAPK4,PRKG2,RAP1A,REL
Dermatan Sulfate Degradation (Metazoa)	2.21	HEXA,HEXB,IDS
Gαs Signaling	2.21	ADCY3,CHRM3,GNA12,GNG5,MAP2K1,MAPK1, MAPK3,RAP1A
Xenobiotic Metabolism Signaling	2.20	ALDH1A1,ALDH4A1,CAMK2G,GSTK1,GSTM3, HSP90AA1,HSP90B1,MAP2K1,MAP2K6,MAPK1, MAPK3,MGMT,RAP1A,REL

Table D4.3 (continued)

Molecular Mechanisms of Cancer	2.20	ADCY3,ARHGEF6,CAMK2G,CASP7,CTNND1, FOXO1,GNA12,GNG5,HDAC3,HDAC9,ITGB8, MAP2K1,MAP2K6,MAPK1,MAPK3,PAK2,RAP1A, REL,RHOQ
Hypoxia Signaling in the Cardiovascular System	2.19	HIF1AN,HSP90AA1,HSP90B1,P4HB,UBE2D3,UBE2H
Stearate Biosynthesis I (Animals)	2.17	ACSL5,DBT,DHRS11,FASN,ZADH2
4-1BB Signaling in T Lymphocytes	2.16	MAP2K1,MAPK1,MAPK3,REL
Arginine Degradation VI (Arginase 2 Pathway)	2.14	ARG2,PYCR2
GDP-mannose Biosynthesis	2.14	GMPPA,GPI
Glioma Signaling	2.14	CAMK2G,HDAC3,HDAC9,IDH2,MAP2K1,MAPK1, MAPK3,RAP1A
IL-15 Signaling	2.10	AKT1S1,MAP2K1,MAPK1,MAPK3,RAP1A,REL
Ferroptosis Signaling Pathway	2.10	CTH,GSS,MAP2K1,MAPK1,MAPK3,PRKAB2, RAP1A,SLC39A14
Signaling by Rho Family GTPases	2.08	ARHGEF6,GFAP,GNA12,GNG5,ITGB8,MAP2K1, MAPK1,MAPK3,PAK2,PPP1R12C,REL,RHOQ, SEPTIN2
Thrombin Signaling	2.07	ADCY3,ARHGEF6,CAMK2G,GNA12,GNG5, MAP2K1,MAPK1,MAPK3,RAP1A,REL,RHOQ
Role of IL-17A in Arthritis	2.04	MAP2K1,MAP2K6,MAPK1,MAPK3,REL
AMPK Signaling	2.03	ADRA2A,AK2,AK3,AKT1S1,CHRM3,CPT2,FASN, FOXO1,GNA12,GNG5,MAPK1,PRKAB2
Apoptosis Signaling	2.03	CAPN7,CASP7,MAP2K1,MAPK1,MAPK3,RAP1A, REL
Methylglyoxal Degradation III	2.01	AKR7A2,DHRS11,ZADH2
Fatty Acid α-oxidation	2.01	ALDH1A1,ALDH4A1,TMLHE
Cancer Drug Resistance By Drug Efflux	2.01	FOXO1,MAP2K1,MAPK1,MAPK3,RAP1A
Protein Ubiquitination Pathway	2.00	AMFR,BAG1,CRYAB,DNAJA1,DNAJC12, HSP90AA1,HSP90B1,HSPA12B,PSMA2,TAP2,UBA1, UBE2D3,UBE2H
G-Protein Coupled Receptor Signaling	1.98	ADCY3,ADRA2A,CAMK2G,CHRM3,GRM1, MAP2K1,MAPK1,MAPK3,NAPEPLD,PDE4A,RAP1A, REL,RGS10
GNRH Signaling	1.97	ADCY3,CAMK2G,GNG5,MAP2K1,MAP2K6,MAPK1, MAPK3,PAK2,RAP1A,REL
JAK/Stat Signaling	1.97	MAP2K1,MAPK1,MAPK3,RAP1A,REL,STAT2
Xenobiotic Metabolism CAR Signaling Pathway	1.96	ALDH1A1,ALDH4A1,GSTK1,GSTM3,HSP90AA1, HSP90B1,MAP2K1,MAP2K6,MAPK1,MAPK3

Table D4.3 (continued)

Paxillin Signaling	1.95	ARHGEF6,ITGB8,MAPK1,NCK1,PAK2,RAP1A,TLN2
Adipogenesis pathway	1.93	CTBP2,FGFR3,FOXO1,HDAC3,HDAC9,LPIN1, RBBP4,SAP18
PEDF Signaling	1.92	ARHGAP22,CASP7,MAPK1,MAPK3,RAP1A,REL
FGF Signaling	1.92	FGFR3,MAP2K1,MAP2K6,MAPK1,MAPK3,RPS6KA5
Aldosterone Signaling in Epithelial Cells	1.91	CRYAB,DNAJA1,DNAJC12,HSP90AA1,HSP90B1, HSPA12B,MAP2K1,MAPK1,MAPK3
LPS-stimulated MAPK Signaling	1.90	MAP2K1,MAP2K6,MAPK1,MAPK3,RAP1A,REL
Rac Signaling	1.88	ITGB8,MAP2K1,MAPK1,MAPK3,PAK2,RAP1A,REL, SH3RF1
Gαi Signaling	1.88	ADCY3,ADRA2A,GNA12,GNG5,MAPK1,MAPK3, RAP1A,RGS10
Apelin Adipocyte Signaling Pathway	1.88	ADCY3,GSTK1,MAPK1,MAPK3,MAPK4,PRKAB2
CDK5 Signaling	1.87	ADCY3,MAP2K1,MAPK1,MAPK3,MAPK4, PPP1R14B,RAP1A
CXCR4 Signaling	1.86	ADCY3,GNA12,GNG5,MAP2K1,MAPK1,MAPK3, PAK2,RAP1A,RHOQ
RAR Activation	1.86	ADCY3,ALDH1A1,MAP2K1,MAPK1,NCOR1,NRIP2, RBP4,RDH13,REL,TAF4
HER-2 Signaling in Breast Cancer	1.86	AKT1S1,CASP7,FOXO1,ITGB8,MAP2K1,MAPK1, MAPK3,RAP1A,REL,YES1
Insulin Receptor Signaling	1.84	FOXO1,MAP2K1,MAPK1,MAPK3,NCK1,PPP1R14B, RAP1A,RHOQ
Ethanol Degradation IV	1.84	ACSS2,ALDH1A1,ALDH4A1
Regulation of Cellular Mechanics by Calpain Protease	1.81	CAPN7,ITGB8,MAPK1,MAPK3,RAP1A,TLN2
Amyotrophic Lateral Sclerosis Signaling	1.81	CAPN7,CASP7,CCS,GLUL,NEFL,NEFM,RAB5C
ErbB2-ErbB3 Signaling	1.80	FOXO1,MAP2K1,MAPK1,MAPK3,RAP1A
Oncostatin M Signaling	1.80	MAP2K1,MAPK1,MAPK3,RAP1A
PI3K Signaling in B Lymphocytes	1.79	CAMK2G,MAP2K1,MAPK1,MAPK3,PLEKHA3, RAP1A,REL,VAV3
Endocannabinoid Cancer Inhibition Pathway	1.79	ADCY3,AKT1S1,CASP7,MAP2K1,MAP2K6,MAPK1, MAPK3,PRKAB2
Ephrin Receptor Signaling	1.79	GNA12,GNG5,ITGB8,MAP2K1,MAPK1,MAPK3, NCK1,PAK2,RAP1A,SDCBP
Heme Biosynthesis II	1.78	ALAD,UROD
Pyridoxal 5'-phosphate Salvage Pathway	1.78	MAP2K1,MAP2K6,MAPK1,MAPK3,PAK2
Coronavirus Pathogenesis Pathway	1.76	CTSL,EEF1A1,EEF1A2,HDAC3,HDAC9,MAPK1, MAPK3,REL,RPS28,STAT2
CD40 Signaling	1.75	MAP2K1,MAP2K6,MAPK1,MAPK3,REL

Table D4.3 (continued)

NGF Signaling	1.75	MAP2K1,MAPK1,MAPK3,RAP1A,REL,RPS6KA2, RPS6KA5
Actin Nucleation by ARP-WASP Complex	1.73	GNA12,ITGB8,NCK1,PPP1R12C,RAP1A,RHOQ
Renin-Angiotensin Signaling	1.72	ADCY3,MAP2K1,MAPK1,MAPK3,PAK2,RAP1A,REL
IL-1 Signaling	1.71	ADCY3,GNA12,GNG5,MAP2K6,MAPK1,REL
Glycine Betaine Degradation	1.69	SARDH,SHMT2
PTEN Signaling	1.68	FGFR3,FOXO1,ITGB8,MAP2K1,MAPK1,MAPK3, RAP1A,REL
Agrin Interactions at Neuromuscular Junction	1.68	ARHGEF6,MAPK1,MAPK3,PAK2,RAP1A
GM-CSF Signaling	1.68	CAMK2G,MAP2K1,MAPK1,MAPK3,RAP1A
Estrogen Receptor Signaling	1.66	ADCY3,ARG2,CTBP2,FOXO1,GNA12,GNG5,HDAC3, HSP90AA1,HSP90B1,MAP2K1,MAPK1,MAPK3, NCOR1,PRKAB2,RAP1A,REL
IL-8 Signaling	1.66	GNA12,GNG5,LASP1,MAP2K1,MAPK1,MAPK3, NAPEPLD,PAK2,RAP1A,RHOQ
Methylthiopropionate Biosynthesis	1.65	ADI1
Glutamine Biosynthesis I	1.65	GLUL
L-cysteine Degradation II	1.65	CTH
Sulfite Oxidation IV	1.65	SUOX
mTOR Signaling	1.64	AKT1S1,MAPK1,MAPK3,NAPEPLD,PRKAB2, RAP1A,RHOQ,RPS28,RPS6KA2,RPS6KA5
Melatonin Signaling	1.63	CAMK2G,MAP2K1,MAP2K6,MAPK1,MAPK3
ERK5 Signaling	1.63	GNA12,RAP1A,RPS6KA2,RPS6KA5,YWHAB
Integrin Signaling	1.63	CAPN7,ITGB8,MAP2K1,MAPK1,MAPK3,NCK1, PAK2,RAP1A,RHOQ,TLN2
Autophagy	1.63	AKT1S1,FOXO1,MAP2K1,MAPK1,MAPK3,PI4K2A, PRKAB2,SESN1,STX17,WIPI1
UVA-Induced MAPK Signaling	1.63	MAPK1,MAPK3,RAP1A,RPS6KA2,RPS6KA5,TNKS
Actin Cytoskeleton Signaling	1.62	ARHGEF6,GNA12,ITGB8,MAP2K1,MAPK1,MAPK3, PAK2,RAP1A,TIAM2,TLN2,VAV3
ERK/MAPK Signaling	1.62	ITGB8,MAP2K1,MAPK1,MAPK3,PAK2,PPP1R14B, RAP1A,RPS6KA5,TLN2,YWHAB
Pancreatic Adenocarcinoma Signaling	1.61	HDAC3,HDAC9,MAP2K1,MAPK1,MAPK3, NAPEPLD,REL
Leptin Signaling in Obesity	1.59	ADCY3,FOXO1,MAP2K1,MAPK1,MAPK3
Melanoma Signaling	1.58	MAP2K1,MAPK1,MAPK3,RAP1A

Table D4.3 (continued)

Huntington's Disease Signaling	1.58	CAPN7,CASP7,GNG5,GRM1,HDAC3,HDAC9, MAPK1,MAPK3,NCOR1,NSF,PSMA2,TAF4
Synaptic Long Term Potentiation	1.56	CAMK2G,GRM1,MAP2K1,MAPK1,MAPK3, PPP1R14B,RAP1A
P2Y Purigenic Receptor Signaling Pathway	1.56	ADCY3,GNG5,MAP2K1,MAPK1,MAPK3,RAP1A, REL
UVC-Induced MAPK Signaling	1.56	MAP2K1,MAPK1,MAPK3,RAP1A
Amyloid Processing	1.56	CAPN7,CSNK1E,MAPK1,MAPK3
Role of NFAT in Cardiac Hypertrophy	1.55	ADCY3,CAMK2G,GNG5,HDAC3,HDAC9,MAP2K1, MAP2K6,MAPK1,MAPK3,RAP1A
GDNF Family Ligand-Receptor Interactions	1.54	MAP2K1,MAPK1,MAPK3,NCK1,RAP1A
Neurotrophin/TRK Signaling	1.54	MAP2K1,MAP2K6,MAPK1,MAPK3,RAP1A
Cleavage and Polyadenylation of Pre-mRNA	1.54	CPSF6,CSTF2
fMLP Signaling in Neutrophils	1.53	GNA12,GNG5,MAP2K1,MAPK1,MAPK3,RAP1A,REL
TNFR1 Signaling	1.53	CASP7,CRADD,PAK2,REL
UVB-Induced MAPK Signaling	1.53	MAP2K1,MAPK1,MAPK3,RPS6KA5
Endothelin-1 Signaling	1.52	ADCY3,CASP7,GNA12,GUCY1A1,MAPK1,MAPK3, MAPK4,NAPEPLD,RAP1A
Production of Nitric Oxide and Reactive Oxygen Species in Macrophages	1.52	ARG2,MAP2K1,MAPK1,MAPK3,PPP1R14B,RAP1A ,RBP4,REL,RHOQ
Angiopoietin Signaling	1.52	FOXO1,NCK1,PAK2,RAP1A,REL
Inhibition of ARE-Mediated mRNA Degradation Pathway	1.52	CNOT3,EXOSC10,EXOSC6,MAPK1,MAPK3,MAPK4, PSMA2,YWHAB
Mouse Embryonic Stem Cell Pluripotency	1.51	DVL2,LIFR,MAP2K1,MAPK1,MAPK3,RAP1A
Xenobiotic Metabolism PXR Signaling Pathway	1.51	ALDH1A1,ALDH4A1,CAMK2G,GSTK1,GSTM3, HSP90AA1,HSP90B1,NCOR1,PPP1R14B
Gα12/13 Signaling	1.50	GNA12,MAP2K1,MAPK1,MAPK3,RAP1A,REL,VAV3
Synaptic Long Term Depression	1.49	CTH,GNA12,GRM1,GUCY1A1,MAP2K1,MAPK1, MAPK3,PRKG2,RAP1A
B Cell Receptor Signaling	1.49	CAMK2G,FOXO1,MAP2K1,MAP2K6,MAPK1, MAPK3,RAP1A,REL,VAV3
IL-3 Signaling	1.48	FOXO1,MAP2K1,MAPK1,MAPK3,RAP1A
Thyroid Cancer Signaling	1.48	FOXO1,MAP2K1,MAPK1,MAPK3,RAP1A
CCR3 Signaling in Eosinophils	1.47	GNA12,GNG5,MAP2K1,MAPK1,MAPK3,PAK2, RAP1A
Renal Cell Carcinoma Signaling	1.46	MAP2K1,MAPK1,MAPK3,PAK2,RAP1A
Chemokine Signaling	1.46	CAMK2G,MAP2K1,MAPK1,MAPK3,RAP1A

Table D4.3 (continued)

Role of PKR in Interferon Induction and Antiviral Response	1.46	HSP90AA1,HSP90B1,MAP2K6,MAPK1,MAPK3,REL, STAT2
Ethanol Degradation II	1.46	ACSS2,ALDH1A1,ALDH4A1
ILK Signaling	1.44	ARHGEF6,ITGB8,MAP2K6,MAPK1,MAPK3, PPP1R14B,REL,RHOQ,RPS6KA5
Role of MAPK Signaling in the Pathogenesis of Influenza	1.44	MAP2K1,MAP2K6,MAPK1,MAPK3,RAP1A
MSP-RON Signaling In Cancer Cells Pathway	1.43	MAP2K1,MAPK1,MAPK3,RAP1A,REL,RPS6KA2, YWHAB
Natural Killer Cell Signaling	1.43	MAP2K1,MAPK1,MAPK3,NCK1,PAK2,PVR,RAP1A, REL,VAV3
Cardiac Hypertrophy Signaling (Enhanced)	1.42	ADCY3,ADRA2A,CAMK2G,DVL2,FGFR3,GNA12, GNG5,HDAC3,HDAC9,ITGB8,MAP2K1,MAP2K6, MAPK1,MAPK3,NAPEPLD,PDE4A,RAP1A,REL, RPS6KA5
Androgen Signaling	1.42	GNA12,GNG5,GTF2A2,HSP90AA1,MAPK1,MAPK3, REL,TAF4
Axonal Guidance Signaling	1.40	ARHGEF6,GNA12,GNG5,ITGB8,L1CAM,MAP2K1, MAPK1,MAPK3,NCK1,NRP1,PAK2,PLXNA3, PLXNB1,RAP1A,SDCBP,SEMA7A,SLIT2,TUBB2B
VEGF Family Ligand-Receptor Interactions	1.38	MAP2K1,MAPK1,MAPK3,NRP1,RAP1A
BAG2 Signaling Pathway	1.38	HSP90AA1,MAPK1,MAPK3,PSMA2,REL
Role of MAPK Signaling in Promoting the Pathogenesis of Influenza	1.38	MAP2K1,MAP2K6,MAPK1,MAPK3,NUP153,RAP1A
Insulin Secretion Signaling Pathway	1.38	ADCY3,CAMK2G,CHRM3,MAPK1,MAPK3,NSF, RAP1A,RPS6KA5,SPCS3,STAT2,YES1
Xenobiotic Metabolism General Signaling Pathway	1.36	GSTK1,GSTM3,MAP2K1,MAP2K6,MAPK1,MAPK3, RAP1A
Telomere Extension by Telomerase	1.36	HNRNPA2B1,TNKS
Cardiac β-adrenergic Signaling	1.35	ADCY3,AKAP12,GNA12,GNG5,NAPEPLD,PDE4A, PKIA,PPP1R14B
Asparagine Degradation I	1.35	ASRGL1
Spermine Biosynthesis	1.35	AMD1
Palmitate Biosynthesis I (Animals)	1.35	FASN
Uridine-5'-phosphate Biosynthesis	1.35	UMPS
4-hydroxyproline Degradation I	1.35	ALDH4A1
Spermidine Biosynthesis I	1.35	AMD1
Fatty Acid Biosynthesis Initiation II	1.35	FASN
Cysteine Biosynthesis/Homocysteine Degradation	1.35	CTH
GDP-L-fucose Biosynthesis I (from GDP-D-mannose)	1.35	GMDS

Table D4.3 (continued)

Glycine Biosynthesis I	1.35	SHMT2
Sertoli Cell-Sertoli Cell Junction Signaling	1.35	GUCY1A1,ITGB8,MAP2K1,MAPK1,MAPK3,PRKG2, RAP1A,TJP1,TUBB2B
Endometrial Cancer Signaling	1.33	MAP2K1,MAPK1,MAPK3,RAP1A
MIF-mediated Glucocorticoid Regulation	1.33	MAPK1,MAPK3,REL
BMP signaling pathway	1.33	MAP2K1,MAPK1,MAPK3,RAP1A,REL
HIF1α Signaling	1.33	CAMK2G,GPI,HIF1AN,HSP90AA1,MAP2K1, MAP2K6,MAPK1,MAPK3,RAP1A
IL-2 Signaling	1.31	MAP2K1,MAPK1,MAPK3,RAP1A
Chondroitin Sulfate Degradation (Metazoa)	1.31	HEXA,HEXB

[a]IPA calculated -log(p-value) for each pathway. Only pathways with $p < 0.05$ are shown. [b]Protein accession numbers and names corresponding to gene names can be found at https://www.uniprot.org/.

Table D4.4. Proteins with significant race x diagnosis interactions.

Accession Number[a]	Protein Name	PSMs[b]	NHW		AA		Race x Diagnosis Interaction		
			AD/CN[c]	p-Value[d]	AD/CN[c]	p-Value[e]	β	Standard Error	p-Value[f]
O15305	Phosphomannomutase 2	48	1.06	**0.0060**	0.82	0.076	-55452	15747	**0.0013**
P17540	Creatine kinase S-type, mitochondrial	820	0.98	0.066	**0.71**	**0.00087**	-13823	3997	**0.0015**
Q5JPF3	Ankyrin repeat domain-containing protein 36C	18	0.88	**0.046**	**1.33**	**0.0024**	15798	5129	**0.0041**
Q9Y3U8	60S ribosomal protein L36	28	0.82	0.31	1.14	0.073	19440	6523	**0.0053**
Q6AI08	HEAT repeat-containing protein 6	13	**1.59**	0.23	**0.51**	0.10	-5257	1755	**0.0057**
Q969U7	Proteasome assembly chaperone 2	19	1.10	0.27	0.85	**0.041**	-9807	3349	**0.0060**
P31749	RAC-alpha serine/threonine-protein kinase	164	0.95	0.14	1.08	0.16	95762	33410	**0.0071**
Q8IYT8	Serine/threonine-protein kinase ULK2	17	**1.30**	**0.048**	0.84	0.16	-8542	3139	**0.010**
P62987	Ubiquitin-60S ribosomal protein L40	991	0.92	0.73	**1.26**	**0.0035**	19107	7031	**0.010**
Q7Z7N9	Transmembrane protein 179B	8	**0.80**	**0.025**	**1.24**	0.14	5479	2065	**0.012**
Q8WUF8	Cotranscriptional regulator FAM172A	29	0.87	**0.029**	1.07	0.48	21722	8260	**0.013**
Q9NX74	tRNA-dihydrouridine(20) synthase [NAD(P)+]-like	15	0.94	0.24	**0.74**	**0.0025**	-6108	2338	**0.013**
Q13404	Ubiquitin-conjugating enzyme E2 variant 1	756	1.02	0.17	0.87	**0.018**	-1322451	514023	**0.015**
Q5TDH0	Protein DDI1 homolog 2	129	1.02	0.29	0.89	**0.0018**	-127941	50376	**0.016**
Q7Z2K6	Endoplasmic reticulum metallopeptidase 1	86	0.92	0.79	1.16	**0.031**	67820	26839	**0.016**
Q9BVT8	Transmembrane and ubiquitin-like domain-containing protein 1	24	1.12	0.82	**0.78**	0.10	-46956	18584	**0.016**

Table D4.4 (continued)

Q8IZD4	mRNA-decapping enzyme 1B	30	0.90	0.13	1.15	0.68	22542	8985	**0.017**
O43424	Glutamate receptor ionotropic, delta-2	13	0.82	0.34	**1.24**	**0.0091**	16028	6454	**0.018**
P41218	Myeloid cell nuclear differentiation antigen	18	1.09	0.79	**0.76**	**0.025**	-25944	10550	**0.019**
Q9H0N5	Pterin-4-alpha-carbinolamine dehydratase 2	50	**0.80**	0.062	1.14	**0.040**	160631	65322	**0.019**
P11229	Muscarinic acetylcholine receptor M1	30	0.94	0.88	**1.24**	**0.029**	45929	18684	**0.019**
Q9NPE2	Neugrin	16	0.82	0.13	1.13	0.23	10397	4313	**0.021**
Q9HA64	Ketosamine-3-kinase	220	0.87	**0.0053**	1.03	0.65	368197	152895	**0.022**
Q8TDI0	Chromodomain-helicase-DNA-binding protein 5	91	0.90	0.52	1.14	**0.011**	9962	4170	**0.023**
O95715	C-X-C motif chemokine 14	16	1.02	**0.044**	**1.32**	**0.038**	16464	6893	**0.023**
Q9Y3B2	Exosome complex component CSL4	14	**0.80**	0.24	1.11	0.44	12159	5093	**0.023**
Q5T9C2	Protein FAM102A	19	1.21	0.79	**0.76**	0.27	-3844	1623	**0.024**
P15104	Glutamine synthetase	1061	1.22	0.062	0.89	0.50	-22975923	9701928	**0.024**
Q8N1W1	Rho guanine nucleotide exchange factor 28	24	0.90	0.66	1.15	0.067	15995	6761	**0.024**
Q9Y4R8	Telomere length regulation protein TEL2 homolog	13	0.84	0.24	1.08	0.24	14012	5953	**0.025**
P11166	Solute carrier family 2, facilitated glucose transporter member 1	139	1.16	0.22	0.81	0.22	-349306	149414	**0.025**
Q6WCQ1	Myosin phosphatase Rho-interacting protein	458	0.94	**0.0052**	1.04	0.28	277697	119175	**0.026**
P07451	Carbonic anhydrase 3	38	1.17	0.75	**0.61**	**0.030**	-195494	84228	**0.026**
O43157	Plexin-B1	389	1.18	**0.00059**	0.99	0.60	-337209	145983	**0.027**
P08913	Alpha-2A adrenergic receptor	39	1.00	0.27	1.18	**0.0055**	17615	7640	**0.027**
Q9NUU7	ATP-dependent RNA helicase DDX19A	311	0.97	0.48	1.02	0.13	158638	69312	**0.028**

Table D4.4 (continued)

Q96EP9	Sodium/bile acid cotransporter 4	18	1.14	**0.037**	0.89	0.27	-8751	3828	**0.029**
P13798	Acylamino-acid-releasing enzyme	381	1.03	0.20	0.92	0.080	-480424	210599	**0.029**
Q9BTE3	Mini-chromosome maintenance complex-binding protein	22	1.20	0.85	**0.77**	**0.033**	-39815	17564	**0.030**
Q9HCS7	Pre-mRNA-splicing factor SYF1	40	1.01	0.41	0.84	**0.015**	-34182	15108	**0.030**
O95347	Structural maintenance of chromosomes protein 2	28	0.98	0.50	0.88	**0.00026**	-12102	5358	**0.030**
P19623	Spermidine synthase	107	0.86	**0.020**	1.05	0.18	123497	54722	**0.031**
O15231	Zinc finger protein 185	20	0.95	0.89		**0.021**	6768	3006	**0.031**
P53990	IST1 homolog	169	1.06	0.89	0.93	**0.016**	-191250	85105	**0.031**
O43524	Forkhead box protein O3	39	0.90	0.25	1.13	0.54	23330	10477	**0.033**
P49736	DNA replication licensing factor MCM2	9	**0.68**	0.30	1.18	0.20	7719	3496	**0.034**
A2A3K4	Protein tyrosine phosphatase domain-containing protein 1	19	0.87	0.078	1.08	0.38	11300	5149	**0.035**
Q8N339	Metallothionein-1M	52	**1.28**	**0.032**	0.88	0.079	-53950	24546	**0.035**
O95922	Probable tubulin polyglutamylase TTLL1	16	0.92	0.55	1.16	0.067	17148	7887	**0.037**
O75832	26S proteasome non-ATPase regulatory subunit 10	101	0.94	0.74	1.11	**0.030**	180335	82971	**0.037**
Q6NUM9	All-trans-retinol 13,14-reductase	46	1.08	0.44	0.85	**0.045**	-41024	18920	**0.037**
P12271	Retinaldehyde-binding protein 1	78	1.09	0.27	**1.54**	0.13	161451	74662	**0.038**
P22570	NADPH:adrenodoxin oxidoreductase, mitochondrial	375	0.88	**0.017**	1.07	0.57	703072	325847	**0.038**
O95926	Pre-mRNA-splicing factor SYF2	13	1.02	0.61	**0.81**	0.11	-6833	3170	**0.038**

Table D4.4 (continued)

Q9H3T3	Semaphorin-6B	13	0.89	0.23	1.06	0.074	4943	2296	**0.039**
Q9BXC9	Bardet-Biedl syndrome 2 protein	73	0.93	0.34	1.05	0.30	47154	21950	**0.039**
Q8IV08	5'-3' exonuclease PLD3	123	0.93	0.31	1.10	**0.037**	214189	100112	**0.040**
Q969E8	Pre-rRNA-processing protein TSR2 homolog	44	0.93	0.068	1.08	0.17	176904	83116	**0.041**
Q9BZL4	Protein phosphatase 1 regulatory subunit 12C	354	0.92	**0.010**	1.01	0.54	114395	53859	**0.041**
Q53EL9	Seizure protein 6 homolog	18	1.01	0.60	0.84	**0.046**	-5711	2692	**0.041**
P15927	Replication protein A 32 kDa subunit	144	0.98	0.44	1.12	**0.015**	188340	88889	**0.041**
Q9H4B7	Tubulin beta-1 chain	4241	0.74	0.11	1.22	0.31	34856	16452	**0.042**
Q86WW8	Cytochrome c oxidase assembly factor 5	38	1.00	0.58	1.22	**0.024**	52071	24662	**0.042**
O43822	Cilia- and flagella-associated protein 410	21	0.86	0.80	1.14	0.18	7438	3541	**0.043**
Q9NZ53	Podocalyxin-like protein 2	49	0.96	0.91	1.14	**0.00046**	37216	17754	**0.044**
P62487	DNA-directed RNA polymerase II subunit RPB7	15	1.04	0.96	0.86	0.24	-8106	3885	**0.044**
Q9UL68	Myelin transcription factor 1-like protein	26	0.86	0.36	1.10	0.11	14068	6758	**0.045**
Q86U44	N6-adenosine-methyltransferase catalytic subunit	30	0.85	**0.037**	1.17	**0.026**	33378	16052	**0.045**
Q96F10	Thialysine N-epsilon-acetyltransferase	28	1.18	0.21	0.87	0.31	-157240	75680	**0.045**
Q9H0E9	Bromodomain-containing protein 8	21	0.95	0.28	1.19	**0.044**	6986	3364	**0.045**
O75094	Slit homolog 3 protein	21	1.14	0.62	**0.76**	0.15	-7422	3587	**0.046**
Q04726	Transducin-like enhancer protein 3	65	1.04	0.40	0.91	0.32	-10661	5162	**0.047**
Q9BXR0	Queuine tRNA-ribosyltransferase catalytic subunit 1	62	0.87	0.083	1.01	0.84	27862	13516	**0.047**

Table D4.4 (continued)

Q96E39	RNA binding motif protein, X-linked-like-1	440	0.90	**0.0061**	1.11	0.30	81284	39530	**0.048**
P02786	Transferrin receptor protein 1	210	1.06	0.46	0.86	0.051	-318255	155063	**0.048**
Q7L8J4	SH3 domain-binding protein 5-like	54	0.88	**0.028**	1.03	0.058	36423	17810	**0.049**
Q93088	Betaine--homocysteine S-methyltransferase 1	44	**0.67**	0.16	1.06	0.66	60273	29484	**0.049**
O60825	6-phosphofructo-2-kinase/fructose-2,6-bisphosphatase 2	255	1.07	0.50	0.91	0.47	-272056	133496	**0.049**
Q96NL8	Protein C8orf37	27	0.95	0.49	1.07	0.10	32320	15881	**0.050**

[a]The accession number from the UniProt human database. [b]PSMs are summed from all batches of samples. cFold changes calculated using the average normalized TMT intensities of each group. Bold indicates fold change < 0.81 or > 1.23. [d]p-values from linear regression model for the main effects of diagnosis in non-Hispanic White adults covaried for age and sex; bold indicates $p < 0.05$. [e]p-values from linear regression model for the main effects of diagnosis in African American/Black adults covaried for age and sex; bold indicates $p < 0.05$. [f]p-values from a linear regression model for the interaction of race and diagnosis on protein intensity covaried for age and sex. Abbreviations: PSMs, peptide spectral matches; NHW, non-Hispanic White; CN, cognitively normal; AD, Alzheimer's disease; AA, African American/Black.

APPENDIX E

Curriculum Vitae

BIOGRAPHICAL

Business Address: Vanderbilt University Chemistry Dept.
5430 Stevenson Center
Office Phone: 615-343-8491

Home Address: 213 Brattlesboro Place
Nashville, TN 37204
Email: kaitlyn.e.stepler@vanderbilt.edu
Personal Phone: 240-405-6919

EDUCATION

Vanderbilt University, Nashville, TN — August 2017-present
Ph.D. in Chemistry, expected graduation August 31, 2021 — Cumulative GPA: 3.912

University of Pittsburgh, Pittsburgh, PA — May 2016-August 2017
Completed first year of Chemistry PhD program — Cumulative GPA: 3.813

McDaniel College, Westminster, MD — May 2015
B.A. in Exercise Science/Chemistry, Spanish Minor — Cumulative GPA: 3.93; Major GPA: 3.97
Honors in Exercise Chemistry — Summa Cum Laude
Honors Program

WORK EXPERIENCE

Quality Control Analyst, MedImmune/AstraZeneca — June 2015-February 2016

- Performed quality control testing on in-process, finished product, and stability samples as assigned and on schedule: appearance, sub-visible particles (HIAC), pH, A280, osmolality, protein A binding (HPLC), deliverable/extractable volume, break loose/glide force for syringes (Instron), container closure integrity
- Trained other analysts on above methods; trained analysts from AstraZeneca facility in Japan on particle appearance test for method transfer
- Entered data in and maintain sample tracker for Quality Control – Analytical Testing group 3x/week and sent weekly updates to management
- Completed appropriate documentation for testing procedures (data capture forms, equipment logbooks)
- Calibrated and maintained laboratory equipment according to standard operating procedures (SOPs)
- Entered data into Laboratory Information Management System (LIMS): assessed compliance to specifications and reported abnormalities
- Understood, followed, and updated SOPs; complied with FDA current Good Manufacturing Practices regulations
- Wrote and executed study protocols and provided data for stability studies and method validation reports
- Operated within all safety regulations in the MedImmune Policies and Procedures

Lab Assistant, McDaniel College Dept. of Kinesiology — January-May 2015

- Assisted in the Exercise Physiology lab course with exercise testing and data collection: Biodex, VO_{2max} testing, underwater weighing, blood pressure measurements, various exercise tests
- Answered individual student questions regarding procedures, calculations, and lab reports

Office Assistant, McDaniel College Office of Institutional Advancement — August 2014-May 2015

- Used public resources for research and data mining, Microsoft Excel data entry, other administrative duties

RESEARCH

Graduate Research, Vanderbilt University & Univ. of Pittsburgh Depts of Chemistry May 2016-present

Advisor: Dr. Renã A. S. Robinson

Synopsis: Alzheimer's disease (AD) proteomics. Optimized a brain proteomics workflow using mouse brain for maximal proteome depth and efficient analysis time to study global differences in proteins. Optimized workflow is being applied to examine differences between non-Hispanic White and African American/Black adults with and without AD in multiple postmortem brain regions. Completed analysis of pilot cohort of human hippocampus, inferior parietal lobule, and globus pallidus samples to identify protein differences in Alzheimer's disease across regions and identify potential racial differences in these changes; manuscript published. Completed similar analysis in a second biracial cohort of inferior parietal lobule samples. Also used proteomics to study HEK 293 cells with a mutation associated with AD in African American/Black adults.

Skills:

- Sample analysis: tissue homogenization, protein concentration assay, enzymatic digestion, desalting/cleanup, tandem mass tags (TMT) labeling, offline fractionation methods, preparation for mass spectrometry (MS), gel electrophoresis, Western blots, Biomek i7 automated workstation
- Liquid chromatography (LC)/MS: Thermo Orbitrap Elite, QExactive HF, Orbitrap Fusion Lumos; MS/MS and (SPS)-MS^3; in-house column pulling/packing, Xcalibur software, instrument troubleshooting
- Data analysis: manual analysis using Microsoft Excel, Xcalibur, Proteome Discoverer v2.1-2.4, Perseus, Ingenuity Pathway Analysis (IPA)

Undergraduate Research, McDaniel College Dept. of Kinesiology May-June 2014

Advisor: Dr. Steve McCole

Title: Cortisol Response to High-Intensity Interval Training

Synopsis: Senior capstone research studied the training effect of high-intensity interval training (HIIT) on cortisol levels, compared to traditional aerobic training (TT), over a three-week exercise program. Collected cortisol samples before and after first and last exercise sessions, and assisted in analyzing samples via radioimmunoassay. Results confirmed cortisol trends with hormonal condition and time of day, but no significant effect was seen from one training session or over the training period.

Skills:

- Worked with research subjects: height/weight measurements, underwater weighing, 12-lead ECG electrode placement, VO_2 max and endurance tests, supervised training sessions via heart rate monitor, collected salivary cortisol samples
- Performed data quality review and analysis using Microsoft Excel
- Calibrated and performed tests with lab equipment: VO_2 system, PhysioFlow cardiography system, underwater weighing software

TEACHING EXPERIENCE

Certificate in College Teaching, Vanderbilt University Center for Teaching Completed October 2019

- Completed 2-semester Certificate in College Teaching program including seminar and practicum courses
- Seminar: learned about various pedagogical styles/theories, active learning strategies, and drafted teaching philosophy statement
- Practicum: learned about collaborative learning activities, teaching in times of crisis, and understanding by design/backward design. Designed a unit for a potential class using the backward design strategy and template, performed a microteaching demonstration, and completed teaching observation sequence in which I was observed guest lecturing and met with a graduate teaching fellow from the Center for Teaching before and after my observation

Specialization in Online Teaching Completed June 2020

- Completed 1-week intensive Specialization in Online Teaching for Certificate in College Teaching recipients
- Introduced to different online teaching technologies such as Hypothe.sis, Pinup, Kaltura, and Brightspace
- Learned about general strategies, accessibility, course design, active learning, and assessments for online teaching
- Created and received peer feedback on a mini module on Brightspace

Specialization in STEM Teaching Completed June 2020

- Completed 1-week intensive Specialization in STEM Teaching for Certificate in College Teaching recipients
- Began building one's STEM teaching persona and teaching community
- Learned about process of and barriers to student learning, as related to students' STEM identities
- Learned active learning, feedback/assessment, and technological strategies specifically for STEM teaching
- Considered approaches to teach problem solving in STEM courses

Guest Lecturer, Vanderbilt University Depts of Chemistry & Neuroscience

Analytical Chemistry November 2018, October 2019

- 75-minute class of ~40-45 students
- 2018: Led class discussion of a mass spectrometry paper and lectured on selected mass spectrometry mass analyzers, detectors, and tandem mass spectrometry
- 2019: Lectured on mass spectrometry including ionization sources, mass analyzers, and applications; was observed during this guest lecture for Certificate in College Teaching practicum course

Forensic Analytical Chemistry February 2020

- Lectured on proteomics and its applications in Alzheimer's disease and forensics; led mass spectrometry lab tour

Analytical Chemistry Laboratory November 2020

- Developed virtual proteomics lab using available online case study and proteomics analysis software with goal to introduce students to bottom-up proteomics sample preparation, data acquisition, and data analysis
- Led four 90-minute virtual lab sessions of 4-8 students each

Methods & Experimental Design in Neuroscience Research, Neuroscience Graduate Program December 2020

- Virtual 50-minute class of 4 graduate students
- Lectured on mass spectrometry and proteomics methods and their applications in neuroscience

Private Tutor, independent August 2014-April 2018

Honors Chemistry, Anatomy & Physiology (high school)

- Taught and reinforced concepts to high school student through assessing knowledge in review of class notes, completing homework assignments, and helping prepare for quizzes and tests
- Helped student reach A average in Chemistry from previous failing marks

Organic Chemistry (collegiate)

- Assisted students in test preparation by teaching and clarifying concepts from lecture and reviewing relevant practice problems

Teaching Assistant, University of Pittsburgh Dept. of Chemistry August-December 2016

- General Chemistry 1 Lab – Independently managed 3 lab sections, including lecture on concepts targeted by lab and how to conduct the experiment, assisting students with performing lab techniques, and grading student lab reports and exams

Tutor, McDaniel College Dept. of Chemistry January 2014-May 2015

- Organic Chemistry tutor – Clarified concepts from lecture, assisted students in preparing for tests, and answered any student questions one night per week August 2014-May 2015
- General Chemistry tutor – Same duties as Organic Chemistry tutor twice per week August 2014-May 2015
- Introductory Chemistry II tutor January2014-May 2014

Peer Tutor, McDaniel College Student Academic Support Services August 2011-December 2014

- One-on-one tutor in Basic Algebra, Calculus I, Intro. Spanish, Human Anatomy, Human Physiology, Nutrition

PUBLICATIONS & PRESENTATIONS

POSTER PRESENTATIONS

November 2020 Poster presentation at the 2nd Annual Vanderbilt Alzheimer's Disease Research Day: *Inclusion of African American/Black Adults in a Pilot Brain Proteomics Study of Alzheimer's Disease*

August 2019 Poster presentation at Vanderbilt Institute of Chemical Biology (VICB) Symposium 2019: *Spatial Brain Proteomics to Understand Racial/Ethnic Disparities in Alzheimer's Disease*

July 2019 Poster presentation at AAIC 2019: *Spatial Brain Proteomics to Understand Racial/Ethnic Disparities in Alzheimer's Disease*

May 2019 Poster presentation at 1st Annual Vanderbilt Alzheimer's Disease Research Day: *Discovery-Based Proteomics to Understand Disparities in Alzheimer's Disease*

September 2018 Poster presentation at NOBCChE 2018: *Discovery-Based Proteomics to Understand Disparities in Alzheimer's Disease*

August 2018 Poster presentation at VICB Symposium 2018: *Characterizing Altered Lipid Metabolism in Health Disparities of Alzheimer's Disease*

June 2018 Poster presentation at ASMS 2018: *Developing Proteomics Platforms to Study Lipid Pathways in Alzheimer's Disease*

October 2017 Poster presentation at NOBCChE 2017: *Proteomics Analysis to Study Lipid Metabolism in Alzheimer's Disease*

May 2017 Poster presentation at Research Day 2017: Celebrating Research on Aging and Rehabilitation (University of Pittsburgh/UPMC): *Optimization of a Brain Proteomics Workflow to Study Proteins in Lipid Metabolism in Alzheimer's Disease*

ORAL PRESENTATIONS

March 2019 Oral presentation at Pittcon 2019: *Spatial Proteomics Analysis of Postmortem Brain in Alzheimer's Disease*

October 2018 Vanderbilt University Chemistry Forum seminar series: *Brain Proteomics to Study Disparities in Alzheimer's Disease*

May 2015 McDaniel College senior capstone presentation: *Cortisol Response to High-Intensity Interval Training*

PUBLICATIONS

1. Ford, K. I.; **Stepler, K. E.**; Arul, A. B.; Pumford, A. D.; Robinson, R. A. S. Proteomics analysis of S-nitrosylation in rabbit aging using Oxidized Cysteine-Selective cPILOT (OxcyscPILOT), *manuscript in preparation.*
2. **Stepler, K. E.**; Gillyard, T. R.; Avery, T. M.; Reed, C. B.; Clemons, T. A.; Davis, J. S.; Robinson, R. A. S. Investigating the proteomic and structural impact of an Alzheimer's disease-associated ABCA7 mutation, *manuscript in preparation*.
3. **Stepler, K. E.**; Reed, C. B.; Avery, T. M.; Davis, J. S.; Robinson, R. A. S. ABCA7, a genetic risk factor associated with Alzheimer's disease risk in African Americans, *manuscript in preparation*.
4. Bowman, E. A.; England, B. L.; Patterson, M. A.; Price, N. S.; **Stepler, K. E.**; Curnutte, H. A.; Lease, R. E.; Bradley, C. A.; Craig, P. R. Pre-assembly required: nickel(II) complexes containing a Schiff-base ligand derived from tris(2-aminoethyl)amine and acetylacetone, salicylaldehyde, or ortho-vanillin, *Inorganica Chimica Acta* **2021**, DOI: 10.1016/j.ica.2021.120415.
5. **Stepler, K. E.**; Mahoney, E. R.; Kofler, J.; Hohman, T. J.; Lopez, O. L.; Robinson, R. A. S. Inclusion of African American/Black Adults in a Pilot Brain Proteomics Study of Alzheimer's Disease, *Neurobiol. Dis.* **2020**, *146*, doi: 10.1016/j.nbd.2020.105129.
6. **Stepler, K. E.** and Robinson, R. A. S. The potential of 'omics to link lipid metabolism and genetic and comorbidity risk factors of Alzheimer's disease in African Americans. In *Reviews on Biomarker Studies in Psychiatric and Neurodegenerative Disorders*, Guest, P. C., Ed. Springer International Publishing: Cham, 2019; Vol. 1118, pp 1-28.

CONFERENCE PROCEEDINGS

1. **Stepler, K. E.** and Robinson, R. A. S. Spatial brain proteomics to understand racial/ethnic disparities in Alzheimer's disease. Alzheimers Dement. 2019, 15 (7), P1316-P1317.
2. **Stepler, K. E.** and Robinson, R. A. S. Discovery-based brain proteomics to understand disparities in Alzheimer's disease. Front. Chem. Conference Abstract: National Organization for the Professional Advancement of Black Chemists and Chemical Engineers (NOBCChE) 45th Annual Conference, 2018. doi: 10.3389/conf.fchem.2018.01.00019.
3. **Stepler, K. E.** and Robinson, R. A. S., Characterizing altered lipid metabolism in health disparities of Alzheimer's disease. Alzheimers Dement. 2018, 14 (7), P1451.
4. Holmes, K. R.; Cannon, A. R.; Wingerd, E. R.; **Stepler, K. E.**; Fish, A. B.; Peterson, M. N.; Laird, R. H.; McKenzie, J. A.; McCole, S. D. Effects of 3-weeks of high-intensity interval training on running economy and endurance. In International Journal of Exercise Science: Conference Proceedings; Harrisburg, 2015; Vol. 9: Iss. 3, Article 41.

HONORS & AWARDS

NIH T32 Training Grant: Vanderbilt Interdisciplinary Training Program in Alzheimer's Disease — May 2019-Apr 2021
Vanderbilt Graduate School Graduate Student Travel Grant to Present Research — February 2018, June 2019
ASMS 2018 Student Stipend Award — February 2018
NOBCChE Advancing Science Conference Grant — October 2017, September 2018
Vanderbilt Institute of Chemical Biology Graduate Fellowship — August 2017, January 2018
Kenneth P. Dietrich School of Arts & Sciences Graduate Fellowship — May 2016
Award for Excellence in Chemistry or Biochemistry – McDaniel College commencement award — May 2015
Phi Beta Kappa — March 2014
Gamma Sigma Epsilon (national chemistry honors society) — December 2013
Phi Sigma Iota (international foreign languages honors society) — April 2014
Alpha Lambda Delta (national first year honors society) — September 2012

PROFESSIONAL MEMBERSHIPS

Alzheimer's Association International Society to Advance Alzheimer's Research and Treatment (ISTAART) — January 2019
American Society for Mass Spectrometry (ASMS) — January 2018
National Organization for the Professional Advancement of Black Chemists & Chemical Engineers (NOBCChE) — March 2017
American Chemical Society — August 2016

INVOLVEMENT, LEADERSHIP, & SERVICE

St. Bartholomew's childcare volunteer — June 2018-present
Vanderbilt Chemical Biology Association of Students – President — August 2019-August 2020
– Executive board — June 2018-August 2020
Second Harvest Food Bank — November 2019
Adventure Science Center Fall Into Science Festival — October 2019
Nashville NOBCChE Chapter – Secretary — May 2018-September 2019
Lunch with a Scientist – STEM Exploration Experience for Kids — June 2018
Governor's School lab demos — June 2018
Walk to End Alzheimer's (Nashville, TN) – Vanderbilt University Medical Center team — October 2017
Volunteer at Brain Fitness Bootcamp (Pitt Clinical & Translational Science Institute) — July 2017
McDaniel College Honors Program – Secretary — August 2011-May 2015
McDaniel College EPE Club – Secretary — May 2014-May 2015
McDaniel College Catholic Campus Ministry – Service coordinator — December 2012-May 2015
Church office volunteer — May 2012-March 2015